Modulation of osteoclasts and their myeloid precursors by specialised pro-resolving mediators in health and rheumatoid arthritis

Patrícia Riedlová

MSc (Eng)

Submitted in fulfilment of the requirements for the degree of Doctor of Philosophy

College of Medical, Veterinary, and Life Sciences

School of Infection & Immunity

University of Glasgow

December 2023

Abstract

Rheumatoid arthritis (RA) is an autoimmune chronic inflammatory disease, which is associated with pathological degradation of bone/cartilage when bone-resorbing osteoclasts dominate over bone-forming osteoblasts. Recent data have shown that novel specialised pro-resolving lipid mediators (SPMs)(e.g., RvE1, RvD1) have the capacity to modulate inflammation, reduce pain and swelling, and assist in cartilage repair, and bone remodelling. However, although prior studies have demonstrated the effect of RvE1 and RvD1 on osteoclast inhibition, this research was limited to murine models and cell lines, and the ability of SPMs to modulate primary human cells in this context has not been investigated.

This thesis therefore investigates modulation of differentiation (osteoclastogenesis) and function (osteolysis) of primary human $CD14^+$ monocytes and pre-dendritic cells by pro-resolving lipid mediators (e.g., RvE1, RvD1, 17-HDHA, and MaR1). Notably, these studies have been done in both a "steady-state" and "TNF-driven" setting to understand the capability of SPMs to function in a pseudo-inflammatory context. The generated results indicate that exposure of $CD14^+$ monocytes to particular SPMs can lead to inhibition of osteoclastogenesis. However, the "pathological" and pseudo-inflammatory context is particularly relevant, as although RvE1 can lead to osteoclast inhibition in cells derived from healthy donors exposed to TNF, it has no impact in cells derived from individuals with RA. In contrast, the reverse is true for RvD1, where it is able to inhibit osteoclastogenesis of $CD14^+$ monocytes from individuals with RA exposed to TNF, but not healthy controls. Mechanistic studies undertaken to examine the cellular pathways associated with this inhibition, revealed that in both the healthy and RA context RvE1 and RvD1 exposure was associated with lower superoxide production, indicative of mitochondrial modulation.

Given the capacity of SPMs to interact with multiple receptors, further studies were performed to understand the cellular requirements for SPM-driven modulation of the observed cell fate decisions. Thus, the expression of SPM receptors present on osteoclasts and osteoclast precursors was examined. Initial analysis was based on RNAseq datasets for healthy monocytes and monocytes from patients with different rheumatic diseases, as well as healthy osteoclasts

differentiated from either monocytes or dendritic cell precursors. Transcriptional profiling showed that RvE1 and RvD1 SPM receptors, namely LTB4R, CMKLR1, and FPR2 were expressed in both, monocytes and osteoclasts. Subsequent evaluation at the protein level, revealed that LTB4R was significantly more expressed in healthy monocytes and osteoclasts compared to RA cells, while the levels of CMKLR1 and FPR2 were comparable. Higher expression of LTB4R receptor in healthy cells supports the inhibitory actions of RvE1 on osteoclastogenesis in healthy but not in RA osteoclasts.

Having identified a potential mechanism of SPM-driven cellular changes through mitochondrial modulation, studies were undertaken to evaluate, whether there are metabolic differences in RA patient and healthy donor monocytes and monocyte-derived osteoclasts, which could explain the differences observed in their response to SPMs. Initial results showed a significant increase in glucose uptake, fatty acid uptake, mitochondrial membrane potential, and increase in mitochondrial mass/number of mitochondria in RA monocytes compared to healthy. Interestingly, no differences were observed in the metabolic enzymes and ATP production. For a better understanding of whether this difference was maintained throughout the differentiation into macrophages and osteoclasts, the metabolic state of these cells was further tested. While glucose and fatty acid uptake was significantly different in RA macrophages and osteoclasts, the size/number of mitochondria and the membrane potential was no longer significantly different when compared to healthy cells.

In conclusion, work in this thesis for the first time demonstrates the ability of RvE1 and RvD1 to inhibit osteoclasts differentiated from primary human cells in health and RA, suggesting a promising role for SPMs and their pathways to modulate the disease. Moreover, these studies have revealed that RA monocytes have a higher glucose and fatty acid uptake, compared to healthy monocytes, which was retained in differentiated macrophages and osteoclasts. These findings suggest overall increased metabolic activity in RA myeloid compartment, which could lead to higher bone resorption and inflammation in RA. Further research is now needed to better understand the drivers of this altered state and to determine the signalling pathways that could potentially be therapeutically targeted to reduce bone resorption and inflammation.

Table of contents

Abstract *2*
Table of contents *4*
List of tables *7*
List of figures *8*
Acknowledgements *11*
Author's declaration *14*
Definitions/abbreviations *15*
Chapter 1 Introduction *22*
1.1 Myeloid cell biology **22**
1.1.1 Monocyte development 23
1.1.2 Macrophages 25
1.1.3 Dendritic cell precursors 27
1.2 Osteoimmunology **28**
1.2.1 Osteoblasts and bone-lining cells 29
1.2.2 Osteocytes 30
1.2.3 Osteoclasts and their precursors 31
1.2.3.1 Osteoclast differentiation 33
1.2.3.1.1 Osteoclast differentiation under inflammatory conditions 34
1.2.3.2 The process of bone resorption 36
1.3 Rheumatoid arthritis **37**
1.3.1 Pathophysiology of the disease 37
1.3.2 Diagnosis of RA 39
1.3.3 RA treatment 41
1.4 Specialised pro-resolving mediators **43**
1.4.1 Specialised pro-resolving mediators and their receptors 43
1.4.2 Biosynthesis of SPMs from fatty acids 44
1.4.2.1 SPM biosynthesis from omega-6 fatty acids 44
1.4.2.2 SPM biosynthesis from omega-3 fatty acids 45
SPMs derived from EPA 46
SPMs derived from DPA 47
SPMs derived from DHA 48
1.4.3 SPMs in RA 50
1.5 Hypothesis and Aims **53**
Chapter 2 Materials and Methods *55*
2.1 Osteoclastogenesis from osteoclast pre-cursors **55**
2.1.1 Sample collection 55
2.1.1.1 PBMC isolation 55
2.1.1.2 $CD14^+$ monocyte isolation 56
2.1.1.3 Dendritic cell precursor isolation 56
2.1.1.4 Osteoclast differentiation 57
2.1.1.5 THP-1 cells 58
2.2 Quantification of osteoclasts **58**
2.2.1 TRAP staining of osteoclast cultures 58
2.2.2 Bone resorption assay 59
2.3 Expression of SPM receptors at a transcript level **59**

2.3.1 RNA sequencing and data analysis 59
2.3.2 Quantitative polymerase chain reaction (qPCR) 60
2.3.2.1 Cell lysis and RNA extraction 60
2.3.2.2 cDNA synthesis 61
2.3.2.3 Primer design 61
2.3.2.4 qPCR 62

2.4 Expression of SPM receptors at the protein level 63
2.4.1 Immunohistochemistry 63
2.4.2 Western blot 64

2.5 Flow cytometry for immunometabolic changes 65
2.5.1 Harvesting cells 65
2.5.2 Staining for metabolic dyes 66
2.5.3 Staining for metabolic enzymes 67
2.5.3.1 Live/dead staining 67
2.5.3.2 Fixation of the cells 67
2.5.3.3 Metabolic enzymes staining 67

2.6 Purity check for $CD14^+$ monocytes 68
2.6.1 Cell preparation 68
2.6.2 Compensation beads preparation 69

2.7 Additional metabolic assays 69
2.7.1 MitoSox 69
2.7.2 ATP assay 70
2.7.3 Seahorse for Mito Stress assay 70
2.7.3.1 Plate and cartridge preparation 70
2.7.3.2 Cell preparation 71
2.7.3.3 Seahorse analysis preparation 71
2.7.3.4 Seahorse measurement 72
2.7.3.5 Fixing cells and SRB assay 72
2.7.3.6 Seahorse analysis 72

2.8 Graphs and statistical analysis 72

Chapter 3 The expression of SPM receptors on osteoclasts and their precursors in health and rheumatoid arthritis 74

3.1 Introduction 74

3.2 Results 76
3.2.1 $CD14^+$ monocyte transcriptional profiles 76
3.2.2 SPM receptor expression on monocytes and osteoclasts at the transcript level 83
3.2.3 The expression of LTB4R is significantly different in RA and healthy monocytes and osteoclasts at the protein level 88

3.3 Discussion 92

3.4 Conclusion 97

Chapter 4 The effect of specialised pro-resolving lipids on osteoclastogenesis 98

4.1 Introduction 98

4.2 Results 100
4.2.1 Differentiation of osteoclasts from THP-1 cells 100
4.2.2 Optimisation of osteoclastogenesis from CD14+ primary monocytes 102
4.2.3 RvE1 inhibits osteoclastogenesis in healthy individuals under inflammatory conditions 110
4.2.4 RvD1 inhibits osteoclastogenesis in RA patients under inflammatory conditions 119
4.2.5 SPMs do not affect the ability of dendritic cell precursors to differentiate into osteoclasts 127

4.3 Discussion 128

4.4 Conclusion 134

Chapter 5 Metabolism of osteoclasts and their precursors in health and rheumatoid arthritis 135

5.1 Introduction 135

5.2 Results 139

5.2.1 Metabolic changes in health and RA 139

5.2.2 ATP production in healthy and RA monocytes and the impact of SPMs stimulation 142

5.2.3 The effect of SPMs on mitochondrial superoxide production in healthy and RA osteoclasts 145

5.2.4 The effect of SPMs on mitochondrial respiration in health and RA 147

5.3 Discussion 150

5.4 Conclusion 154

Chapter 6 General discussion 156

Impact of COVID-19 162

Conferences 163

Published papers 164

Appendices 165

Media 165

Complete α-MEM media 165

Complete RPMI media 165

Buffers and solutions 165

Cell separation buffer 165

FACS buffer 165

TRAP fixative solution 165

TRAP staining solution 166

2x RT master mix for cDNA synthesis 166

qPCR master mix 166

TBST 166

Milk blocking buffer 166

PFA 167

2% formaldehyde 167

0.1% Triton 167

2% BSA 167

MitoSOX master mix 167

Seahorse media 167

Cell-Tak solution 168

Sulforhodamine B (SRB) sodium salt solution 168

List of references 169

List of tables

Table 1.1 ACR/EULAR classification criteria for RA diagnosis 40
Table 2.1 2x RT master mix for cDNA synthesis 61
Table 2.2 Human primers designed for qPCR 62
Table 2.3 Antibodies used for immunohistochemistry with the used dilutions 64
Table 2.4 Antibodies used for western blot with the used dilutions 65
Table 2.5 Summary of metabolic dyes used for flow cytometry 66
Table 2.6 Summary of metabolic enzymes and antibodies used for flow cytometry..... 68
Table 3.1 Overall gene expression in RA..... 76
Table 3.2 SPM receptor expression on healthy and diseased monocytes 83
Table 3.3 SPM receptor expression on monocytes and osteoclasts 88

List of figures

Figure 1.1 Cell differentiation from hematopoietic stem cells. 22
Figure 1.2 Different monocyte subsets in inflammation and resolution. 25
Figure 1.3 Metabolism of pro-inflammatory and anti-inflammatory macrophages. 27
Figure 1.4 Bone remodelling. 31
Figure 1.5 Osteoclast differentiation from its precursors. 33
Figure 1.6 Osteoclastogenic bone resorption process. 37
Figure 1.7 Pathophysiology of RA. 38
Figure 1.8 The mechanism of biosynthesis of lipoxins from arachidonic acid. 45
Figure 1.9 The mechanism of biosynthesis of E-series resolvins from eicosapentaenoic acid. 46
Figure 1.10 The mechanism of biosynthesis of n-3 DPA SPMs and T-series resolvins from docosapentaenoic acid. 48
Figure 1.11 The mechanism of biosynthesis of D-seried resolvins, maresins, protectins, aspirin-triggered Rvs, and cys-SPMs from docosahexaenoic acid. 50
Figure 2.1 Experimental workflow. 58
Figure 3.1 SPM receptors and their ligands. 75
Figure 3.2 The most differentially expressed genes in RA vs healthy monocytes. 77
Figure 3.3 Upregulated signalling pathways in RA $CD14^+$ monocytes. 79
Figure 3.4 Selected upregulated inflammatory pathways in RA $CD14^+$ monocytes. 82
Figure 3.5 Heatmap of the SPM receptor expression on monocytes in health and RA. 84
Figure 3.6 SPM receptor expression on monocytes in different conditions. 85
Figure 3.7 SPM receptor expression on healthy monocytes and osteoclasts. 87
Figure 3.8 BCA assay 89
Figure 3.9 SPM receptor expression at the protein level in healthy and RA $CD14^+$ monocytes. 89
Figure 3.10 SPM receptor expression at the protein level in healthy and RA macrophages and osteoclasts. 90
Figure 3.11 Summary of the LTB4R, FPR2 and CMKLR1 SPM receptor expression in monocytes, macrophages, and osteoclasts in RA and health. 91
Figure 3.12 SPM receptor expression on macrophages and osteoclasts at the protein level with IHC. 92
Figure 4.1 Resolution of inflammation via lipid mediator class switching. 99
Figure 4.2. THP-1 cell differentiation into osteoclasts with their qPCR transcripts. 101

Figure 4.3 Differentiation of osteoclasts from macrophages and their precursors with RANKL addition on day 1, 3, and 6. 103
Figure 4.4 Inhibition of osteoclastogenesis with TNF added 24 hours after M-CSF addition. 104
Figure 4.5 The addition of TNF 72 hours post M-CSF and RANKL addition. 105
Figure 4.6 The addition of TNF 96 hours after the addition of M-CSF with the RANKL concentration of 25 ng/ml. 106
Figure 4.7 Enhancement of osteoclastogenesis with the addition of TNF 96 hours after the addition of M-CSF with the suboptimal RANKL concentration. 108
Figure 4.8 The effect of TNF and synovial fluid on osteoclastogenesis. 109
Figure 4.9 Evaluation of the right timepoint of SPM addition. 110
Figure 4.10 The effect of SPMs on osteoclast differentiation under standard or TNF-driven conditions with 25 ng/ml of RANKL. 112
Figure 4.11 The effect of SPMs under standard or TNF-driven conditions at sub-optimal RANKL concentration (1 ng/ml). 113
Figure 4.12 RvE1 inhibits osteoclastogenesis under inflammatory conditions. 114
Figure 4.13 Microscope pictures of mature $TRAP^{+}$ osteoclasts and their precursors in the presence of SPMs. 115
Figure 4.14 Bone resorption with RvE1 in healthy donors. 116
Figure 4.15 Gene expression involved in osteoclast differentiation and bone resorption for various SPMs in healthy osteoclasts. 118
Figure 4.16 The effects of SPMs under physiological and inflammatory settings in RA. 120
Figure 4.17 The effect of SPMs on osteoclasts under inflammatory conditions in RA. 121
Figure 4.18 Bone resorption with RvD1 in RA. 122
Figure 4.19 Gene expression involved in osteoclast differentiation and bone resorption with various SPMs in RA. 124
Figure 4.20 RvD1 and RvE1 inhibit osteoclastogenesis in RA and healthy donors, respectively. 125
Figure 4.21 Comparison of osteoclastogenic gene expression between healthy and RA donors. 126
Figure 4.22 Osteoclast differentiation from pre-DCs from whole blood. 127
Figure 4.23 Osteoclast differentiation from DC precursors from leukocyte cones with the addition of SPMs. 128
Figure 5.1 The metabolism of glucose including glycolysis, Krebs cycle, electron transport chain, and OXPHOS. 138

Figure 5.2 Representative image for staining of the metabolic dyes and enzymes..... 139
Figure 5.3 Metabolic enzyme expression in healthy and RA monocytes. 140
Figure 5.4 Metabolic dyes in healthy and RA monocytes. 141
Figure 5.5 Comparison of metabolic dyes in healthy and RA macrophages and osteoclasts. 142
Figure 5.6 ATP production in healthy and RA monocytes. 143
Figure 5.7 ATP production in healthy and RA osteoclasts. 144
Figure 5.8 MitoSOX assay in healthy osteoclasts with the addition of SPMs. 146
Figure 5.9 MitoSOX assay in RA osteoclasts with the addition of SPMs. 147
Figure 5.10 Seahorse cell mito-stress test for mitochondrial respiration. 148
Figure 5.11 Cellular respiration in healthy and RA monocytes in the presence of SPMs. 150

Acknowledgements

First and foremost, I would like to thank my supervisor, Professor Carl Goodyear for his guidance, support, and wise words, without which, this work would not be possible, and I am very grateful for that. Thank you for giving me this amazing opportunity of conducting my PhD in your lab, which has helped me to become a better scientist. Thanks also for reading my thesis and providing your valuable feedback, for finding time when I needed it, and for letting me participate in several national and international conferences, which allowed me to present my research, meet new people, and experience science from a different angle. Thanks also goes to my assessors Professor Simon Milling and Professor Kevin Maloy for their valuable insight and guidance throughout my PhD and also thanks to my secondary supervisor Professor Mariola Kurowska-Stolarska. I would also like to thank Dr. Bart Evert for being my supervisor for almost 3 months during my secondment in the Netherlands at LUMC and to Luís Almeida for the collaboration and for teaching me new metabolic techniques. A huge thanks goes to everyone involved with the ArthritisHeal project, which was responsible for this incredible journey. This project has given me many valuable experiences, I got to participate at various conferences, see how different scientific companies work, and most importantly I was surrounded by awesome people, who I can now call my friends. This project turned out to be so much better than I could have ever dreamed of, and I am very grateful for being a part of it with you all, for sharing our struggles and successes, and for all the amazing memories. Hope we meet again soon! Major thanks goes to the European Union's Horizon 2020 research and innovation programme under the Marie Skłodowska-Curie Grant (agreement No. 812890) for funding my PhD project. Thanks also to all the doctors and nurses for their kindness and help with recruiting patients for this project, and thanks to all the patients who volunteered to donate blood for my research. Thanks

A special thanks also goes to the members of the Goodyear lab, past and present. Thanks to Cecilia and Shiny, who were incredibly helpful when I needed them and were always willing to help whether it was in scientific or personal matters. You taught me a lot and thanks to you I discovered my passion for osteoclasts. Thanks to Kieran for letting me use his RNAseq dataset and for being a great conference travel buddy. Thanks also goes to Yuriko for her help when I needed her vampire skills for taking blood and to everyone who donated blood for my project. A special

thanks also goes to Annie, Andy, Maria Laura, Lauren, Lewis, Bogdan, Aysin, Flavia, Aurélie, Andrew, Sam, and Carmen for not only your help, but also for all the chats, encouragements, pub nights, fun, and your friendship. I would also like to thank The Lunchables for making every day better. You all made this PhD journey very memorable, and I am extremely thankful that I could be a part of this amazing lab. You are the reason Glasgow feels like home.

Huge thanks also goes to my family and friends for their support, love, and positive words. Thanks to Hana for making sure I have a more normal work/life balance, for being an incredible flatmate and an awesome friend, for all our trips and adventures and for all the fun activities during lockdown. You were there during my ups and downs and always did your best to cheer me up. Thanks to Badders for our badminton nights, which were a great de-stressing break from work. Thanks also to the people I got to know through the PhD society on our trip in Pitlochry, who are great friends and thanks for all our camping trips, wild swimming, and adventures, which were a great way to relax after long days in the lab and writing. I would also like to thank MCAA group in Glasgow for our pub nights, supportive talks, and for going through our PhD journeys together.

Finally, massive thanks goes to my mum, dad, and brother for always being there for me. Thank you for long calls, frequent visits to Scotland, and mainly for your love, encouragement, and for supporting me in my scientific career from when I was a little child. Special thanks to my grandma who was diagnosed with rheumatoid arthritis and was one of the reasons why I decided to pursue my PhD degree in rheumatology. Sadly, you can’t be here for the end of this journey but I am very grateful for you, for our talks full of great stories, for being invested in my research, being my top fan, for your incredible optimism, and for always believing in me.

I would like to dedicate this thesis to my grandma, Zdenka Vojtková.

Author's declaration

I declare that this thesis is the result of my own work. No part of this thesis has been submitted or is pending submission for any other degree at The University of Glasgow, or any other institution. Appropriate acknowledgements have been made where any necessary support has been provided by another individual.

……

Patrícia Riedlová

Definitions/abbreviations

13R-HDPA - 13*R*-hydroxy-docosapentaenoic acid

14S-HpDPA - 14S-hydroperoxy-docosapentaenoic acid

15S-HETE - 15S-hydroxyeicosatetraenoic acid

15S-HpETE - 15S-hydroperoxyeicosatetraenoic acid

17-HDHA - 17-hydroxydocosahexaenoic acid

17-HpDPA - 17-hydroperoxy-docosapentaenoic acid

17S-HpDHA - 17S-hydroperoxy-docosahexaenoic acid

18R-H(p)EPE - 18R-hydro(peroxy)-eicosapentaeonic acid

2DG - 2 Deoxy D-glucose

7-Hp-13R-HDPA - 7-hydroperoxy-13(R)-hydroxy-docosapentaenoic acid

AA - arachidonic acid

ACC1 - Acetyl-CoA carboxylase 1

Acetyl coA - acetyl coenzyme A

ACPA - anti-citrullinated protein antibodies

ACR - American college of rheumatology

ATLs - aspirin-triggered LX

ATP - adenosine triphosphate

ATRvs - aspirin-triggered resolvins

bDMARDs – biological DMARDs

BLT1 - leukotriene B4 receptor

c-fms – colony stimulating factor-1 receptor

CA^{2+} - calcium ions

CCCP - Carbonyl cyanide 3-chlorophenylhydrazone

CCL2 – C-C motif chemokine ligand 2

CCR2 - C-C chemokine receptor type 2

cDCs - classical (conventional/myeloid) dendritic cells

cDMARDs - Conventional DMARDs

ChemR23 - chemerin receptor 23

CMKLR1 - Chemokine receptor-like 1

CO_2 - carbon dioxide

COX – cyclooxygenase

CPT1A - carnitine palmitoyltransferase 1A

CRP - C-reactive protein

CSB – cell separation buffer

CSF-1 – colony stimulating factor 1

CX_3CL1 - CX3C motif chemokine receptor 1

Cys-SPMs - cysteinyl specialised pro-resolving mediators

CytC - cytochrome C

DAMPs - damage-associated molecular patterns

DAS - disease activity score

DC stamp - dendritic cell-specific transmembrane protein

Dc_OCs – osteoclasts differentiated from dendritic cell precursors

DCs – dendritic cells

dcSSc - diffuse cutaneous systemic sclerosis

dH_2O - distilled water

DHA - docosahexaenoic acid

DMARDs - disease modifying antirheumatic drugs

DMPI - dentin matrix protein

DPA - docosapentaenoic acid

DPEP - dipeptidase

eaSSc - early systemic sclerosis

EDTA - Ethylenediamine tetraacetic acid

EPA - eicosapentaenoic acid

ERK - extracellular signal-regulated kinase

ESR - erythrocyte sedimentation rate

ETC - electron transport chain

EULAR - European League against rheumatism

$FADH_2$ - flavin adenine dinucleotide

FBS – fetal bovine serum

FPR2 - formyl peptide receptor 2

FSC-A – forward scatter area

FSC-H – forward scatter height

G6PD - Glucose-6-phosphate dehydrogenase

GeoMFI - Geometric mean fluorescence intensity

GGT - gamma-glutamyl transferase

GLUT (1) – glucose transporter (1)

GPCRs - G-protein coupled receptors

GSTM4 - glutathione s-transferase mu4

HC – healthy controls

HCQ – hydroxychloroquine

HLA-DR - class II major histocompatibility complex human leukocyte antigens

HRP - Horseradish peroxidase

IFN - interferon

IGF-1 – insulin-like growth factor 1

IgG - immunoglobulin G

IL – interleukin

JAK - Janus kinase

KEGG - Kyoto Encyclopedia of Genes and Genomes

LCs - Langerhans cells

lcSSc - limited cutaneous systemic sclerosis

LDS - lithium dodecyl sulfate

LGR6 - Leucine-rich repeat-containing

LO – lipoxygenase

LTB4 - leukotriene B4

LTB4R - leukotriene B4 receptor

LTC4S - leukotriene C4 synthase

LTs – leukotrienes

LX - lipoxin

M – macrophages differentiated with M-CSF

M-CSF – monocyte/macrophage colony-stimulating factor

mAb – monoclonal antibody

MAPK - mitogen-activated protein kinase

MaR - maresin

MEPE - matrix extracellular phosphoglycoprotein

MHC II - histocompatibility complex II

MitoTracker DR - MitoTracker Deep Red FM

MMPs – metalloproteinases

Mo – monocytes

Mo_OCs – osteoclasts differentiated from monocytes

Mo-DC – monocyte-derived dendritic cell

MOPS - 3-(N-morpholino)propanesulfonic acid

MR – osteoclasts differentiated with M-CSF and RANKL

$MR_{1/25}$ - osteoclasts differentiated with M-CSF and 1 or 25 ng/ml of RANKL

MRT – osteoclasts differentiated with M-CSF, RANKL, and TNF

$MRT_{1/10}$ - osteoclasts differentiated with M-CSF, RANKL, and 1 or 10 ng/ml of TNF

MRTV - osteoclasts differentiated with M-CSF, RANKL, TNF, and ethanol vehicle

MTX – methotrexate

n – number of donors

NADH - nicotinamide adenine dinucleotide

$NaHCO_3$ – sodium hydrogen carbonate (sodium bicarbonate)

NETs - neutrophil extracellular traps

NF-κB - nuclear factor kappa B

NFATc1 - nuclear factor of activated T cells 1

NK cells – natural killer cells

NO – nitric oxide

nPDs – neuroprotectins

NSAIDs - non-steroidal anti-inflammatory drugs

NTC – non-template control

OC stamp - osteoclast stimulatory transmembrane protein

OCR - oxygen consumption rate

OPG – osteoprotegerin

OSCAR - osteoclast-associated receptor

OXPHOS – oxidative phosphorylation

PBMCs - peripheral blood mononuclear cells

PBS – phosphate-buffered saline

PD - protectin

pDCs - plasmacytoid dendritic cells

PG – prostaglandin

PKM - pyruvate kinase muscle isozyme

PMA - phorbol 12-myristate-13-acetate

PMNs - polymorphonuclear leukocytes

Pre-DCs – immature dendritic cells/dendritic cell precursors

PTPN22 - protein tyrosine phosphatase non-receptor type 22

RA - Rheumatoid arthritis

RANK - receptor activator of nuclear factor kappa B

RANKL - receptor activator of nuclear factor kappa B ligand

RF - rheumatoid factor

RIPA - radioimmunoprecipitation assay

RNS - reactive nitrogen species

ROS – reactive oxygen species

RPMI - Roswell Park Memorial Institute

RT – room temperature

Rv - resolvin

RvDs - D-series resolvins

RvEs - E-series resolvins

RvTs – T-series resolvins

SD – standard deviation

SDHA - Succinate Dehydrogenase Complex Flavoprotein Subunit A

SDS - sodium dodecyl sulfate

SF – synovial fluid

$SF_{1/10}$ – differentiation in the presence of 1 or 10 ng/ml of synovial fluid

siRNA - small interfering ribonucleic acid

SLE - systemic lupus erythematosus

SPMs - specialised pro-resolving lipid mediators

SRB - sulforhodamine B sodium salt

SSc – systemic sclerosis

SSC-A – side scatter area

SSZ – sulfasalazine

TCA - tricarboxylic acid

TCA - trichloroacetic acid

TNF - tumour necrosis factor

TNFR - tumour necrosis factor receptor

TRANCE - TNF-related activation-induced cytokine

TRAP - tartrate-resistant acid phosphatase

V-ATPase – vacuolar H+ type ATPase

α-MEM - alpha Minimum Essential Medium

ΔΨm - mitochondrial membrane potential

Chapter 1 Introduction

1.1 Myeloid cell biology

Myeloid cells originate in bone marrow from hematopoietic stem cells and can differentiate from myeloid progenitor cell into various cell types, including granulocytes, also known as polymorphonuclear leukocytes (PMNs; i.e., basophils, neutrophils, eosinophils, mast cells), monocytes, macrophages, different subsets of dendritic cells (DCs), erythrocytes, and platelets (figure 1.1). They constantly circulate in blood to be supplied to all tissues during infection or damage repair, which is an orchestrated process facilitated by various chemokine receptors. Additionally, they are also present in steady-state tissues where they control homeostasis and development (De Kleer et al., 2014). As this thesis is focused on osteoclasts, further emphasis will be placed on their precursors, namely monocytes, macrophages, and different subsets of DCs.

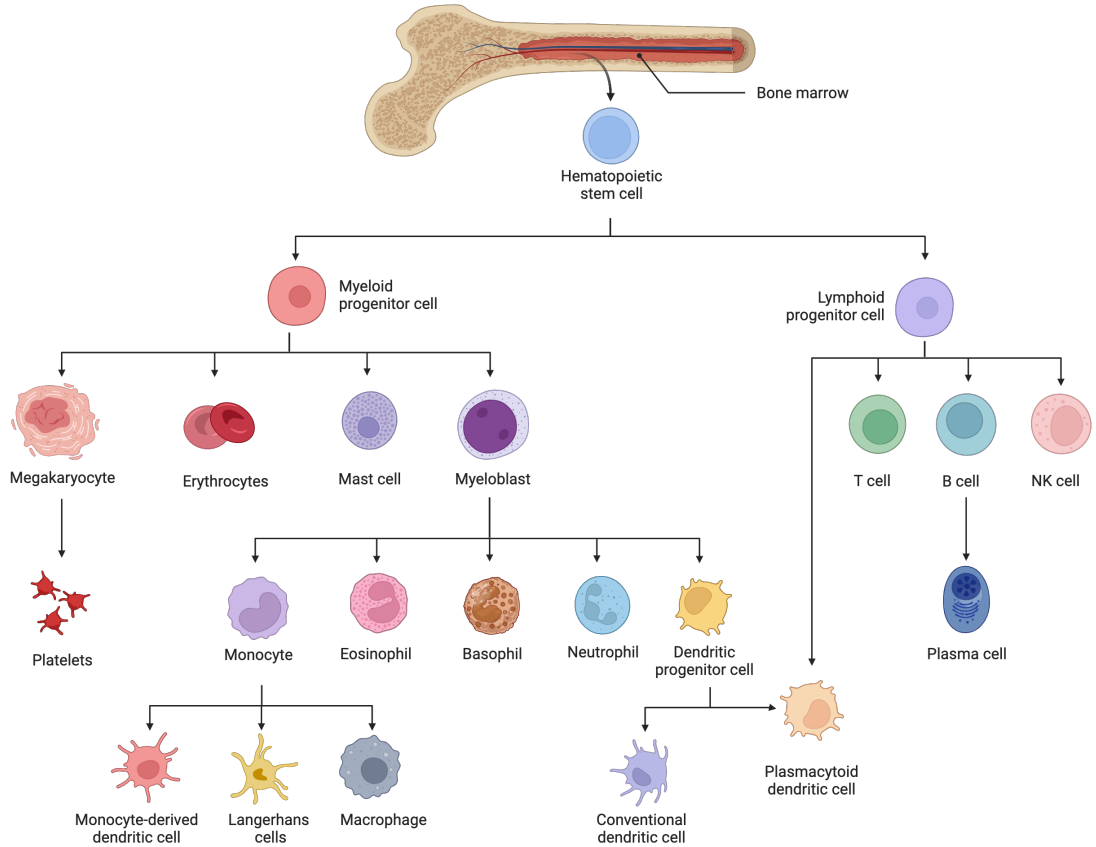

Figure 1.1 Cell differentiation from hematopoietic stem cells.
Hematopoietic stem cell originated in bone marrow can differentiate into either myeloid or lymphoid progenitor cell. Myeloid cells can give rise to several immune cells like PMNs, DCs, monocytes, or macrophages, while lymphoid cells give rise to T cells, B cells, natural killer cells (NK cells) or plasmacytoid DCs. Created in BioRender - figure made based on Khan et al. (2022), Rocamonde et al. (2019), and Zhou & Wu (2017).

1.1.1 Monocyte development

Monocytes are cells of innate immune system that play key roles in inflammation through for example the release of cytokines or phagocytosis. They are the largest leukocytes originating from myeloid precursor cells in the bone marrow before their release into the blood stream where they circulate during homeostasis (Galli et al., 2022; Monie, 2017). Monocytes make up between 3-8% of circulating cells under steady-state conditions with higher cell counts recorded during infection, and between 10-30% of peripheral blood mononuclear cells (PBMCs). Although 90% of monocytes are CD14 positive, there is some variability and three subsets are distinguished, namely classical ($CD14^{++}CD16^{-}$), intermediate ($CD14^{++}CD16^{+}$), and non-classical ($CD14^{Dim}CD16^{++}$), from which classical monocytes are the most abundant (Kapellos et al., 2019; Nielsen et al., 2019). The lifespan of monocytes is relatively short, usually 1 day for classical monocytes, 4.3 days for intermediate monocytes, and 7.4 days for non-classical monocytes (Patel et al., 2021). In this time range, the majority of monocytes undergoes apoptosis, while the rest migrate to tissues or the site of injury or infection, where they differentiate into macrophages (Monie, 2017).

Classical monocytes are inflammatory cells, which means they can infiltrate tissues, produce pro-inflammatory cytokines and mature into inflammatory macrophages. They can also remove dying cells and microorganisms through phagocytosis thanks to their pattern recognition receptors (Mirjam & Broos, 2019). Additionally, they can regulate inflammation, which can later result in its resolution (Kapellos et al., 2019). Intermediate monocytes are mainly pro-inflammatory, secreting tumour necrosis factor (TNF), interleukin 1 (IL-1), IL-6 or IL-12 cytokines once stimulated, while non-classical monocytes are anti-inflammatory. Under physiological conditions, non-classical monocytes can differentiate into tissue-resident macrophages, while during inflammation, their differentiation shifts towards anti-inflammatory macrophages, which actively assist in tissue repair processes (Mirjam & Broos, 2019).

Apart from the differences in monocyte function and the variable expression of CD14 and CD16 markers, classical monocytes also express CCR2 receptor (C-C chemokine receptor type 2) and act in response to CCL2 (C-C chemokine ligand

type 2), which attracts monocytes from bone marrow to the site of inflammation. In contrast non-classical monocytes act in response to CX_3CL1 (CX3C motif chemokine receptor 1, also known as fractalkine), which is a non-classical monocyte chemoattractant maintaining tissue homeostasis and helps with resolution (figure 1.2) (Tsou et al., 2007). Notably, classical monocytes only possess CCR2 receptor and lack CX_3CR1, while non-classical monocytes, express CX_3CR1 and lack CCR2. Intermediate monocytes, have receptors for both ligands (CCR2 and CX_3CR1), which means they can respond to both chemokines, and even though they are mainly pro-inflammatory, they can also exhibit anti-inflammatory actions. However, it is not clear whether they can secrete pro-inflammatory and anti-inflammatory cytokines simultaneously or whether there is another mechanism involved (Kapellos et al., 2019; Wacleche et al., 2018).

Additionally, circulating monocytes, in rheumatoid arthritis (RA) were shown to be leaning towards an intermediate phenotype, and their numbers are also enhanced in RA patients compared to healthy individuals (McGarry et al., 2021). Moreover, monocytes, from inflammatory conditions, like RA, are hyper-inflammatory and primed to become inflammatory macrophages, which is mediated via a STAT3 pathway. They express more pro-inflammatory cytokines and chemokines than healthy individuals, have altered mitochondria, and show enhanced oxidative phosphorylation and glycolysis, which can lead to pannus formation (thickening of synovial tissue) and cartilage damage (McGarry et al., 2021).

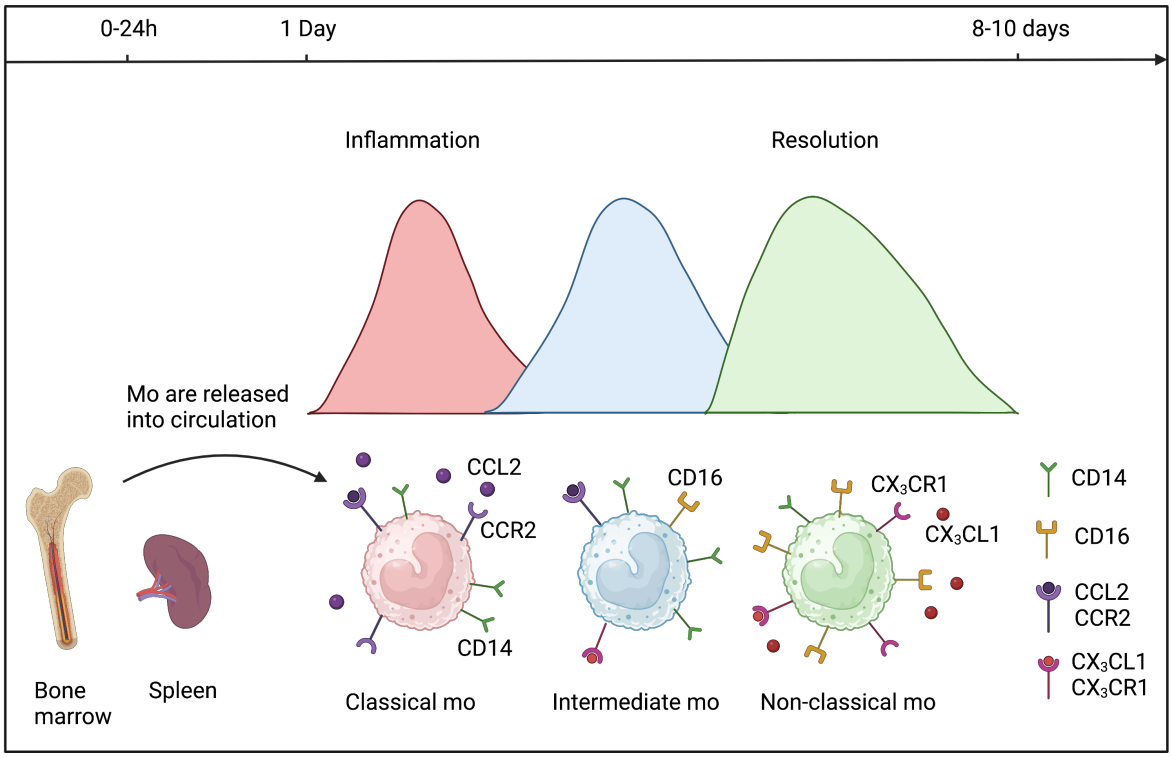

Figure 1.2 Different monocyte subsets in inflammation and resolution.
Monocytes (Mo) are released from bone marrow or spleen to migrate to the inflammatory site due to chemokines. Classical monocytes, which are $CD14^{++}CD16^{-}$ migrate due to CCL2, which interacts with their CCR2 receptor, while non-classical monocytes, which are $CD14^{Dim}CD16^{++}$ express CX3CR1 receptor binding CX3CL1 to achieve resolution. Intermediate monocytes, which are $CD14^{++}CD16^{+}$ express both types of receptors. Created in BioRender - figure adapted from Marsh et al. (2017) and Tahir & Steffens (2021).

1.1.2 Macrophages

Macrophages are the most abundant immune cells in the majority of tissues. They play a key role in innate immunity, where they are involved in immunological response against pathogens and inflammation, as well as in cancer or autoimmune diseases like RA, where their presence is increased (Lee et al., 2018; Laria et al., 2016; Yang et al., 2020). Macrophages are also found at higher numbers in synovial tissues where they can produce pro-inflammatory cytokines after their activation. Moreover, the number of macrophages in synovial tissue can also be used as a biomarker for RA disease activity (Laria et al., 2016).

For many years, it has been thought that macrophages differentiate from circulating blood monocytes, however, it is now known that there are two types of macrophages. These include blood-borne macrophages and tissue-resident macrophages, which were formed during the development of an embryo and last throughout a lifetime (Epelman et al., 2014). Macrophages can have inflammatory

and pro-resolving properties. Tissue resident macrophages have the ability to self-renew, influence bone-remodelling and cell turnover, maintain homeostasis by the clearance of apoptotic cells and by tissue repair, while blood-borne macrophages are ready to respond to inflammation or infection (Gu, et al., 2017; Laria et al., 2016).

Under physiological conditions, pro-inflammatory and anti-inflammatory macrophages are balanced to help maintain homeostasis. However, in the inflamed joints of RA patients for example, active macrophages release numerous pro-inflammatory cytokines (i.e., TNF, IL-1, IL-6, IL-8) and chemokines as a response to inflammation, which then attracts/activates other immune cells (monocytes, neutrophils, T cells, or fibroblasts). As a result, this can lead to chronic inflammation followed by bone/cartilage or tissue damage (Laria et al., 2016). Additionally, based on various factors in the microenvironment, macrophages can also switch between pro-inflammatory and anti-inflammatory state, which is essential for resolution of inflammation (Porcheray et al., 2005).

In RA, polarization of pro-inflammatory and anti-inflammatory macrophages in synovial tissue depends on the level of disease activity, where patients with high disease activity score (DAS) have more pro-inflammatory macrophages, while patients in remission have more anti-inflammatory macrophages (Laria et al., 2016). Moreover, pro-inflammatory macrophages produce more prostaglandins and leukotrienes, which are necessary for the initiation of transcription of enzymes (12- and 15-lipoxygenase (LO)) needed for the production of specialised pro-resolving mediators (SPMs) (Sahni & Van Dyke, 2023). In contrast, the release of prostaglandins is downregulated in anti-inflammatory macrophages and the production of SPMs (discussed later) is upregulated, which further leads to the resolution of inflammation. This process is called lipid mediator class-switching and results in reparative and anti-inflammatory actions (Serhan, 2014).

Another difference in pro-inflammatory and anti-inflammatory macrophages after the phenotypic switch is in their metabolism, where pro-inflammatory macrophages utilise aerobic glycolysis, while anti-inflammatory macrophages use Krebs cycle and oxidative phosphorylation (OXPHOS), which dominates over glycolysis. Pro-inflammatory macrophages primarily use glycolysis for rapid

activation during inflammation or infection, while anti-inflammatory macrophages use fatty acid oxidation critical for the Krebs cycle. This mechanism is more suitable for supplying energy for cell survival to keep macrophages alive for a longer time period while fighting infection and for resolution of inflammation. Moreover, pro-inflammatory macrophages also possess a broken Krebs cycle, which contributes to the production of prostaglandins, nitric oxide (NO), reactive oxygen species (ROS) or IL-1 due to accumulated citrate and succinate, while anti-inflammatory macrophages have an intact Krebs cycle contributing to the resolution of inflammation (figure 1.3) (O'Neill & Pearce, 2015; O'Neill, 2015).

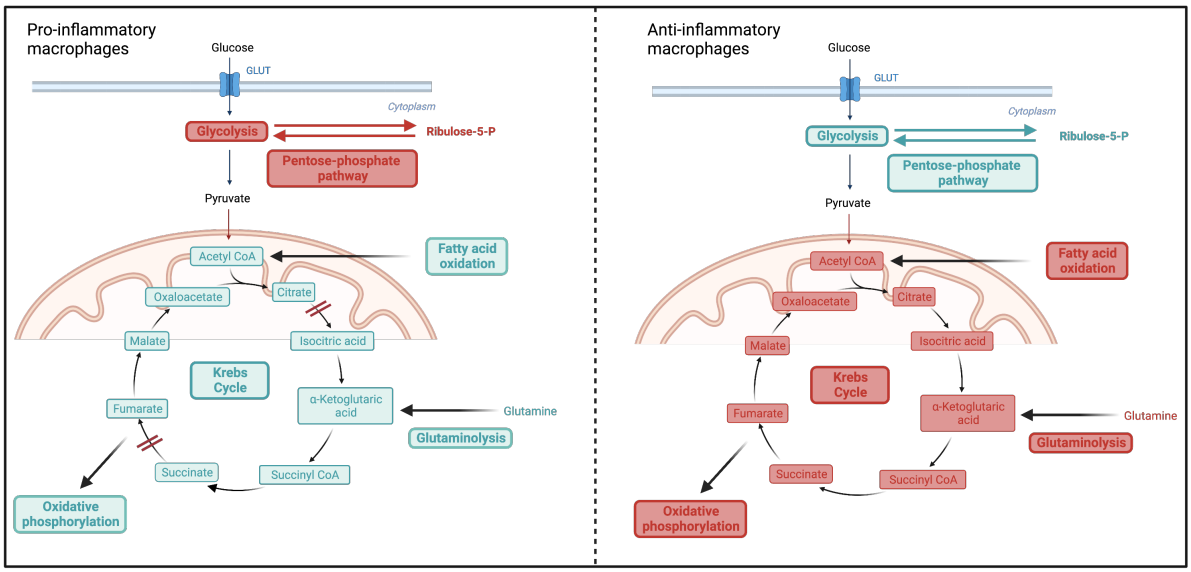

Figure 1.3 Metabolism of pro-inflammatory and anti-inflammatory macrophages. Glucose is transported into the cell via glucose transporters (GLUT) and converted into pyruvate in the process of glycolysis. Proinflammatory macrophages (left) express increased glycolysis and pentose-phosphate pathways (in red), while they possess 2 breaks in Krebs cycle (after citrate and succinate), which reduces its efficiency (in blue). Anti-inflammatory macrophages (right) prefer Krebs cycle and oxidative phosphorylation (red) over glycolysis and pentose-phosphate pathway (blue). Created in BioRender - figure adapted from Sadiku & Walmsley, 2019.

1.1.3 Dendritic cell precursors

DCs are the most important antigen-presenting cells in our immune system and connect innate immunity to adaptive. DCs are relatively rare and only comprise less than 1% of circulating PBMCs (Hoeffel et al., 2012). Similarly to monocytes and macrophages, DCs have a series of pattern recognition receptors on their surface, which allows for their quick response to pathogens or damaged cells (Mirjam & Broos, 2019). They originate from pluripotent hematopoietic stem cells in bone marrow and can differentiate either from a myeloid precursor (same

precursor as for monocytes, and macrophages) or from lymphoid precursors (figure 1.1), however their phenotypes and location differ (Zanna et al., 2021).

DCs are divided into several groups, namely steady-state DCs, inflammatory DCs, and Langerhans cells (LCs). Steady-state DCs can further be divided into classical (conventional or myeloid) DCs (cDCs) and plasmacytoid DCs (pDCs). These subtypes are rich in major histocompatibility complex II (MHC II; needed for the activation of antigen-specific immune response) and lack most of monocyte, T cell, B cell or NK cell markers (Balan et al., 2019). The pDC subset is characterised by high production of anti-inflammatory interferon type I during an infection, while cDCs promote naïve T cell activation, which can respond to new pathogens and trigger immune response (Balan et al., 2019; Granot et al., 2017). In addition, cDCs also express CD11c, which is necessary for osteoclast differentiation, however this receptor is absent in pDCs (Ansalone et al., 2021). Inflammatory subsets are only present during inflammation (e.g., RA) and are monocyte-derived (either classical or non-classical monocytes) (Balan et al., 2019). LCs are a special DC subset in skin epidermis and have an embryonic origin. They are the first form of defence against infections and have a capacity to self-renew (Hoeffel et al., 2012).

DCs can also be divided based on their location into blood DCs (cDCs or pDCs), or by the location in the tissue into lymphoid resident or migratory DCs. The migratory DCs migrate from peripheral tissue, where they collect antigen, to lymph nodes, where the antigen is presented to T cells. The resident DCs capture antigen in the lymphoid organs either directly or receive it from other cells like migratory DCs (Radford et al., 2014). Lastly, DCs can be mature, or immature based on the expression of their phenotype markers, from which only immature DCs (pre-DCs) can differentiate into osteoclasts (Ansalone et al., 2021; Balan et al., 2019).

1.2 Osteoimmunology

Bone is a mineralised living connective tissue composed of 4 cell types, namely osteoblasts, osteocytes, osteoclasts, and bone lining cells. The role of a bone is to protect or support inner organs and soft tissues, to gather calcium and phosphate, and to store bone marrow (Florencio-Silva et al., 2015). Bones are very

dynamic and bone modelling and remodelling are essential processes during growth or injuries when the bone changes shape and size (modelling) or in order to maintain strength and mineral homeostasis (remodelling). In bone remodelling, old bone is removed (by osteoclasts) and replaced by new bone (by osteoblasts) at the same ratio which takes approximately 2-3 weeks (Katsimbri, 2017). The disruption in the balance of osteoclasts and osteoblasts can, however, lead to various bone diseases like osteoporosis (lack of bone-formation) or osteopetrosis (too much bone formation and lack of bone resorption).

1.2.1 Osteoblasts and bone-lining cells

Osteoblasts are mononuclear cells formed from mesenchymal stem cells. They are found on the bone surface and are responsible for the formation of new bone. Osteoblasts form bone matrix by producing osteoid (non-mineralised bone), which is mostly composed of type I collagen (90%), proteoglycans, proteins and growth factors. Osteoid is then mineralised via calcification facilitated by matrix vesicles released from osteoblasts (Florencio-Silva et al., 2015). Matrix vesicles contain calcium and phosphate ions which then interact together forming hydroxyapatite crystals via nucleation. This causes the vesicle to break, and the crystals are spread throughout the osteoid, binding organic material and proteoglycans, thus mineralising the matrix and forming the new bone (Anderson, 2003).

After osteoblasts produce new mineralised bone, they can either become quiescent and transform into bone-lining cells, undergo apoptosis, become chondroids (cartilage-like structure), or become osteocytes. The ratio of the transformation varies, however, the majority of osteoblasts (65%) undergoes apoptosis. Once osteoblasts get embedded in the osteoid (either by themselves or by the surrounding cells), they become osteocytes (Franz-Odendaal et al., 2005). When osteoblasts do not differentiate into osteocytes or undergo apoptosis, it is believed that they become bone-lining cells, which are flat, long, thin, quiescent cells found on the bone surface (Karsdal et al., 2002).

Bone-lining cells act as important players in bone remodelling and contribute to the bone tissue repair. In contrast with osteoblasts, they do not contain osteocalcin, which is necessary for bone formation (Everts et al., 2002). When they are not activated, they do not contribute to either bone resorption or bone

formation. However, after the contact with osteocytes embedded in bone matrix (after a mechanical stress, microcracks, or microfractures in bone), bone-lining cells can produce receptor activator of nuclear factor kappa B (NF-κB) ligand (RANKL) and activate RANK receptor on osteoclast precursors. This then leads to osteoclastogenesis and bone resorption, which can then be repaired by new bone formation. When bone resorption is no longer needed, bone lining cells start producing osteoprotegerin (OPG) that blocks osteoclast differentiation (Florencio-Silva et al., 2015; Matsuo & Irie, 2008). Additionally, it has been shown that quiescent bone-lining cells also have the ability to de-differentiate back into mature osteoblasts when bone formation is necessary and during healthy bone turnover in adults (Matic et al., 2016; Sawa et al., 2019).

1.2.2 Osteocytes

Osteocytes are the most abundant cells in bone (90-95% of cells) and can live up to 25 years (Franz-Odendaal et al., 2005). Osteoblasts comprise approximately 4-6% while osteoclasts form only 1-2% of bone cells (Schaffler & Kennedy, 2012). Osteocytes have a DC-like shape and can be found in mineralised bone matrix. They are also mechanosensory cells, which gives them the ability to sense mechanical changes, deformation and fluid movement (e.g., weight-bearing, physical exercise, load or pressure) in the bone, respond to the local or systemic stimuli by generating biochemical signals, and control bone remodelling. They do this thanks to their interconnected network via which they communicate between each other and the bone surface (Rochefort et al., 2010; Florencio-Silva et al., 2015) (figure 1.4). They can then adapt the bone to mechanical stress via bone remodelling and replace the bone if it undergoes any impairment from recurring mechanical load or injuries.

After osteoblasts become osteocytes, some of the osteoblast markers (alkaline phosphatase, osteocalcin and type I collagen) are downregulated/lost, while osteocyte markers (CD44 marker, or sclerostin, which inhibits osteoblast differentiation) are upregulated (Capulli et al., 2014; Huang, 2007; Miron & Zhang, 2012). They also highly express dentin matrix protein (DMPI) and matrix extracellular phosphoglycoprotein (MEPE), which are necessary for bone mineralisation, where MEPE inhibits and DMPI enhances mineralisation of extracellular matrix (Santos et al., 2009; Schaffler & Kennedy, 2012).

It has also been found that osteocytes can release OPG and RANKL, therefore can contribute to the regulation of new bone formation and bone-resorption (Goldring, 2015). However, these cells are understudied due to difficulty of including them in *in vitro* assays, therefore, their full potential is still not fully understood. Moreover, when osteocytes reduce sclerostin production, e.g., during mechanical stress, osteoblasts start to form new bone (figure 1.4). Additionally, mechanical load upregulates the expression of prostaglandin E2 (PGE2), Prostaglandin I2 (PGI2), nitric oxide (NO) and insulin-like growth factor 1 (IGF-1), which are also responsible for bone formation by osteoblasts, however when mechanical load decreases or is no longer present, these factors are downregulated and osteoblast inhibitors (e.g., sclerostin) are upregulated (Schaffler & Kennedy, 2012).

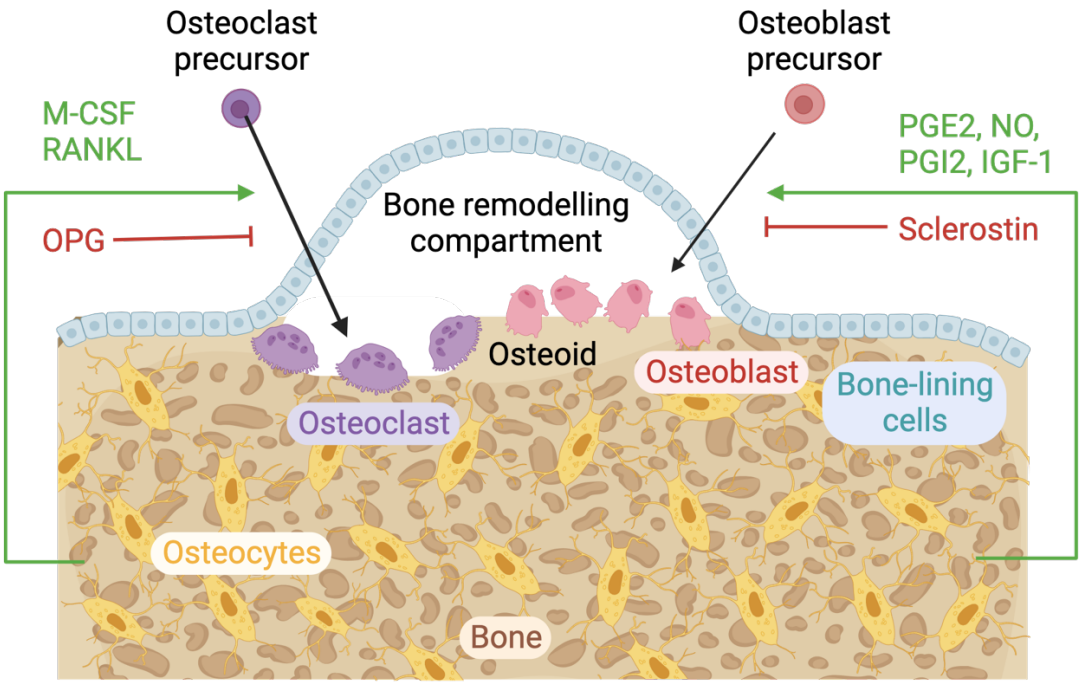

Figure 1.4 Bone remodelling.
Osteoclasts resorb old bone, which is replaced by new bone formed by osteoblasts, while bone-lining cells form the outer area of bone-remodelling compartment and can be activated and differentiate into osteoblasts. Osteocytes can regulate bone-resorption by the release of monocyte/macrophage colony-stimulating factor (M-CSF) and RANKL, and bone formation by prostaglandin E2 and I2 (PGE2, PGI2, respectively), NO and IGF-1. Additionally, they can release OPG and sclerostin for osteoclast and osteoblast inhibition, respectively. Created in BioRender - figure adapted from Gasser & Kneissel, 2017; Salhotra et al., 2020.

1.2.3 Osteoclasts and their precursors

Osteoclasts are multinucleated (3 or more nuclei), bone-resorbing cells responsible for the normal physiological bone remodelling. Unlike osteoblasts, osteocytes, and bone-lining cells, which are derived from mesenchymal stem

cells, osteoclasts are of hematopoietic origin and are created by fusion of their mononuclear precursors like monocytes, macrophages, or pre-DCs (Muto et al., 2011; Bhagavatham et al., 2021; Wang et al., 2021; Parvizi and Kim, 2010). Notably, previous studies reported that only pure immature $CD11c^+$ DCs with $MHCII^{low}$ $CD80^-$ $CD86^-$ phenotype can be differentiate into osteoclasts, both *in vitro* and *in vivo*, where their differentiation potential is lost after maturation (Alnaeeli & Teng, 2009). Therefore, only the cDCs subset with $CD14^-CD16^-CD11c^+$ phenotype can be successfully differentiated into osteoclasts, with a comparable differentiation rate as for $CD14^+$ monocytes, because pDCs are $CD11c^-$ (Ansalone et al., 2021).

It has also been shown that even though both classical and intermediate monocytes can differentiate into osteoclasts, the bone-resorbing activity of these osteoclasts differs. Osteoclasts from classical monocytes can resorb bone most efficiently, while osteoclasts differentiated from intermediate monocytes resorb bone to a lower extent. Under inflammatory conditions (e.g., IL-17), however, intermediate monocyte-derived osteoclasts showed enhanced efficiency in bone resorption, while the resorption activity of classical osteoclasts remained the same (Vuoti et al., 2023). In contrast, non-classical monocytes were believed to be incapable of differentiating into osteoclasts, however, in 2023 Vuoti el al. reported that non-classical monocytes can differentiate into osteoclasts, but they are not able to resorb bone (figure 1.5).

Additionally, it is believed that classical monocytes are the main source of osteoclasts, while intermediate monoctytes are mainly responsible for the production of pro-inflammatory cytokines. In the terms of RA, however, intermediate monocytes are the most abundant and can migrate to RA synovium, where they can produce pro-inflammatory cytokines like TNF, IL-1 or IL-6. This could further contribute to higher production of IL-17, thus, to enhanced formation of osteoclasts from $CD14^+$ monocytes (Xue et al., 2020; Komano et al., 2006).

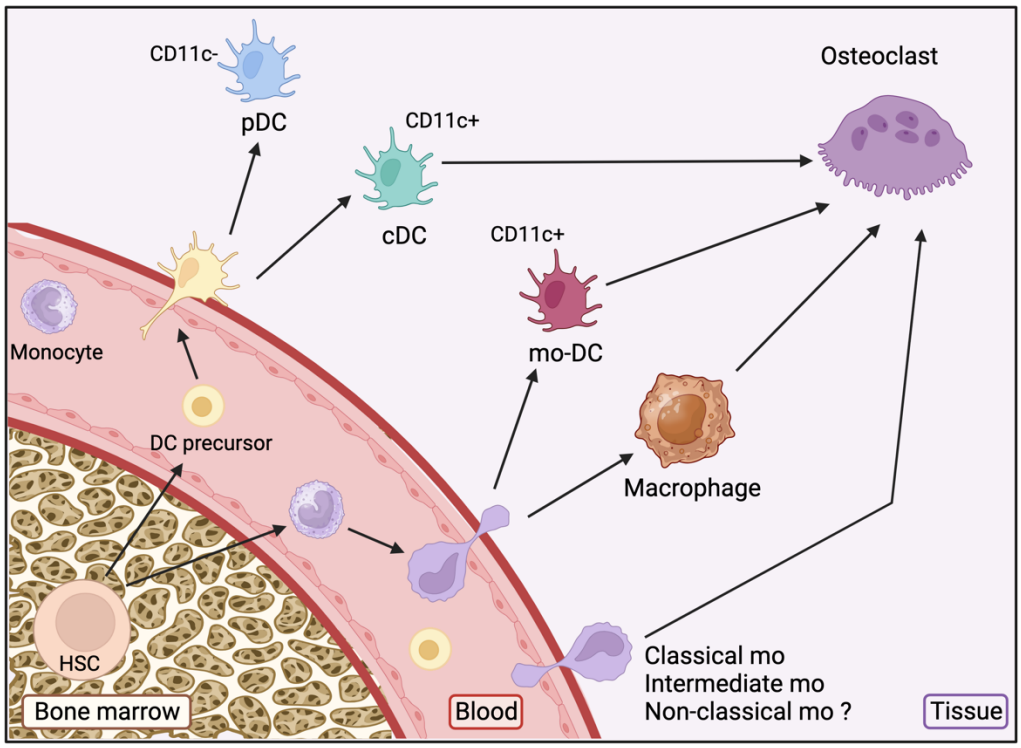

Figure 1.5 Osteoclast differentiation from its precursors.
Differentiation of mature osteoclasts from their precursors originating from hematopoietic stem cells (HSC), namely classical and intermediate monocytes (mo), macrophages, monocyte-derived dendritic cells (mo-DC), and conventional DCs (cDCs). Plasmacytoid DCs (pDCs) cannot be differentiated into osteoclasts as they lack CD11c marker. The differentiation into osteoclasts from non-classical monocytes could be possible but it is not well explored. Created in BioRender.

1.2.3.1 Osteoclast differentiation

In RA, the balance between osteoclasts and osteoblasts is tipped towards osteoclasts, which results in bone resorption (Feng and Teitelbaum, 2013). The two most important cytokines involved in osteoclastogenesis are monocyte/macrophage colony-stimulating factor (M-CSF, also known as CSF-1) and RANKL.

M-CSF is secreted by a variety of cells such as osteoblasts, monocytes, synovial fibroblasts, T cells and macrophages (Dai and Stanley, 2003; Fleetwood et al., 2016). It is a key growth factor responsible for the development of macrophages (Markey and Hill, 2017). It binds and acts through its tyrosine kinase colony stimulating factor-1 receptor c-fms (also known as CSF-1R & CD115), promoting not only monocyte differentiation, but also their proliferation and survival (Teitelbaum, S., 2007). It also plays a role in lysosome formation and function, which is important in the bone resorption process (Kimura et al., 2015; Lacombe et al., 2013).

RANKL also known as TRANCE (TNF-related activation-induced cytokine) is a cytokine belonging to the TNF superfamily (Silva and Bilezikian, 2015), and is expressed by T cells, synovial cells, osteocytes, and osteoblasts (Boyce and Xing, 2008). RANKL can be found as a membrane-bound protein or can be released by the cells. It interacts with the RANK receptor, expressed on osteoclast precursors, osteoclasts, pre-DCs and cancer cells, and plays an important role in osteoclastogenesis (Boyce and Xing, 2008; Fata et al., 2000; Ito and Hata, 2004; Park et al., 2017; Thomas et al., 1999). In comparison to M-CSF, which controls monocyte proliferation and survival, RANKL is directly responsible for differentiation of osteoclast precursors (Faccio et al., 2011). Additionally, RANK competes for RANKL with a soluble decoy receptor OPG, secreted by osteoblasts. OPG prevents RANKL from binding its receptor, which leads to the inhibition of osteoclastogenesis (Pettit et al., 2001).

Apart from RANKL and M-CSF, which are both essential for osteoclastogenesis, several other pro- and anti-inflammatory cytokines can exhibit stimulatory or inhibitory effects on osteoclastogenesis. In chronic inflammatory diseases, pro-inflammatory cytokines such as TNF and IL-1 can stimulate the osteoclastogenic process. They do it by inhibiting maturation and differentiation of osteoblasts, inducing their apoptosis, and regulating RANKL and OPG release, which results in articular bone erosion and inflammation in RA (Baum & Gravallese, 2013; Boyce & Xing, 2007; Feng & Teitelbaum, 2013; Silva and Bilezikian, 2015). When inflammation occurs and synovial fluid is inflamed, activated macrophages and leukocytes infiltrate the affected joint. This infiltration further contributes to the release of more pro-inflammatory cytokines such as TNF, IL-1, IL-6, IL-17 and growth factors like M-CSF. As a result, this can impair bone remodelling and lead to bone damage (Karmakar et al., 2010).

1.2.3.1.1 Osteoclast differentiation under inflammatory conditions

TNF is the key pro-inflammatory cytokine stimulating inflammation in RA. Besides it being a contributing factor for chronic inflammation, it also contributes to pathological bone resorption (Jang et al., 2021). This has also been shown in transgenic mice that overexpress TNF, where mice develop arthritis very similar to human disease (Keffer et al., 1991; Zhao et al., 2015). TNF is released by

activated macrophages, T-cells and NK cells, playing a role in various autoimmune and inflammatory conditions, where it can activate several inflammatory molecules (i.e., cytokines and chemokines) (Jang et al., 2021). TNF has an impact on bone resorption and metabolism via its direct actions on the differentiation of tartrate-resistant acid phosphatase (TRAP) positive osteoclasts from osteoclast precursors. TNF can increase osteoclast differentiation by the activation of osteoblasts and tissue stromal cells, which further release RANKL or through the upregulation of M-CSF and RANKL receptors on osteoclast precursors (Amarasekara et al., 2018; Zhao et al., 2015). TNF also increases the secretion of IL-34 via activation of JAK and NF-κB in RA synovial cells, resulting in enhanced osteoclastogenesis (Amarasekara et al., 2018). Additionally, TNF can promote osteoclastogenesis in synergy with RANKL and other cytokines like IL-6 but is unable to cause osteoclast differentiation in the absence of RANKL (Zhao et al., 2012). In contrast, when monocytes are stimulated with TNF and RANKL *in vitro* early in the differentiation process (<24h), it leads to osteoclast inhibition, showing a dual role of TNF in osteoclastogenesis. The mechanism of early stimulation with TNF is driven via tumour necrosis factor receptor 1 (TNFR1), which activates canonical NF-κB pathway resulting in osteoclast inhibition, while the TNF addition later in the process to osteoclast precursors stimulated with RANKL acts via tumour necrosis factor receptor 2 (TNFR2) activating non-canonical NF-κB pathway leading to an enhancement of osteoclasts. Interestingly, it has also been shown that $CD11c^+$ DC precursors do not respond to TNF in the same way as $CD14^+$ monocytes, which is most likely due to the lower expression of TNFR1 receptor (Ansalone et al., 2021).

Apart from TNF, other pro-inflammatory cytokines were also shown to induce osteoclast differentiation, like IL-1, IL-6, IL-7, IL-8, IL-11, IL-15, IL-17, IL-23 or IL-34, however the presence of RANKL is required in most cases. These cytokines lead to osteoclastogenesis indirectly by upregulating the expression of RANKL and other pro-inflammatory cytokines. Apart from these cytokines, chemokines like CXCL8, CXCL9, CXCL10 and CCL20 also play a role in osteoclastogenesis by enhancing the release of IL-6, RANKL, or TNF (Amarasekara et al., 2018).

1.2.3.2 The process of bone resorption

After the contact of osteoclasts with extracellular mineralised matrix, actin cytoskeleton in osteoclasts gets rearranged and F-actin ring forms continuous dense dynamic podosomes. This allows osteoclasts to attach via vitronectin, osteopontin, or sialoprotein (bone proteins) on the bone surface through their surface integrins (e.g. integrin $\alpha_V\beta_3$) and CD44 adhesion molecule (Feher, 2017; Silva and Bilezikian, 2015). After the attachment of osteoclasts, a ruffled border, which is a membrane formed by microvilli, is created. The ruffled border then separates area that is going to be resorbed from the surrounding tissue by a sealing zone, which comprises of an actin ring and other proteins. Osteoclasts can resorb bone via the use of a vacuolar proton/protein pump known as V-ATPase, which can create an acidic environment within the ruffled border boundaries and solubilise hydroxyapatite crystals in bone (Silva and Bilezikian, 2015). The next step of bone resorption is the release of degrading enzymes such as cathepsin k, TRAP, and metalloproteinases (MMPs), which are transported to the resorption area under the sealing zone; also known as Howship's lacunae (Bolamperti et al., 2022).

During the resorption process, resorbed material from bone matrix degradation is continuously endocytosed by osteoclasts and transported through the cell to the opposite side, where they are exocytosed via the secretory domain found at the top part of basolateral membrane of osteoclasts (figure 1.6). This ensures that osteoclasts are firmly attached to the bone matrix throughout the whole process of bone resorption (Bolamperti et al., 2022). Once bone resorption is completed, osteoclasts can either undergo an apoptosis or de-differentiate into their daughter cells called osteomorphs (once RANKL is inhibited). Osteomorphs stay in the bone marrow nearby the resorption area and are ready to fuse back together and recycle back into functional mature osteoclasts (McDonald et al., 2021).

Similarly, in cell cultures mature osteoclasts usually live only between 2-4 days after the stimulation with RANKL and fusion of their precursors. These multinucleated mature osteoclasts then die, usually by undergoing apoptosis. However, after osteoclasts undergo apoptosis, they are renewed by fusion of other pre-osteoclasts or by incomplete cytokinesis to form new mature osteoclasts (Takegahara et al., 2016). Notably, osteoclast cell cultures will never have all the

cells differentiated into mature osteoclasts, and there will always be some mononuclear cells that are unable to differentiate (Akchurin et al., 2008; Cappariello et al., 2014).

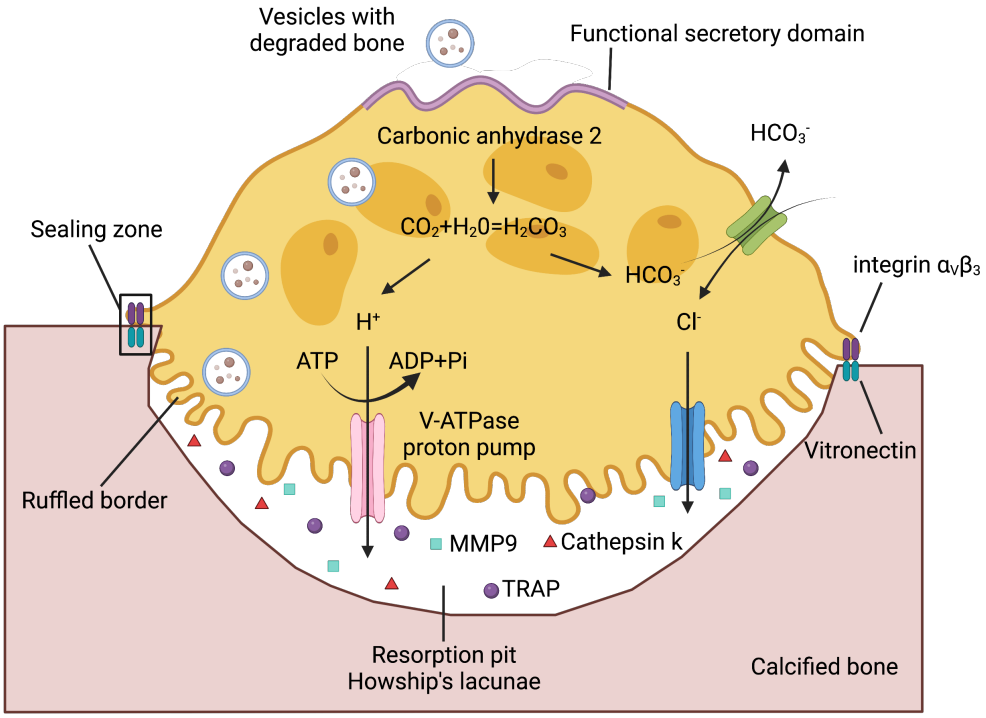

Figure 1.6 Osteoclastogenic bone resorption process.
Osteoclast attaches to vitronectin present on the calcified bone via its receptor (integrin $\alpha_V\beta_3$) creating a sealing zone, which separates resorption pit from the surrounding area. Calcified bone is then resorbed via various enzymes cathepsin k, TRAP, and MMPs, and acids and resorbed bone is transported in vesicles through the osteoclast's functional secretory domain. Created in BioRender - adapted from Cappariello et al., 2014.

1.3 Rheumatoid arthritis

1.3.1 Pathophysiology of the disease

RA is an autoimmune disease characterised by chronic inflammation of the synovium, with subsequent bone and cartilage destruction (Tsukasaki and Takayanagi, 2019). The cells responsible for bone loss in RA are bone-resorbing osteoclasts. Importantly, these cells are essential in the normal physiological bone remodelling process, which in order to maintain skeletal health remove old bone via degradation and replace it through osteoblast-driven mineralisation (Feng and Teitelbaum, 2013). Bone remodelling is a highly regulated process, where the ratio of osteoclasts to osteoblasts has to be optimal. Perturbation of normal homeostasis, with a dominance of osteoclasts, can lead to various disease-

associated bone pathologies, e.g., RA or metastatic cancer (figure 1.7) (Feng and Teitelbaum, 2013).

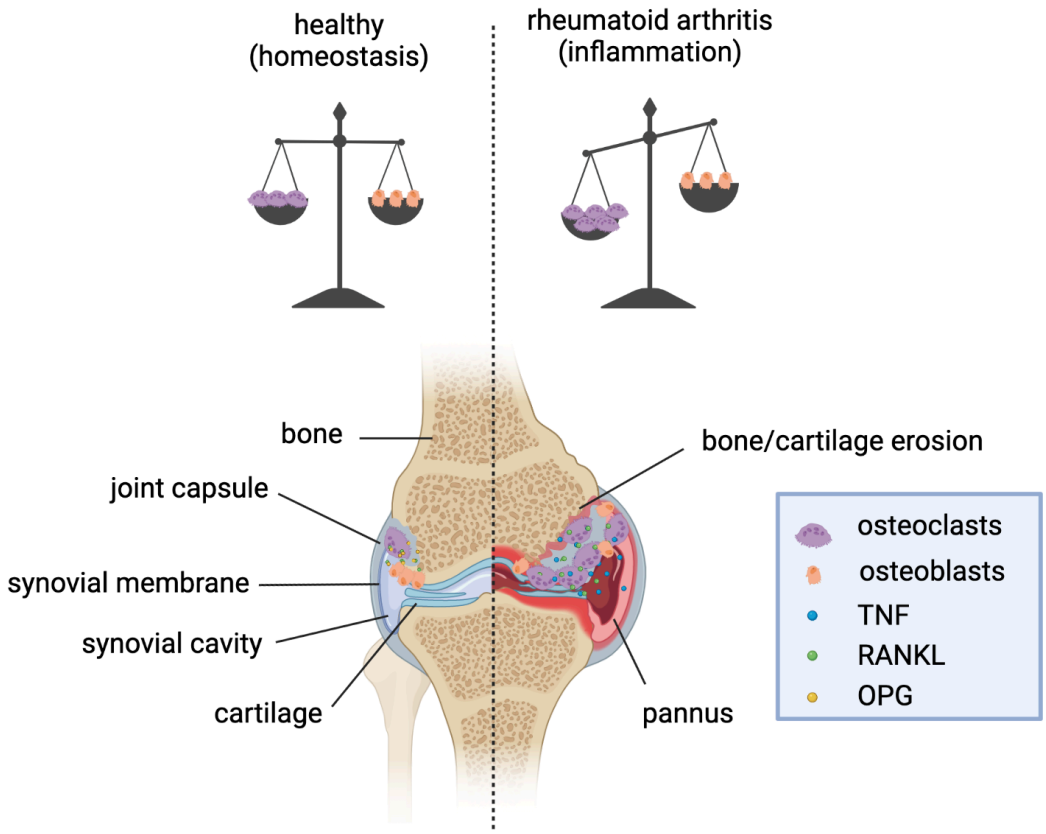

Figure 1.7 Pathophysiology of RA.
In health, osteoclasts and osteoblasts are in balance to maintain homeostasis and healthy bone remodelling, however, in RA, this balance is disrupted, which leads to higher osteoclast numbers, thus higher degree of bone resorption. The difference between healthy (left) and inflamed joint with visible pannus formation (right) involving higher concentration of various pro-inflammatory cytokines (e.g. TNF), higher RANKL and lower OPG production, which leads to more osteoclasts, which all contribute to enhanced bone resorption and chronic inflammation (right). Created in BioRender.

RA has a prevalence of 1% and can affect individuals of all ethnic groups and ages, with the highest occurrence in the geriatric population. It is more common in women than in men (approximately 3:1), which could be due to genetic factors (X-linked) and hormones (e.g., estrogen, progesterone) (O'Brien et al., 2007; van Vollenhoven, 2009; van Vollenhoven and McGuire, 1994). In general, RA tends to improve during pregnancy, as higher levels of prolactin are produced, which has been shown to have an effect on the immune system. Enhanced prolactin levels can lead to improved RA symptoms and reduced DAS, while progesterone can supress the immune system (van Vollenhoven and McGuire, 1994). RA can be seropositive (40-65% heritability) or seronegative (20% heritability), where

patients with seropositive RA have detectable autoantibodies against anti-citrullinated protein (ACPA) and/or antibodies against Fc part of immunoglobulin G (IgG) known as a rheumatoid factor (RF) (Nordberg et al., 2018; Smolen, et al., 2016). However, both genetic and environmental factors are known to contribute to the development of RA.

Genetic factors contributing to the development of RA are mostly class II major histocompatibility complex human leukocyte antigens (HLA-DR), mainly HLA-DRB1 gene and non-HLA genes such as protein tyrosine phosphatase non-receptor type 22 (PTPN22), which is the second biggest genetic contributor to RA (Kurkó et al., 2013). It was first discovered in 1976 that patients with RA share the identical HLA haplotype (Stastny, 1976). It was later identified that several alleles in HLA-DRB1 gene are highly associated with RA risk. They encode for molecules containing a conserved 5 amino acid sequence, known as the shared epitope, found on the MHC class II antigen-binding site. It has also been observed that HLA-DRB1 gene aids in ACPA antibodies development and therefore to ACPA positive RA (Viatte et al., 2013). Environmental factors contributing to the RA development include smoking (associated with a higher risk of development of ACPA positive and not ACPA negative RA), vitamin D deficiency, red meat digestion, bacterial and viral infections, air pollution and silica (Liao et al., 2009; Edwards and Cooper, 2006; Stolt et al.,2005).

1.3.2 Diagnosis of RA

There is no single test that could determine RA, therefore diagnosis is generally based on clinical presentation. Thus, evaluation of disease revolves around classification criteria from the American College of Rheumatology (ACR) and the European League against rheumatism (EULAR). These criteria help to distinguish RA from other forms of arthritis (table 1.1) (Tanaka, 2020). After the doctor's examination and medical history, laboratory tests are performed, which gives information on C-reactive protein (CRP) and erythrocyte sedimentation rate (ESR). Both of these factors are strongly correlated with the disease severity and radiography changes. RF and ACPA are also essential for the disease diagnosis and increase the specificity of the diagnosis. Synovitis (inflamed synovium tissue) is another sign of early RA and can lead to bone erosion (Heidari, 2011). To diagnose RA progression, imaging can be used, as it monitors narrowing of joint space or

bone erosion. Radiography is usually not as reliable, therefore, sonography or MRI can be used for more precise techniques (Wakefield et al., 2000).

ACR/EULAR scoring system serves as a guideline for clinicians to help distinguish between non-RA or destructive RA. If the score is 6 or higher, the patient is diagnosed with RA and is prescribed treatment (Taylor, 2020). There are several scoring systems to assess the DAS, from which DAS28 is the most commonly used. DAS28 takes into account swelling and tenderness of specific joints (28 joints), together with other factors like 1-hour ESR (CRP can be assessed as an alternative), and the physician's, as well as patient's assessment of the disease activity, which is then used for the calculation of DAS with a specific formula (Gossec, 2018). When DAS28 is <2.6, it is classified as remission, <3.2 is low disease activity, 3.2-5.1 is moderate disease activity, and the score above 5.1 is high disease activity (Gossec, 2018; Tanaka, 2020).

Table 1.1 ACR/EULAR classification criteria for RA diagnosis
RF – Rheumatoid Factor, ACPA – Anti-Citrullinated Protein Antibodies, CRP – C-Reactive Protein, ESR – Erythrocyte Sedimentation Rate (Taylor, 2020)

Joint distribution (0-5)	
1 large joint	0
2-10 large joints	1
1-3 small joints (large joints not counted)	2
4-10 small joints (large joints not counted)	3
>10 joints (at least 1 small joint)	5
Serology (0-3)	
Negative RF and negative ACPA	0
Low positive RF or low positive ACPA	2
High positive RF or high positive ACPA	3
Symptom duration (0-1)	
<6 weeks	0
≥6 weeks	1
Acute phase reactants (0-1)	
Normal CRP and normal ESR	0
Abnormal CRP or abnormal ESR	1

1.3.3 RA treatment

Currently, there is no cure for RA, however several treatments are used to reduce symptoms such as inflammation, swelling and pain. Most of the treatments are focused on diminishing inflammation but it is also important for patients with RA to exercise daily (mostly swimming, yoga) to improve the disease outcome (Bullock et al., 2018). It has also been noted that supplementation with fish oil, calcium with vitamin D, and folic acid can reduce side effects, slow down the disease progression and relieve pain. Vitamin D deficiency is quite common in patients with RA and this has been associated with an increased risk of severe RA or osteoporosis (Kostoglou-Athanassiou et al., 2012). Fish oil supplementation triggers the production of SPMs and has been recommended for patients with RA. SPMs have been shown to improve pain, reduce the number of tender joints, and decrease IL-1 and IL-6 levels. Furthermore, some patients were able to stop routine treatment with non-steroidal anti-inflammatory drugs (NSAIDs) without any further complications after taking these supplements (Kremer et al., 1995).

NSAIDs, together with corticosteroids, are the most common form of treatment for RA. NSAIDs work by blocking the cyclooxygenase (COX) pathway (promotes production of prostaglandins causing bone resorption), either non-selectively (acetylsalicate (Aspirin), ibuprofen) or selectively (celecoxib (Celebrex)), which has less adverse side effects (Bullock et al., 2018; Hadjicharalambous et al., 2021). Corticosteroids appear to be slightly more effective, however, they tend to have more side effects (e.g. immunosuppression, diabetes, bone thinning, bone loss) than NSAIDs and therefore these treatments should only be used temporarily for a short period of time (<6 months) (Bullock et al., 2018). They reduce inflammation by activating some of anti-inflammatory genes and by enhancing the degradation of mRNA which encodes inflammatory proteins, thus switching them off (Barnes, 2009).

The second-line treatments for RA include disease modifying antirheumatic drugs (DMARDs), which are used for slowing down the progression of the disease and joint destruction, and they are known to reduce the expression of bone resorption markers (Combe et al., 2016). They are divided into 3 groups, namely conventional, biological, and targeted synthetic DMARDs (Smolen et al., 2010;

Chatzidionysiou et al., 2017). DMARDs can either be used as a monotherapy or in a combination with corticosteroids or most often with other DMARDs, mainly methotrexate (MTX) (Smolen et al., 2010).

Conventional DMARDs (cDMARDs) include MTX, sulfasalazine (SSZ) or hydroxychloroquine (HCQ) and work by supressing the immune system. MTX was originally developed as an anti-cancer drug for acute leukaemia. It was later discovered that lower doses of MTX are effective for RA treatment and thus MTX is nowadays considered an anchor drug and used as the first DMARD for treating RA (Koźmiński et al., 2020). It is often advised to be used in combination with corticosteroids or other DMARDs (Köhler et al., 2019). MTX as an immunosuppressive drug acts on the metabolism of folic acid, and therefore folic acid supplements are generally proscribed to reduce this side effect (Shea et al., 2013). In general, less than 5% of patients have to terminate the treatment because of side effects. Unlike MTX, SSZ was specifically designed as an antirheumatic drug. It has antibacterial and anti-inflammatory effects and is usually prescribed to patients with intolerance to other DMARDs. It is also suitable during pregnancy, which is not possible with MTX (Köhler et al., 2019). It is relatively safe and is effective as a monotherapy or can be used in combination with other DMARDs (Amaral et al., 2016). HCQ is an antimalarial drug used in RA treatment, however, it is not as effective at inhibiting structural damage, as for example SSZ (Smolen et al., 2010). Additionally, HCQ, as well as MTX, manage to inhibit osteoclasts *in vitro* by supressing RANKL secretion, which further prevents bone erosion in RA (Carbone et al., 2020).

If patients are intolerant or unresponsive to cDMARDs, biological DMARDs (bDMARDs or biologics) can be introduced. They are administered by injection, either as an infusion or as self-injection every week or two (Scott, 2010). bDMARDs (e.g., adalimumab - a TNF inhibitor) are genetically engineered to mimic natural proteins of the immune system (e.g., monoclonal antibodies) and their target is more specific (Kornu et al., 2012). Some of the most common side effects of bDMARDs are an increased chance of infection (Scott, 2010). bDMARDs target and inhibit pro-inflammatory cytokines such as TNF, which is most widely used, IL-6 receptors, B cells and T cells. TNF inhibitors can work as neutralising antibodies (e.g., Infliximab) binding to a cytokine, preventing further binding to its receptor

or as a recombinant soluble receptor (e.g., Etanercept) binding to circulating cytokine preventing its binding to endogenous receptor (Rider et al., 2016). IL-6 and B cells are inhibited by recombinant monoclonal antibodies called tocilizumab and rituximab, respectively (Kester, et al, 2012). Interestingly, murine *in vivo* studies showed that anti-TNF therapy in combination with an anti-IL-6 antibody led to the reprogramming of bone-resorbing osteoclasts to non-resorbing osteoclasts (Matsuura et al., 2018). Similarly, anti-TNF with OPG reduced bone resorption in arthritic mice (Sakthiswary et al., 2022). Lastly, anti-TNF therapy (infliximab) in RA patients, led to higher levels of osteocalcin (protein released by osteoblasts to regenerate bone) and decreased bone erosion markers (Lange et al., 2005). Similarly to cDMARDs, the effect of bDMARDs is stronger when combined with other cDMARDs, most often MTX. The combined therapy could reduce the dose of MTX and bDMARDs, which could lead to lower toxicity, less adverse side effects, and enhanced immunological tolerance, thus reduce the chance of immune system developing antibodies against bDMARDs (Inui & Koike, 2016).

Lastly, targeted synthetic DMARDs block a particular pathway inside immune cells, and include baricitinib, and tofacitinib. These drugs are small molecules used to inhibit the intracellular Janus kinase (JAK) family enzymes, by blocking their signalling pathway, thus preventing a pro-inflammatory immune response in RA (Bullock et al., 2018; Smolen et al., 2016).

1.4 Specialised pro-resolving mediators

1.4.1 Specialised pro-resolving mediators and their receptors

As mentioned earlier, RA is a chronic inflammatory disease caused by unresolved inflammation (Cash, et al., 2014). In non-chronic inflammatory settings, acute inflammation is a natural response that protects the host from infections and ideally leads to resolution. This resolution is believed to be achieved in part by SPMs, which if harnessed appropriately could serve as potential therapeutics for RA (Arnardottir et al., 2016).

SPMs are a group of lipids, which are biosynthesized during the early stages of acute inflammation and subsequently in the resolution phase. They can be found in tissues, organs, condensates of exhaled breath, plasma, serum, lymph nodes or

in tears (Abdolmaleki et al., 2019; Serhan & Levy, 2018). They are produced by immune cells, such as monocytes, macrophages, and neutrophils or are biosynthesised by a transcellular interplay between e.g., neutrophils/macrophages and endothelial/epithelial cells (Chatterjee et al., 2017).

SPMs can be classified into 4 groups, namely lipoxins (LXs), resolvins (Rvs), protectins (PDs), and the most recently identified maresins (MaRs) (Serhan, 2014). They act via the activation of G-protein coupled receptors (GPCRs). Currently, there are 8 receptors identified, namely formyl peptide receptor 2 (FPR2), leukotriene B4 receptor (BLT1), chemerin receptor 23 (ChemR23), GPR37, Leucine-rich repeat-containing GPCR 6 (LGR6), GPR18, GPR32 and GPR101 (Bang et al., 2018; Flak et al., 2019; Hughes et al., 2021; Park et al., 2020). SPM receptors and their ligands are further discussed in chapter 3.

1.4.2 Biosynthesis of SPMs from fatty acids

1.4.2.1 SPM biosynthesis from omega-6 fatty acids

The process of SPMs biosynthesis can take many forms and can start with various fatty acids as the originating molecule. For instance, LXs, the first discovered SPMs with anti-inflammatory and pro-resolving effects, are biosynthesised from omega-6 fatty acid, more specifically arachidonic acid (AA) by macrophages and/or neutrophils with the help of lipoxygenase (LO) enzymes (Serhan, 2005). LXs can resolve inflammation via several mechanism. They prolong the lifespan of macrophages via the activation of PI3K and AKT pathways, control neutrophil levels by guiding them to the site of inflammation and further block their proliferation. They also modulate the secretion of pro-inflammatory cytokines (e.g., IL-8) and prevent tissue injury at the inflamed area (Sharma-walia & Chandrasekharan, 2015).

The process of biosynthesis from AA can take the form of oxygenation by 15-LO generating either 15S-hydroperoxyeicosatetraenoic acid (15S-HpETE) or 15S-hydroxyeicosatetraenoic acid (15S-HETE). These act as substrates for 5-LO, leading to the production of LXs with the help of hydrolases producing either LXA4 or LXB4. This process occurs either within the same cell type or transcellularly.

Alternatively, 5-LO (found in leukocytes) can generate leukotriene A4 (LTA4) hydrolase, which is transformed by 12-LO (found in platelets) into LXA4 and LXB4 (1:1 ratio). Notably, this mechanism relies on the interaction of neutrophils and platelets, which can uptake the secreted LTA4. Finally, it is possible for LXs to be produced when aspirin is present. This scenario results in COX-2 acetylation, producing 15R-HETE followed by 5-LO to create aspirin-triggered LXs (ATLs; also known as 15-epi LX or 15R-lipoxins) (Serhan, 2005). ATLs are formed in healthy humans taking low-dose aspirin, where they have anti-inflammatory effects, which can further lead to the resolution process (figure 1.8) (Recchiuti et al., 2019).

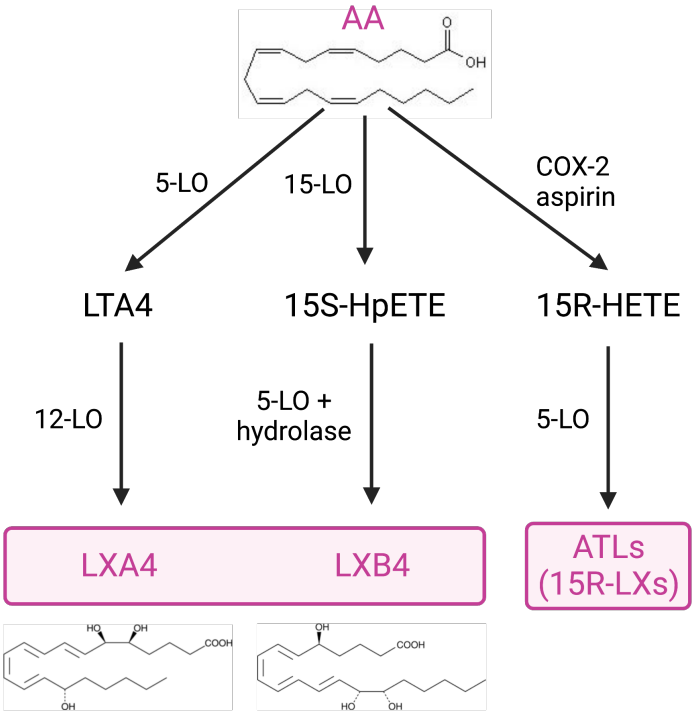

Figure 1.8 The mechanism of biosynthesis of lipoxins from arachidonic acid.
Arachidonic acid (AA) is converted into lipoxin A4 (LXA4) or lipoxin B4 (LXB4) from LTA4 or 15S-HpETE intermediates with a series of different lipoxygenases (LOs), or into aspirin-triggered lipoxins (ATLs), also known as 15R-LXs via 15R-HETE in the presence of aspirin. Created in BioRender.

1.4.2.2 SPM biosynthesis from omega-3 fatty acids

Unlike LXs, which are derived from omega-6 fatty acids, MaRs, PDs and Rvs are derived from omega-3 fatty acids. Once again there are multiple originating molecules that can be utilised for biosynthesis. In the case of MaRs, PDs, D-series Rvs (RvDs) and cysteinyl-SPMs (cys-SPMs), they are derived from docosahexaenoic acid (DHA). In comparison, E-series Rvs (RvEs) are biosynthesised from

eicosapentaenoic acid (EPA), whilst T-series Rvs (RvTs) and the n-3 DPA-derived SPMs are biosynthesised from docosapentanoic acid (DPA); discussed in more details below (Dyall et al., 2022; English et al., 2017; Serhan, 2014).

SPMs derived from EPA

Biosynthesis of SPMs from EPA leads to the production of RvEs. They have pro-resolving properties and can limit production of pro-inflammatory cytokines (e.g., IL-17, IL-23), prevent neutrophil and DC infiltration, or promote macrophage phagocytosis and efferocytosis (Serhan et al., 2022). The mechanism of biosynthesis for RvEs is very similar to LXs, where EPA is transformed by acetylated COX-2 or cytochrome P450 to 18R-hydro(peroxy)-eicosapentaeonic acid (18R-H(p)EPE), which is further converted by 5-LO into RvE1 and RvE2. If 18R-HEPE is converted by 12-LO or 15-LO, it gives rise to RvE3 (López-Vicario et al., 2016). For a long time, these were the only known RvEs, until a recent discovery in 2021 uncovered RvE4. Recent data suggest that RvE4 contributes to resolution of inflammation via an increase in efferocytosis of apoptotic cells by macrophages. RvE4 is biosynthesised from EPA by 15-LO to 15S-HpEPE, which can be further reduced to 15S-HEPE and converted to RvE4 by 5-LO or 15-LO (figure 1.9) (Libreros et al., 2021).

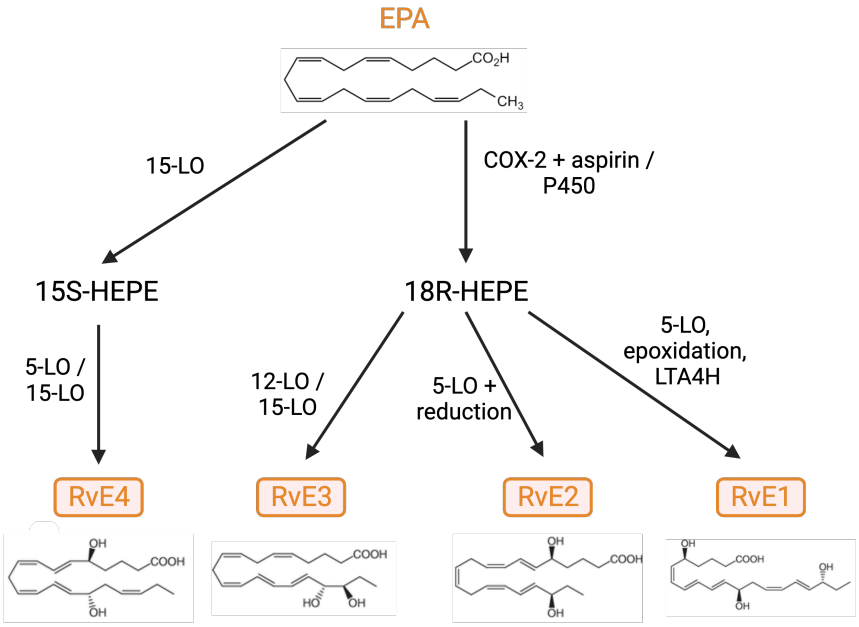

Figure 1.9 The mechanism of biosynthesis of E-series resolvins from eicosapentaenoic acid. Eicosapentaenoic acid (EPA) is converted into RvE1-RvE3 from 18R-HEPE in the presence of aspirin via COX-2 or cytochrome P450, or into RvE4 from 15S-HEPE with different lipoxygenases (LO). Created in BioRender.

SPMs derived from DPA

Another group of SPMs was recently discovered and is derived from DPA, which is an EPA intermediate and a precursor of DHA. These SPMs are either T-series (RvT1-RvT4; also called 13-series SPMs because of the addition of an alcohol group in the 13th position; Dalli, et al., 2015), or the n-3 DPA-derived SPMs, namely $RvD1_{n-3\ DPA}$, $RvD2_{n-3\ DPA}$, $RvD5_{n-3\ DPA}$, $MaR1_{n-3\ DPA}$, $MaR2_{n-3\ DPA}$, $MaR3_{n-3\ DPA}$, $PD1_{n-3\ DPA}$, $PD2_{n-3\ DPA}$ (Dubé et al., 2022).

RvTs have been shown to have protective properties in mice. Notably, they are able to protect mice from lethal doses of E.coli and serve as antibiotics alternatives, where they can also increase resolution of inflammation and increase survival of the mice (Dalli, et al., 2015). Additionally, RvTs, similarly to some other SPMs can reduce neutrophil extracellular traps (NETs) in human blood. NETs are produced by neutrophils (first cells to arrive to the site of infection) to trap pathogens, however, high number of NETs can lead to tissue damage. These SPMs can regulate NET formation and clearance, which can then be useful in infection and organ protection and can lead to resolution of inflammation without overt immunosuppression (Chiang et al., 2022). In RA, the administration of atorvastatin in humans or pravastatin in mice, upregulated the productions of RvTs, which was associated with a reduction in disease activity in RA, e.g., reduced joint inflammation and reduction in DAS (Walker, et al., 2017). For the biosynthesis of RvT1-RvT4, DPA is converted by COX-2 into 13*R*-hydroxy-docosapentaenoic acid (13R-HDPA) and further reduced into 7-hydroperoxy-13(R)-hydroxy-docosapentaenoic acid (7-Hp-13R-HDPA), which is further converted into RvT4 by reduction or into RvT2 and RvT3 by epoxidation. RvT4 can then be converted to RvT1 by 5-LO after the endothelial cell-neutrophil interaction (Rodriguez & Spur, 2020).

The n-3 DPA-derived SPMs have anti-inflammatory and protective effects in RA, cardiovascular diseases, or neurodegenerative diseases. Similarly to other SPMs, they regulate pro-inflammatory cytokines biosynthesis, modulate leukocyte recruitment and inflammation, and increase macrophage phagocytosis (Dalli et al., 2013). To form n-3 DPA Rvs, DPA is converted by 17-LO to 17-hydroperoxy-docosapentaenoic acid (17-HpDPA) and 5-LO to yield $RvD1_{n-3\ DPA}$, $RvD2_{n-3\ DPA}$, and $RvD5_{n-3\ DPA}$. 17-HpDPA can also be enzymatically converted to an epoxide

intermediate and further hydrolysed to $PD1_{n\text{-}3\ DPA}$, $PD2_{n\text{-}3\ DPA}$. Lastly, arachidonate 12-LO can convert DPA to 14S-hydroperoxy-docosapentaenoic acid (14S-HpDPA) that is then converted to an epoxide intermediate and further hydrolysed to form $MaR1_{n\text{-}3\ DPA}$ or $MaR2_{n\text{-}3\ DPA}$. Additionally, 14S-HpDPA can be oxidised to form $MaR3_{n\text{-}3\ DPA}$ (figure 1.10) (Dalli, et al., 2013).

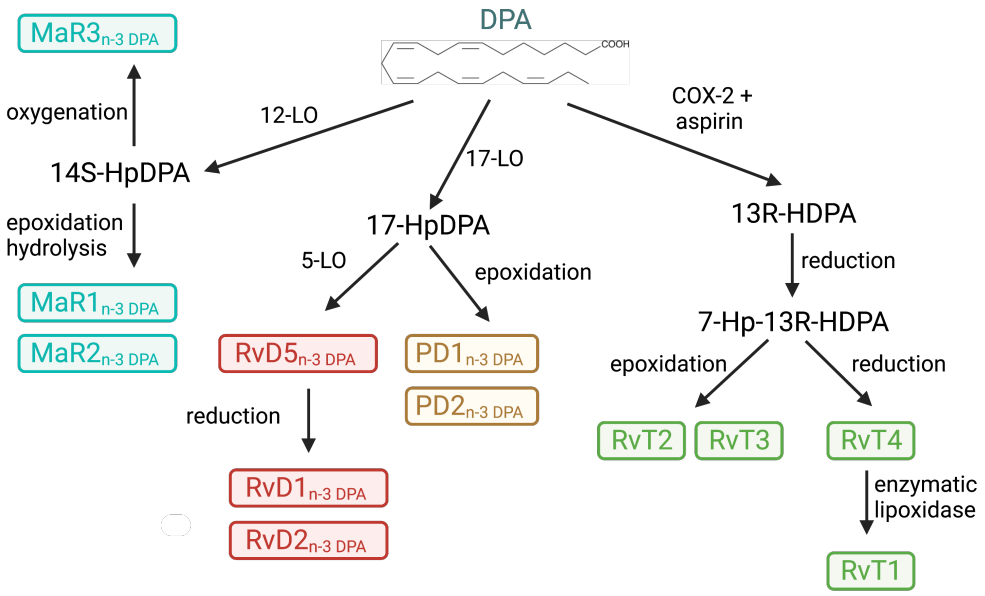

Figure 1.10 The mechanism of biosynthesis of n-3 DPA SPMs and T-series resolvins from docosapentaenoic acid.
Docosapentaenoic acid (DPA) is converted into T-series resolvins RvT1-RvT4 (green) via acetylated COX-2, while n-3 DPA SPMs are converted from DPA via 12-LO into $MaRs_{n\text{-}3\ DPA}$ (blue), or by 17-LO into $RvDs_{n\text{-}3\ DPA}$ (red) and $PDs_{n\text{-}3\ DPA}$ (light brown). Created in BioRender.

SPMs derived from DHA

As discussed in section 1.4.2.2, processing of DHA results in the biosynthesis of RvDs, MaRs and PDs, or neuroprotectins (nPDs) when biosynthesised in the neurvous system. RvDs have been shown to have stronger anti-inflammatory and pro-resolving effects than their precursors. They also exhibit neuroprotective actions, protect cells from injuries caused by oxidative stress, reduce pro-inflammatory actions via inhibition of NF- κB and IL-6, increase T-cell counts and can inhibit tumour growth (Ferreira et al., 2022). MaRs can promote resolution of acute inflammation and promote tissue regeneration, as well as enhance macrophage phagocytosis and efferocytosis, and reduce pro-inflammatory cytokines (TNF, IL-1, IL-6) (Hwang et al., 2019). PDs, apart from their anti-inflammatory and pro-resolving actions also show anti-apoptotic properties, limit neutrophil infiltration. Moreover, recent studies have demonstrated that PDs can

lower insulin resistance and inflammation in human primary adipocytes (Jung et al., 2018). Whereas, nPDs have been shown to protect human retinal pigment epithelium cells, human brain cells, and rat brain with ischemia-reperfusion from oxidative stress induced apoptosis, promote cell survival, and protect against ischemic injury (Bazan, 2006; Bazan, 2009; Mu et al., 2020).

D-series Rvs are generated from DHA either with 15-LO to form 17S-hydroperoxy-docosahexaenoic acid (17S-HpDHA), which is followed by 5-LO and peroxidases or by hydrolysis to form RvD1-D6. An alternative mechanism relies on the presence of acetylated COX-2 to form 17R-HpDHA, which is subsequently converted by 5-LO to aspirin-triggered Rvs (ATRvs; R-epimers). The conversion of DHA by 12-LO into 14S-HpDHA leads to the production of MaR1 and MaR2 with the help of a hydrolase or by epoxidation hydrolysis, respectively. When DHA is transformed by 15-LO into 17S-HpDHA, it can be further transformed with epoxidation hydrolysis into nPD1 and its isomer protectin DX (PDX; figure 1.11) (Balas et al., 2014).

Additionally, a new group of SPMs termed cys-SPMs consisting of SPM conjugates in tissue regeneration (CTR) has recently been identified. These macrophage-derived SPMs showed apart from pro-resolving properties also tissue-regenerative and tissue-protective actions in planaria (Chiang et al., 2021; Serhan et al., 2018). They include maresin, protectin and resolvin CTRs (MCTR, PCTR, RCTR, respectively), with each group consisting of 3 members, e.g., MCTR1, MCTR2, and MCTR3 (Chiang et al., 2021). The suggested role of cys-SPMs is to prevent tissue damage, remove bacteria and debris, and promote tissue regeneration (Serhan, et al., 2018). The biosynthesis is very similar to other SPMs from DHA, where for MCTR, DHA is converted by 12-LO into 14S-HpDHA and further into epoxide that is converted into MCTR1 by glutathione s-transferase mu4 (GSTM4) and by leukotriene C4 synthase (LTC4S). MCTR1 can then be converted by gamma-glutamyl transferase (GGT) into MCTR2, which can then be biosynthesised into MCTR3 by dipeptidase (DPEP). The process is similar for PCTRs and RCTRs, however, instead of MaR precursor 14S-HpDHA, PD1 precursor (16S,17S-epoxy-PD), and RvD1 and RvD2 precursor (7S(8)-epoxy-Rv) are used for the final step of the biosynthesis (figure 1.11) (de la Rosa et al., 2018; Recchiuti et al., 2019; Serhan, et al., 2018).

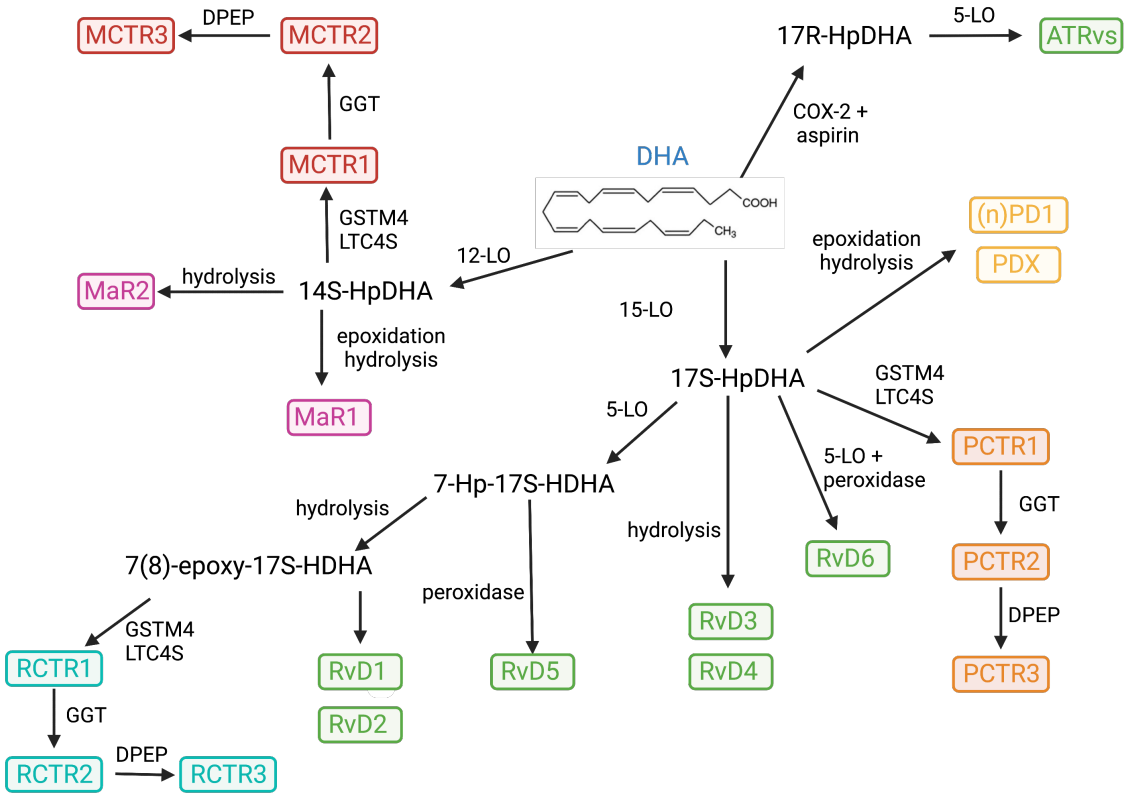

Figure 1.11 The mechanism of biosynthesis of D-seried resolvins, maresins, protectins, aspirin-triggered Rvs, and cys-SPMs from docosahexaenoic acid.
Docosahexaenoic acid (DHA) intermediate 17-S-HpDHA gives rise to D-seried SPMs (RvDs; RvD1-RvD6, green), protectins (PDs; PDX, (n)PD1, yellow), PD/Rv conjugates in tissue regeneration (PCTR, orange/RCTR, blue). Maresin (MaR) conjugates in tissue regeneration (MCTR, red) and MaRs (pink) are biosynthesised through 14S-HpDHA, while aspirin-triggered resolvins (ATRvs, green) are biosynthesised via COX-2 and aspirin. Created in BioRender.

1.4.3 SPMs in RA

As mentioned earlier, SPMs play an important role in inflammation resolution by their ability to limit the recruitment of PMNs, they promote efferocytosis, reduce pain, clear bacteria, protect tissue from neutrophil infiltration, block ROS, can counter-regulate pro-inflammatory cytokines and increase the production of anti-inflammatory cytokines (Funaki et al., 2018; Norling et al., 2016; Zetoune et al., 2014). SPMs have numerous positive properties when it comes to inflammation or tissue/cartilage repair, however, for the purpose of this thesis the focus will be on the actions of SPMs in RA.

There is only limited research about SPMs in the modulation of disease pathology and the vast majority of studies focused on processes involved in RA (e.g. osteoclastogenesis, bone resorption) were conducted in murine models or cell

lines. For example, in murine RA models, LXs have been shown to reduce joint oedema and inflammation, lower levels of pro-inflammatory cytokines, and reduce immune cell infiltration in murine zymosan-induced arthritis models when given intra-articularly either as a pre-treatment or post-treatment (Conte et al., 2010). LXA4 also blocked the IL-1 induced activation of human fibroblast-like synoviocytes *in vitro*, which are key cell types to promote inflammation and activation of immune cells in RA (Sodin-Semrl et al., 2004; Jaén, et al., 2021). In OA murine models, LXA4 reduced severity of OA symptoms like cartilage loss and proteoglycan reduction when administered to mice for 8 weeks one day after medical meniscus destabilisation surgery (Habouri et al., 2017).

Apart from LXA4, some other SPMs biosynthesised from omega-3 fatty acids were tested in the context of RA. MaR1 reduced arthritic clinical score, levels of pro-inflammatory cytokines (TNF, IL-1, IL-6) and enhanced IL-10 production in murine models (Zaninelli et al., 2021). RvD1 has been tested on RAW264.7 cells, where it inhibited the ability of these cells to become mature osteoclasts with the ability to resorb bone. Furthermore, it decreased the ability of RAW264.7 cells to produce pro-inflammatory cytokines. Similar results were observed in *in vitro* osteoclast cultures from human monocytes, which lead to reduced bone resorption. RvD1 in mice reduced disease activity, bone resorption and cartilage degradation by reducing the production of TRAP, cathepsin k, TNF, IL-1, IFN-γ, and PGE2 (Benabdoun et al., 2019; Zaninelli et al., 2021). Similarly to RvD1, RvE1 also managed to inhibit osteoclastogenesis, bone erosion and secretion of pro-inflammatory cytokines like IL-17, which further inhibited expression of RANKL and PGE2 in RAW264.7 cells, however, RvE1 has not been tested in primary human cells (Funaki et al., 2018).

Lastly, different levels of SPMs were recorded in plasma from RA patients with different disease activity. RA patients with active disease showed lower levels of LXA4, MaR1, RvD1 and RvE1 in plasma and serum compared to those in remission or healthy individuals, while the levels of pro-inflammatory chemokines and cytokines were increased in RA patients with active disease, which suggests impaired synthesis of SPMs in RA (Özgül Özdemir et al., 2020; Zaninelli et al., 2021). Interestingly, a study conducted in 2016 by Barden et al. examined the level of SPMs in plasma and synovial fluid in patients with arthritis compared to

healthy individuals. Both groups were taking omega-3 fatty acids supplements, while patients were also treated with anti-rheumatic drugs. As a result, SPM levels were increased in individuals with arthritis and the conversion rate of the majority of SPMs (RvEs, RvDs) was higher compared to healthy volunteers, despite a similar concentration of omega 3 fatty acid supplements. Additionally, conversion from precursors 18-HEPE and 17-HDHA to RvEs and RvDs was greater in synovial fluid rather than in plasma, which could lead to enhanced inflammation resolution in joints, lower cartilage damage, and reduced symptoms as a result of omega-3 fatty acids supplements (Barden et al., 2016).

1.5 Hypothesis and Aims

Previous research has suggested numerous advantages of SPMs in controlling inflammatory cascades and inhibiting osteoclastogenesis. However, the majority of this research has been predominantly conducted in murine models or cell lines rather than in primary human cells. This is particularly the case for osteoclast, where osteoclast differentiated from human myeloid cell lineage, more specifically $CD14^+$ monocytes or $CD14^-CD16^-CD11c^+$ pre-DCs, has not been investigated. Therefore, the overall hypothesis of this work is that SPMs possess inhibitory properties that could modulate osteoclast differentiation from primary human cells *in vitro* and decrease their bone resorbing activity.

Additionally, prior research has shown that RA monocytes have different epigenetic and transcriptomic profiles. Moreover, the SPM receptor expression in primary human cells is not well understood. Therefore, it can be hypothesised that SPM receptors are differentially expressed in health and RA, which can lead to different potential effect of SPMs on osteoclastogenesis and bone resorption in different cell types. More specifically, if an SPM receptor is predominantly expressed in RA than in health, it can be hypothesised that SPMs binding this receptor may have a stronger effect in RA, potentially leading to a more evident inhibitory effect on osteoclastogenesis.

Moreover, previous research has shown perturbation in the myeloid compartment of RA patients compared to healthy individuals, with altered metabolic activity in RA monocytes, however, whether this difference is maintained throughout the differentiation into osteoclasts is not explored. Therefore, it can be hypothesised that osteoclasts as highly metabolically active cells will show metabolic differences between healthy and RA cells, which could potentially be linked to their function.

Lastly, increased superoxide production, which is linked to mitochondrial damage, has previously been associated with increased osteoclastogenesis, therefore another hypothesis that needs to be investigated is that the effect of SPMs may reduce osteoclastogenesis via the inhibition of superoxide production. Understanding the difference in metabolism of healthy and RA osteoclasts and

their precursors (in the presence and absence of SPMs) could aid with targeting various pathways, which could contribute to the resolution of inflammation and reduced bone resorption and could be a step forward as a potential treatment for RA.

This thesis aims to:

1. Establish a reliable model for osteoclast differentiation.

2. Identify SPM receptors present on osteoclasts and their precursors in healthy individuals and RA patients at a transcriptional and protein level.

3. Evaluate the actions of selected SPMs on $CD14^{+}$ monocyte-derived and pre-DC-derived osteoclasts and their monocytic precursors under TNF-driven inflammatory conditions and standard culture conditions in terms of osteoclastogenesis and bone resorption.

4. Understand metabolic changes in healthy and RA monocytes, macrophages, and osteoclasts and the impact of SPMs on metabolism.

5. Investigate whether SPMs can inhibit superoxide production, which could lead to the inhibition of osteoclasts.

Chapter 2 Materials and Methods

2.1 Osteoclastogenesis from osteoclast pre-cursors

2.1.1 Sample collection

Patients with rheumatoid arthritis (RA) were recruited at either the Gartnavel General Hospital Rheumatology Unit or the Queen Elizabeth Hospital Rheumatology Unit in Glasgow. Only patients with active RA (disease activity score (DAS) 28 > 2.6) and those who were naïve to biological therapies but treated with conventional disease-modifying antirheumatic drugs (cDMARDs), more specifically Methotrexate, were recruited. Age and sex matched healthy donors were recruited at the University of Glasgow, Glasgow Biomedical Research Centre. Informed consent was obtained from all the donors before sample collection under the auspice of ethical approval (West of Scotland REC 4 approval 14/WS/1035, project reference: CG_2021_17_A). All donors remained anonymous after a collection of a maximum of 50 ml of peripheral blood into sodium heparin tubes (BD Vacutainer™).

2.1.1.1 PBMC isolation

Peripheral blood mononuclear cells (PBMCs) were isolated by density gradient from either blood collected in sodium heparin tubes (<50 ml) or leukocyte cones of healthy donors. Blood was diluted 1:1 (or 1:3 for leukocyte cones) with sterile phosphate-buffered saline (PBS; Gibco, 14190-094), and layered over 3 ml of Ficoll-Paque Plus (cytiva, 17144003) in 15ml falcon tubes and centrifuged (400g, 30 min, room temperature (RT), no brake). The top plasma layer was aspirated with a Pasteur pipette and discarded whilst the next layer containing PBMCs was carefully aspirated off and transferred into a new 50 ml falcon tube. The PBMC layer collected in a new falcon tube was increased in volume to approximately 45 ml with PBS and centrifuged at 300g for 10 min with the brake on. The resulting pellet was resuspended in 45 ml of PBS two more times with additional centrifugation, as a means of washing the cells. After washing, PBMCs were resuspended in cell separation buffer (CSB; PBS supplemented with 2% fetal bovine serum (FBS; gibco, 10500-064) and 1 mM ethylenediaminetetraacetic acid (EDTA; Sigma-Aldrich, E7889-100ML) to the final volume of 25 ml. To count the cells, 10 µl of cell suspension was mixed with 10 µl of Trypan Blue (Gibco, 15250061) to

exclude dead cells. Afterwards, 10 µl of cells mixed with Trypan Blue was added to a haemocytometer and counted using a light microscope.

2.1.1.2 CD14$^+$ monocyte isolation

CD14$^+$ monocytes were isolated from PBMCs with the EasySep™ Human CD14 Positive Selection Kit (94.7% purity; see section 2.6 for purity check) according to the manufacturer's instructions (Stemcell Technologies, 17858). Briefly, PBMCs were pelleted via centrifugation and resuspended at 1x10^8 cells/ml in CSB. The cell suspension was transferred into a 5 ml round-bottom polystyrene tube (Stemcell Technologies, 38007) and incubated at RT (lid on) for 10 minutes with an antibody cocktail (100 µl/ml; included in the isolation kit). After 10 minutes, nanoparticle beads (included in the kit) were added at 100 µl/ml and the suspension was incubated for another 3 minutes. The volume was increased to 2.5 ml with CSB and the tube was placed in an EasySep™ magnet for column-free immunomagnetic separation (lid off) for 3 minutes. Then, in one continuous movement, the magnet with the tube was inverted to discard the supernatant. The tube was removed from the magnet and the CD14$^+$ monocytes were resuspended in 2.5 ml of CSB, placed back into the magnet and incubated for 3 minutes prior to removal of supernatant, as mentioned above. This procedure was repeated twice. Once supernatant was discarded after the last incubation step, 3 ml of complete alpha Minimum Essential Medium (α-MEM; gibco, 22571-020), supplemented with 1% L-glutamine (gibco, 25030-024), 1% penicillin/streptomycin (Sigma Aldrich, P0781), and 10% FBS (gibco, 10500-064) was added to the cells. The isolated cells were counted with haemocytometer as described in the above section (see 2.1.1.1) and diluted to the final concentration of 1x10^6 cells/ml.

2.1.1.3 Dendritic cell precursor isolation

Dendritic cell (DC) precursors were isolated from PBMCs with EasySep™ Human Myeloid DC Enrichment Kit (Stemcell Technologies, 19061). Briefly, the PBMC cell pellet was resuspended at 5x10^7 cells/ml and transferred to a 5 ml round bottom tube (Fisher Scientific, 352054) fitting the EasySep™ magnet. FcR blocker was added at 15 µl/ml together with 50 µl/ml of Myeloid DC Enrichment Cocktail (both components A and B; part of the kit), cells were mixed and incubated for 30 minutes at RT. Magnetic beads were briefly vortexed and added to the sample at 100 µl/ml and incubated for another 10 minutes at RT. CSB was topped up to 2.5

ml, the tube was placed into the magnet without the lid, and incubated for 5 minutes. The tube with cell suspension was inverted while still in the magnet and cells were collected into a new 5 ml round bottom tube, which was subsequently placed in the magnet for 5 more minutes. Finally, the tube in the magnet was inverted and the isolated cells were transferred to a new 5 ml round bottom tube and counted with a haemocytometer as for $CD14^+$ monocytes (see 2.1.1.1). Counted cells were centrifuged (400g, 5 min, 4°C, no brake), and resuspended in complete α-MEM at $1x10^6$ cells/ml.

2.1.1.4 Osteoclast differentiation

Isolated $CD14^+$ monocytes or DC precursors resuspended in complete α-MEM at $1x10^6$ cells per ml were plated on a 96-well flat bottom cell culture plate (Corning, 3596) at $1x10^5$ cells/well (100 µl/well). Plated cells were stimulated with 25 ng/ml of recombinant human macrophage colony-stimulating factor (M-CSF; PEPROTECH, 300-25-100UG) and all surrounding wells were filled with PBS to avoid media evaporation. The cells were incubated at 37°C with 5% CO_2. After approximately 18 hours, 50 µl of media was replaced with fresh media containing a final concentration of 25 ng/ml of M-CSF and 25 ng/ml of recombinant human soluble receptor activator of NF-κB ligand (RANKL, E. coli-derived; PEPROTECH, 310-01-100UG). Recombinant human tumour necrosis factor (TNF; PEPROTECH, 300-01A) was added to certain wells at 10 ng/ml on day 5 (120 hours after the M-CSF addition) to emulate an "inflammatory" environment. In some instances, 10 ng/ml of specialised pro-resolving lipids (Cayman Chemicals), namely resolvin D1 (RvD1; CAY13060-10ug), RvE1 (CAY10007848-10ug), 17-HDHA (CAY33650-25ug) and Maresin 1 (MaR1; CAY10878-10ug) were added together with TNF. All experiments were done in triplicates and media was refreshed every 3 days. Finally, cells were stained with tartrate-resistant acid phosphatase (TRAP) on day 10 or were used for other experiments (figure 2.1).

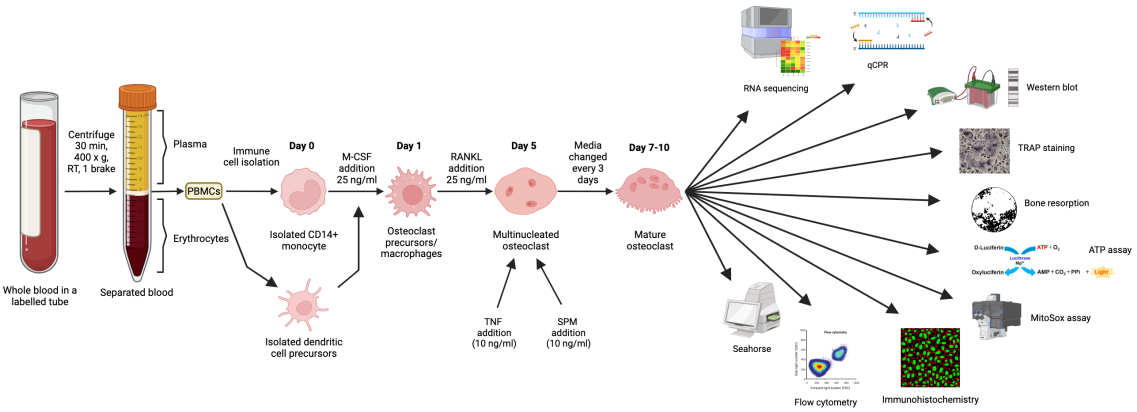

Figure 2.1 Experimental workflow.
Human in vitro osteoclast differentiation from whole blood, where monocytes or dendritic cell precursors were isolated from PBMCs and differentiated into osteoclasts with M-CSF, RANKL ±TNF ± SPMs for 7-10 days. Further applications of osteoclasts in various assays, namely RNA sequencing, qPCR, western blot, TRAP staining, bone resorption assay, ATP assay, MitoSox assay, Immunohistochemistry, flow cytometry, and seahorse are listed (created in BioRender).

2.1.1.5 THP-1 cells

THP-1 cells were grown in a 75 cm^2 tissue culture treated flask (Greiner Bio-One, 658175) in complete Roswell Park Memorial Institute (RPMI) media (Invitrogen, 31870-025) supplemented with 10% FBS, 1% penicillin/streptomycin, and 1% L-glutamine. Media was changed every 3 days. Cells were split once a week and transferred to a new 75 cm^2 flask at a concentration of $2x10^5$ cells/ml. Several passages were performed to ensure stable cellular properties. Subsequently, cells were centrifuged (300g, 5 min, RT), counted using haemocytometer, resuspended in fresh complete RPMI media, and plated on a 96-well plate at a concentration of $1x10^5$ cells/well. Cells were grown in the presence of 100 ng/ml phorbol 12-myristate-13-acetate (PMA) for 4 days. After 4 days, M-CSF and RANKL were added at the final concentration of 50 ng/ml and incubated for another 10 days. Cells were TRAP stained on day 14.

2.2 Quantification of osteoclasts

2.2.1 TRAP staining of osteoclast cultures

Media was removed from wells and cells were fixed with fixative solution (12.5 ml citrate solution (Sigma Aldrich, 91-5; from kit, Cat No. 387A-1KT), 32.5 ml acetone (VWR, 20066.330), 5 ml 37% formaldehyde (Sigma-Aldrich, F-8775)) for 1 minute at RT. Wells were washed 3 times with distilled water, dried, and fixed cells were

incubated with 100 µl of TRAP staining solution according to the manufacturer's protocol (Acid Phosphatase, Leukocyte (TRAP) Kit, see appendix; Sigma-Aldrich, 387A-1KT) for 20 minutes at 37°C in the dark. Stained cells were washed 3 times with distilled water and were allowed to dry overnight. Images of TRAP-stained cells were taken at 10x or 20x magnification with the EVOS FL Auto cell Imaging System (Life Technologies). Mature osteoclasts (3≤ nuclei, stained in purple) were manually counted with ImageJ software with a cell counter plugin.

2.2.2 Bone resorption assay

$CD14^+$ cells were plated on a special 96-well osteo assay Stripwell plate (Corning, 3989) coated with calcium phosphate at $1x10^5$ cells/well and cultured as for TRAP staining in the presence of M-CSF, RANKL, ±TNF and SPMs for 12 days. Afterwards, media was discarded, and cells were lysed with sodium hypochlorite solution (Sigma-Aldrich, 425044-1L). Plates were imaged with EVOS microscope and images were analysed by IMAGE J.

2.3 Expression of SPM receptors at a transcript level

2.3.1 RNA sequencing and data analysis

$CD14^+$ monocyte RNAseq dataset used in this thesis was previously generated in the Goodyear laboratory (Kieran Woolcock, 2022). Briefly, peripheral blood was obtained from RA patients at Gartnavel General Hospital Rheumatology unit Glasgow (DAS28 > 2.7) and age-matched healthy volunteers were recruited at the University of Glasgow. Informed consent was obtained from all donors prior to sample collection together with an appropriate ethical approval (West of Scotland REC 4 approval 19/WS/0111, project reference CG_2019_09_A_AM01). All donors were treated anonymously after sample collection. $CD14^+$ monocytes were isolated from PBMCs with CD14 Positive Selection Kit and isolated cells were subsequently lysed with RNA lysis buffer supplemented with ß-mercaptoethanol. RNA extraction was conducted with the PureLink™ RNA Mini Kit (Invitrogen, 12183018A). RNA samples were sequenced by GenomeScan BV (Leiden, The Netherlands). For RNA library preparation, the NEBNext Ultra II Directional RNA Library Prep Kit for Illumina (New England BioLabs) was used. RNA sequencing was conducted according to the manufacturer's instructions with NovaSeq 6000

(Illumina), using 1.1 nM of DNA. The sequencing reads were aligned to the reference genome (GRCh38.p13, Ensembl). DESeq2 package in RStudio was used for normalisation of read counts and for identification of genes that are differentially expressed between sample groups. Further analysis was undertaken with Rstudio (see section 2.8 for Rstudio packages).

2.3.2 Quantitative polymerase chain reaction (qPCR)

2.3.2.1 Cell lysis and RNA extraction

Cells were lysed with RLT lysis buffer (part of the RNeasy Micro Kit; QIAGEN, 74004) supplemented with 1% ß-mercaptoethanol (Sigma-Aldrich, M3148-100ML). 70% ethanol was added to the lysate (1 volume) and mixed by pipetting. RNA was extracted according to the Manufacturer's manual (RNeasy Micro Kit, QIAGEN, 74004). Briefly, samples were transferred to an RNeasy MinElute spin column in a 2 ml collection tube, centrifuged for 15 seconds at 8000g and flow through was discarded. Samples were incubated with DNase I solution (10 µl of DNase I stock solution in 70 µl RDD buffer; Qiagen, 79254) for 15 minutes. Next, 350 µl of RW1 buffer (part of the RNeasy Micro Kit) was added and samples were centrifuged as previously described. RNeasy MinElute spin columns were placed into a new collection tube and 500 µl of RPE buffer (included in the kit) was added. After the centrifugation (15s, 8000g), 500 µl of 80% ethanol was added to the column and the samples were centrifuged for 2 minutes. To dry out the membrane, samples were centrifuged again at maximal speed for 5 minutes in a new collection tube (lid open). Finally, columns were transferred into a new 1.5 ml tube and 14 µl of RNase free water was directly applied to the centre of the membrane. Samples were centrifuged one last time for 1 minute at full speed to elute the extracted RNA, which was then kept on ice. Concentration of every sample was measured by Nanodrop2000 Spectrophotometer (ThermoFisher Scientific). The ratio of absorbance at 260 and 280 (A260/A280) for pure RNA should be between 1.8-2.1 and the ratio of 260/230, showing possible contamination, should be between 2.0-2.2. If cDNA could not be synthesised the same day, extracted RNA was stored at -80 degrees.

2.3.2.2 cDNA synthesis

cDNA was synthesised using High-Capacity cDNA synthesis kit (Applied Biosystems, 4368814). Isolated RNA samples were diluted in RNase free water to achieve a uniform concentration (10 ng/µl or higher) for all samples. 100 ng of RNA was used per reaction, which is expected to yield 100 ng of cDNA. To prepare the samples for qPCR, 10 µl of diluted RNA was added to a PCR tube and mixed with 10 µl of 2x RT master mix per each reaction on ice (table 2.1). Components of the kit were thawed on ice.

Table 2.1 2x RT master mix for cDNA synthesis

Component	Volume
10X RT Buffer	2.0 µL
25X dNTP Mix (100 mM)	0.8 µL
10X RT Random Primers	2.0 µL
MultiScribe™ Reverse Transcriptase	1.0 µL
Nuclease-free H_2O	4.2 µL
Total per reaction	**10.0 µL**

Afterwards, tubes were centrifuged (30s, 400g), and put in the thermocycler where they were initially incubated at 25°C for 5 minutes, then at 37°C for 2 hours and finally at 95°C for 5 minutes. cDNA samples were stored at -20°C until qPCR was performed.

2.3.2.3 Primer design

qPCR primers were designed using the Integrated DNA Technologies Ltd (IDT) and ENSEMBL website. An exon sequence of a particular gene was identified, and the selected sequence copied to the IDT website where further primer parameters were implied. Primer length was designed to be between 18-23 base pairs yielding a PCR amplicon between 90-150 bp. GC nucleotide content was between 40-60% (optimally 50%) and optimal melting temperature was 60°C with a range between 59.5 - 61°C. The selected sequence of the primers was subsequently confirmed with BLAST software (National Centre for Biotechnology Information, USA) to prevent any non-specific binding and amplification. Primers specific for a particular gene meeting all the requirements above were ordered via the IDT

website and are shown in the table 2.2. Before use, primers were resuspended in nuclease free water to the final concentration of 100 μM.

Table 2.2 Human primers designed for qPCR

Primer	Sequence 5'3'
RANK Forward	GCT GTA ACA AAT GTG AAC CAG GA
RANK Reverse	GCC TTG CCT GTA TCA CAA ACT
CD115 Forward	TCC CAG TGA TAG AGC CCA GT
CD115 Reverse	CAG GGT CCA GTG AGG TGA TG
TRAP Forward	GAC CAC CTT GGC AAT GTC TCT G
TRAP Reverse	TGG CTG AGG AAG TCA TCT GAG TTG
Cathepsin K Forward	TTG GAA GGG AGT TGG TGT G
Cathepsin K Reverse	TGG GTG GAG AGA AGC AAA GT
PU.1 Forward	TGC CCT ATG ACA CGG ATC TAT A
PU.1 Reverse	GTA ATG GTC GCT ATG GCT CTC
MITF Forward	CTT AAA AGC ATC CGT GGA C
MITF Reverse	AGA CCC GTG GAT GGA ATA A
DCSTAMP Forward	CCT TGC CAC TCC ACT AAG TGT
DCSTAMP Reverse	CTC TGT GGT TGT TGC CAT CTG
OCSTAMP Forward	GCT CCA GCG AAG ACA CGA C
OCSTAMP Reverse	AGC CTG TAG TCT ATC CAT GCC
OSCAR Forward	CGC TTG GAG ATT TGG ACT TTT CA
OSCAR Reverse	GCA GCG GTA AAT TCC CCC TT
GAPDH Forward	CAA GGC TGA GAA CGG GAA G
GAPDH Reverse	GGT GGT GAA GAC GCC AGT
MMP9 Forward	CAG TAC CGA GAG AAA GCC TAT TT
MMP9 Reverse	TAG GTC ACG TAG CCC ACT T
NFATc1 Forward	AGA ATT CGG CTT GCA CAG G
NFATc1 Reverse	CTC TGG TGG AGA AGC AGA GC

2.3.2.4 qPCR

Primers and cDNA were defrosted on ice. cDNA samples were diluted in RNase free water to final concentration of 1 ng/μl. 1 μl of cDNA sample was added to the PCR master mix (for 1 sample – 5 μl Power Sybr green dye (Invitrogen, 4367659), 3.8 μl RNase free water, 0.1 μl forward primer, 0.1 μl reverse primer). Samples were run in duplicates. GAPDH was used as a housekeeping gene for normalisation.

Nuclease free water was used instead of cDNA as a non-template control (NTC) for each primer. Plates were sealed, centrifuged at 400g for 30 seconds, and run with Applied Biosystems QuantStudio 7 Flex Real-time PCR system for 384-well plates with the following cycle: 10 minutes at 95°C, 40 cycles for 15 seconds at 95°C, and 1 minute at 60°C.

2.4 Expression of SPM receptors at the protein level

2.4.1 Immunohistochemistry

Isolated $CD14^+$ monocytes resuspended in complete α-MEM were plated on 8-well glass-bottom chamber slides at $4x10^5$ cells/well (400 µl; Ibidi, 80807) and differentiated into fully mature osteoclasts in the presence of M-CSF, RANKL ± TNF for 10 days. After 10 days, media was removed, and cells were washed twice with PBS. PBS was removed and cells were fixed with 300 µl of 2% formaldehyde (diluted in distilled water; Sigma-Aldrich, F-8775) for 10 minutes at RT. Cells were again washed twice with PBS and permeabilised with 300 µl of 0.1% Triton X-100 (diluted in PBS; Sigma-Aldrich, 9002-93-1) for 10 minutes on a shaker. Cells were washed with PBS twice and blocked with 300 µl of 2% bovine serum albumin (BSA, diluted in PBS; Sigma-Aldrich, A9418-100G) for 20 minutes on a shaker. Block solution was subsequently replaced with 300 µl of primary antibody diluted in 2% BSA (see table 2.3 for dilutions), and slides were incubated overnight in the dark at 4°C on a shaker. Rabbit polyclonal antibodies were used for CMKLR1 (ThermoFisher Scientific, PA5-100933), FPR2 (ThermoFisher Scientific, 720367), and LTB4R receptors (ThermoFisher Scientific, BS-2654R).

The next day, cells were washed twice with PBS and stained with 200 µl of secondary antibody (goat anti-rabbit IgG H&L (Alexa Fluor 647; ThermoFisher Scientific, 31460) and phalloidin (acting ring staining, Alexa Fluor 488; ThermoFisher Scientific, A12379) diluted in 0.2% BSA (see table 2.3 for dilutions). Cells were incubating for 1h on a shaker in the dark and afterwards were washed twice with PBS. 300 µM of DAPI nuclei staining solution (358/461 nm; ThermoFisher Scientific, D3571) was added and slides were incubating on a shaker for 10 minutes. Afterwards, cells were washed with PBS, 300 µl of PBS was added to each well, and slides were scanned with Nikon confocal microscope at 20x magnification.

Table 2.3 Antibodies used for immunohistochemistry with the used dilutions

Antibody	Dilution
LTB4R	1:200
FPR2	1:250
CMKLR1	1:100
Anti-rabbit antibody	1:1000
Phalloidin	1:500

2.4.2 Western blot

After the cells were differentiated on a 96-well plate (section 2.1.1.4), media was removed from the wells and cells were washed with PBS twice. 20 µl of radioimmunoprecipitation assay (RIPA) buffer (ThermoFisher Scientific, 89900) was applied per $1x10^5$ cells (80 µl in total for 4 technical replicates) to lyse the cells. Samples can be stored at -20°C until processed. 15 µl of sample lysate was transferred into a new 1.5 ml Eppendorf tube and 4x NuPage lithium dodecyl sulfate (LDS) sample buffer (Invitrogen, NP0007) and 10x NuPage sample reducing agent (Invitrogen, NP0004) were added to each tube. Afterwards, cells were incubated at 95°C for 5 mins, and then moved to ice to cool down. A pre-casted 10-well gel (NuPAGE 4 to 12%, Bis-Tris, 1.0–1.5 mm, Mini Protein Gels; Invitrogen, NP0321BOX) was rinsed with water and white tape was removed from the cassette. Gels were assembled in a SureLock gel tank and 500 ml of running buffer (25 ml of NuPAGE MOPS SDS running buffer 20x (Invitrogen, NP0001)) with 475 ml of distilled water (dH_2O) was added in between the gels. Before applying the samples, the well forming comb was removed from the cassette. 35 µl of a sample, which is the maximum for a 10-well gel, was loaded per well. One well was reserved for the protein ladder; 7 µl of ladder was loaded (Precision Plus Protein Dual Color Standards; Bio-Rad, 1610374). The gels were run with an electrophotometer (BIO-RAD), first at 100V (until the samples crossed the well barrier) and then the voltage was increased to 140V for 40 minutes or until the samples reached the bottom of the well. The gel was then carefully moved to a tank with dH_2O and transferred on a nitrocellulose membrane using the iBlot 2 gel transfer device with dry transfer system (23V, 6 mins; Life Technologies). Membrane was quickly transferred to a tank with dH_2O to prevent drying out and blocked with 5% non-fat dried milk (milk) in TBST (1x Tris-buffered saline with

0.1% Tween) for 1h on a shaker. After an hour, the solution was replaced with 7 ml of 5% milk in TBST with the correct dilution of primary antibodies (table 2.4) and incubated on a shaker at 4°C overnight.

Next day, the membrane was washed 3x10 mins with TBST on a shaker at RT. Secondary antibody was diluted in 5% milk in TBST, added to the membrane, and incubated for 1h on a shaker at RT. Then, the membrane was washed 4x10 min in TBST as before. Lastly, the membrane was covered in 2 ml of a chemiluminescent substrate for 2-3 minutes (SuperSignal™ West Pico PLUS Chemiluminescent Substrate, 1:1 ratio; ThermoFisher Scientific, 34577) and scanned with an imaging system (Azure Biosystems). For applying another antibody/beta-actin control (ß-Actin (13E5) Rabbit mAb (HRP Conjugate); Cell Signaling Technology, 5125S) to the same membrane, stripping buffer (Restore™ Western Blot Stripping Buffer; ThermoFisher Scientific, 46430) was applied to the membrane for 10 minutes (on a shaker, RT) to remove the primary and secondary antibodies. The membrane was washed with TBST, blocked with 5% milk in TBST for an hour and the process was repeated as before.

Table 2.4 Antibodies used for western blot with the used dilutions

Antibody	Dilution
LTB4R	1:500
FPR2	1:500
CMKLR1	1:1000
Anti-rabbit antibody	1:1000
Beta actin	1:2000

2.5 Flow cytometry for immunometabolic changes

2.5.1 Harvesting cells

$CD14^+$ monocytes were isolated from PBMCs, plated on a 24-well flat-bottom plate ($5x10^5$ cells/well) and differentiated to either macrophages or osteoclasts. Differentiated cells were centrifuged (600g, 5 min, 4°C) and media was discarded. Cold PBS was added to wash the cells, which was followed by another centrifugation step. PBS was then removed, and ice-cold Accutase (STEMCELL Technologies, 07920) was added to each well to detach the cells from the surface

of the plate. Cells were incubated at 37°C for 10-12 minutes. Plates were tapped/gently vortexed after 5-7 minutes of incubation. Supernatant was collected and transferred into a V-bottom plate. Accutase was added one more time and the process was repeated. Plates were centrifuged (400g, 5 mins, at 4°C for enzymes or RT for metabolic dyes). Supernatant was discarded and cells were washed in cold PBS for enzyme assays or warm PBS for metabolic dye assays and centrifuged as before. Cells were resuspended in PBS and same conditions were pooled together. Pooled samples were centrifuged and stained.

2.5.2 Staining for metabolic dyes

Once cells were washed with warm PBS, 50 µl of master mix was added to each well except the controls. For master mix, all the metabolic dyes were diluted in warm PBS (table 2.5). The cells were then incubated at 37°C for 10 minutes. Afterwards, cells were washed with cold PBS twice (600g, 5 min, 4°C). Next, 50 µl of antibody cocktail diluted in PBS was added per well as follows: OSCAR (1:25, FITC; Miltenyi Biotec,130-107-617), FC block (1:100), Hoechst (1:500, DAPI channel), CD16 (1:100, APC-Cy7; BD Biosciences, 557758), and live/dead dye (1:1000, Zombie NIR; Biolegend, 423106). In case of unstained and single-stained cells, 50 µl of PBS was added. Cells were resuspended and incubated at RT for 20 minutes protected from the light. Afterwards, cells were washed with PBS and centrifuged as before. Cells were resuspended in FACS buffer and transferred into FACS tubes. The data was acquired on a Cytek's Aurora flow cytometer. Cell data was unmixed using SpectroFlo version 3, and data was analysed using FlowJo software.

Table 2.5 Summary of metabolic dyes used for flow cytometry

Dye	Dilution	Peak	Company	Cat. number
2-NBDG	1:100 Stock 10 mM	B3	ThermoFisher Scientific	N13195
Bodipy C16	1: 100 000 Stock 10 mM	B2	ThermoFisher Scientific	D3821
TMRM	1: 1 000 000 Stock 5 mM	YG1	ThermoFisher Scientific	M20036
MitoTracker Deep Red (DR)	1: 100 000 Stock 1 mM	R2	ThermoFisher Scientific	M22426

2.5.3 Staining for metabolic enzymes

2.5.3.1 Live/dead staining

Unlike with metabolic dyes, which had to be applied to live cells, metabolic enzymes were added after the cells were fixed. Prior to fixation, 50 µl of live/dead staining (see table 2.6 for enzyme/antibody details) was added to each well except for the controls, which were given 50 µl of PBS. Samples were resuspended and incubated at 4 °C with an aluminium foil for 15-40 minutes. After the incubation 150 µl of PBS was added to each well to wash the cells and the plate was centrifuged (400g, 5 min, 4 °C).

2.5.3.2 Fixation of the cells

To fix the cells, PBS was removed from the wells and 100 µl/well of 2% para formaldehyde in PBS (PFA) was added, cells were resuspended, and the plate was incubated for 15 minutes in the dark at RT. Cells were washed with PBS, centrifuged (400g, 5 min, 4°C), and 200 µl of FASC buffer (PBS with 2% FBS and 2 mM EDTA) was added to each well. Fixed cells were stored at 4°C in aluminium foil until metabolic enzymes and antibodies were added. Fixed plates can be stored under these conditions for up to 1 week.

2.5.3.3 Metabolic enzymes staining

Fixed cells were centrifuged (400g, 5 min, 4°C), washed with PBS, and centrifuged again. 50 µl of CD16, OSCAR (table 2.6), and FC block (1:100) were added to each well, except for the unstained and single-stained cells, which only contained a particular antibody, not a combination of them. Cells were incubated for 20 minutes in the dark at RT. After the incubations, cells were washed with PBS. For wells that included the biotinylated OSCAR antibody, Streptavidin-BV785 was added, and the cells were incubated for another 20 minutes in the dark at RT. The cells were then washed in PBS and centrifuged as before.

Prior to enzyme addition, cells were washed in 1X eBioscience™ permeabilization buffer (ThermoFisher Scientific, 00-8333-56). Afterwards, 50 µl of enzyme cocktail consisting of a combination of all enzymes, or individual enzyme for single-stained cells (diluted in 1X permeabilization buffer, not PBS; table 2.6) was applied to the

cells and cells were incubated for 2 hours at 4°C. Cells were then washed in permeabilization buffer, resuspended in 100 µl of FACS buffer and transferred to FACS tubes. Cells were acquired on a Cytek's Aurora 5-laser spectral flow cytometer, data were unmixed using SpectroFlo version 3, and analysed using FlowJo software.

Table 2.6 Summary of metabolic enzymes and antibodies used for flow cytometry

Antibodies	Fluorescence	Excitation peak	Dilution	Company	Cat. number
Glut 1	BSA/Azide free				ab252403
Lightning link	DL405	V2	1:1000	Abcam	ab210438
PKM	BSA/Azide free				ab206129
Lightning link	PE	YG1	1:1000	Abcam	ab102918
SDHA	BSA/Azide free				ab240098
Lightning link	AF647	R2	1:1000	Abcam	ab269823
G6PD	BSA/Azide free				ab231828
Lightning link	APC-Cy7	R7	1:5000	Abcam	ab102859
CytC	BSA/Azide free				ab237966
Lightning link	PE-Cy7	YG9	1:1000	Abcam	ab102903
ACC1	BSA/Azide free				ab272704
Lightning link	AF488	B2	1:1000	Abcam	ab236553
CPT1a	BSA/Azide free				ab235841
Lightning link	PE-Cy5	YG5	1:1000	Abcam	ab102893
CD16	bUV496	UV7	1:100	BD Biosciences	564653
OSCAR	Biotin	-	1:25	Miltenyi Biotec	130-107-614
Streptavidin	BV785	V15	1:400	Biolegend	405249
Live/Dead	Zombie NIR	R6	1:25	Biolegend	423106

2.6 Purity check for CD14$^+$ monocytes

2.6.1 Cell preparation

Purity check was performed on a new CD14$^+$ isolation kit. Several conditions were tested, namely unstained and stained PBMCs, stained negative selection, and stained and unstained positive selection including isolated CD14$^+$ monocytes. For the staining, 1x10^6 cells were transferred to a FACS tube and the volume was topped to 1 ml with FACS buffer (PBS with 2% FBS, 2 mM EDTA). The tubes were centrifuged at 350g for 5 min and supernatant was discarded. The cells were then stained with the following antibodies: 20 µl of CD3 (BioLegend, 300408), 5 µl of

CD19 (BioLegend, 302208), and 20 µl of CD56 (BioLegend, 318306) all in PE channel, 10 µl of CD14 (PB channel; BD Biosciences, 558121), and 5 µl of CD16 (FITC; BioLegend, 302006) diluted in 500 µl of FACS buffer. Unstained cells contained only 500 µl of FACS buffer. Tubes were centrifuged (350g, 5 min), supernatant was discarded, cell pellets were resuspended in 250 µl of fixation buffer (BioLegend, 420801), and incubated at 4°C for 20 minutes. Cells were washed with FACS buffer, centrifuged as before, and resuspended in 350 µl of FACS buffer. Cells were then stored on ice until they were acquired.

2.6.2 Compensation beads preparation

Compensation controls were stained similarly to cells (section 2.6.1), but instead of cells, compensation beads (Invitrogen,15385356) were used. 1 drop of beads was applied to each tube and resuspended in 100 µl of FACS buffer. Similarly as with the cell staining, CD3, CD56 and CD19 (PE channel) were added to 1 tube, CD14 (PB) to another tube, and CD16 (FITC) to the third tube. The tubes were vortexed and incubated for 30 minutes at RT, protected from light. After the incubation, 2 ml of FACS buffer was added to each tube and the tubes were centrifuged at 200g for 10 minutes. Supernatant was discarded and stained beads were resuspended in 300 µl of FACS buffer and stored on ice. Cells and compensation beads were subsequently acquired on the BD FACSCanto Flow cytometry machine (BD BioSciences).

2.7 Additional metabolic assays

2.7.1 MitoSox

For MitoSOX assay, isolated $CD14^+$ monocytes were plated on 8-well glass bottom chamber slides at $4x10^5$ cells/well (400 µl; Ibidi, 80807), and differentiated into osteoclasts in the presence of M-CSF, RANKL ±TNF and SPMs (see section 2.1.1.4). Afterwards, media was discarded and cells on slides were washed with warm PBS. 400 µl of MitoSOX master mix (PBS, 5 µM MitoSOX dye (Invitrogen, M36008) and 4 µM Hoechst 33342 nuclei staining (stock=16.2 mM; Invitrogen, H3570)) was added to each well. Two controls were used, i.e., Menadione as a positive control (2-Methyl-1,4-naphthoquinone, 98%; fisher scientific, A13593) and Mito-TEMPO as a negative control (MedChemExpress, HY-112879). 50 µM of Menadione (0.0172g of

Menadione in 2 ml of methanol) was added to MitoSOX master mix in one control well while 100 µM of Mito-TEMPO (10 mM stock) was added to the other control well. The slide was incubated for 10 minutes at 37°C. Afterwards, the cells were washed twice with warm PBS, which was then replaced with sufficient volume of warm complete α-MEM media. The slides were then imaged with Nikon confocal microscope (MitoSOX - AF 555 nm, Hoechst - 460-490 nm). Results were analysed with a MitoSOX pipeline created by Leandro Lemgruber Soares from the College of Medical, Veterinary & Life Sciences imaging facility, using CellProfiler software.

2.7.2 ATP assay

The adenosine triphosphate (ATP) assay was conducted using a luminescent ATP detection kit (ATPlite 1step, PerkinElmer, 6016731). Isolated monocytes were differentiated in triplicates into osteoclasts on a 96-well plate as before (section 2.1.1.4), however, 4 additional conditions in triplicates (as discussed below) were added for controls. 10 ml of substrate buffer solution was added to lyophilised substrate solution (provided in the kit) and left at room temperature for 30 minutes. In the meantime, the controls were prepared. 10 mM and 100 mM of Alfa Aesar 2 Deoxy D-glucose (2DG, 98%, 2M stock; Fisher Scientific, 11321867), which is a glycolysis inhibitor, 1 µM oligomycin from Streptomyces Diastatochromogenes (5 mM stock; Sigma-Aldrich, Q4876-5MG), an oxidative phosphorylation inhibitor, or a combination of oligomycin with 100 mM 2DG were used. The plate was incubated for 30-40 minutes at 37°C (making sure not to exceed 40 minutes). After the incubation, 50 µl of the prepared ATPlite mix was added to each well and the plate was incubated on a shaker for 5-10 minutes at RT protected from light. Finally, 100 µl of supernatant from each well was transferred to a special 96-well ATP assay white-bottom plate (cell culture microplate, 96-well, PS, F-bottom; Greiner bio-one, 655083). The plate was immediately read on a Pherastar machine using the luminescence method via the Pherastar software.

2.7.3 Seahorse for Mito Stress assay

2.7.3.1 Plate and cartridge preparation

Cell-Tak solution was prepared (0.02 mg/ml of Corning™ Cell-Tak Cell and Tissue Adhesive (Fisher Scientific, 10217081) in 0.1 M $NaHCO_3$) with a pH between 6-8

and 25 µl was added to each well of a Seahorse plate (XFe96/XF Pro Flux Pak; Agilent Technologies, 103792-100). The plate was incubated at RT for 30 minutes, washed twice with distilled water and allowed to air-dry. The plate can be left at RT overnight or it has to be prepared at least 2 hours before plating the cells. In addition to plate preparation, the cartridge (part of Seahorse FluxPaks) was hydrated by adding 200 µl of Seahorse calibrant per well (Agilent, 100840-000). The hydrated cartridge was wrapped in parafilm and put in an incubator overnight at 37°C (no CO_2).

2.7.3.2 Cell preparation

Isolated $CD14^+$ monocytes were plated on a 96-well Seahorse plate at $1x10^5$ cells/well. The wells on the sides had only media with no cells in them. For a calibration curve, which was used for the normalisation of the cell count, cells were also plated on a regular 96-well plate. For normalisation, cells were diluted in complete media at $5x10^6$ cells, from which 200 µl was transferred in the first two wells (A1, A2), while the other wells B1,B2 - H1,H2 were filled with 100 µl of complete media. Serial dilutions were made by adding 100 µl from the first well to the well below (B1, B2), and then from B wells to C wells until H1 and H2 wells to reach the concentration between 500,000 cells/well to 3,906 cells/well. The plate was incubated under the same conditions as the Seahorse plate at 37°C with 5% CO_2.

2.7.3.3 Seahorse analysis preparation

50 ml of Seahorse media (no serum; Agilent Technologies, 102353-100) was supplemented with 4 mM glutamine, 5.5 mM glucose, 1 mM penicillin/streptomycin and 1 mM sodium pyruvate (Gibco, 11360070), with a pH of 7.4. Cell media was gently removed from each well and replaced with 175 µl of supplemented Seahorse media. The cells were incubated at 37°C for 45-60 minutes (no CO_2). While the cells were incubating, necessary drugs for the measurement were prepared. 25 µl of each drug was injected into a suitable port as follows: oligomycin (1.5 µM; Sigma-Aldrich, O4876-5MG) was injected into port A, Carbonyl cyanide 3-chlorophenylhydrazone (CCCP, 1 µM; Sigma-Aldrich, C2759) was injected into port B, and a combination of rotenone (1 µM; Sigma-Aldrich,

R8875) and antimycin A (1.25 µM; Sigma-Aldrich, A8674) was injected into port C. The cartridge was then incubated for 15 minutes at 37°C with no CO_2.

2.7.3.4 Seahorse measurement

For the analysis, the Seahorse cartridge plate with injected drugs was inserted into the Seahorse machine (Seahorse XF Pro Analyzer) without the lid and the calibration was done. After the calibration, the plate with cells was taken out of the incubator and loaded into the machine without the lid, and the run was performed.

2.7.3.5 Fixing cells and SRB assay

After the run was finished, cells were fixed with 25 µl (for Seahorse plate) or 12.5 µl (for calibration control for cell normalisation) of cold 50% w/v trichloroacetic acid (TCA; Sigma-Aldrich, 91228), which was added straight into the media, and incubated at 4°C for an hour. The wells were washed 4 times with running water and air dried at RT. 50 µl of 0.057% w/v of sulforhodamine B sodium salt (SRB; Sigma-Aldrich, S1402) solution (0.2 g of SRB dissolved in 50 ml of 1% acetic acid) was added to each well and the wells were incubated at RT for 30 minutes. The plates were washed 4 times with 200 µl of 1% acetic acid and air dried at RT. 100 µl of 10 mM TRIS base solution (pH=10.5) was then added to every well and the plate was put on a shaker for 10 minutes. Finally, the absorbance was measured at 510 nm.

2.7.3.6 Seahorse analysis

The data was analysed with Seahorse Wave software and normalised with the cell count from the calibration plate based on the absorbance data after the SRB staining.

2.8 Graphs and statistical analysis

All graphs and their statistical analyses were generated either in Rstudio with appropriate packages (listed below) or in GraphPad Prism 9. Normality test was performed for t-tests in order to know whether the data is normally distributed - parametric (Gaussian distribution) or non-parametric. For the statistical analysis,

95% confidence intervals were used and p-values of ≤0.05 were considered significant. Graphs generated in Rstudio from RNAseq datasets used adjusted p-value generated and normalised by “DESeq2” package. Other packages used in Rstudio included “ggplot2”, “reshape2”, “amap”, “dplyr”, “org.Hs.eg.db”, “clusterProfiler”, “readr”, “pathview”, “readxl”, “tidyverse”, “data.table”, and “BiocManager”.

Chapter 3 The expression of SPM receptors on osteoclasts and their precursors in health and rheumatoid arthritis

3.1 Introduction

Specialised pro-resolving mediators (SPMs) are a class of lipids generated during an early stage of acute inflammation (Abdolmaleki et al., 2019). They are produced from polyunsaturated fatty acids by a series of enzymatic reactions (Krishnamoorthy et al., 2018) and consist of 4 groups, namely resolvins (Rv; E- or D- series), maresins (MaR), protectins (PD), and lipoxins (LX) (Flak et al., 2019). SPMs act via specific G protein-coupled receptors (GPCRs) to produce anti-inflammatory and pro-resolving signals necessary for the resolution of inflammation. This involves reduced platelet and macrophage activation, lower neutrophil activation and recruitment, and enhanced macrophage phagocytosis (Cash et al., 2014). They mainly act via 8 GPCRs; namely formyl peptide receptor 2 (FPR2; also known as ALX/FPR2), leukotriene B4 receptor (LTB4R; other name BLT1), chemerin receptor 23 (ChemR23; also known as ERV1 or CMKLR1), GPR37, Leucine-rich repeat-containing GPCR 6 (LGR6), GPR32 (known as DRV1), GPR18 (known as DRV2), and GPR101 (Bang et al., 2018; Flak et al., 2019; Hughes et al., 2021; Park et al., 2020). Each SPM receptor interacts with various SPMs and these interactions have a range of affinities (figure 3.1).

It has been shown that the absence of SPMs or the impairment of SPM-receptor signalling can contribute to chronic inflammatory disorders (Serhan & Levy, 2018). Therefore, targeting SPM receptors with their SPM ligands revealed their importance as therapeutic agents. Notably, in humans and in preclinical animal studies they were able to prevent inflammation, organ fibrosis, reduce pain, promote tissue regeneration, and wound healing (Chiang & Serhan, 2017). It also should be appreciated however, that most SPMs have no known receptor and thus further studies are needed in order to identify these receptors and characterise related signalling pathways (Chiurchiù et al., 2018).

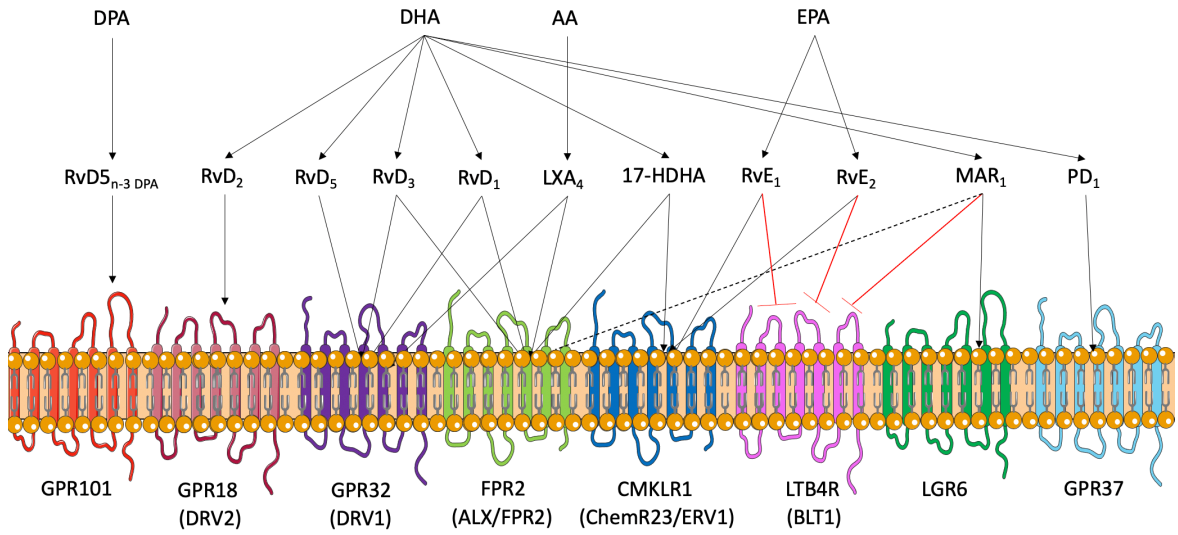

Figure 3.1 SPM receptors and their ligands.
The figure shows multiple specialised pro-resolving mediators biosynthesised from omega-3 (docosahexaenoic acid (DHA), eicosapentaenoic acid (EPA)), docosapentaenoic acid (DPA) or omega-6 (arachidonic acid (AA)) fatty acids and their known receptors, namely GPR101, GPR18, GPR32, ALX/FPR2, CMKLR1, LTB4R, LGR6, and GPR37. All SPMs act as agonists except RvE1, RvE2 and MaR1, which also act as antagonists to LTB4R receptor and block its pro-inflammatory signalling pathways (shown in red). MaR1 binds ALX/FPR2 receptor with lower affinity compared to LGR6 receptor (dashed line).

The main emphasis of this work is on rheumatoid arthritis (RA), however, other inflammatory autoimmune diseases (systemic lupus erythematosus (SLE) and systemic sclerosis (SSc)) are included as relevant comparators. These diseases are complex and of unknown origin. Yet, it is accepted that genetics and/or environmental factors play a role in disease initiation, and that hormonal and immunological factors contribute to initiation and perpetuation (Aliko et al., 2011). RA is characterised by inflammation of synovium (lining of the joints) and bone erosion, which leads to further joint deformities, cartilage destruction, and associated disability (Tsukasaki & Takayanagi, 2019; Scherer et al., 2020). The cells responsible for bone loss in RA are multinucleated (3 or more nuclei) bone-resorbing osteoclasts, which are created by fusion of their mononuclear precursors. The classical mononuclear precursor is the bone marrow or peripheral blood monocyte (Muto et al., 2011), however, osteoclasts can also be differentiated from dendritic cell (DC) precursors (pre-DCs) (Wang et al., 2021) or macrophages (Bhagavatham et al., 2021).

Circulating monocytes play an important role in RA and their phenotype differs from monocytes in healthy individuals. Previous research has shown that

circulating monocytes in RA display higher levels of pro-inflammatory cytokines (e.g. TNF, IL-6 or IL-1) and are primed to become inflammatory macrophages (McGarry et al., 2021). Additionally, monocyte levels are enhanced in RA and positively correlate with the disease activity. For instance, $CD14^{++}$ $CD16^{-}$ monocytes differentiate into osteoclasts and cause bone erosion while $CD14^{++}$ $CD16^{+}$ monocytes release pro-inflammatory cytokines, which further contribute to osteoclastogenesis (Rana et al., 2018).

This chapter focuses on bioinformatic analysis to define the altered transcriptional pathways in RA. It investigates the expression of SPM receptors in RA monocytes in comparison to other related inflammatory autoimmune diseases, i.e., SLE and SSc, and healthy individuals. It also evaluates the SPM receptor expression in osteoclasts differentiated from monocytes or pre-DCs due to variations in their phenotype. Lastly, SPM receptor expression was further confirmed at the protein level in osteoclasts and their precursors.

3.2 Results

3.2.1 $CD14^{+}$ monocyte transcriptional profiles

$CD14^{+}$ monocyte RNAseq data from both healthy individuals and RA patients was already available in the Goodyear laboratory (*Woolcock, 2022*). A re-analysis was undertaken to determine the overall transcriptional profiles and differential changes between the groups. Notably, differential transcripts were filtered based on their significance i.e., adjusted p-value lower than 0.05 and the absolute value of log2 fold change higher than 1. This enabled the selection of both upregulated (log2fold>1) and downregulated (log2fold<1) genes. A total of 3,031 differentially expressed genes were identified between RA vs healthy, from which 1,114 were downregulated and 1,917 genes were upregulated in RA (table 3.1).

Table 3.1 Overall gene expression in RA

Expression	Number of genes
Downregulated	*1,114*
Unchanged (Non-Significant)	*2,1536*
Upregulated	*1,917*

Within the significantly upregulated genes, some of those with most increased fold changes were TNF, CCL4, CCL4L2, NFKB2, PTX3 or CCRL2 (figure 3.2 A), with TNF (the major pro-inflammatory factor in RA) being the most expressed (figure 3.2 B).

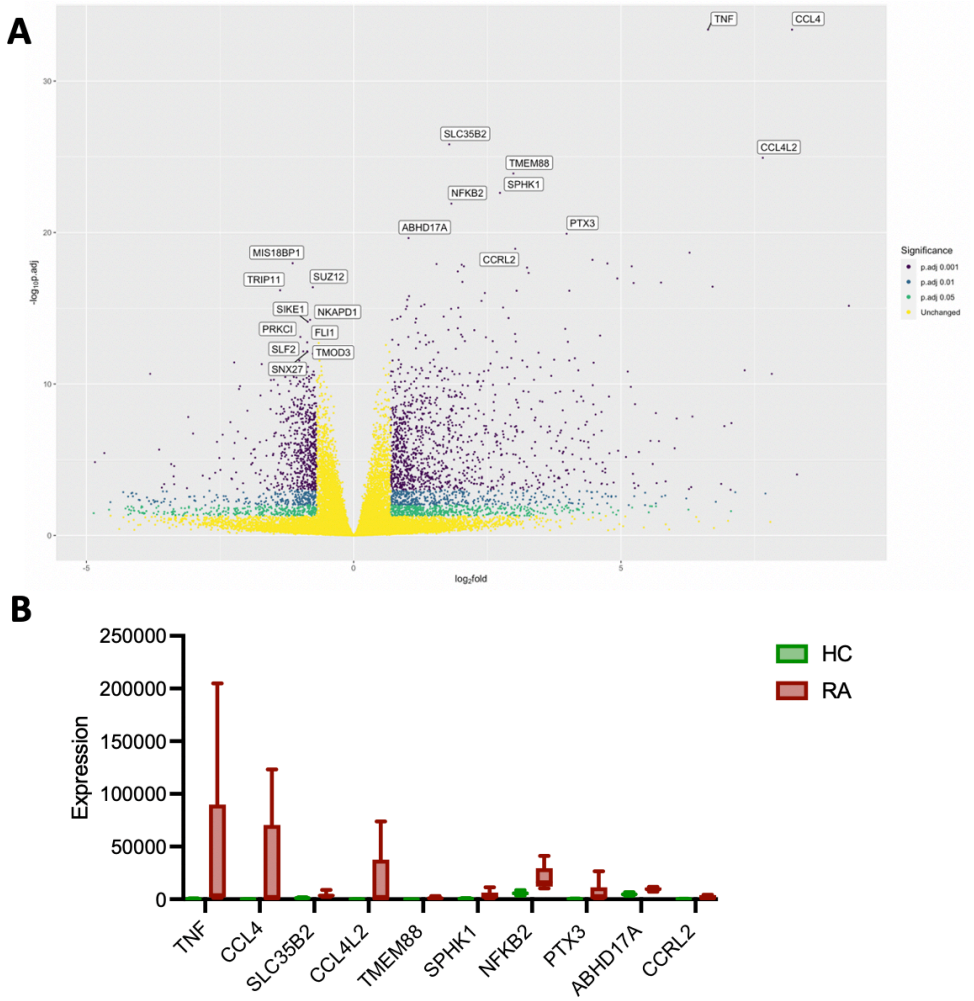

Figure 3.2 The most differentially expressed genes in RA vs healthy monocytes.
A - 10 most upregulated and 10 most down-regulated genes in RA samples compared to healthy individuals were labelled. Upregulated genes in RA compared to healthy are in the positive values and downregulated genes are in the negative values on the log_2fold x-axis. 3 different ranges of significance were applied with significant genes shown in green (p.adj ≤0.05 and >0.01), more significant shown in blue (p.adj ≤0.01 and >0.001), and most significant shown in purple (p.adj ≤0.001). Non-significant genes are shown in yellow. **B -** Boxplots for most expressed genes (p.adj ≤0.001) in RA (red) based on the volcano plot compared to healthy individuals (HC, green).

To understand potential implications of these observed changes, signalling pathway analysis using the KEGG (Kyoto Encyclopedia of Genes and Genomes) pathway database was undertaken. This revealed a number of pathways with varying degrees of identified gene contribution and significance. Of the top 25 upregulated pathways in RA, the most enriched was the cytokine-cytokine receptor interaction pathway (figure 3.3). Other interesting pathways included MAPK (mitogen-activated protein kinase) signalling pathway, TNF signalling

pathway, IL-17 signalling pathway, nuclear factor kappa B (NF-κB) signalling pathway, RA, and osteoclast differentiation. Interestingly, interaction mapping of the identified pathways suggests a direct link between osteoclast differentiation, MAPK signalling pathway, IL-17 signalling pathway, and c-type lectin receptor signalling pathway (figure 3.3 B). As noted above, the contribution of the identified genes differed across the various signalling pathways. To understand the contribution of genes to each of the pathways, they were visualised in KEGG pathway diagrams (Figure 3.4), revealing the inter-linked nature of the changes right across the signalling cascades. For instance, in the osteoclastogenesis pathway there is perturbation in both the extra-cellular, cytoplasmic and nuclear compartments (figure 3.4 F). Taken together this suggests that multiple pathways related to inflammation and osteoclastogenesis are potentially perturbed in RA, which is consistent with our prior understanding of drivers of the disease (Auréal et al., 2020; Fennen et al., 2016).

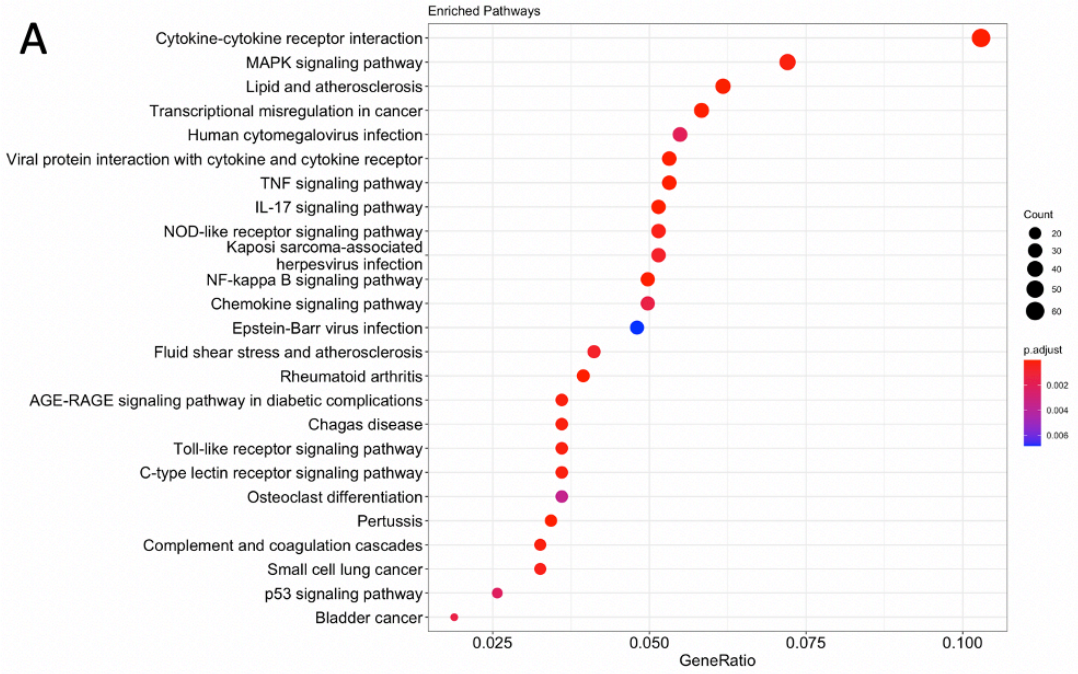

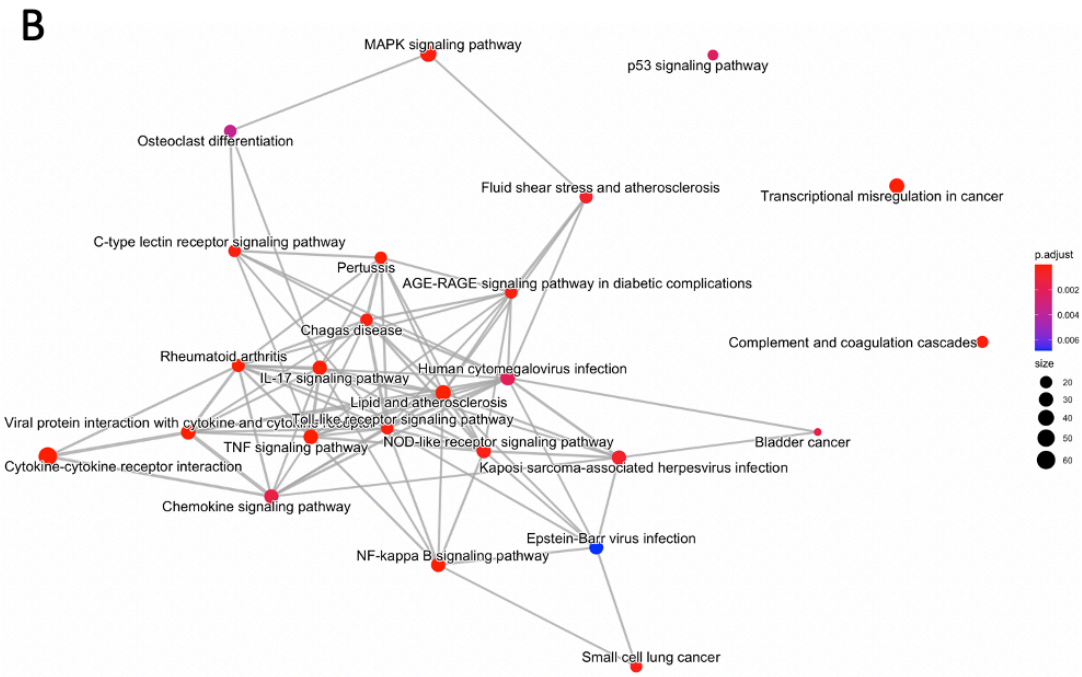

Figure 3.3 Upregulated signalling pathways in RA CD14⁺ monocytes.
A - A dotplot showing 25 most upregulated KEGG signalling pathways of all the upregulated genes in RA vs healthy monocytes. **B** - An Emapplot showing interactions between the signalling pathways showed in the dotplot. The bigger the dot, the more genes are involved. Red – more significant, blue – less significant based on the p.adj value.

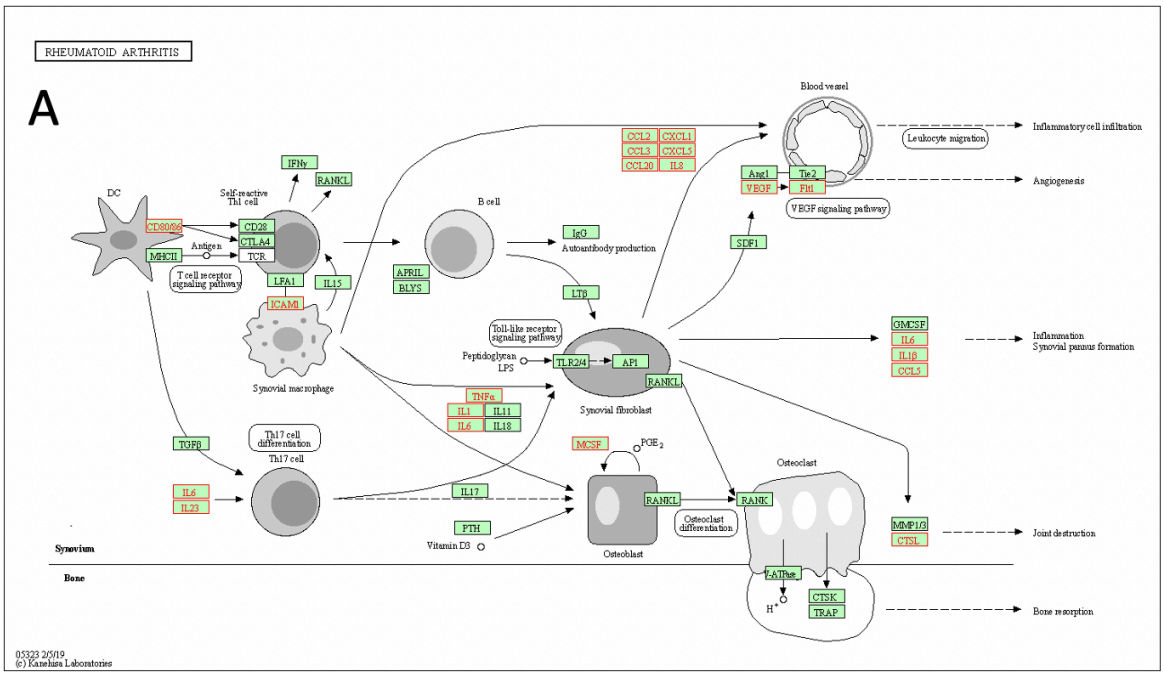
RHEUMATOID ARTHRITIS
A
Blood vessel
Leukocyte migration
Inflammatory cell infiltration
Angiogenesis
VEGF signaling pathway
DC
Self-reactive Th1 cell
IFNγ
RANKL
CD80/86
CD28
CTLA4
TCR
Antigen
MHCII
T cell receptor signaling pathway
LFA1
IL15
ICAM1
B cell
IgG
Autoantibody production
APRIL
BLYS
LTβ
SDF1
CCL2
CXCL1
CCL3
CXCL3
CCL20
IL8
Ang1
Tie2
VEGF
Flt1
Toll-like receptor signaling pathway
Peptidoglycan
LPS
TLR2/4
AP1
RANKL
Synovial fibroblast
Synovial macrophage
TNFα
IL1
IL11
IL6
IL18
GMCSF
IL6
IL1β
CCL5
Inflammation
Synovial pannus formation
TGFβ
Th17 cell differentiation
Th17 cell
IL6
IL23
IL17
MCSF
PGE2
Osteoclast
RANKL
RANK
Osteoclast differentiation
PTH
Vitamin D3
Osteoblast
MMP1/3
CTSL
Joint destruction
Synovium
Bone
V-ATPase
H+
CTSK
TRAP
Bone resorption
03323 2/5/19
(c) Kanehisa Laboratories

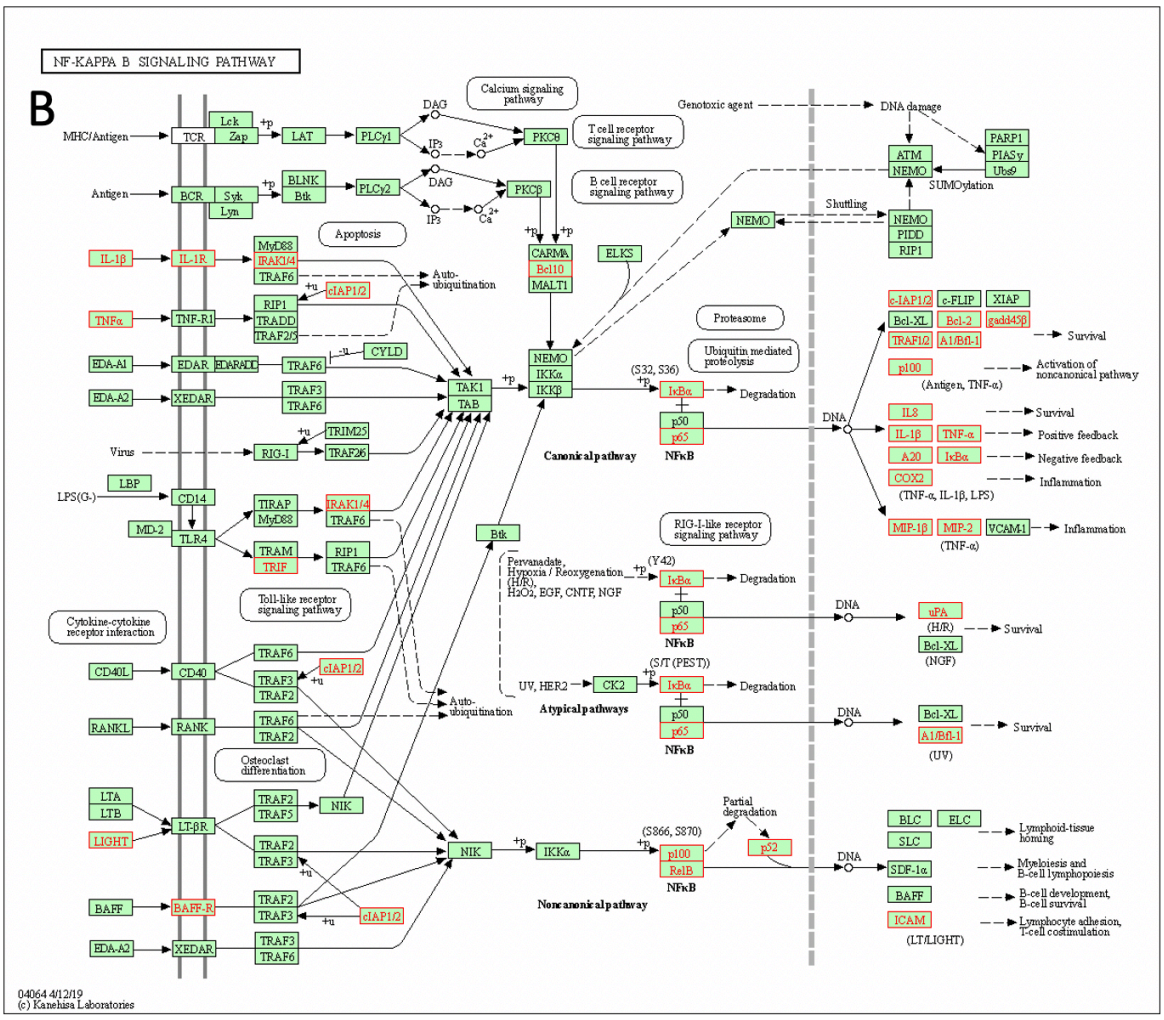
NF-KAPPA B SIGNALING PATHWAY
B
Calcium signaling pathway
DAG
IP3
Ca2+
PKCθ
PKCβ
T cell receptor signaling pathway
B cell receptor signaling pathway
MHC/Antigen
TCR
Lck
Zap
LAT
PLCγ1
Antigen
BCR
Syk
Lyn
BLNK
Btk
PLCγ2
Genotoxic agent
DNA damage
PARP1
PIASy
Ubc9
ATM
NEMO
SUMOylation
Shuttling
NEMO
NEMO
PIDD
RIP1
Apoptosis
IL-1β
IL-1R
MyD88
IRAK1/4
TRAF6
Auto-ubiquitination
cIAP1/2
TNFα
TNF-R1
RIP1
TRADD
TRAF2/5
CYLD
EDA-A1
EDAR
EDARADD
TRAF6
EDA-A2
XEDAR
TRAF3
TRAF6
CARMA
Bcl10
MALT1
ELKS
TAK1
TAB
NEMO
IKKα
IKKβ
(S32, S36)
IκBα
p50
p65
Degradation
Canonical pathway
NFκB
Proteasome
Ubiquitin mediated proteolysis
Virus
RIG-I
TRIM25
TRAF26
LBP
LPS(G-)
CD14
MD-2
TLR4
TIRAP
MyD88
IRAK1/4
TRAF6
TRAM
TRIF
RIP1
TRAF6
Toll-like receptor signaling pathway
Cytokine-cytokine receptor interaction
RIG-I-like receptor signaling pathway
Btk
Pervanadate, Hypoxia / Reoxygenation (H/R), H2O2, EGF, CNTF, NGF
(Y42)
Degradation
UV, HER2
CK2
(S/T (PEST))
Atypical pathways
CD40L
CD40
TRAF6
TRAF3
TRAF2
cIAP1/2
RANKL
RANK
TRAF6
TRAF2
Osteoclast differentiation
LTA
LTB
LIGHT
LT-βR
TRAF2
TRAF5
NIK
TRAF2
TRAF3
BAFF
BAFF-R
TRAF2
TRAF3
cIAP1/2
EDA-A2
XEDAR
TRAF3
TRAF6
NIK
IKKα
(S866, S870)
p100
RelB
Partial degradation
p52
Noncanonical pathway
NFκB
DNA
c-IAP1/2
c-FLIP
XIAP
Bcl-XL
Bcl-2
gadd45β
TRAF1/2
A1/Bfl-1
Survival
p100
Activation of noncanonical pathway
(Antigen, TNF-α)
IL8
Survival
IL-1β
TNF-α
Positive feedback
A20
IκBα
Negative feedback
COX2
Inflammation
(TNF-α, IL-1β, LPS)
MIP-1β
MIP-2
VCAM1
Inflammation
(TNF-α)
uPA
(H/R)
Survival
Bcl-XL
(NGF)
Bcl-XL
A1/Bfl-1
Survival
(UV)
BLC
ELC
Lymphoid-tissue homing
SLC
SDF-1α
Myelopiesis and B-cell lymphopoiesis
BAFF
B-cell development, B-cell survival
ICAM
Lymphocyte adhesion, T-cell costimulation
(LT/LIGHT)
04064 4/12/19
(c) Kanehisa Laboratories

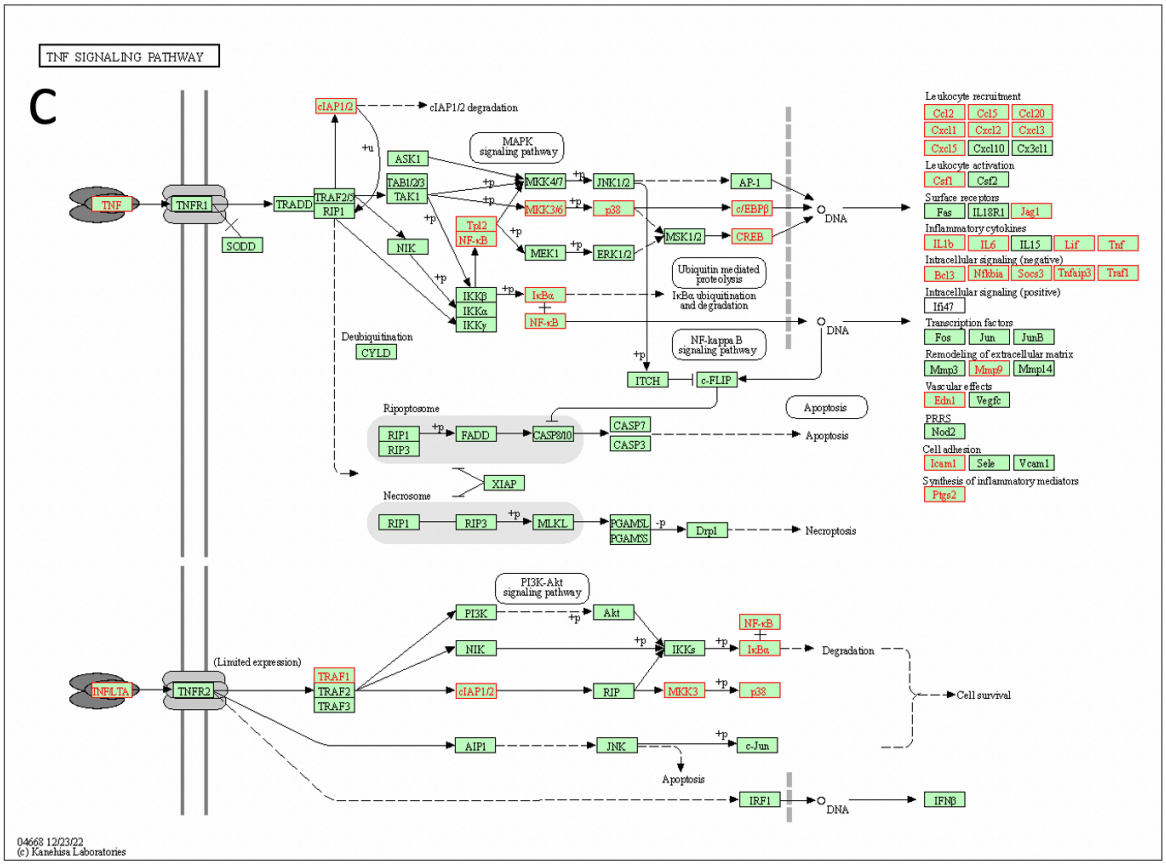
TNF SIGNALING PATHWAY
C
cIAP1/2
cIAP1/2 degradation
MAPK signaling pathway
ASK1
TAB1/2/3
TAK1
MKK4/7
JNK1/2
AP-1
MKK3/6
p38
c/EBPβ
Tpl2
NF-κB
MSK1/2
CREB
MEK1
ERK1/2
DNA
TNF
TNFR1
TRADD
TRAF2/5
RIP1
SODD
NIK
IKKβ
IKKα
IKKγ
IκBα
NF-κB
Ubiquitin mediated proteolysis
IκBα ubiquitination and degradation
Deubiquitination
CYLD
NF-kappa B signaling pathway
ITCH
c-FLIP
Ripoptosome
RIP1
RIP3
FADD
CASP8/10
CASP7
CASP3
Apoptosis
XIAP
Necrosome
MLKL
PGAM5L
PGAM5S
Drp1
Necroptosis
Leukocyte recruitment
Ccl2
Ccl5
Ccl20
Cxcl1
Cxcl2
Cxcl3
Cxcl5
Cxcl10
Cx3cl1
Leukocyte activation
Csf1
Csf2
Surface receptors
Fas
IL18R1
Jag1
Inflammatory cytokines
IL1b
IL6
IL15
Lif
Tnf
Intracellular signaling (negative)
Bcl3
Nfkbia
Socs3
Tnfaip3
Traf1
Intracellular signaling (positive)
Ifi47
Transcription factors
Fos
Jun
JunB
Remodeling of extracellular matrix
Mmp3
Mmp9
Mmpl4
Vascular effects
Edn1
Vegfc
PRRS
Nod2
Cell adhesion
Icam1
Sele
Vcam1
Synthesis of inflammatory mediators
Ptgs2
PI3K-Akt signaling pathway
PI3K
Akt
NIK
IKKs
NF-κB
IκBα
Degradation
(Limited expression)
TNFLTA
TNFR2
TRAF1
TRAF2
TRAF3
cIAP1/2
RIP
MEKK3
p38
Cell survival
AIP1
JNK
c-Jun
Apoptosis
IRF1
IFNβ
04668 12/23/22
(c) Kanehisa Laboratories

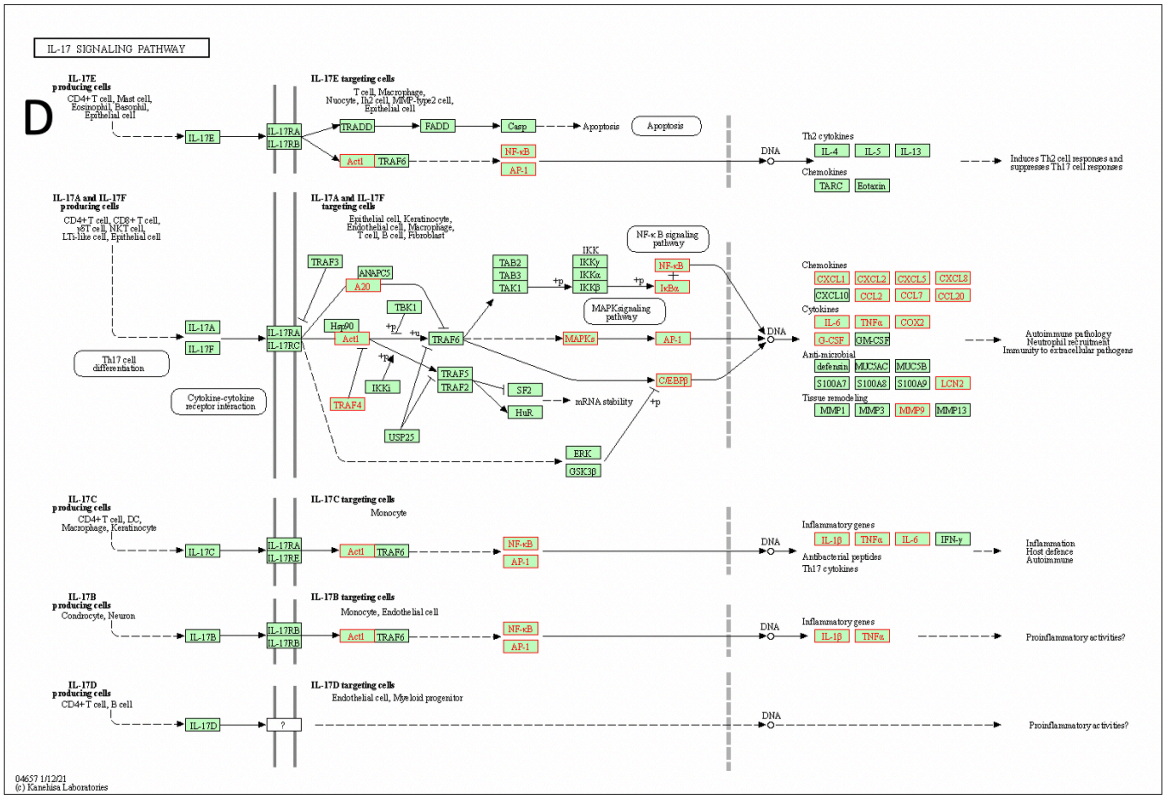
IL-17 SIGNALING PATHWAY
D
IL-17E producing cells
CD4+ T cell, Mast cell, Eosinophil, Basophil, Epithelial cell
IL-17E
IL-17E targeting cells
T cell, Macrophage, Nuocyte, Th2 cell, MMP-type2 cell, Epithelial cell
IL-17RA
IL-17RB
TRADD
FADD
Casp
Apoptosis
Act1
TRAF6
NF-κB
AP-1
DNA
Th2 cytokines
IL-4
IL-5
IL-13
Chemokines
TARC
Eotaxin
Induces Th2 cell responses and suppresses Th17 cell responses
IL-17A and IL-17F producing cells
CD4+ T cell, CD8+ T cell, γδT cell, NKT cell, LTi-like cell, Epithelial cell
IL-17A and IL-17F targeting cells
Epithelial cell, Keratinocyte, Endothelial cell, Macrophage, T cell, B cell, Fibroblast
TRAF3
ANAPC5
A20
TBK1
Hsp90
TAB2
TAB3
TAK1
IKK
IKKγ
IKKα
IKKβ
NF-κB signaling pathway
IκBα
MAPK signaling pathway
MAPKs
IL-17A
IL-17F
IL-17RA
IL-17RC
TRAF6
Th17 cell differentiation
Cytokine-cytokine receptor interaction
TRAF5
TRAF2
TRAF4
USP25
SF2
HuR
mRNA stability
C/EBPβ
ERK
GSK3β
Chemokines
CXCL1
CXCL2
CXCL3
CXCL8
CXCL10
CCL2
CCL7
CCL20
Cytokines
IL-6
TNFα
COX2
G-CSF
GM-CSF
Anti-microbial
defensin
MUC5AC
MUC5B
S100A7
S100A8
S100A9
LCN2
Tissue remodeling
MMP1
MMP3
MMP9
MMP13
Autoimmune pathology
Neutrophil recruitment
Immunity to extracellular pathogens
IL-17C producing cells
CD4+ T cell, DC, Macrophage, Keratinocyte
IL-17C
IL-17C targeting cells
Monocyte
Inflammatory genes
IL-1β
TNFα
IL-6
IFN-γ
Antibacterial peptides
Th17 cytokines
Inflammation
Host defence
Autoimmune
IL-17B producing cells
Chondrocyte, Neuron
IL-17B
IL-17B targeting cells
Monocyte, Endothelial cell
Proinflammatory activities?
IL-17D producing cells
CD4+ T cell, B cell
IL-17D
IL-17D targeting cells
Endothelial cell, Myeloid progenitor
04657 1/12/21
(c) Kanehisa Laboratories

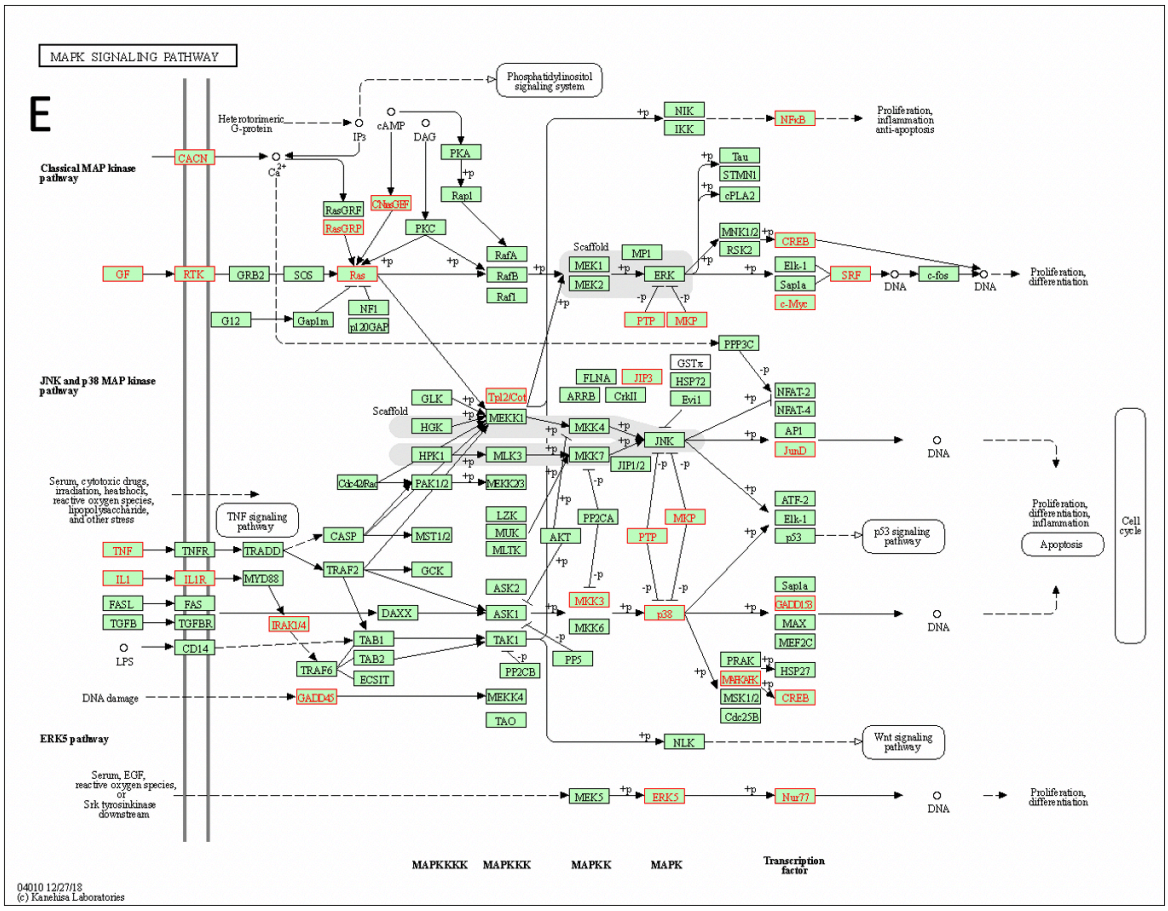

Figure 3.4 Selected upregulated inflammatory pathways in RA CD14⁺ monocytes.
Selected upregulated pathways were rheumatoid arthritis (A), NF-kappa B signalling (B), TNF signalling (C), IL-17 signalling (D), MAPK signalling (E), and osteoclast differentiation (F). Upregulated RA genes are shown in red.

3.2.2 SPM receptor expression on monocytes and osteoclasts at the transcript level

Having revealed that there is an altered transcriptional profile in RA monocytes, a focused analysis was performed to evaluate expression of the main SPM receptors. However, this analysis was not restricted to healthy individuals and RA but also included samples from patients with systemic lupus erythematosus (SLE), diffuse cutaneous SSc (dcSSc), early SSc (eaSSc), and limited cutaneous SSc (lcSSc)). SLE and SSc were added as similarly to RA they are autoimmune, inflammatory diseases, and the presence of SPM receptors on monocytes from these diseases could indicate a plausible anti-inflammatory/pro-resolving effect of various SPMs. However, these diseases are not the main interest of this study and therefore are not further studied in this thesis.

RNAseq analysis revealed that of the 8 studied GPCR SPM receptors, only 5 had detectable transcripts in $CD14^+$ monocytes obtained from either healthy or those with an autoimmune inflammatory condition. These were GPR18, CMKLR1, FPR2, LTB4R and LGR6, while GPR32, GPR101, and GPR37 transcripts were not expressed. More specifically, LTB4R was the most expressed and was followed by FPR2, CMKLR1, GPR18 and LGR6, which had the lowest expression values across healthy and diseased monocytes and was barely expressed (table 3.2).

Table 3.2 SPM receptor expression on healthy and diseased monocytes
Mean of normalised counts for SPM receptor expression on healthy monocytes (HC) compared to monocytes from RA, SLE and patients with SSc, namely dcSSc, eaSSc, and lcSSc.

	HC	RA	SLE	dcSSc	eaSSc	lcSSc
CMKLR1	910.35	518.87	1206.09	898.20	916.71	1135.59
GPR18	46.35	92.09	87.94	61.72	57.3	57.14
FPR2	1270.92	2737.30	2734.74	2186	1870.93	1939.96
LTB4R	3281.38	3832.96	3055.94	3451.07	3051.95	3324.33
LGR6	6.63	6.33	7.08	3.04	10.77	10.62

The expressed SPM receptors were further visualised using heatmaps (figure 3.5) and boxplots (figure 3.6). GPR18 and FPR2 showed significantly higher expression in RA compared to healthy monocytes (figure 3.6 A, B). LTB4R was also slightly

more expressed in RA than in healthy, however, the difference was not significant (figure 3.6 D). In contrast, CMKLR1 was significantly more expressed in healthy monocytes (figure 3.6 C). LGR6 was similarly expressed in healthy and RA monocytes and no significant difference was observed (figure 3.6 E). Additionally, GPR18 also showed a significant difference between SLE and healthy, while FPR2 exhibited significant increase in SLE and dcSSc compared to healthy (figure 3.6 A, B).

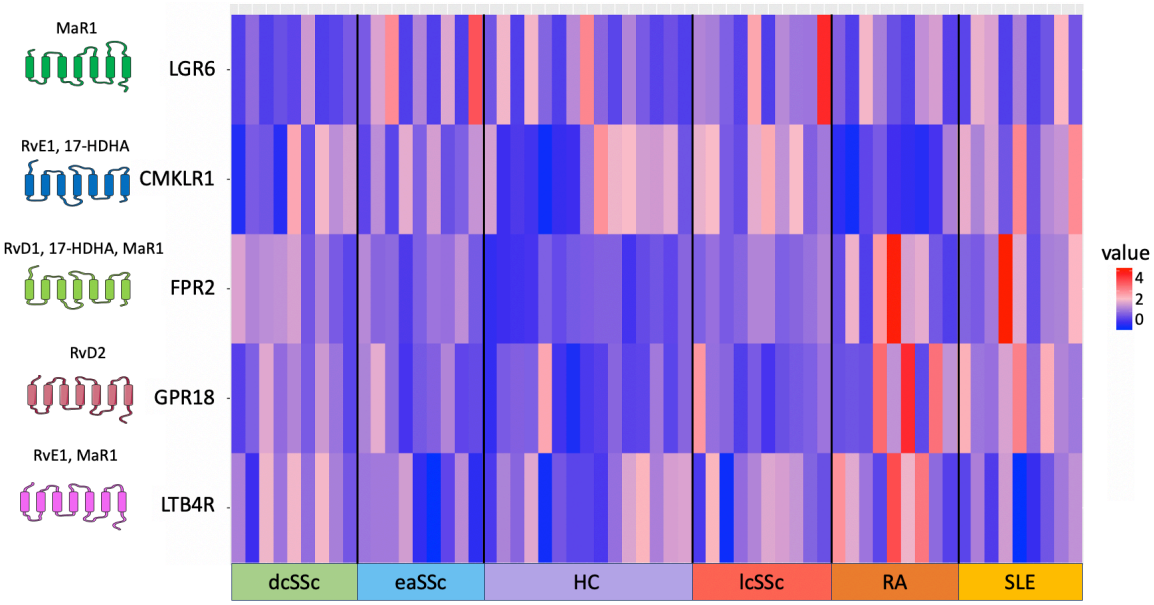

Figure 3.5 Heatmap of the SPM receptor expression on monocytes in health and RA. RNAseq data analysis of expressed SPM receptors, namely LGR6, CMKLR1, FPR2, GPR18, and LTB4R SPM receptors in healthy donors (HC, n=15), rheumatoid arthritis (RA, n=9), systemic lupus erythematosus (SLE, n=9) and different types of systemic sclerosis (SSc), namely diffuse cutaneous (dcSSc, n=9), early (eaSSc, n=9), and limited cutaneous SSc (lcSSc, n=10). Red values – high expression, blue values – low expression. Ligands of individual SPM receptors (MaR1, RvE1, 17-HDHA, RvD1, and RvD2) are shown as well.

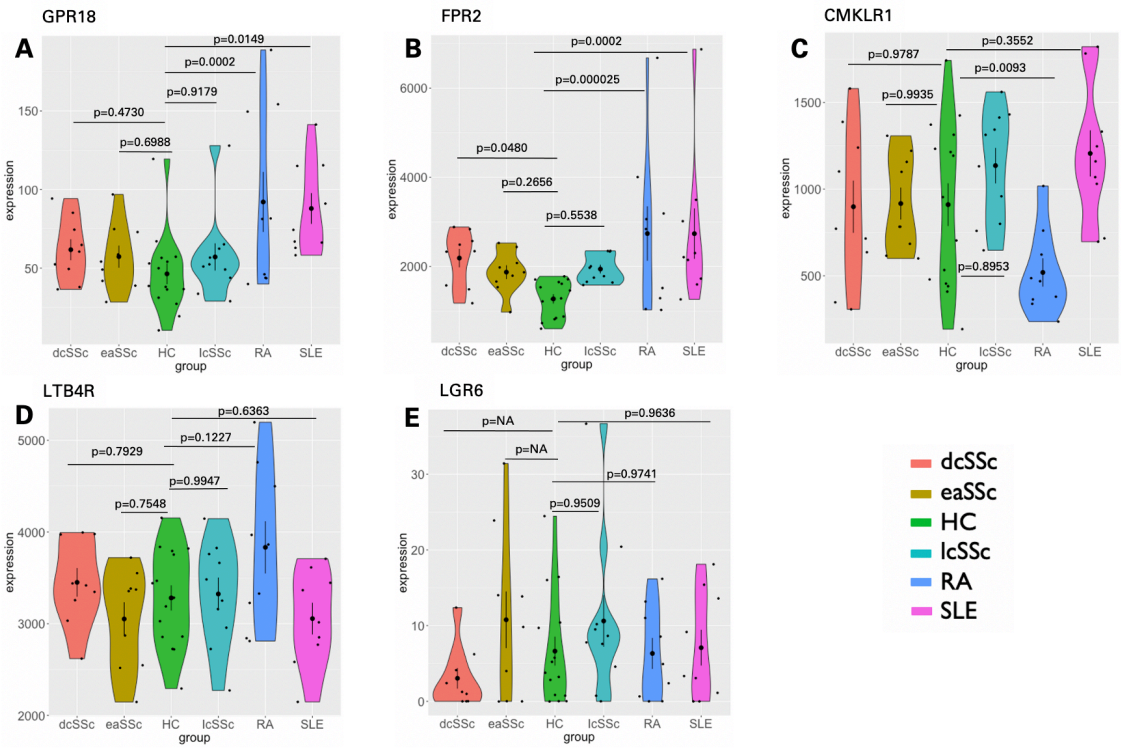

Figure 3.6 SPM receptor expression on monocytes in different conditions.
Violin plots for GPR18 **(A)**, FPR2 **(B)**, CMKLR1 **(C)**, LTB4R **(D)**, LGR6 **(E)** genes with their adjusted p value (calculated with DESeq2 package in Rstudio; p<0.05 is considered significant) are shown for monocytes from diffuse cutaneous systemic sclerosis (dcSSc), early systemic sclerosis (eaSSc), limited cutaneous systemic sclerosis (lcSSc), rheumatoid arthritis (RA), and systemic lupus erythematosus (SLE) compared to healthy monocytes.

As previously mentioned, KEGG pathway analysis showed an involvement of upregulated RA genes in monocytes in osteoclast differentiation pathway. $CD14^+$ monocytes, which are important osteoclast precursors, have been shown to have different phenotypes in RA and healthy individuals, where RA monocytes are metabolically reprogrammed to induce pro-inflammatory signals, which are important for RA onset (McGarry et al., 2021). RA and healthy monocytes also respond differently to TNF (Ansalone et al., 2021), which is the most upregulated gene in RA monocytes (figure 3.2) and is also an important factor in osteoclast differentiation. Therefore, pre-existing RNAseq data from osteoclasts derived from monocytes (mo_OCs) or dendritic cell precursors (dc_OCs) was assessed for SPM receptor expression (data generated in the Goodyear laboratory by Cecilia Ansalone). The SPM receptor expression in osteoclasts was also compared to monocytes, to investigate whether the SPM receptors expressed in monocytes are preserved throughout the differentiation into osteoclasts. The aim of this experiment was to determine the presence of SPM receptors, which is crucial for assessing the optimal timing for the SPM addition (effects of SPMs are studied in

chapter 4), either during the osteoclast precursor state (monocytes) or after they mature into osteoclasts.

The receptor expression compared on healthy monocytes, mo_OCs, and dc_OCs, suggested much higher expression of LTB4R, FPR2 and CMKLR1 receptors on monocytes rather than on osteoclasts (338-fold, 90-fold, and 10-fold, respectively), with a higher expression on mo_OCs than on dc_OCs. FPR2 was not expressed on dc_OCs at all. GPR18 receptor was similarly expressed in monocytes and osteoclasts differentiated from both, monocytes, and DC precursors, although the expression of GPR18 was relatively low. LGR6 receptor was not expressed on osteoclasts at all (figure 3.7 A, table 3.3). Therefore, based on the SPM receptor expression, further work was focused on CMKLR1, FPR2 and LTB4R receptors, as they all have multiple ligands and are highly expressed on healthy and RA monocytes. Receptors GPR18 and LGR6 were not further analysed as LGR6 was not expressed on osteoclasts and was barely expressed on monocytes, and GPR18 only had one ligand (RvD2), which was not the main interest of this thesis.

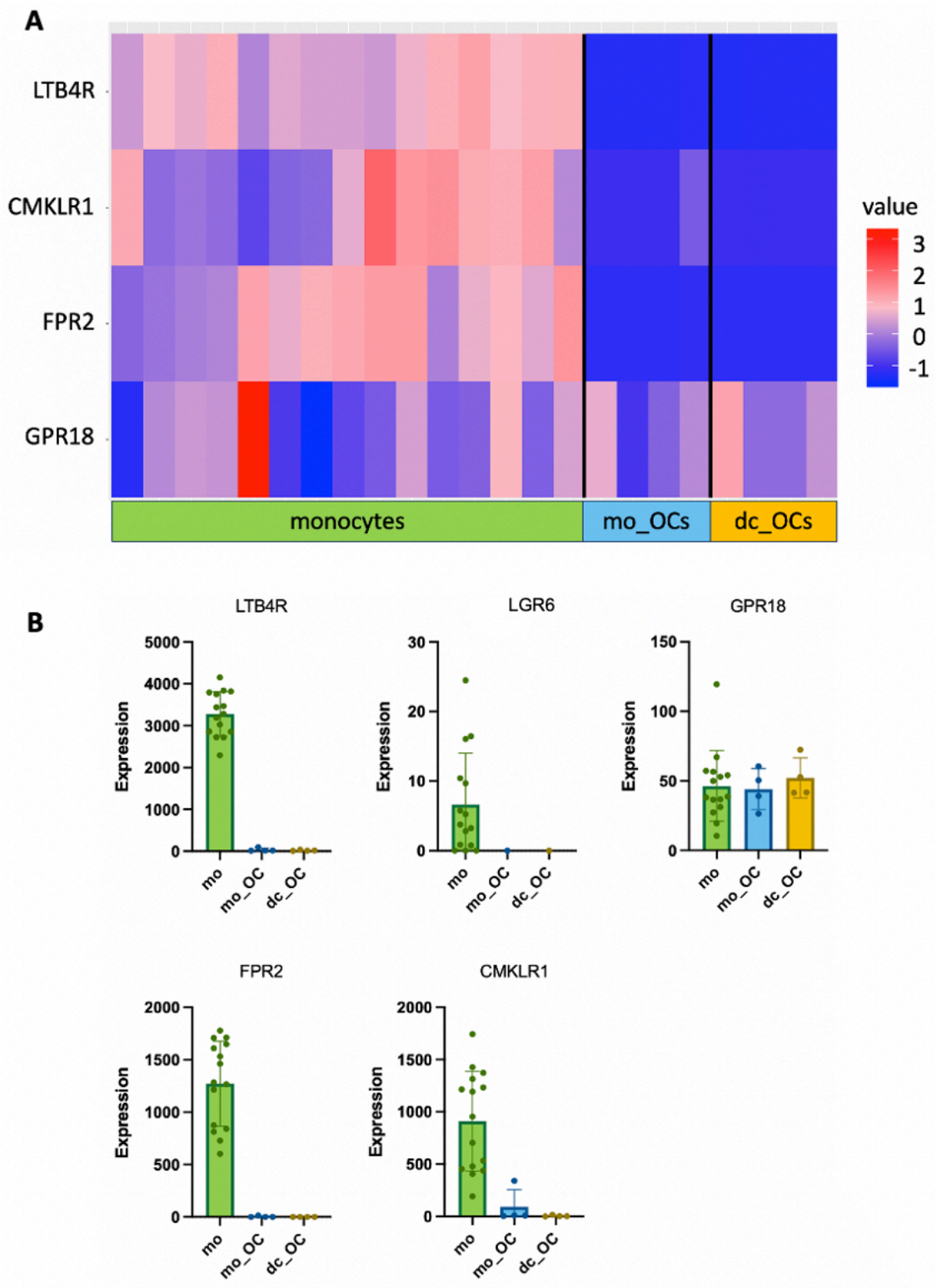

Figure 3.7 SPM receptor expression on healthy monocytes and osteoclasts.
A - Heatmap of 4 expressed SPM receptors, namely LTB4R, GPR18, FPR2 and CMKLR1 on healthy monocytes (n=15), monocyte-derived osteoclasts (mo_OCs; n=4), and osteoclasts differentiated from dendritic cell precursors (dc_OCs; n=4). Red values – high expression, blue values – low expression. **B** - Boxplots showing normalised expression of SPM receptors, namely LTB4R, LGR6, GPR18, FPR2, and CMKLR1 on monocytes (mo, green; n=15), monocyte-derived osteoclasts (mo_OC, blue; n=4), and dendritic cell precursor-derived osteoclasts (dc_OC, yellow; n=4). Dots represent individual donors. Error bars show mean±SD.

Table 3.3 SPM receptor expression on monocytes and osteoclasts
Mean of normalised counts for SPM receptor expression on healthy monocytes (mo) compared to healthy monocyte-derived osteoclasts (mo_OCs) and dendritic cell precursor-derived osteoclasts (dc_OCs).

Receptor	Mean of mo	Mean of mo_OCs	Mean of dc_OCs
GPR18	46.35	44.08	52.03
FPR2	1270.92	3.76	0
CMKLR1	910.35	90.79	5.42
LTB4R	3281.38	36.14	20.40
LGR6	6.63	0	0

3.2.3 The expression of LTB4R is significantly different in RA and healthy monocytes and osteoclasts at the protein level

To understand whether the transcript levels correlate with protein expression, CMKLR1, FPR2 and LTB4R were assessed via western blot. Therefore, in order to investigate the expression of these SPM receptors at the protein level, BCA assay was conducted prior to western blot to acquire the absorbance of all the samples at 570 nm in order to quantify the overall amount of protein in all the samples and to ensure that cells from different donors were applied to the gel at the same concentration (figure 3.8). All the quantified samples were then diluted with RIPA buffer to match the final concentration of the monocytes, which had the lowest overall protein concentration. Monocytes were not further diluted as their concentrations were similar and were already relatively low. Moreover, beta-actin was used as a protein loading control to ensure the same amount of protein was loaded, and all the samples were normalised according to the ß-actin control.

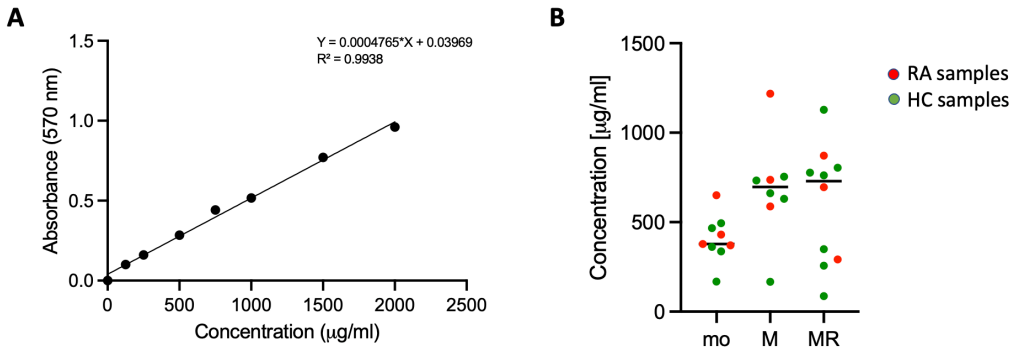

Figure 3.8 BCA assay
A - BCA standard curve at 570 nm absorbance. **B** - A graph showing concentration for monocyte (mo), macrophage (M), and osteoclast (MR) samples from healthy (HC) and RA donors. RA samples are shown in red, while healthy samples are shown in green.

Western blots showed the expression of CMKLR1, FPR2 and LTB4R SPM receptors with 4 RA and 5 healthy CD14⁺ monocytes samples. Based on the ß-actin, one RA sample (RA2) was excluded as no ß-actin band was visible on the western blot membrane. Overall, LTB4R receptor was significantly more expressed in healthy compared to RA monocytes, while CMKLR1 and FPR2 receptors were similarly expressed (figure 3.9). Notably, this does not correlate with the expression at the transcript level evaluated with RNAseq, which showed higher expression of FPR2 in RA, CMKLR1 in healthy, and comparable expression of LTB4R in healthy and RA monocytes; discussed later. However, the expression of ß-actin was not uniform in all the samples, therefore quantification of the expression levels of the SPM receptors is not as reliable.

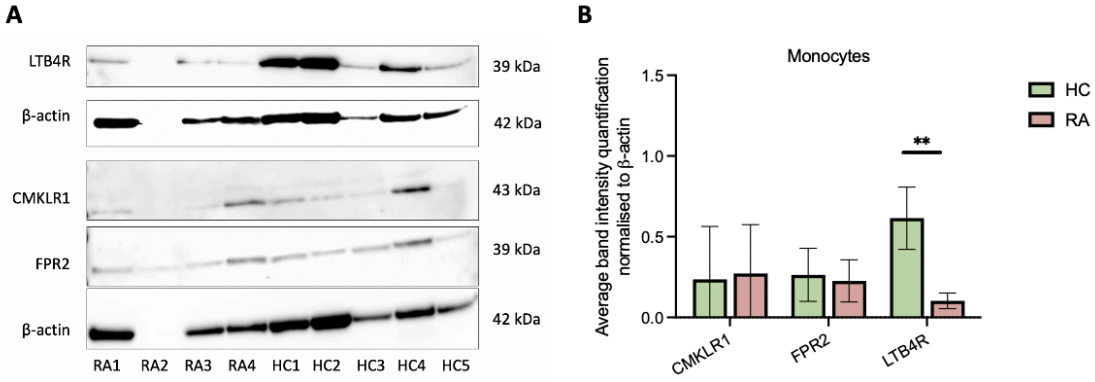

Figure 3.9 SPM receptor expression at the protein level in healthy and RA CD14⁺ monocytes.
A - Western blot showing the expression of 3 SPM receptors (LTB4R, CMKLR1, FPR2) together with 2 ß-actin controls. 2 gels were run in parallel, therefore 2 ß-actin controls were used, 1 for LTB4R and the other for CMKLR1 and FPR2. The results were normalised to ß-actin based on the intensity of the bands analysed by ImageJ. **B** - An average of the band signal intensity for all the RA and healthy samples normalised to ß-actin. RA samples are shown in red, healthy samples are shown in green. Significance is shown with an asterisk (**p≤0.005; unpaired t-test). Error bars show mean±SD (n_{RA}=3, n_{HC}=4).

The expression of these 3 SPM receptors at the protein level was also investigated on macrophages and osteoclasts. These samples were diluted to match the concentration of monocytes, in order to be able to compare the expression on osteoclasts to the SPM receptor expression on their precursors. CMKLR1 receptor was on average (5 healthy and 3 RA donors) similarly expressed in macrophages and osteoclasts, and in healthy compared to RA cells. FPR2 expression was comparable between healthy and RA samples and was slightly higher in osteoclasts than in macrophages, although this was not significant. Lastly, LTB4R was more abundant in healthy compared to RA, with significantly higher expression in healthy osteoclasts. Additionally, its overall expression was more pronounced in macrophages rather than in osteoclasts (figure 3.10 A, B).

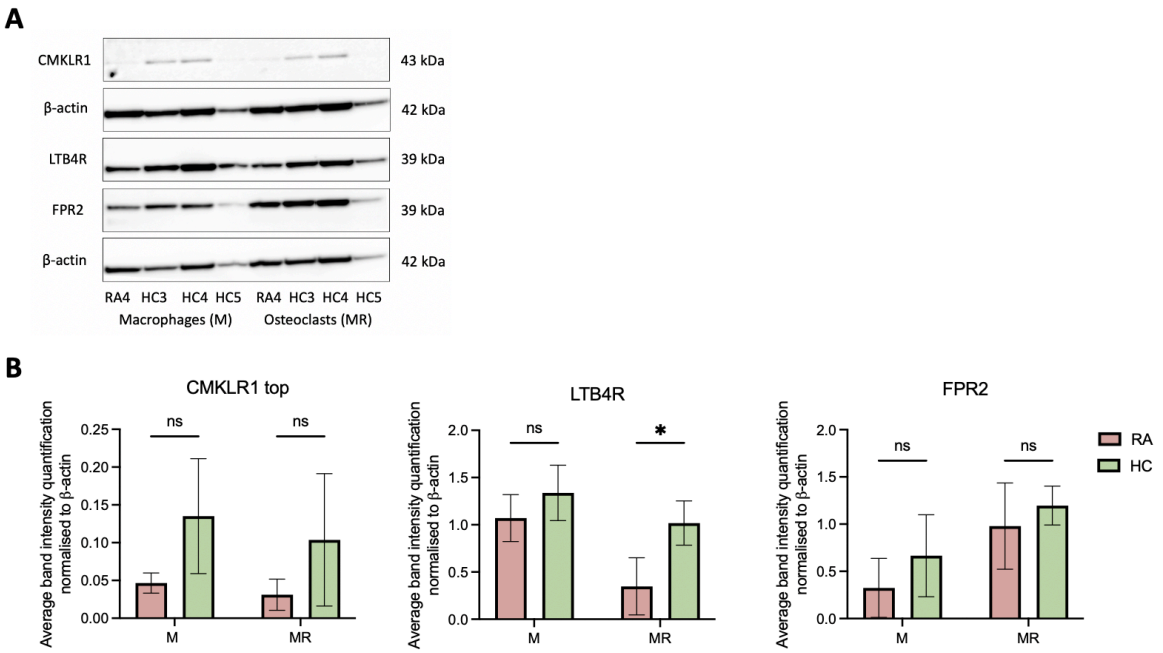

Figure 3.10 SPM receptor expression at the protein level in healthy and RA macrophages and osteoclasts.
A - Representative image of a western blot showing the expression of 3 SPM receptors together with 2 ß-actin controls (one for CMKLR1, and one for LTB4R and FPR2 as they were run on 2 separate gels) on RA and healthy (HC) macrophages (M) and osteoclasts (MR). **B** - Graphs showing average signal intensities for CMKLR1, LTB4R, and FPR2 in healthy (green) and RA (red) macrophages (M) and osteoclasts (MR). Significance is marked with an asterisk (*$p \leq 0.05$; unpaired t-test) and ns means non-significant difference. All the band intensity values are normalised to beta-actin. Error bars show mean±SD ($n_{RA}=3$, $n_{HC}=5$).

In summation, at the protein level, LTB4R was significantly more expressed in healthy compared to RA monocytes and osteoclasts. CMKLR1 and FPR2 were similarly expressed in RA and healthy monocytes, macrophages and osteoclasts at

the protein level. Additionally, LTB4R was most expressed in macrophages, FPR2 expression showed the highest expression on osteoclasts, and CMKLR1 was similarly expressed in different cell types (figure 3.11). Notably, the SPM receptor expression at the protein level was in contrast with the RNAseq data, where CMKLR1 was more expressed in healthy monocytes, FPR2 in RA monocytes, and LTB4R was similarly expressed. Additionally, the expression of these SPM receptors was more pronounced in monocytes compared to osteoclasts at the transcript level, while at the protein level, LTB4R and FPR2 were more expressed in differentiated cells. Notably, the levels of ß-actin were variable between the samples, thus the quantification is a limitation of this experiment. However, the main purpose of this experiment was to confirm the presence of the SPM receptors on osteoclasts and their precursors.

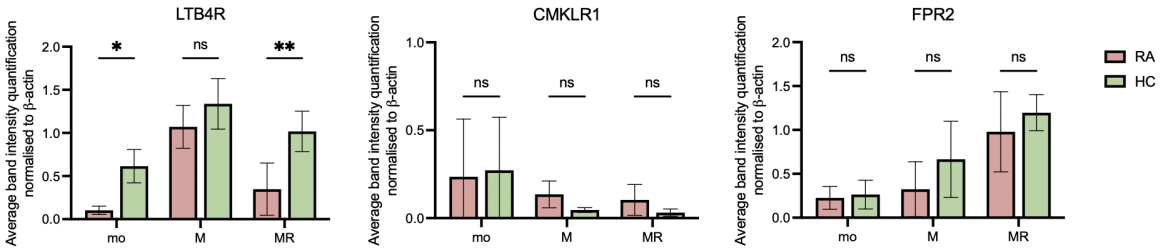

Figure 3.11 Summary of the LTB4R, FPR2 and CMKLR1 SPM receptor expression in monocytes, macrophages, and osteoclasts in RA and health.
Graphs showing average signal intensities for LTB4R, CMKLR1, and FPR2 in RA (red) and healthy (green) monocytes (mo), macrophages (M), and osteoclasts (MR). Significance is marked with an asterisk (*p≤0.05, **p≤0.005; unpaired t-test), while ns means non-significant difference. All the band intensity values are normalised to beta-actin. Error bars show mean±SD.

Lastly, after observing the expression of the SPM receptors at the transcript level and via western blot at the protein level, immunohistochemistry (IHC) was performed. It is important to note that IHC is not a quantitative method and these experiments for different healthy or RA donors were not conducted at the same time. As a result, comparisons between healthy and RA donors cannot be made due to variations in microscope settings, however different conditions (macrophages vs osteoclasts) within the same donor for the same antibody can be compared. Notably, no positive controls were included in this experiment, therefore, it cannot be proved that primary antibodies are not binding non-specific proteins (mainly given their unexpected cytoplasmic localisation). However, this experiment was conducted just to confirm the presence of LTB4R, FPR2 and CMKLR1 on macrophages (3.12 A) and osteoclasts (3.12 B). In conclusion,

the presence of all 3 SPM receptors was observed on healthy and RA macrophages and osteoclasts (healthy donor not shown due to similarity to RA donors, thus, only images from 1 representative RA donor are shown; figure 3.12).

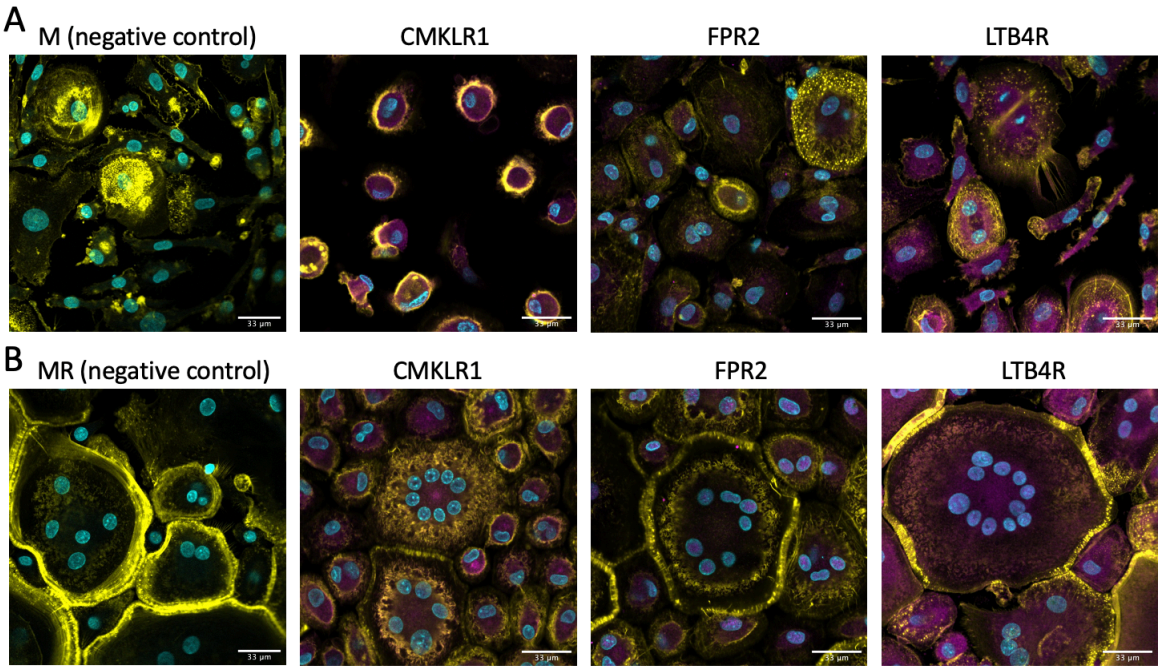

Figure 3.12 SPM receptor expression on macrophages and osteoclasts at the protein level with IHC.
Representative IHC images (n=1) of CMKLR1, FPR2 and LTB4R receptors in RA expressed on **A -** macrophages, i.e., only in the presence of M-CSF (M) and **B -** on osteoclasts, i.e., in the presence of M-CSF and RANKL (MR) with negative controls (20x magnification; scale bar = 33 μm). Yellow – actin ring (Phalloidin), blue – nuclei (DAPI), magenta – expressed receptor.

3.3 Discussion

This chapter focused on assessing SPM receptor expression on osteoclasts and their precursors in health and RA. This was important as currently there is only limited research on SPM receptors, especially when it comes to primary human cells and osteoclasts. Understanding the expression of these receptors on osteoclasts and their precursors can inform not only about which signalling can be modulated via the addition of specific SPMs but also the right timepoint for their stimulation, which will be further evaluated in chapter 4.

Analysis of RNAseq data revealed that certain SPM receptors were expressed in both osteoclasts and their precursors, while some were only expressed in monocytes (e.g., LGR6), and some were not expressed on either cell type at all (e.g., GPR32). Therefore, it can be speculated that stimulation of the expressed

SPM receptors with specific SPMs could potentially modulate osteoclast differentiation. Many SPM receptors act in a promiscuous manner, which essentially means they can be activated by various ligands. For example, FPR2 receptor can not only interact with RvD1 and LXA4 but can also bind anti-inflammatory annexin-1 or serum amyloid A, which is essential in tracking inflammation (Wang & Colgan, 2017). Similarly, CMKLR1 binds RvE1 and/or chemerin, and LTB4R binds RvE1, RvE2, and LTB4 (Serhan, 2020). This thesis shows that the selected SPM receptors are expressed in healthy and RA monocytes, as well as in monocytes from patients with other rheumatic diseases like SSc and SLE. The expression of FPR2 was significantly more expressed in dcSSc and SLE monocytes compared to healthy monocytes, while the expression of all 3 SPM receptors (CMKLR1, FPR2, and LTB4R) was relatively high in SSc and SLE. Therefore, there is a possibility that the contribution of SPMs via the expressed SPM receptors in disease pathogenesis could be beneficial not only in RA, but also in SSc and SLE. However, as the main focus of this work is on RA, and SSc and SLE were beyond the scope of this thesis, future studies are needed to explore the effect of SPMs in these diseases. This analysis was also necessary to understand the expression of SPM receptors, which might provide insights into potentially active pathways following SPM signalling in healthy individuals and in patients with RA, as the receptor expression varies in different settings. For example, based on these data, SPMs binding CMKLR1 may work better in healthy individuals as CMKLR1 is more expressed in healthy monocytes, while the SPMs binding FPR2 receptor might have a higher impact in RA patients. The effect of SPMs on osteoclast differentiation and function will be tested in chapter 4.

Consistent with data from the literature, pathway analysis of upregulated genes in RA monocytes highlighted the bone destruction/damage typical for the disease pathology. Some of the upregulated pathways in RA compared to healthy monocytes involved NF-κB pathway, TNF signalling, IL-17 signalling, MAPK signalling, RA, and osteoclast differentiation, which are all linked to inflammation and osteoclastogenesis. These pathways are interesting as there is a lot of overlap and potential cooperation with each other, and it is necessary to understand their actions in order to be able to attenuate them. The osteoclast differentiation pathway was the main interest of this study. This pathway involved a number of upregulated RA genes like TNF, M-CSF, IL-1, NFκB1, NFκB2, IκB, PU.1 or PPaR

gamma, from which TNF was the most upregulated. The osteoclast differentiation pathway was also linked with several other pathways like PI3K/Akt, MAPK, NF-κB, JAK/STAT and calcium signalling pathways. Some of these genes and pathways are also associated with the SPM signalling and are necessary for osteoclast differentiation, bone resorption and inflammation. For example, RvE1 activates PI3K/Akt pathway, and together with MaR1 blocks MAPK, ERK (extracellular signal-regulated kinase), and NF-κB signalling pathways, thus contributes to the resolution of inflammation (Cezar et al., 2019; Li et al.,2020; El Kholy et al., 2018; Keinan et al., 2013). RvD1, similarly to MaR1 also blocks NF-κB pathway (Krishnamoorthy et al., 2010; Wu et al., 2021). Therefore, these SPMs have a potential to inhibit/activate these pathways and contribute to the inhibition of osteoclastogenesis and bone resorption, and resolution of inflammation.

After investigating the SPM receptor expression at the transcript level, their expression was also evaluated at a protein level. All the assessed receptors were expressed in both, osteoclasts and their precursors, but their distribution in healthy vs RA did not correspond to the RNAseq data. In the RNAseq data, the highest expression of FPR2 was recorded in RA, while CMKLR1 was more expressed in healthy monocytes, and LTB4R was similarly expressed. At the protein level, LTB4R was more expressed in healthy and CMKLR1 and FPR2 were similarly expressed in health and RA. These differences in the expression at the transcript and protein level might be due to several factors. One of the reasons could be that the antibody used for western blot did not target all isoforms of the SPM receptors, therefore it is possible that different isoforms have variable levels of expression, which could also contribute to variations between transcript and protein level. Notably, the levels of ß-actin were variable in different samples, which could have an effect on quantification of the SPM receptors. Other factors could be different rate of protein expression kinetics in monocytes and osteoclasts, and in RA compared to healthy samples, mRNA decoy, or protein degradation (Stein & Frydman, 2019).

Notably, to provide a comprehensive analysis of SPM receptor expression, further studies are required in a larger cohort. Furthermore, paired experiments like RNA sequencing on monocytes, macrophages, and osteoclasts could be done. The same donors could also be used for the protein validation (i.e., western blot). This

would reduce the variations between different experiments, allow comparisons between monocytes, macrophages, and osteoclasts and provide more accurate data on the transcript and protein expression in these cells. Additionally, it would provide information about the SPM receptor expression at the transcript level in RA compared to healthy osteoclasts and their precursors. Currently different donors were used for all the experiments, which resulted in different datasets, bigger donor variations and inconsistencies. Donor variability is another important factor in protein expression experiments, which in some samples contributed to non-significant differences possibly due to low sample size. However, only 50 ml of blood could be taken from every patient, which after $CD14^+$ monocytes isolation led to very low cell numbers, varying from donor to donor. This only allowed for limited experiments with carefully planned conditions and was not enough to do 3 or more paired experiments. Another complementary experiment that could be done would be flow cytometry, which could detect the SPM receptor expression on osteoclasts and their precursors. Flow cytometry, however, would require more donors and a lengthy optimisation for the new antibodies, which was not feasible due to lack of time and donors.

There is only limited research on SPM receptor expression on human monocytes and osteoclasts. Moreover, there is also lack of knowledge on the role of these receptors and SPMs in health and RA, which makes it challenging to compare the results from this work to other studies. However, one study investigated the expression of CMKLR1 in healthy undifferentiated cells, osteoclast precursors and osteoclasts from murine bone marrow by qPCR. Their findings showed the highest expression in monocytes. They also show downregulation of CMKLR1 in pre-osteoclasts (differentiated with RANKL for 24 or 48 hours), with the gene being gradually upregulated again in osteoclasts 72h post-RANKL addition. Although the expression was still higher on monocytes, the difference in expression on mature osteoclasts was less distinct than in pre-osteoclasts (3-fold) (Ramos-Junior et al., 2016). This thesis analysed osteoclasts differentiated for 120 hours, however, high levels of CMKLR1 transcript were recorded in monocytes, while osteoclasts showed much lower expression, which would be consistent with the above-mentioned study. Another study by Bouchareychas et al. tested the LTB4R expression on murine bone marrow macrophages and osteoclasts via their DNA-microarray analysis. They observed a higher expression on macrophages than osteoclasts

(Bouchareychas et al., 2017). However, this thesis did not use DNA-microarray analysis and even though the expression levels cannot be directly compared to the protein expression due to various epigenetic modifications, these results showed slightly higher expression on macrophages than on osteoclasts at the protein level, which would also be consistent with this study. Bouchareychas et al. also described the importance of the LTB4R receptor, suggesting that LTB4R regulates RANKL signalling and osteoclastogenesis activation. When RvE1 binds LTB4R, it prevents the binding of leukotriene B4 (LTB4), a proinflammatory SPM, thus attenuates NF-κB pathway, which further leads to the reduction of osteoclast differentiation and inflammation resolution. LTB4 on the other hand, counter regulates the effect leading to the NF-κB and IκB activation and Ca^{2+} signalling via LTB4R receptor contributing to synovial inflammation *in vivo* and bone resorption *in vitro*. No similar studies defining the expression of SPM receptors on osteoclasts and their precursors were found for the FPR2 receptor.

The findings in this thesis suggest that as LTB4R and FPR2 were more expressed on differentiated cells than on monocytes, therefore, the SPM addition might be more beneficial later on in the differentiation process, i.e., to osteoclast precursors/osteoclasts rather than monocytes. The next chapter will delve further into the evaluation of the SPM addition at both early and late timepoints. The addition of SPMs to monocytes could lead to the prevention and early inhibition of osteoclastogenesis and bone resorption. However, investigating the addition of SPMs to osteoclasts could be valuable, as it may help to halt the progression of bone degradation and osteoclast differentiation in patients with active RA. Therefore, to address this, the following questions need to be answered, which will be further elaborated in chapter 4.

1. *Can the addition of various SPMs early on in the differentiation process prevent osteoclastogenesis and osteoclast functions?*

2. *Can the addition of SPMs at later time points block the actions of mature osteoclasts and halt their function which could further reduce bone erosion in patients with RA?*

3.4 Conclusion

This chapter provides an insight into the expression patterns of specific SPM receptors on monocytes and osteoclasts in healthy individuals and patients with RA and other rheumatic diseases. The results suggest differences in expression levels of these receptors between different cell types in healthy donors and RA patients at a transcript and protein level. In summation, 3 SPM receptors were selected for further investigation based on their expression namely CMKRL1, FPR2, and LTB4R. These findings show the importance of investigating the impact of ligands binding to SPM receptors on osteoclasts and their precursors in health and disease in order to elucidate their potential as a novel treatment option.

Chapter 4 The effect of specialised pro-resolving lipids on osteoclastogenesis

4.1 Introduction

SPMs are lipids that have shown to be effective in inflammation, infection, arthritis or treating pain. It has also been observed that supplementation with omega 3 fatty acids (e.g., fish oil consumption), which are SPM precursors, can enhance the production of plasma SPMs and limit RA activity (Serhan & Levy, 2018). Furthermore, SPMs have a wide range of positive effects in health and disease (e.g., RA, cardiovascular diseases, diabetes, and cancer) and are essential in the resolution of inflammation and tissue regeneration (Abdolmaleki et al., 2019; Headland & Norling, 2015). Functionally, SPMs have the ability to reduce recruitment of leukocytes, stimulate neutrophil apoptosis and increase macrophage efferocytosis (Headland and Norling, 2015). SPMs can also regulate pro-inflammatory mediators (cytokines (e.g., IL-17, IL-23, IL-6, IFN-γ), prostaglandins, or leukotrienes), involved in the inflammatory process (Arnardottir et al., 2016). Additionally, they can contribute to the switch of macrophages from pro-inflammatory to pro-resolving macrophages, which are further involved in tissue repair and recovery (Headland & Norling, 2015) (figure 4.1).

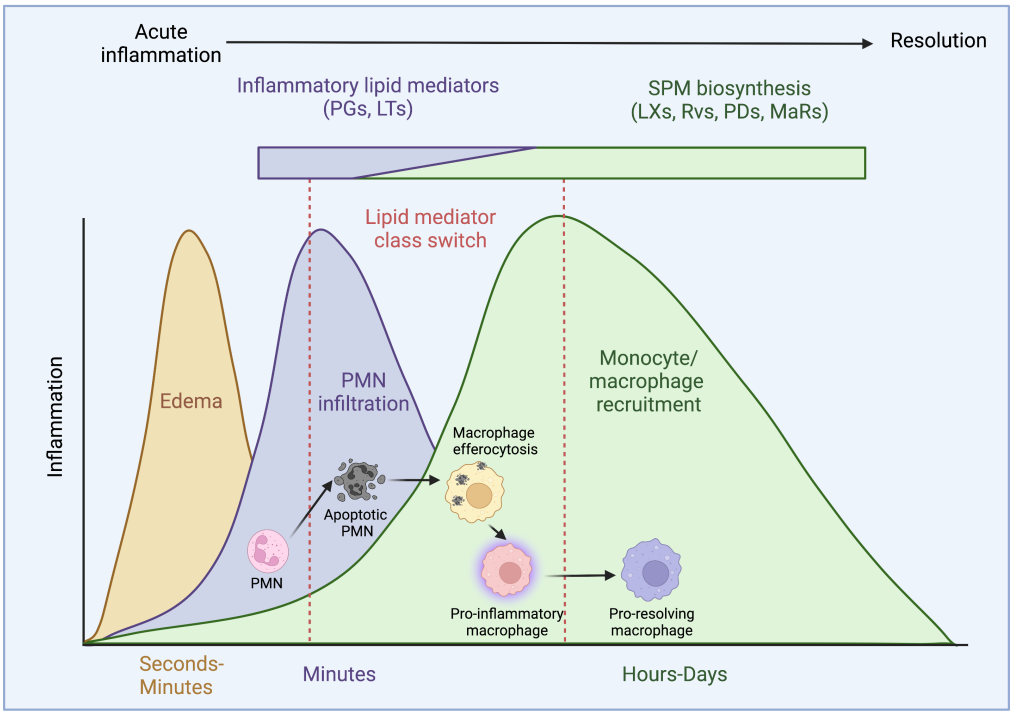

Figure 4.1 Resolution of inflammation via lipid mediator class switching.
The ideal result of inflammation is its resolution, which can be done by lipid mediator class switching. First stage of inflammation is edema, which is due to the release of pro-inflammatory lipid mediators like prostaglandins (PGs) and leukotrienes (LTs). As a response to pro-inflammatory mediators, polymorphonuclear neutrophils (PMNs) are released to help with the inflammation by removing the pathogen. As a result, PMNs undergo apoptosis and start releasing pro-resolving lipid mediators (i.e., resolvins (Rvs), lipoxins (LXs), maresins (MaRs), and protectins (PDs)) instead of pro-inflammatory mediators (PGs and LTs). Macrophages then remove apoptotic PMNs by efferocytosis, which results in a phenotypic switch from pro-inflammatory to anti-inflammatory macrophages, which release more pro-resolving mediators. Pro-resolving mediators further stop the recruitment of PMNs, which further leads to the resolution of inflammation. Created in BioRender, figure adapted from Sansbury & Spite, 2016 and Serhan & Levy, 2018.

SPM research is still in its early stage, but there is the potential that SPMs could not only help modulate pathology and drive repair (e.g., bone and cartilage regeneration) across a variety of diseases, but also provide anti-infective and analgesic properties. Previous studies have indicated a role of certain SPMs and their precursors in the context of macrophage and osteoclast differentiation. For example, RvE1 can inhibit RANKL-induced osteoclastogenesis and bone resorption by supressing the expression of some key osteoclast markers i.e., tartrate-resistant acid phosphatase (TRAP), cathepsin K, and metalloproteinase-9 (MMP-9) in osteoclastic cells from murine bone marrow (Funaki et al., 2018). Similarly, RvD1 can also reduce TRAP and cathepsin K production and inhibit osteoclastogenesis and bone resorption in RAW 264.7 cells and arthritic mice (Benabdoun et al., 2019). Additionally, it can regulate pro-inflammatory and anti-inflammatory cytokines and reduce reactive oxygen species (ROS) production,

which affect osteoclast differentiation and survival, as well as bone resorption (Agidigbi & Kim, 2019; Leuti et al., 2019).

Even though RvE1 and RvD1 showed an inhibitory effect on osteoclastogenesis, these experiments were conducted in murine models or RAW264.7 cell lines, but their effect on primary human cells remains unclear (Kholy et al., 2018; Funaki et al., 2018; Herrera et al., 2008; Benabdoun et al., 2019; Yuan et al., 2010; Klein et al., 2022). Therefore, this chapter investigated the effect of RvE1, RvD1, MaR1, and 17-HDHA on osteoclasts created through the cell fusion of their primary human mononuclear precursors in the presence of M-CSF and RANKL with or without tumour necrosis factor (TNF). The effect of SPMs was tested on monocyte-derived and dendritic cell precursor (pre-DC)-derived osteoclasts in health and RA in order to investigate the effect on osteoclastogenesis, bone resorption, and signalling pathways involved in osteoclastogenic processes.

4.2 Results

4.2.1 Differentiation of osteoclasts from THP-1 cells

THP-1 is a human monocytic cell line derived from patients with acute leukaemia and was established as a reliable human osteoclast model (Li et al., 2017). The main advantages of this cell line are that it is a human cell line, it has a high rate of proliferation, the cells are immortal, osteoclasts can be differentiated in a relatively short time, there are no ethical issues and there are no major individual variations, as is the case with primary human cells (Li et al., 2017).

THP-1 cells were used in this thesis as an alternative plan for osteoclast differentiation as it was not possible to obtain fresh blood and isolate primary human cells due to the Covid-19 pandemic. Therefore, experiments with THP-1 cells were conducted according to a protocol used by other members of the lab, however, the differentiation was not successful as THP-1 cells failed to differentiate into osteoclasts. Despite the experiments being repeated a few times with new THP-1 cell lines, the results were comparable. Following the TRAP staining, none of the cells displayed the characteristic purple colour, which indicated a lack of mature osteoclasts. Moreover, no multinucleated cells were present and the cells with the RANKL addition resembled the undifferentiated

cells in the control wells. To investigate why THP-1 cells remained in their precursor state and did not differentiate into mature osteoclasts, qPCR was performed to assess the receptor expression of CSF-1R (M-CSF receptor), RANK (RANKL receptor), and TRAP (marker of mature osteoclasts) with 18s as a housekeeping gene. The expression was evaluated 24 hours after the addition of phorbol 12-myristate 13-acetate (PMA), M-CSF or RANKL and on day 14 of osteoclast differentiation. The results suggested that RANK, CSF-1R and TRAP transcripts were barely expressed on cells lysed 24 hours post PMA or cytokine addition. The expression of CSF-1R and TRAP was increased in transcripts of cells lysed after 14 days, however, the lack of purple colour also suggests no TRAP expression at the protein level. RANK receptor's C_T values after qPCR were above 30, indicating very low or almost non-detectable expression (figure 4.2). Given the need for RANK expression to initiate osteoclastogenesis, the absence of RANK transcript expression was most likely the reason for the non-differentiation of THP-1 cells into osteoclasts. After several unsuccessful attempts and after the lab's and clinics' reopening after the COVID-19 pandemic, THP-1 cells were no longer used and were replaced with primary human cells obtained from whole blood or leukocyte cones. Leukocyte cones contain blood that is enriched with different cell types found in blood, which provides much higher cell counts compared to cells isolated from fresh whole blood.

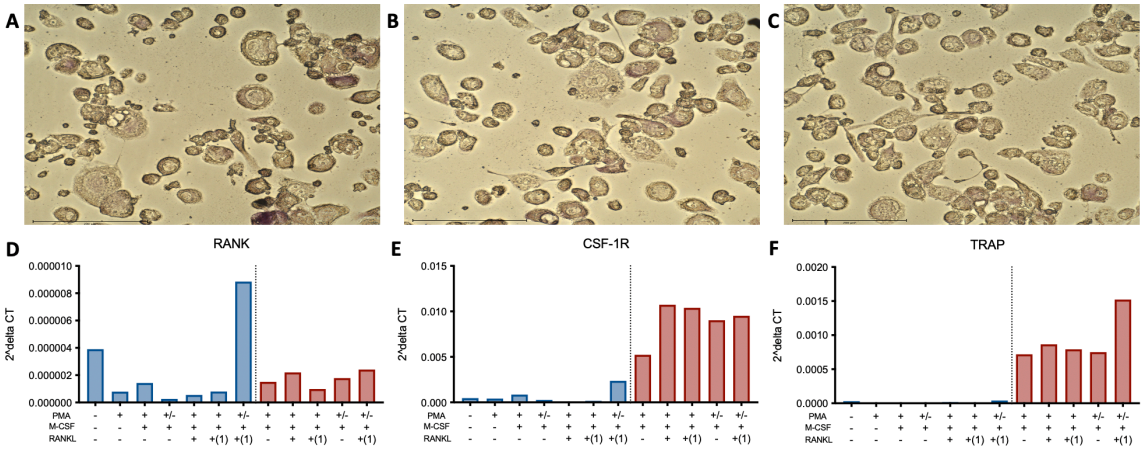

Figure 4.2. THP-1 cell differentiation into osteoclasts with their qPCR transcripts.
THP-1 cells were differentiating in the presence of PMA only (A), with PMA and M-CSF (B), or in the presence of PMA, M-CSF and RANKL (C) for 14 days. Transcripts of RANK (D), CSF-1R (E) and TRAP (F) receptors under different conditions were assessed by qPCR. Blue bars – cells were lysed 24 hours after the addition of PMA, M-CSF or RANKL, red bars – cells were lysed after 14 days. "+" means the addition of M-CSF, RANKL or PMA, while "-" shows its absence. "+/-" shows that the cells were pre-incubated with PMA for 4 days, after which PMA was removed and the cells were incubated only in the presence of M-CSF and RANKL. "+(1)" means the addition of RANKL a day after M-CSF and not simultaneously as indicated with "+". 20x magnification; scale bar = 200 μm.

4.2.2 Optimisation of osteoclastogenesis from CD14+ primary monocytes

It is well established that osteoclasts can be differentiated from monocytes or macrophages (Yao et al., 2021). However, to verify this, $CD14^+$ monocytes were isolated and subsequently stimulated with M-CSF for 1 day (24h), 3 days or 6 days prior to the addition of RANKL. This was undertaken to achieve three separate states within the cultured cells. In explanation, exposure to M-CSF for 1 day results in cells that retain a monocyte state, 3 days results in cells that are primed to become macrophages but are not yet fully differentiated, whilst 6 days results in fully mature macrophage.

Overall, the highest number of mature osteoclasts was recorded once RANKL was added to cell cultures 24h post M-CSF addition after 10 days of differentiation (~400 osteoclasts when added on day 1, compared to ~300 when added on day 3, and ~200 when added on day 6). Additionally, osteoclasts observed with the RANKL addition 24h after M-CSF were the biggest (figure 4.3 A). After further inspection, sealing zone-like structures could be observed around the largest osteoclasts in the cultures that received M-CSF for either 1 or 3 days, but not for 6 days. This suggests lower capacity of macrophages compared to monocytes to differentiate into mature osteoclasts as after 6 days with M-CSF only, cells are commited to become macrophages, which makes them less effective for osteoclast differentiation (figure 4.3 B). Notably, the sealing zone is created when osteoclasts attach to a bone during the resorption and separate the resorption area from the rest of the environment, causing the released degrading enzymes to stay within the resorption area (see chapter 1.2.3.2 for bone resorption process). However, when osteoclasts are adherent on plastic or glass instead of mineralised matrix, as in this case, they do not form a sealing zone, but a similar sealing zone-like structure called the “podosome belt” or the “actin ring” (Georgess et al., 2014; Takito et al., 2018). Therefore, for further experiments, RANKL was added 24h after the M-CSF addition as it exhibited the highest number of mature $TRAP^+$ osteoclasts with clear actin ring formed around the osteoclasts.

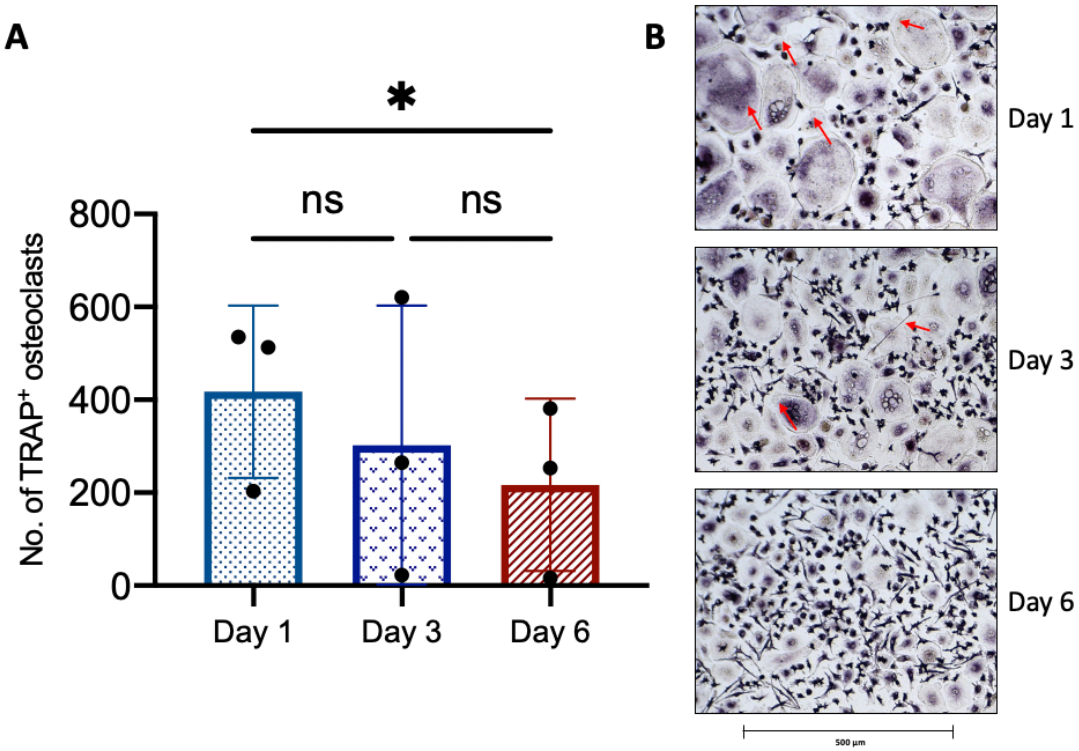

Figure 4.3 Differentiation of osteoclasts from macrophages and their precursors with RANKL addition on day 1, 3, and 6.
A - Number of mature osteoclasts with the addition of RANKL at different timepoints, specifically on day 1 to monocyte, day 3 to cells primed to become macrophages, and day 6 to mature macrophages. Bars show mean±SD of n=3. Significance is shown with an asterisk, where *p≤0.05. Statistical analysis was performed using paired parametric t-test after passing the Shapiro-Wilk's normality test. Individual dots represent individual donors. **B** - Representative images of TRAP-stained osteoclasts (10x magnification; scale bar = 500 µm) with the RANKL addition on day 1, day 3 and day 6. Examples of actin rings ("sealing zone") are shown with red arrows.

In addition to optimising the right time-point for the RANKL addition, it was also necessary to optimise TNF addition. TNF was added to simulate inflammation; a hallmark of RA. Given the limited availability of RA samples, all the experiments were initially optimised in healthy cells due to easier accessibility. Moreover, the number of RA samples was limited, and blood volume was restricted to 50 ml per patient, which would not be sufficient for complete optimisation. Initial experiments compared addition of 1 and 10 ng/ml of TNF 24h post M-CSF addition but simultaneously with 25 ng/ml of RANKL. Consistent with previous finding (Ansalone et al., 2021), both concentrations of TNF led to a significant inhibition of osteoclastogenesis when compared to the control with no TNF (figure 4.4 A). The inhibition was dose-dependent with higher effect recorded with 10 ng/ml of TNF (68.8% inhibition compared to 19.6% inhibition with 1 ng/ml of TNF). This can also be observed in TRAP-stained osteoclasts resulting in smaller osteoclasts with 10 ng/ml of TNF compared to 1 ng/ml, with even lower cell fusion and well

coverage (figure 4.4 C). Even though the conducted experiments were confirmatory with known outcomes, it was important to verify that the assay works and that TNF addition after 24h really results in the inhibition of osteoclasts within this experimental setup.

To further examine the impact of TNF on the function of osteoclasts, a bone resorption assay was performed. These results showed that the differentiated cells had a similar ability to resorb bone with 1 ng/ml of TNF when compared to the control, while 10 ng/ml of TNF led to a ~13% reduction in bone resorption (figure 4.4 B, D). Based on the findings, all subsequent experiments used 10 ng/ml of TNF.

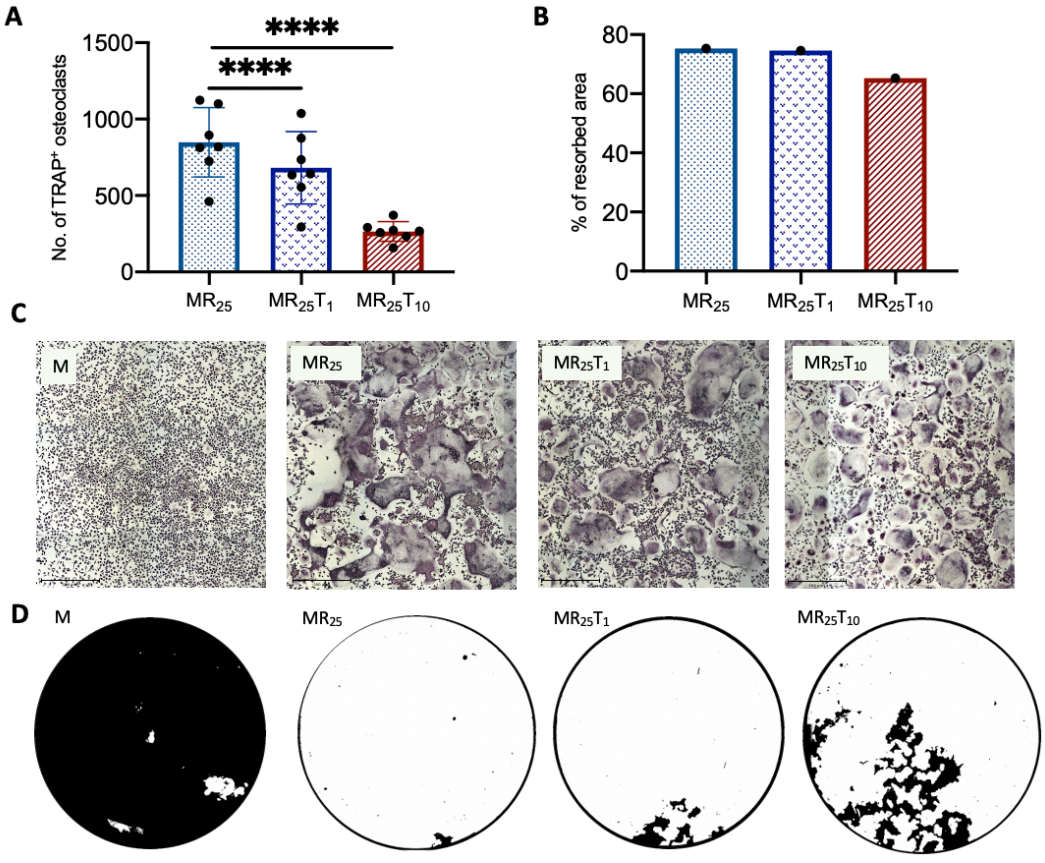

Figure 4.4 Inhibition of osteoclastogenesis with TNF added 24 hours after M-CSF addition.

A - Number of osteoclasts differentiated only with M-CSF and 25 ng/ml RANKL (MR25) in the absence of TNF, with 1 ng/ml of TNF ($MR_{25}T_1$), or with 10 ng/ml of TNF ($MR_{25}T_{10}$). Bars show mean±SD of n=7. Significance is shown with asterisks, ****p≤0.0001. Statistical analysis was performed using paired parametric t-test after passing the Shapiro-Wilk's normality test. **B** - Percentage of resorbed area of calcium phosphate plates under the same conditions, i.e., no TNF, 1 ng/ml or 10 ng/ml of TNF (n=1). **C** - TRAP-stained images (10x magnification) of macrophages (M), osteoclasts without TNF (MR_{25}), osteoclasts with 1 ng/ml of TNF ($MR_{25}T_1$) and 10 ng/ml of TNF ($MR_{25}T_{10}$). 10x magnification; scale bar = 500 µm. **D** - Representative digital images of resorption pits in the absence or presence of RANKL and/or TNF. Mineral substrate in black and resorption pits in white.

The above-mentioned study by Ansalone et al. (2021) had also shown that the inhibition of osteoclastogenesis was due to the activation of canonical NF-κB pathway via TNFR1 receptor. In comparison, TNF added to $CD14^+$ monocytes 72 hours after stimulation with RANKL lead to an upregulation of the TNFR2 receptor, which resulted in the activation of non-canonical NF-κB pathway and enhanced osteoclastogenesis synergically with RANKL (Lam et al., 2000; Luo et al., 2018). However, when the same timing of cytokine exposure was applied in this thesis, the number of osteoclasts remained comparable in the presence and absence of TNF at both concentrations (figure 4.5 A). Ansalone et al. (2021) also proposed that it is at the sub-optimal level (1 ng/ml) of RANKL that the synergistic effect of TNF is observed, however, no differences were observed when a sub-optimal RANKL concentration (1 ng/ml) was implemented in this work 72h post RANKL addition (Figure 4.5 B).

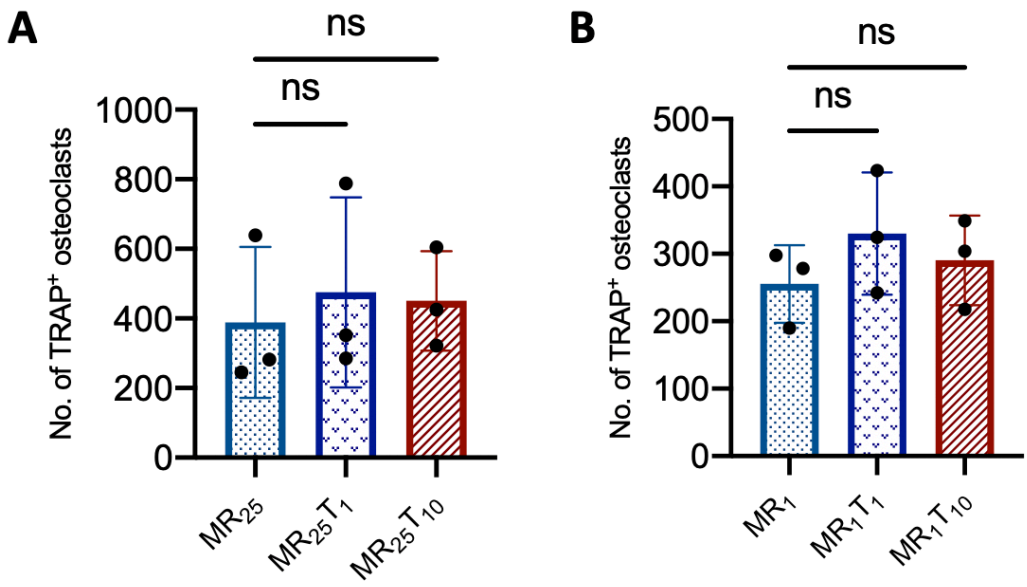

Figure 4.5 The addition of TNF 72 hours post M-CSF and RANKL addition.
A - Quantification of $TRAP^+$ osteoclasts differentiated with 25 ng/ml of M-CSF and 25 ng/ml RANKL (MR_{25}) used as a control, with the addition of 1 ng/ml of TNF ($MR_{25}T_1$), or with 10 ng/ml of TNF ($MR_{25}T_{10}$) **B -** Quantification of $TRAP^+$ osteoclasts at 1 ng/ml of RANKL. MR_1 – 25 ng/ml M-CSF and 1 ng/ml RANKL used as a control, MR_1T_1 – differentiation with MR_1 in the presence of TNF at 1 ng/ml, MR_1T_{10} - differentiation with MR_1 in the presence of TNF at 10 ng/ml. Error bars are shown as mean±SD for n=3. Paired parametric t-test was conducted after passing the Shapiro-Wilk's normality test (ns means non-significant).

Since no significant effect of TNF was observed when added 72h after the addition of RANKL, it was investigated whether TNF can enhance osteoclastogenesis in our setting. Here, $CD14^+$ monocytes were treated with M-CSF and RANKL as previously,

however, TNF was added 96h post RANKL exposure, and different $CD14^+$ isolation kit was used, which might explain discrepancies in the results when compared to Ansalone et al. (2021). Despite the later TNF addition, number of osteoclasts and bone resorption were comparable to the control with no TNF (figure 4.6).

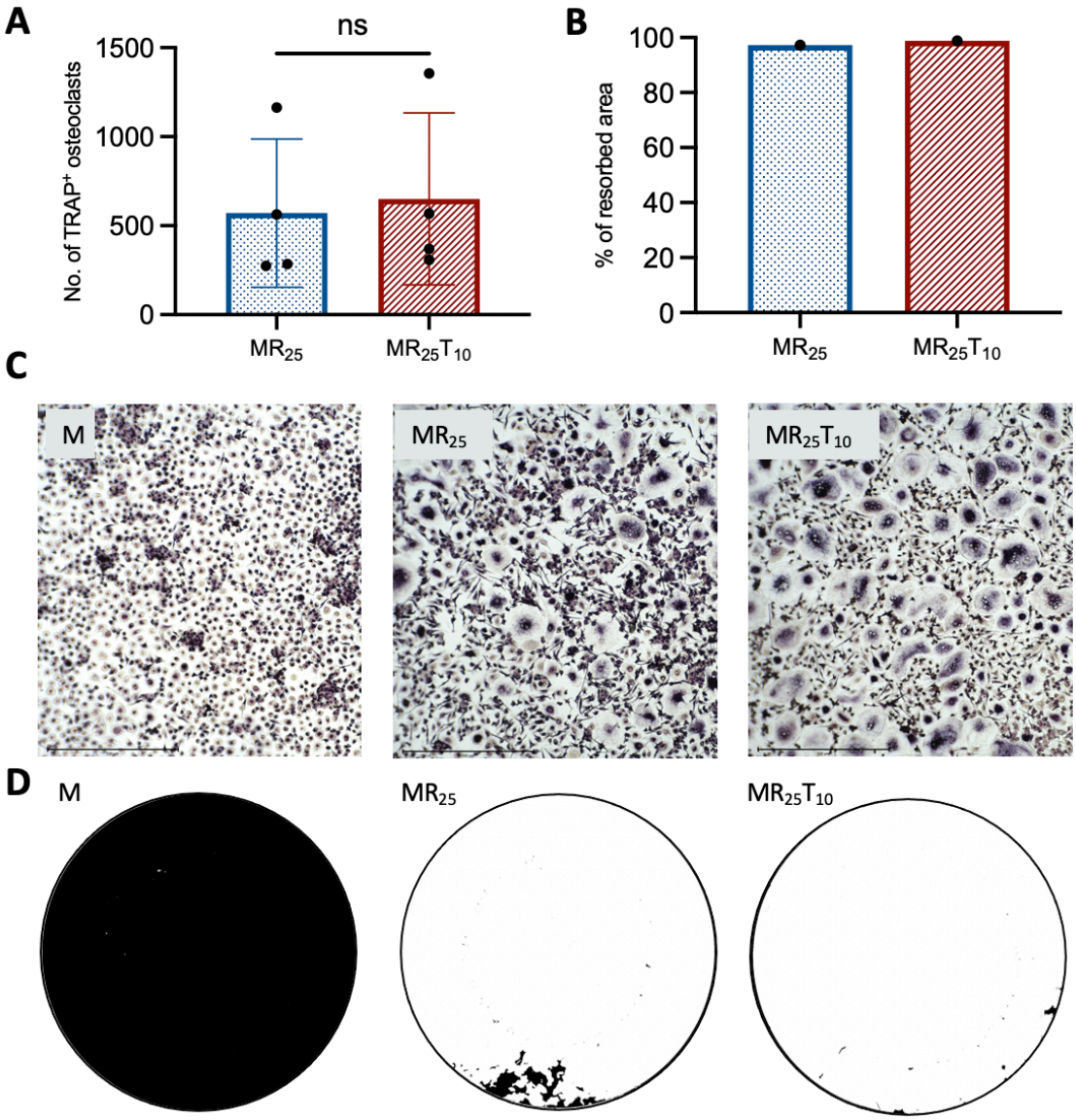

Figure 4.6 The addition of TNF 96 hours after the addition of M-CSF with the RANKL concentration of 25 ng/ml.
A - Number of osteoclasts differentiated only with 25 ng/ml of M-CSF and 25 ng/ml RANKL (MR_{25}) in the absence of TNF or with 10 ng/ml of TNF ($MR_{25}T_{10}$). Error bars are shown as mean±SD for n=4. Paired parametric t-test was conducted for significance, ns – non-significant. **B** - Percentage of resorbed area of calcium phosphate plates under the same conditions, i.e., no TNF or 10 ng/ml of TNF, n=1. **C** - TRAP-stained images of macrophages differentiated with M-CSF only (M), osteoclasts without TNF differentiated with M-CSF and 25 ng/ml of RANKL (MR_{25}), or 10 ng/ml of TNF ($MR_{25}T_{10}$). 10x magnification; scale bar = 500 µm. **D** - bone resorption images in the absence or presence of RANKL ± TNF. White area represents resorption.

Given the inability of TNF to enhance osteoclastogenesis in the context of 25 ng/ml of RANKL, the concentration of RANKL was decreased to its sub-optimal level (1 ng/ml), which led to a noticeable enhancement of osteoclastogenesis in the presence of 10 ng/ml of TNF. Additionally, this effect was clearly visible in TRAP-stained images of osteoclasts (figure 4.7 A, C).

To gain a deeper insight into the resorptive activity of mature osteoclasts, calcium phosphate-coated osteo-assay plates were used to assess osteoclast resorption activity. The data from TRAP staining corresponds with the results observed in bone resorption assay, where the resorbed area is greater in the presence of TNF, leading to a ~55 % enhancement in bone resorption compared to the cells without TNF (figure 4.7 B, D). Cells with only M-CSF were used as a control. Even though no osteoclasts were differentiated under this condition, some resorbed areas (white spots) were visible. This was most likely caused by $TRAP^{+}$ macrophages (differentiated from monocytes), which are mono- or binuclear and have the ability to resorb bone into a much smaller extend than osteoclasts (figure 4.7 C, D).

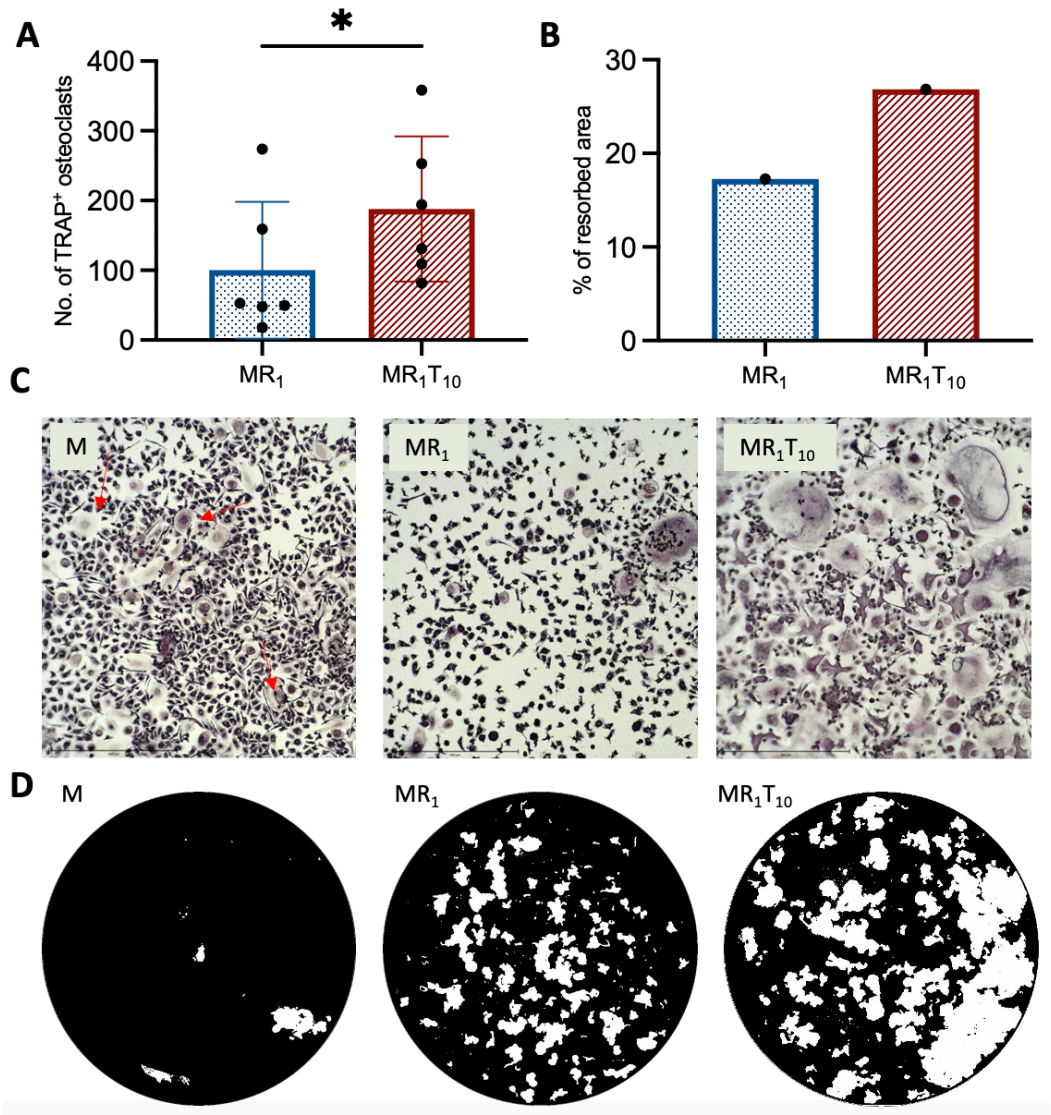

Figure 4.7 Enhancement of osteoclastogenesis with the addition of TNF 96 hours after the addition of M-CSF with the suboptimal RANKL concentration.
A - Number of osteoclasts differentiated only with M-CSF and suboptimal 1 ng/ml concentration of RANKL (MR_1) in the absence of TNF or with 10 ng/ml of TNF (MR_1T_{10}), n=6. Error bars show mean±SD. Paired parametric t-test was done for significance, where significance is shown with an asterisk, *p≤0.05. **B** - Percentage of resorbed area of calcium phosphate plates under the same conditions, i.e., no TNF or 10 ng/ml of TNF, n=1. **C** - TRAP-stained images of monocytes cultured with M-CSF only (M; mono- and bi-nuclear cells are shown with a red arrow) or osteoclasts without TNF (MR_1) and 10 ng/ml of TNF (MR_1T_{10}). 10x magnification; scale bar = 500 μm. **D** - bone resorption images in the absence or presence of RANKL and/or TNF. White area represents resorption.

Once the cytokine exposure kinetics that allowed TNF to inhibit or enhance osteoclast differentiation was optimised, synovial fluid (SF) was collected from patients with active RA and was used with the aim to recapitulate the disease environment with a wide spectrum of pro-inflammatory cytokines, chemokines, growth factors, damage-associated molecular patterns (DAMPs), etc. (Sayegh et al., 2019). The rationale behind this experiment was to observe the impact of SF

on osteoclastogenesis, as in RA, monocytes enter the synovial compartment, and the environment within the SF might influence their differentiation process. The results showed that both early and late SF addition (added on day 1 or on day 5, respectively) reduced osteoclastogenesis. This was in contrast with the data observed with the addition of TNF on day 1, which led to an inhibition while the addition on day 5 resulted in an enhancement of osteoclasts. Inhibition with the SF was comparable in both conditions and was more pronounced than the inhibitory effect of TNF added on day 1 (figure 4.8). The inhibitory effect of RA SF was also observed in prior research in the Goodyear laboratory, where the work showed that multiple factors (e.g., interferon alpha (IFNα), immune complexes, and toll-like receptors binding DAMPs) present in RA SF inhibited levels of various chemokines. The effect on osteoclastogenesis was not addressed, however, the inhibition was unexpected due to several pro-inflammatory DAMPs in SF. Notably, more research is needed to fully understand the mechanisms of action behind the inhibition of osteoclastogenesis in the presence of SF (Kidger, 2017).

Overall, TNF was consistently able to inhibit but also enhance osteoclast differentiation depending on the time of exposure, while SF failed to enhance osteoclast differentiation and led to inhibition in both investigated settings. Therefore, further experiments aiming to evaluate the effect of SPMs on osteoclasts used the enhancing TNF culture system.

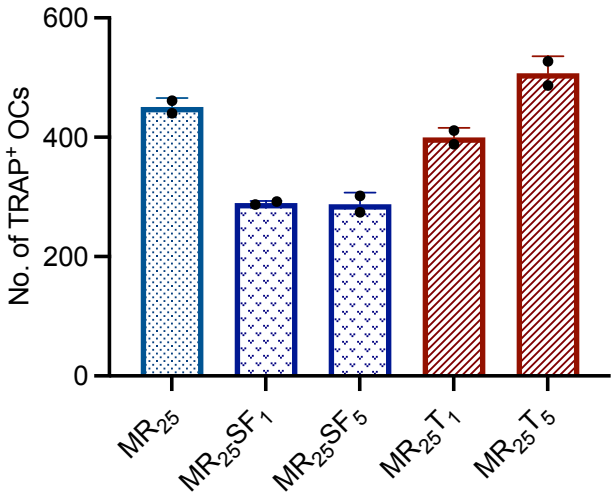

Figure 4.8 The effect of TNF and synovial fluid on osteoclastogenesis.
A bar chart showing the addition of synovial fluid (SF; in purple) on day 1 ($MR_{25}SF_1$), on day 5 ($MR_{25}SF_{10}$) or the addition of 10 ng/ml of TNF (in red) on day 1 and day 5 compared to the control (MR_{25}; in blue), where cells were incubated with 25 ng/ml of M-CSF and 25 ng/ml of RANKL for 12 days. Error bars are shown as mean±SD for n=2.

4.2.3 RvE1 inhibits osteoclastogenesis in healthy individuals under inflammatory conditions

To establish the optimal concentration of SPMs to be added to osteoclast cultures, three different half-log concentrations, namely 3, 10, and 30 ng/ml (equivalent to 8.6, 28.5, and 85.6 nM) were tested. These concentrations were selected based on prior research and also because the aim of this work was to test whether SPMs have an effect under lower concentrations. Prior studies investigating an effect of RvE1 on osteoclastogenesis used, 50-100 nM (Funaki et al., 2018), 100 nM (Kholy et al., 2018) or 1, 3, and 10 ng/ml, with the highest effect observed at 3 ng/ml (Herrera et al., 2008). The concentrations for RvD1 were slightly higher, ranging between 500 nM (Benabdoun et al., 2019), and 2, 20 or 200 ng/ml, with significant effect on osteoclastogenesis observed with 20 and 200 ng/ml (Klein et al., 2022).

The results with 3, 10, and 30 ng/ml showed no significant difference under standard culture conditions (M-CSF+RANKL) with either RvE1 or 17-HDHA (figure 4.9 A). However, when the effect of these SPMs was tested under TNF-driven inflammation, 3 and 10 ng/ml of RvE1 and 17-HDHA showed an osteoclast inhibition, while 30 ng/ml did not exhibit an inhibitory effect (figure 4.9 B). Therefore, based on these results and previous studies, further experiments were conducted using 10 ng/ml of SPMs.

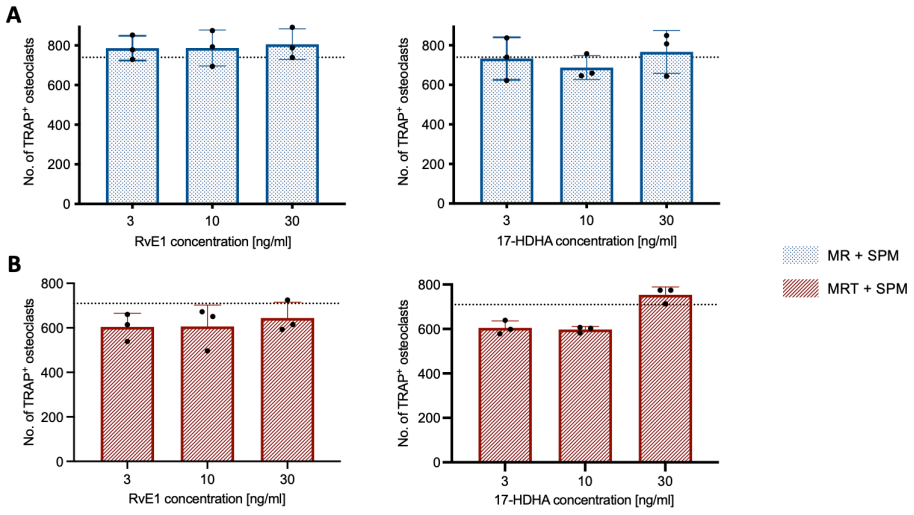

Figure 4.9 Evaluation of the right timepoint of SPM addition.
A - The addition of RvE1 and 17-HDHA at 3 ng/ml, 10 ng/ml or 30 ng/ml under standard culture conditions with 25 ng/ml of M-CSF and RANKL (blue; MR) compared to the control with no SPMs (dotted line). **B** - the addition of RvE1 and 17-HDHA at 3, 10, and 30 ng/ml under TNF-driven conditions with 10 ng/ml of TNF (red) compared to the control without SPMs (dotted line; MRT). SPMs were added on day 5 in the absence or presence of TNF. Bars show mean±SD for n=1, each dot represents a replicate of the same donor.

To observe the effect of RvD1, RvE1, 17-HDHA, MaR1 (selected based on the SPM receptor expression discussed in chapter 3), and their combination on osteoclastogenesis, these SPMs were tested in the presence of M-CSF and optimal concentration of RANKL (25 ng/ml) ± TNF. These SPMs were initially tested in osteoclasts differentiated from $CD14^+$ monocytes isolated from leukocyte cones. To assess their effect during early pre-osteoclast differentiation, SPMs were added on day 1 (figure 4.10 A). In contrast, to observe their impact on mature osteoclasts, SPMs were added on day 5 (figure 4.10 B). Both additions were done in the absence of TNF to mimic steady-state conditions. To investigate the effect of SPMs under TNF-driven inflammation, SPMs were added simultaneously with TNF on day 5 (figure 4.10 C). A condition where TNF would be added on day 1 alongside the SPMs was not included as earlier addition would lead to osteoclast inhibition, which would not be suitable for observing possible inhibitory effect of SPMs.

The addition of RvD1, RvE1, 17-HDHA, MaR1, and their combination in the absence of TNF on day 1 or day 5 did not significantly affect RANKL-driven osteoclast differentiation and no significant differences were observed when compared to the control (figure 4.10 A, B). In contrast, RvE1, significantly inhibited osteoclastogenesis when added alongside TNF on day 5 (figure 4.10 C). The inhibition with RvE1 was donor-dependent ranging between 11 to 42 % with an average of 20.9 ± 12.5 % decrease in the number of osteoclasts. Although MaR1 also led to an inhibition across the donors, these results were not statistically significant ($p=0.055$), most likely due to sample variation and low number of donors ($n=3$). The average inhibition with MaR1, however, resulted in 24.7±10.5 % decrease of osteoclast numbers with the inhibition ranging between 14.2 % to 24.8 %. Therefore, despite the non-significant results with MaR1, MaR1 managed to inhibit osteoclastogenesis with a slightly higher average inhibition than RvE1, however, more donors would be needed for confirmation. Additionally, the effect of RvD1, 17-HDHA, and the SPM combination was non-significant under TNF-driven conditions.

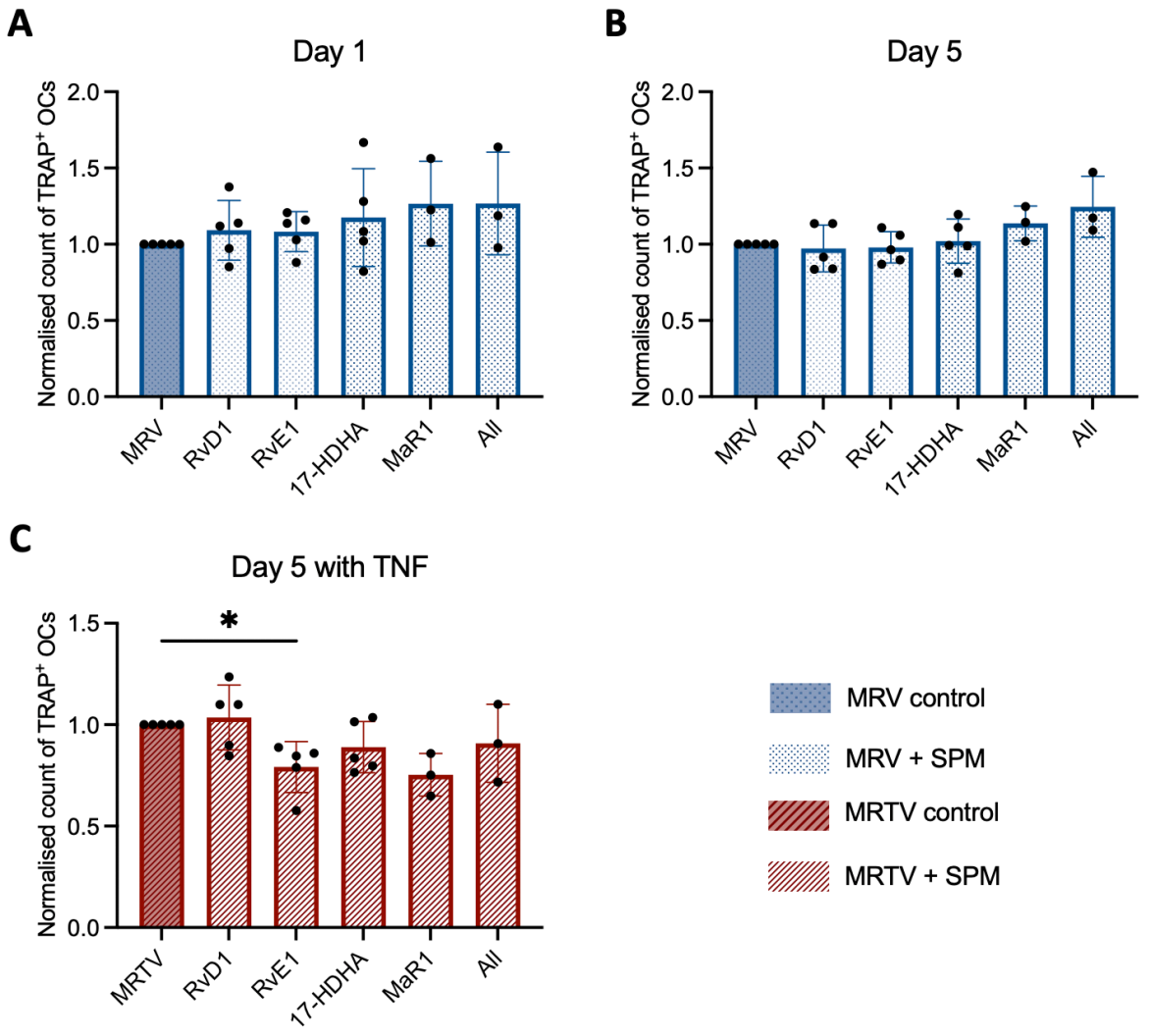

Figure 4.10 The effect of SPMs on osteoclast differentiation under standard or TNF-driven conditions with 25 ng/ml of RANKL.
Normalised number of osteoclasts under standard culture conditions differentiated from $CD14^+$ monocytes isolated from leukocyte cones. Filled blue bar – MRV control (25 ng/ml of M-CSF, 25 ng/ml of RANKL, and ethanol vehicle) with no SPMs, dotted blue bar – standard culture condition (MRV) with SPMs (10 ng/ml), namely RvD1, RvE1, 17-HDHA, MaR1 and their combination added on day 1 (**A**) or on day 5 (**B**). **C** – Normalised number of osteoclasts under TNF-driven conditions. Filled red bar – MRTV control (25 ng/ml M-CSF, 25 ng/ml RANKL, 10 ng/ml TNF, and ethanol vehicle) without SPMs, striped red bar - MRT condition with the SPM addition (10 ng/ml) on day 5. Parametric paired t-test assuming Gaussian distribution was done. Significance is shown with an asterisk, where *p≤0.05 and ns means non-significant. Each dot represents one donor (n=3-5).

To assess whether the effect would be more pronounced, SPMs were also tested at the sub-optimal concentration of RANKL (1 ng/ml). Interestingly, the effect of SPMs was comparable to that at a higher RANKL concentration. Similarly, the addition of RvE1 alongside with TNF resulted in a significant inhibition of osteoclastogenesis (22±8.3 % less osteoclasts than in the control). In contrast, the effect with MaR1 was inconsistent across the donors, with 1 donor showing no effect, while the other 2 donors inhibited osteoclast differentiation. No significant

differences were observed with any of the SPMs added under standard culture conditions (figure 4.11). Therefore, in the following experiments, SPMs were no longer tested under standard culture conditions.

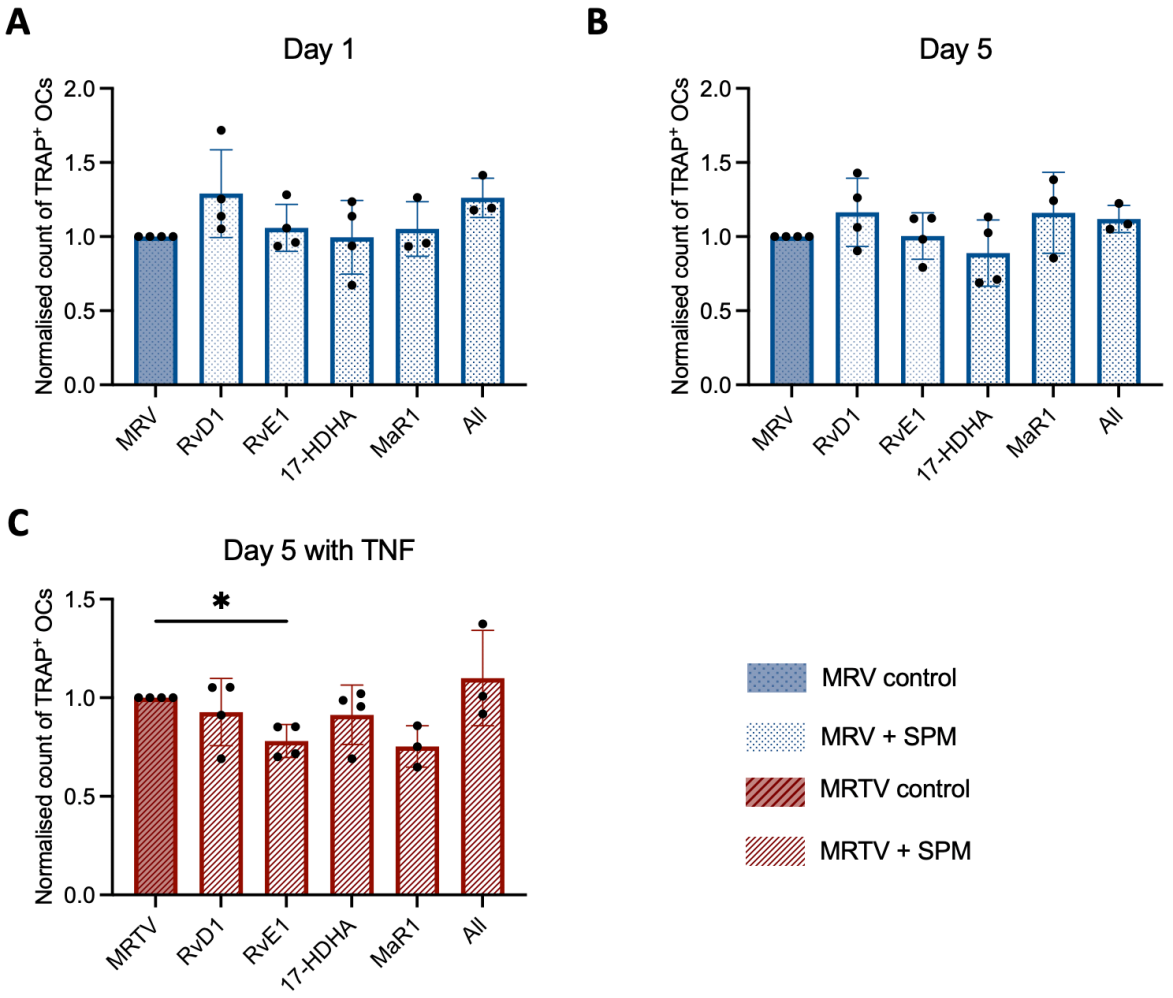

Figure 4.11 The effect of SPMs under standard or TNF-driven conditions at sub-optimal RANKL concentration (1 ng/ml).
Normalised number of osteoclasts differentiated from $CD14^+$ monocytes isolated from leukocyte cones under TNF-driven inflammatory conditions. Filled blue bar – MRV control (25 ng/ml of M-CSF, 1 ng/ml of RANKL, and ethanol vehicle) with no SPMs, dotted blue bar – standard culture condition (MRV) with 10 ng/ml of SPMs, namely RvD1, RvE1, 17-HDHA, MaR1 and their combination added on day 1 (**A**) or on day 5 (**B**). **C** – Normalised number of osteoclasts under TNF-driven conditions. Filled red bar – MRTV control (25 ng/ml M-CSF, 1 ng/ml RANKL, 10 ng/ml TNF, and ethanol vehicle) without SPMs, striped red bar - MRT condition with the SPM addition (10 ng/ml) on day 5. Parametric paired t-test assuming Gaussian distribution was done. Significance is shown with an asterisk, where *p≤0.05 and ns means non-significant. Each dot represents one donor. Error bars show mean±SD for n=3-4.

To obtain more reliable comparisons between healthy and RA donors, it was necessary to confirm the effect of SPMs in TNF cultures in primary human cells acquired from fresh whole blood rather than leukocyte cones. Notably, RvE1 significantly inhibited osteoclast differentiation from monocytes isolated from

whole blood of healthy donors with 15±6.7 % higher osteoclast reduction in every donor compared to control, which was slightly less pronounced than with the leukocyte cones. The effect of the other SPMs that were tested, namely RvD1, 17-HDHA, MaR1 and their combination resulted in non-significant changes (figure 4.12).

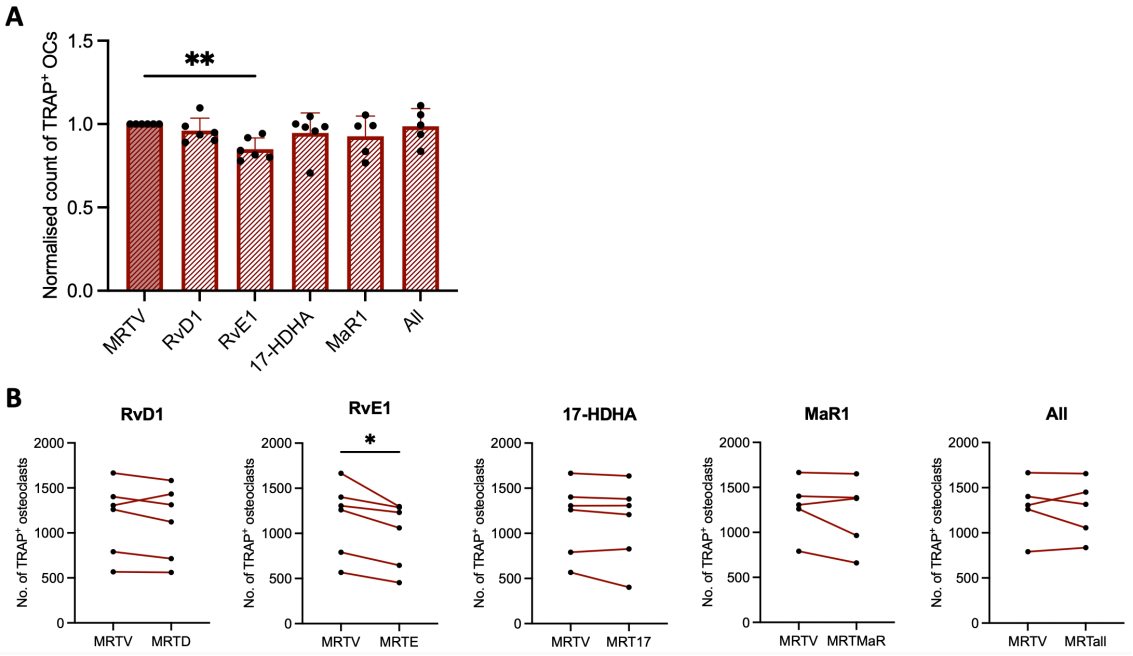

Figure 4.12 RvE1 inhibits osteoclastogenesis under inflammatory conditions.
A - Normalised number of osteoclasts differentiated from fresh whole blood monocytes under inflammatory conditions with 25 ng/ml of M-CSF, 25 ng/ml of RANKL, and 10 ng/ml of TNF with ethanol vehicle (MRTV) in the absence or presence of SPMs (10 ng/ml), namely RvE1, RvD1, 17-HDHA, MaR1, and their combination (All). Paired parametric t-test was performed to observe the difference between conditions with the added SPMs and the MRTV control after passing the normality test (n=5-6); **p≤0.005. Error bars show mean±SD. **B** - pairwise comparison of number of TRAP⁺ osteoclasts of individual donors for different SPMs compared to the MRTV control. Statistical significance was done using paired parametric t-test; *p≤0.05.

Notably, the inhibitory effect of RvE1 was also evident in TRAP-stained images of osteoclasts. This was characteriesed by a reduced number of mature osteoclasts, which also appeared smaller (figure 4.13). Additionally, more osteoclast precursors with 1 or 2 nuclei were observed, however, this observation was not confirmed due to time restraints, and the counts of mono- and binulear cells compared to mature osteoclasts could be conducted in future work. This could suggest that a higher number of cells failed to differentiate into mature osteoclasts and remained in their precursor state, as suggested by Zhu et al., (2013).

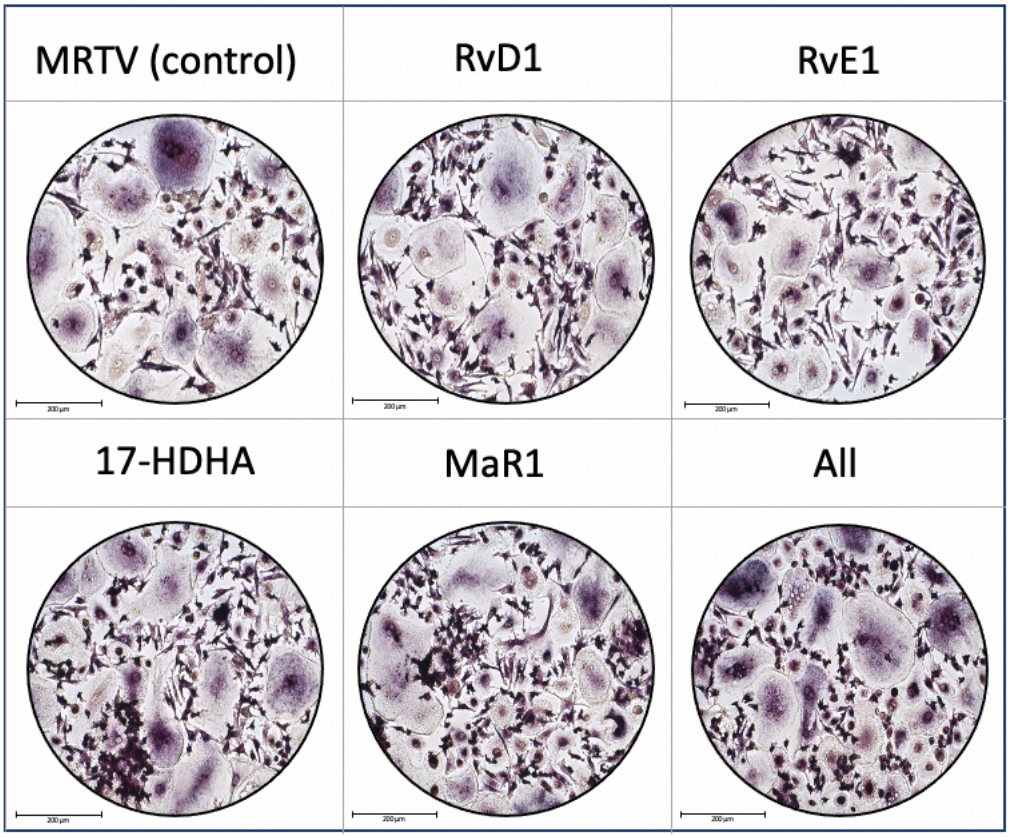

Figure 4.13 Microscope pictures of mature TRAP$^+$ osteoclasts and their precursors in the presence of SPMs.
Osteoclasts differentiated in the presence of 25 ng/ml of M-CSF, 25 ng/ml of RANKL, 10 ng/ml of TNF ± 10 ng/ml of SPMs. Ethanol was added as a vehicle to the control (MRTV). Cells with 3 or more nuclei are characterised as mature osteoclasts, while cells with less than 3 nuclei are osteoclast precursors. Elongated cells are macrophages not differentiated into osteoclasts (20x magnification; scale bar = 200 µm).

To investigate the relationship between the osteoclast inhibition caused by RvE1 and bone degradation, a bone resorption assay was conducted using calcium phosphate coated plates. The results suggest that the effect of RvE1 on bone resorption was very donor-dependent and the results were non-significant. However, despite the non-significant results, a slight inhibition was seen in 3 out of 4 donors ranging between 2.5-8.8 %. One donor remained unchanged (figure 4.14). More donors would be needed to fully conclude the impact of RvE1 on bone resorption and to understand its connection with osteoclast inhibition. Based on power calculations, for 80% power assuming a 5% significance level using 2-tailed test, a minimum of 743 patients per group would be needed. This is, however, not possible, therefore no significant results of this assay can be expected. Moreover, this experiment was not possible to repeat as the bone resorption plates were discontinued.

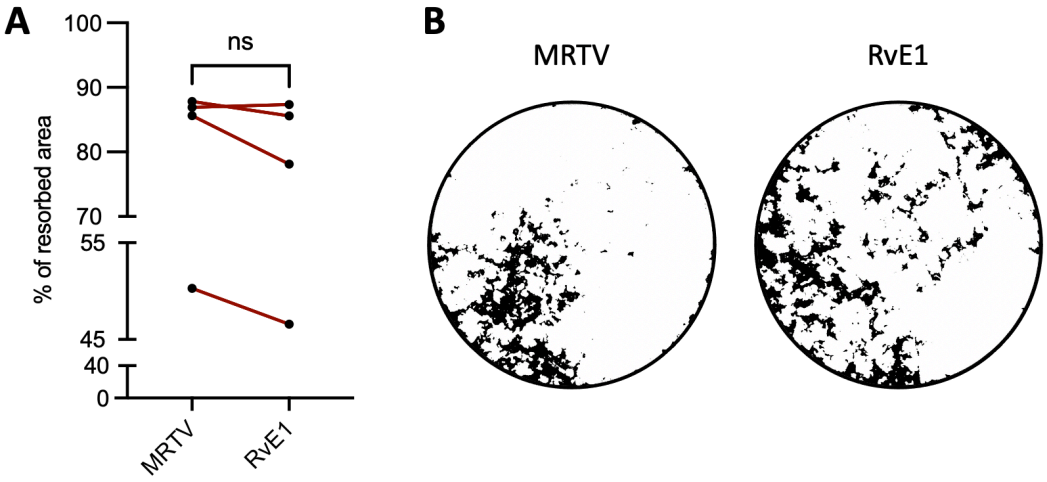

Figure 4.14 Bone resorption with RvE1 in healthy donors.
A - Percentage of resorbed area with the addition of RvE1 (10 ng/ml) compared to its MRTV control (25 ng/ml M-CSF, 25 ng/ml RANKL, 10 ng/ml TNF, ethanol as a vehicle). Error bars show mean±SD for n=4. Statistical analysis was performed using paired parametric t-test; ns – non-significant. **B** - Representative image showing resorbed area for the MRTV control, and MRTV with the addition of RvE1. White area shows resorption.

In summation, RvE1 inhibited osteoclast differentiation from leukocyte cones at both, optimal and sub-optimal RANKL concentrations (25 ng/ml and 1 ng/ml, respectively) under TNF-driven conditions. The inhibitory effect was also confirmed in osteoclasts differentiated from whole blood of healthy donors. No effect of SPMs (RvD1, RvE1, 17-HDHA, MaR1) was observed under standard culture conditions after their addition on day 1 or day 5 in osteoclasts differentiated from leukocyte cones. Aditionally, the inhibition of osteoclasts by RvE1 was also observed with TRAP-staining, which resulted in smaller osteoclasts. Furthermore, RvE1 might have an inhibitory effect on bone resorption, however, it was very donor-dependant. As according to the power calculations, 743 patients would be needed, these results are not significant and RvE1 did not have an effect on bone resorption when using the bone resorption assay plates. However, different experiments using for example bone slices or fluorescent bone resorption assay kits could be used to conduct further investigations.

Lastly, the actions of SPMs on the expression of key genes involved in TNF-driven osteoclastogenesis was also assessed to gain a deeper understanding of the underlying mechanism and signalling pathways of SPMs. The genes selected for this qPCR analysis were all associated with osteoclast differentiation, bone resorption or inflammation. These genes included dendritic cell-specific

transmembrane protein (DC stamp; cell-cell fusion in osteoclasts), osteoclast stimulatory transmembrane protein (OC stamp; osteoclast fusion and bone resorption), RANK (RANKL receptor marker; osteoclast formation, activation, and survival), CD115 (M-CSF receptor marker; survival and differentiation of myeloid cells), osteoclast-associated receptor (OSCAR; osteoclast marker), TRAP (bone resorption), matrix metalloproteinase 9 (MMP9; bone resorption), cathepsin k (bone resorption), nuclear factor of activated T cells 1 (NFATc1; osteoclast differentiation), PU.1 (myeloid cell development, commitment to monocyte/macrophages), and MITF (osteoclast differentiation). $CD14^{+}$ monocytes were differentiated into osteoclasts using M-CSF, RANKL, and TNF, with SPMs added simultaneously on day 5. The cells were lysed 24h after the addition of the SPMs±TNF. The control was lysed 24h after the addition of the vehicle, and mRNA expression for the selected genes was assessed via qPCR. Genes that consistently showed expression levels below or above the MRTV average across all biological replicates were further analysed for significance.

In healthy cells isolated from whole blood, RvD1 and MaR1 did not significantly impact any of the analysed genes. RvE1 exhibited a significant enhancement on the NFATc1 transcript, without impacting RANK, which is upstream of NFATc1. These observations in the transcript increase, however, do not correspond with the functional outcomes showing RvE1's inhibitory effect on osteoclastogenesis and an inhibition of NFATc1 was expected. Additionally, 17-HDHA led to a significant upregulation of RANK, MMP9 and NFATc1 across the donors. Lastly, the combination of all SPMs lead to a significant enhancement of NFATc1 gene (figure 4.15).

Overall, RvE1, 17-HDHA and the SPM combination significantly enhanced NFATc1 transcript, with 17-HDHA also enhancing RANK and MMP9 expression. Notably, no SPM showed an increase of 2-fold or higher compared to the control in all the biological replicates, thus even though these SPMs possibly had an effect on the transcript expression, the changes were relatively small and did not correspond with the functional outcomes of SPMs. To observe whether these SPMs could have an effect on the transcript expression, more donors would be needed, and different time-points could be tested, as in this experiment the mRNA expression was only tested 24h after the SPM addition.

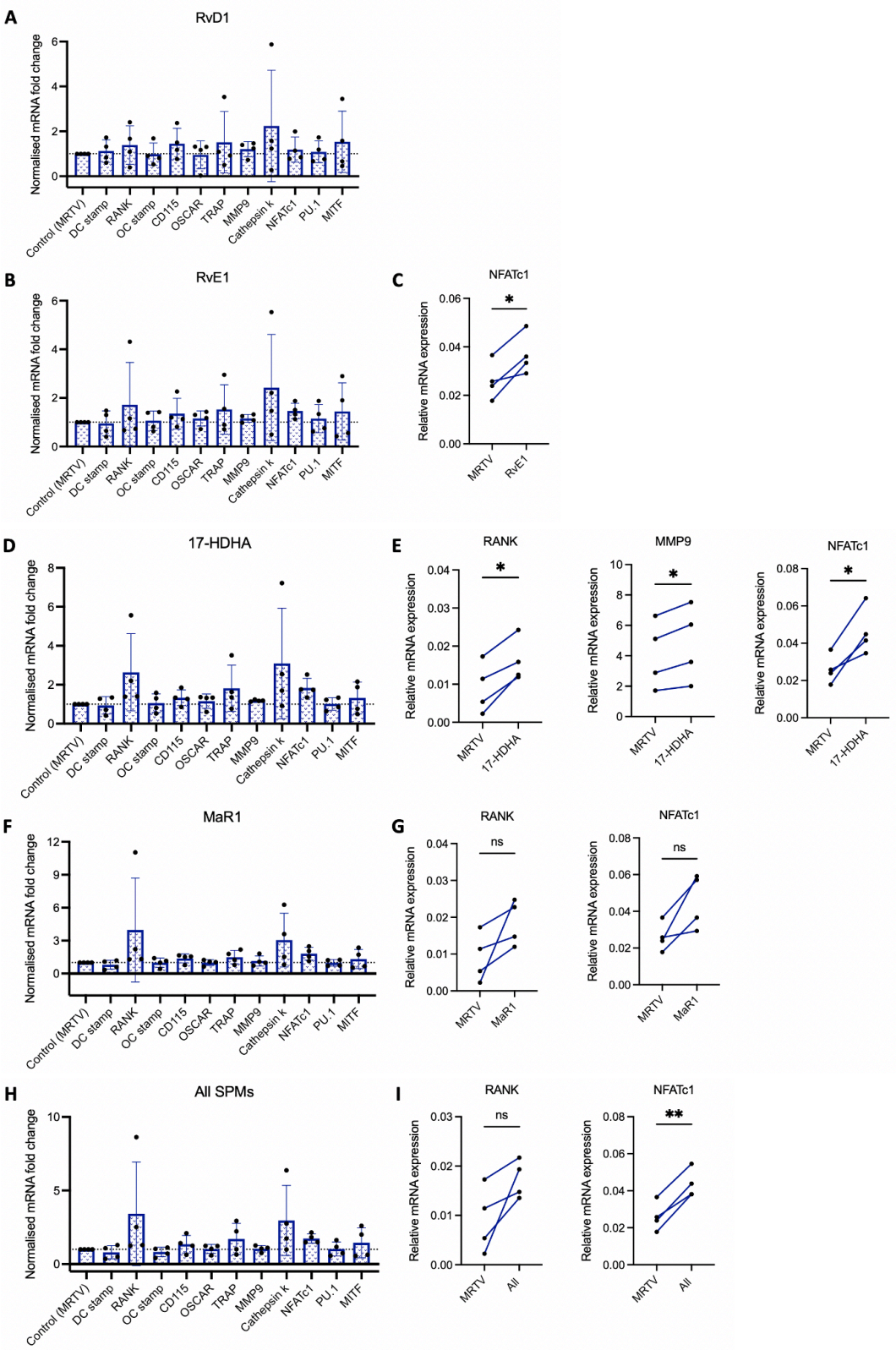

Figure 4.15 Gene expression involved in osteoclast differentiation and bone resorption for various SPMs in healthy osteoclasts.

mRNA fold change was counted for different osteoclastogenic pathways for RvD1 (A), RvE1 (C), 17-HDHA (D), MaR1 (F) and a combination of all the SPMs (H) compared to the MRTV control with no SPM (dotted line). Fold change was counted as $2^{-\Delta\Delta CT}$ normalised to the MRTV control, where $\Delta\Delta C_T$ was counted as $\Delta C_{T(\text{with SPM})} - \Delta C_{T(\text{control})}$ and ΔC_T was counted as $C_{T(\text{gene of interest})} - C_{T(\text{GAPDH})}$. Selected pathways where all donors showed either an enhancement or an inhibition with RvE1 (C), 17-HDHA (E), MaR1 (G), or all SPMs (I) compared to the MRTV control were selected and plotted as relative mRNA expression counted as $2^{-\Delta C_T}$. Parametric paired t-test was done for statistical analysis and significance is shown with an asterisk (*p≤0.05; **p≤0.005) for n=4.

4.2.4 RvD1 inhibits osteoclastogenesis in RA patients under inflammatory conditions

Due to variations in phenotype, gene expression and metabolism between healthy and RA myeloid compartment (chapters 1.1.1, 3, and 5.1), it is necessary to examine the effect of SPMs in RA precursors since their actions may vary from healthy osteoclasts. RA monocytes were isolated from whole blood of patients with active RA and were cultured under standard culture conditions (no TNF) or TNF-driven inflammatory conditions (with TNF) ± SPMs, as previously described with healthy osteoclasts. Under standard culture conditions, none of the SPMs added on day 5 exhibited a significant effect on osteoclastogenesis, which was consistent with the effect of SPMs observed in healthy osteoclasts. In contrast, under TNF-driven conditions, RvD1 and MaR1 significantly inhibited osteoclastogenesis, with RvD1 showing higher significance ($p=0.004$) than MaR1 ($p=0.04$) (figure 4.16 A). The other SPMs, including their combination, did not affect osteoclastogenesis in the presence of TNF. Interestingly, in contrast to healthy individuals, RvE1 was unable to inhibit osteoclastogenesis in RA samples.

SPMs were also tested at a sub-optimal RANKL concentration (1ng/ml), which resulted in a comparable effect to that seen at 25 ng/ml under standard culture conditions (figure 4.16B). However, due to the limited number of RA cells, some conditions under standard culture settings could not be performed or replicated, as the primary focus was on investigating the SPMs in inflammation. Under TNF-driven conditions, RvD1 maintained its inhibitory actions (10.8±4.2 % fewer osteoclasts compared to the control), however, the significance was lower ($p=0.05$) than with the optimal concentration of RANKL. No significant difference was observed with any other SPMs (figure 4.16 B).

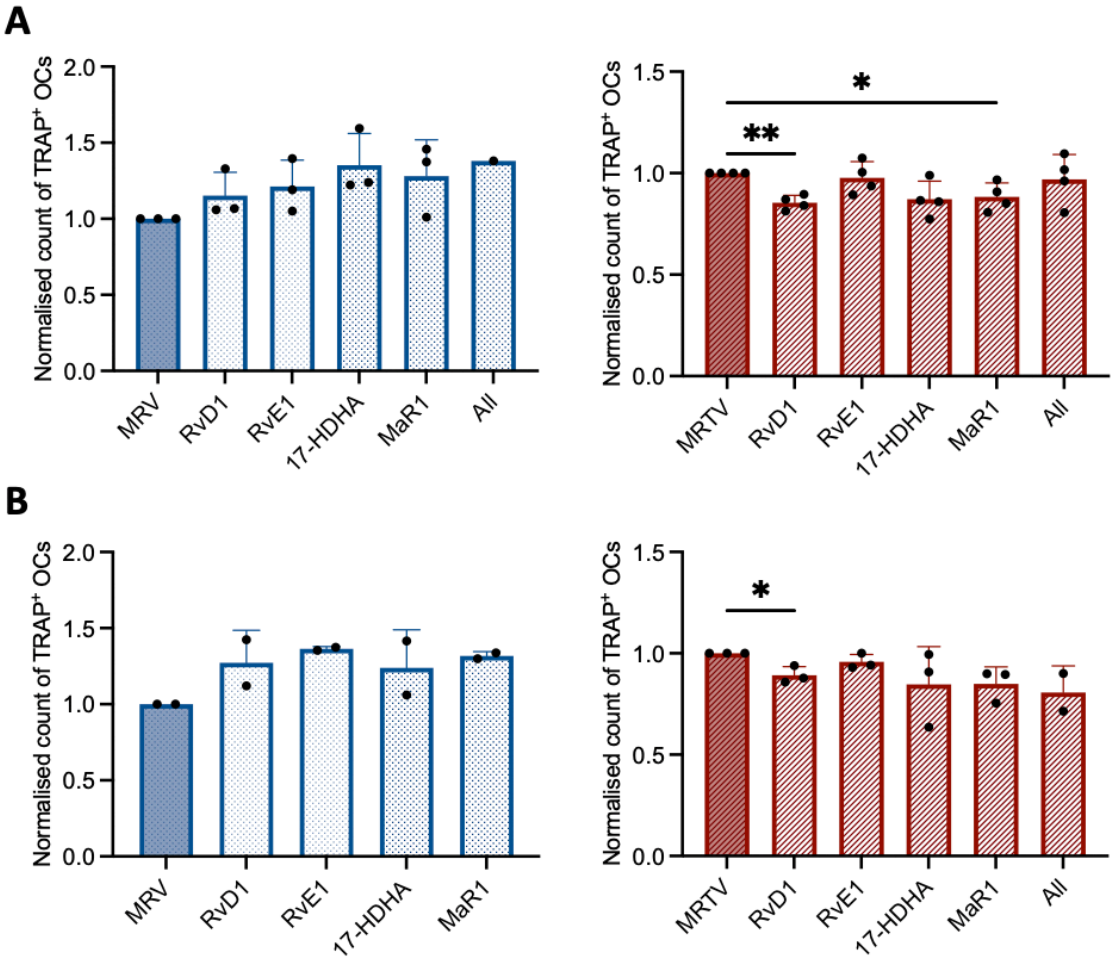

Figure 4.16 The effects of SPMs under physiological and inflammatory settings in RA.
A - Normalised counts for TRAP⁺ osteoclasts with the addition of 10 ng/ml SPMs (RvD1, RvE1, 17-HDHA, MaR1, and their combination – All) under standard culture conditions (blue) or TNF-driven conditions (red). Under standard culture conditions, osteoclasts were differentiated in the presence of 25 ng/ml of M-CSF, 25 ng/ml of RANKL and ethanol vehicle (MRV), while under TNF-driven conditions, apart from M-CSF and RANKL, TNF was added (MRTV). Ethanol was added as a vehicle to the control as SPMs are dissolved in ethanol. **B -** Normalised counts for TRAP⁺ osteoclasts differentiated at sub-optimal RANKL concentration (1 ng/ml) in the absence or presence of TNF (MRV and MRTV, respectively). Full bar shows the MRV and MRTV control (blue and red, respectively). Due to limited number of cells, the combination of all SPMs could not be tested under standard culture conditions with 1 ng/ml of RANKL so it was not included. Paired parametric t-test was done for the statistical analysis. Significance is shown with an asterisk, ns means non-significant results; *p≤0.05, **p≤0.01 for n=1-4.

Additionally, inhibition of osteoclastogenesis was also observed in TRAP-stained images, which resulted in smaller osteoclasts in the presence of RvD1 and MaR1 (4.17 A). Notably, only RvD1 exhibited osteoclast inhibition (15.6±2.4 % inhibition compared to the control) when raw data with actual osteoclast counts were used rather than normalised data (4.17 B). Therefore, for more reliable results and a clear conclusion about the possible inhibitory actions of MaR1, a larger sample size would be needed.

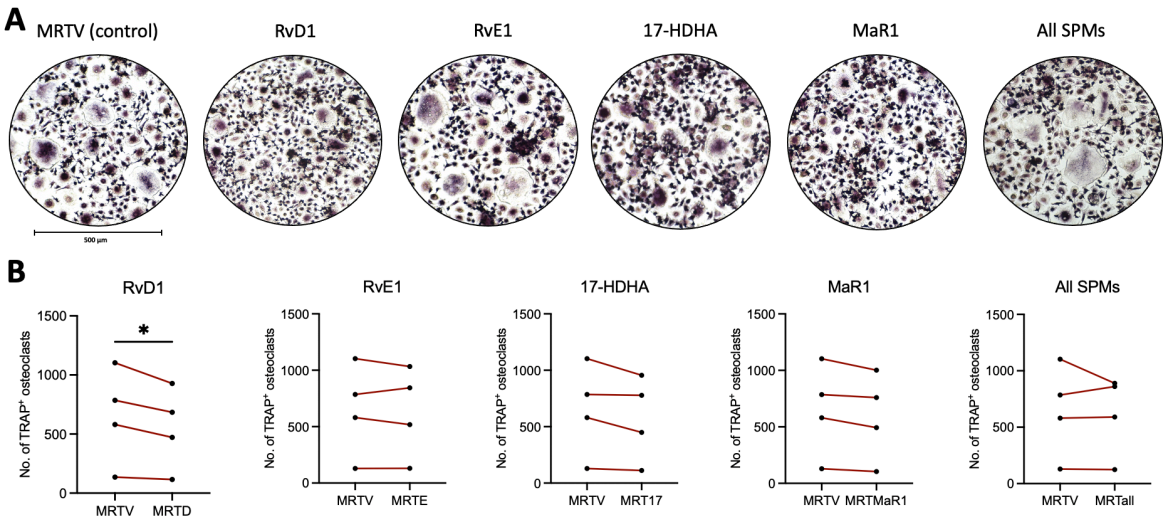

Figure 4.17 The effect of SPMs on osteoclasts under inflammatory conditions in RA.
A - TRAP⁺ osteoclasts with the addition of various SPMs, namely RvD1, RvE1, 17-HDHA, MaR1, and the combination of all SPMs compared to the control with M-CSF, RANKL, TNF and vehicle (MRTV) (20x magnification). Mature osteoclasts are shown in purple and have 3 or more nuclei. 10x magnification; scale bar = 500 µm. **B -** Number of TRAP⁺ osteoclasts. The effect of RvD1 (MRTD), RvE1 (MRTE), 17-HDHA (MRT17), MaR1 (MRTMaR1), and all SPMs (MRTall) was tested on osteoclastogenesis compared to the MRTV control (M-CSF, RANKL, TNF and vehicle) for individual donors (n=4). Paired parametric t-test was done after passing the normality test; *p≤0.05.

The bone resorbing activity of RvD1 was also evaluated, however, there were no significant differences compared to the control. The results varied between the donors with one donor enhancing osteoclastogenesis, the other inhibiting, and the third remained unchanged (figure 4.18). Therefore, despite RvD1's inhibitory actions on osteoclastogenesis, it did not have an inhibitory effect on bone resorption in osteoclasts differentiated from primary human cells from RA patients. This could be due to oversaturation of the wells with cells or because cells were left in cell cultures for longer than for TRAP staining (14 days compared to 10 days), which led to high degree of resorption. Additionally, higher concentration of SPMs could be used, as prior studies used 500 nM (Pinto et al., 2023; Benabdoun et al., 2019), while this work used 10 ng/ml, which is comparable to 26.6 nM. Therefore, even though lower concentration might be sufficient for osteoclast inhibition, higher concentration might be needed in order to see a possible effect on bone resorption.

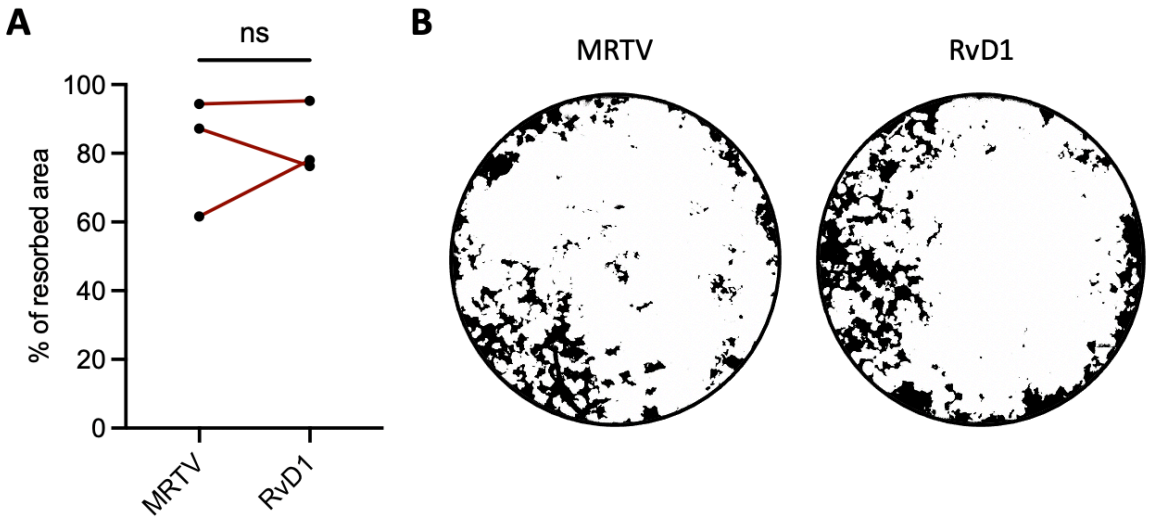

Figure 4.18 Bone resorption with RvD1 in RA.
A - Graph showing the percentage of resorbed area by osteoclasts differentiated in the presence of 25 ng/ml of M-CSF, 25 ng/ml of RANKL, 10 ng/ml of TNF, and a vehicle (MRTV) used as a control compared to osteoclasts differentiated with the addition of 10 ng/ml of RvD1 for 14 days (n=3). Paired parametric t-test was conducted, which resulted in non-significant results. **B** - Pictures of resorbed area for RvD1 and its MRTV control. White area is resorbed area.

In summation, RvD1 inhibited osteoclastogenesis under TNF-driven inflammatory conditions in RA at both, optimal and sub-optimal concentrations, however, its effect on bone resorption was not significant. Additionally, even though MaR1 showed an inhibitory effect on osteoclast differentiation, the difference was not significant, and more donors would be needed to better observe its effect. Notably, none of the SPMs exhibited an inhibitory effect on osteoclastogenesis under standard culture conditions.

Lastly, the effect of SPMs on osteoclastogenic gene transcripts in RA was also tested in the same way as for healthy donors, however, the number of donors was limited (n=3). Preliminary data suggest that the addition of RvD1 decreased OSCAR, NFATc1 and PU.1 transcripts, which corresponds with RvD1's functional cellular outcome, although the differences were not significant (figure 4.19). Despite RvE1 not having an effect on osteoclastogenesis in RA, it exhibited a significant decrease in OSCAR and PU.1 transcript expression. 17-HDHA showed a non-significant inhibition on DC stamp and PU.1 genes, however, upon further analysis of the C_T values and fold changes of these genes, the values were comparable to the PU.1 gene expression after the exposure to RvE1, which was statistically significant, therefore 17-HDHA could also exhibit an inhibitory effect. Additionally, MaR1 showed no effect on any of these transcripts. The combination of all SPMs significantly enhanced the expression of CD115, although despite the

statistical significance, the differences were very subtle (3-5%) (figure 4.19). Notably, none of these fold change values was bigger than 2-fold, therefore the actions of these SPMs were not as pronounced, and more donors would be needed to draw more reliable conclusions. As already mentioned, gene expression was only tested at a single time-point, therefore it is possible that an earlier/later time-point could lead to more pronounced effects for some of the genes but further experiments would be required, which was not possible due to time restrains.

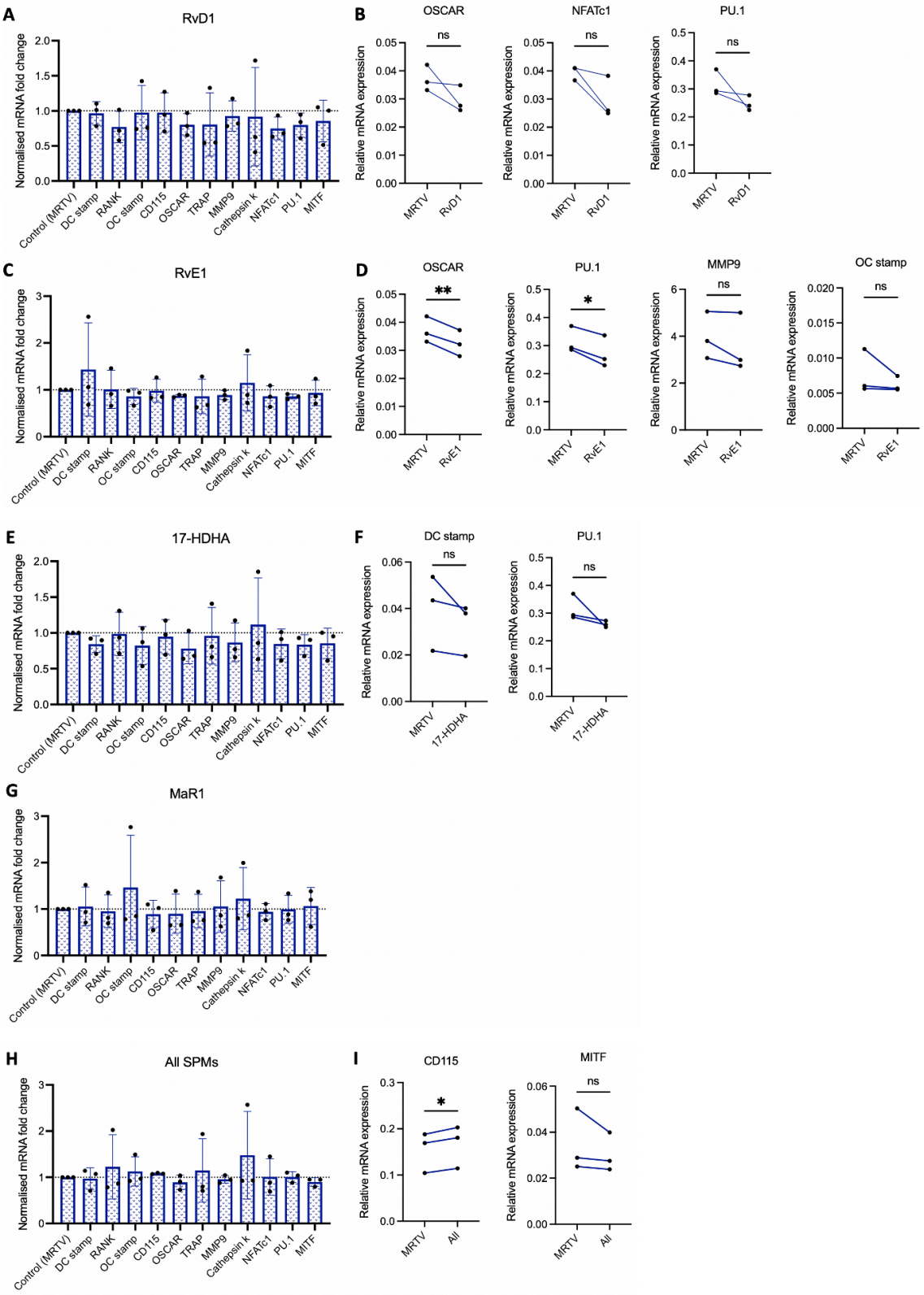

Figure 4.19 Gene expression involved in osteoclast differentiation and bone resorption with various SPMs in RA.

mRNA fold change was counted for different osteoclast pathways for RvD1 (A), RvE1 (C), 17-HDHA (E), MaR1 (G) and a combination of all the SPMs (H) compared to MRTV. It was counted as $2^{-\Delta\Delta C_T}$ normalised to the MRTV control, where $\Delta\Delta C_T$ was counted as $\Delta C_{T(\text{with SPM})} - \Delta C_{T(\text{control})}$ and ΔC_T was counted as $C_{T(\text{gene of interest})} - C_{T(\text{GAPDH})}$. Selected pathways where all donors showed either an enhancement or an inhibition with RvD1 (B), RvE1 (D), 17-HDHA (F), or all SPMs (I) compared to the MRTV control were selected and plotted as relative mRNA expression counted as $2^{-\Delta C_T}$. Parametric paired t-test was done for statistical analysis and significance is shown with an asterisk (*$p \leq 0.05$; **$p \leq 0.01$) for n=3.

In summary, when evaluating the impact of SPMs on osteoclast differentiation, a significant difference between healthy and RA donors was observed with regards to RvE1 and RvD1. Notably, RvD1 had a significantly higher inhibitory effect in RA osteoclasts, while RvE1 showed significantly higher inhibition in healthy osteoclasts under TNF-driven conditions (figure 4.20). No major differences were noted with 17-HDHA, MaR1, and the combination of all the SPMs.

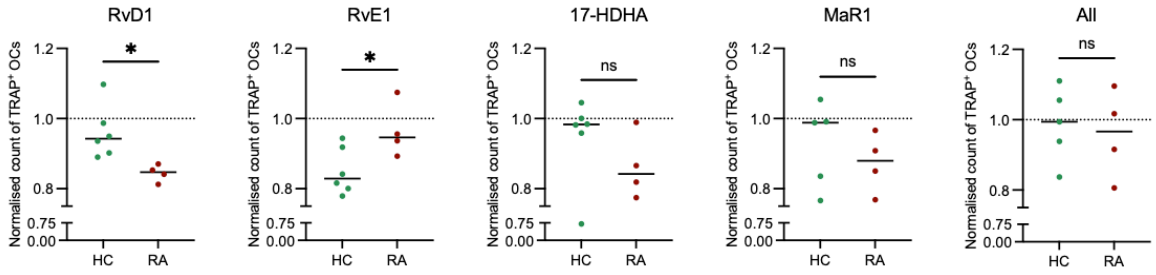

Figure 4.20 RvD1 and RvE1 inhibit osteoclastogenesis in RA and healthy donors, respectively. Comparison of the effect of RvD1, RvE1, 17-HDHA, MaR1, and the combination of all SPMs (All) in healthy and RA osteoclasts under TNF-driven conditions. Each dot shows individual donor compared to the normalised MRTV control (M-CSF, RANKL, TNF, vehicle; dotted line). Paired parametric t-test was done to statistically establish the significance between the number of normalised $TRAP^+$ osteoclasts in the presence of SPMs between healthy (HC; green) and RA (red) donors. Statistical significance is shown with an asterisk; *$p \leq 0.05$, ns is non-significant.

Similarly, mRNA fold change of the osteoclastogenic genes were compared between healthy and RA donors. This comparison was only done for the genes selected in figures 4.15 and 4.19, which were more/less expressed in all of the donors when compared to the control. Notably, only NFATc1 showed a significant difference between healthy and RA donors in the presence of RvE1, 17-HDHA, and the combination of all SPMs, which could suggest an inhibitory effect on osteoclast differentiation in RA compared to healthy donors. Interestingly RA donors showed lower transcript expression in the presence of these SPMs, while the expression in healthy donors was slightly enhanced when compared to their normalised controls (figure 4.21). To fully understand the difference between the expression of NFATc1 transcripts in healthy and RA osteoclasts in the presence of certain SPMs, more experiments would be needed, such as looking at the protein expression by western blot, investigating upstream/downstream signalling pathways, or using different time-points.

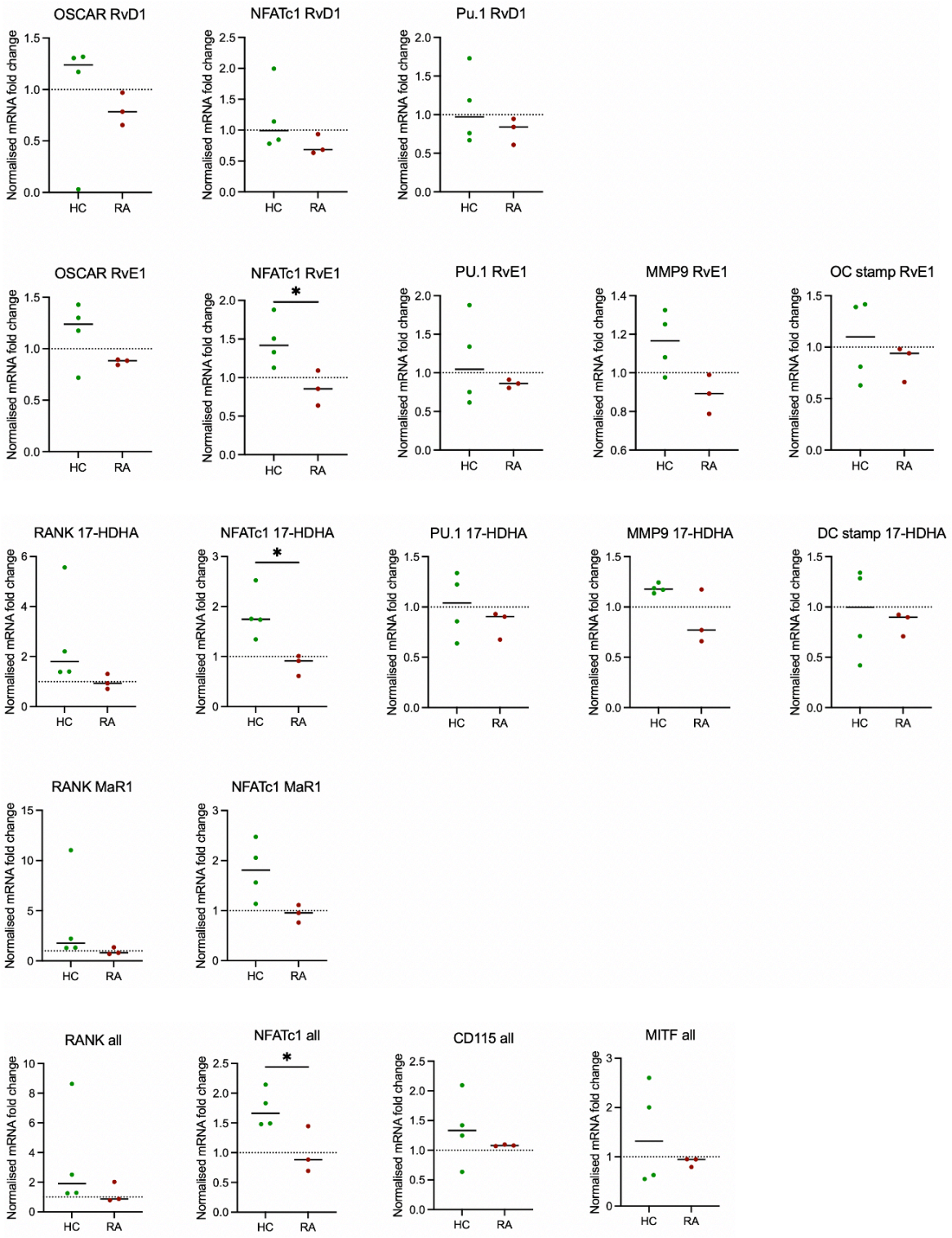

Figure 4.21 Comparison of osteoclastogenic gene expression between healthy and RA donors. Normalised transcript expression of selected genes of healthy (HC; green) and RA (red) donors as compared to the MRTV control (M-CSF, RANKL, TNF, vehicle; dotted line). Unpaired parametric t-test was done, where *p≤0.05. Individual dots represent individual donors, n_{HC} = 4, n_{RA} = 3.

4.2.5 SPMs do not affect the ability of dendritic cell precursors to differentiate into osteoclasts

To investigate the impact of SPMs on pre-DCs, initial experiments were performed using whole blood. However, due to limited number of pre-DCs obtained from whole blood, the cells were differentiated in 384-well plates, as opposed to the standard 96-well plate (figure 4.22 A). In comparison with 96-well plates, these plates only required 25,000 cells per condition instead of the usual 100,000 cells. The use of smaller wells, however, resulted in large variations and inconsistent cell differentiation between replicates and no reliable conclusions could be drawn based on these results (figure 4.22 B, C). However, despite the inter-donor variations, RvD1 showed an inhibitory effect on osteoclastogenesis in all technical replicates (N=1), therefore, it might have an effect on osteoclastogenesis, however, more experiments would be needed. Notably, only a very small volume (25 µl) was used per well, which may have contributed to variations in the number of plated cells and their distribution in the well. For half-changing the media, only 12.5 µl of media was exchanged, which was too little and sometimes the fresh media including the cytokines would stick to the wall of the well or it was not as precise as it would be with larger volumes.

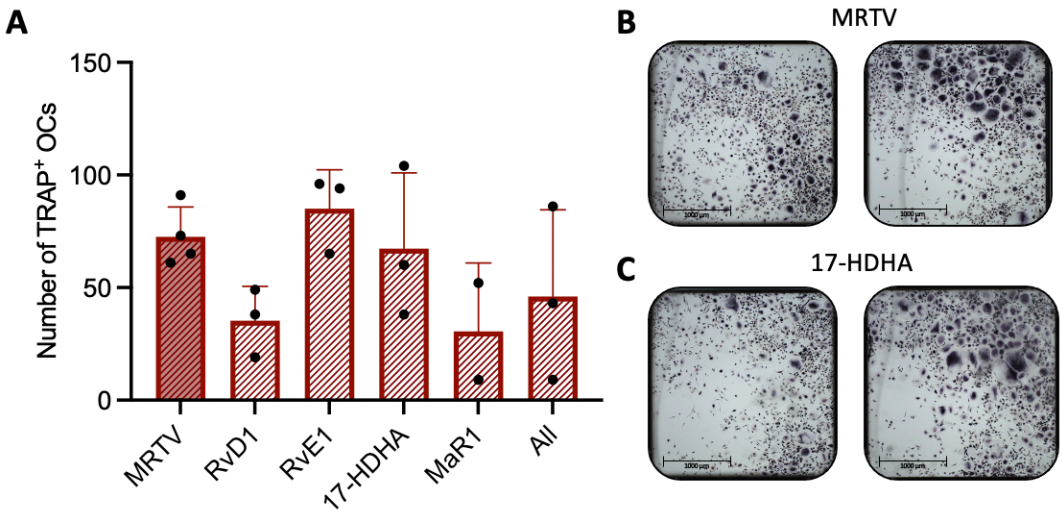

Figure 4.22 Osteoclast differentiation from pre-DCs from whole blood.
A - Number of TRAP$^+$ osteoclasts differentiated from DC precursors isolated from whole blood with the addition of SPMs on day 5. The effect of RvD1, RvE1, 17-HDHA, MaR1, and all SPMs was tested on osteoclastogenesis compared to the MRTV control (M-CSF, RANKL, TNF, and vehicle). Each dot represents a replicate of the same donor (n=1). **B -** Variations in the number of TRAP-stained osteoclasts between the MRTV replicates of the same donor in two different wells. **C -** Variation between the number of TRAP$^+$ osteoclasts in the presence of 17-HDHA in two different replicates of the same donor (scale bar = 1000 µm).

Due to limitations of a 384-well plate, further experiments were conducted using 96-well plates. However, due to limited number of cells obtained from RA or healthy whole blood, leukocyte cones were used to observe whether any of the SPMs has an effect on osteoclastogenesis. If an SPM would have an effect on osteoclastogenesis, it would further be tested with RA and healthy cells on 384-well plates with whole blood. As osteoclasts differentiate more rapidly from pre-DCs than from $CD14^+$ monocytes (~6 days compared to 7-10 days), SPMs were introduced either on day 5 as before, or a day earlier, on day 4 alongside TNF. However, the results suggest no significant differences between any of the SPMs compared to the control on either of these days. Therefore, due to donor variations, it can be concluded that none of these SPMs demonstrated an inhibitory effect on pre-DC-derived osteoclasts (figure 4.23).

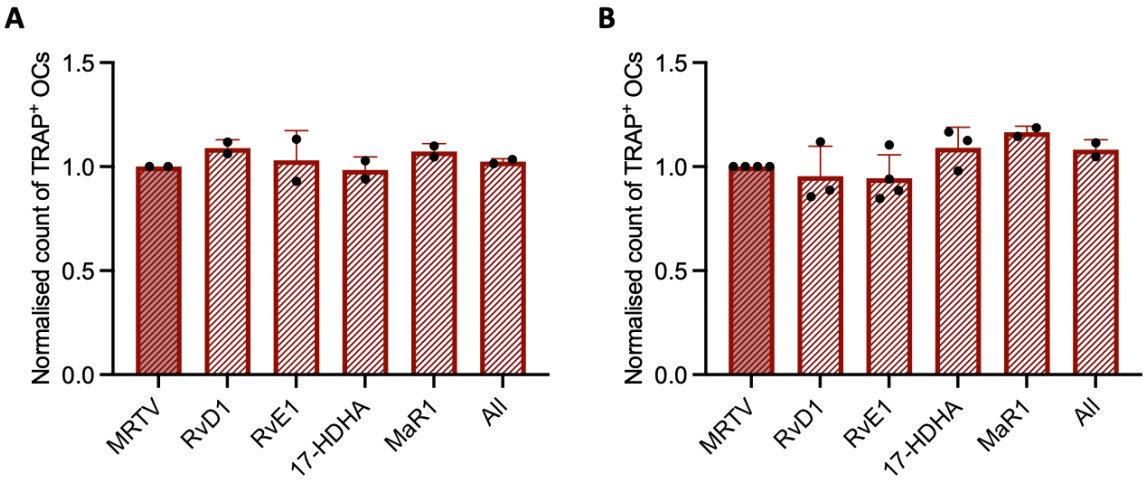

Figure 4.23 Osteoclast differentiation from DC precursors from leukocyte cones with the addition of SPMs.
Normalised counts of osteoclasts with the addition of SPMs on day 4 (**A**) or on day 5 (**B**) with 25 ng/ml of M-CSF, 25 ng/ml of RANKL, 10 ng/ml of TNF ± 10 ng/ml of SPMs, namely RvD1, RvE1, 17-HDHA, MaR1, and their combination (All). Filled bar shows the MRTV control to which the other conditions are compared to. Error bars show mean±SD while dots represent individual donors. Paired parametric t-test was done for the conditions with 3 or more donors after passing the normality test (n=2-4), however, no significance was observed.

4.3 Discussion

This chapter revolved about studying the effect of RvD1, RvE1, 17-HDHA, and MaR1 on osteoclastogenesis in standard culture conditions (no TNF) and TNF-driven conditions with the aim to elucidate their role in modulating the differentiation process. Additionally, the effect of SPMs was tested in bone resorption in healthy and RA osteoclasts. The investigation of the actions of SPMs aimed to elucidate

the underlying mechanisms, identify prominent receptors, and reveal the genes and pathways affected by the addition of these lipids.

Firstly, the effect of TNF on osteoclasts was confirmed following previous research (Ansalone et al., 2021). TNF, known for its pro-inflammatory properties, was added to cell cultures to mimic the RA environment. Initially, TNF was introduced early alongside RANKL (on day 1), which led to an inhibition of osteoclastogenesis. Further experiments in this thesis introduced TNF on day 5, which no longer resulted in an inhibition of osteoclastogenesis, but led to its enhancement at lower concentration of RANKL (1ng/ml). Additionally, RANKL was introduced 24h after M-CSF, as RANK levels are upregulated once the cells are preincubated with M-CSF for 24h (Thümmler et al., 2022), resulting in higher osteoclast numbers compared to later time-points (day 3 and day 6). Lastly, the concentration of SPMs used for this experiment was optimised.

Previous studies reported various SPM concentrations ranging between 1-500 nM (~0.35 – ~175 ng/ml) (El Kholy et al., 2018; Funaki et al., 2018; Gao et al., 2013; Herrera et al., 2008). Even though most of the studies used 100 nM, (~35 ng/ml) of SPMs (El Kholy et al., 2018; Funaki et al., 2018), in this thesis 10 ng/ml (26.6 nM) was used to investigate the effect of SPMs at a lower concentration to minimise the potential influence of ethanol, in which the SPMs are dissolved. Notably, despite several studies investigating the effect of SPMs on osteoclastogenesis, the majority of them was conducted in animal models or murine cell lines. Therefore, due to lack of research, this thesis aims to investigate the effect of SPMs on primary human cells and osteoclasts in healthy and RA individuals.

The findings of this chapter revealed that SPMs had no effect on osteoclastogenesis when added on day 1 or 5 under standard culture conditions in healthy donors. In contrast, under TNF-driven conditions, RvE1 exhibited inhibitory effect on osteoclastogenesis in healthy osteoclasts (15±6.7% inhibition compared to the control). These data correspond with previous murine studies where the inhibition of osteoclasts by RvE1 was recorded. It has been proposed that SPM-mediated inhibition of osteoclastogenesis is due to the prevention of pre-osteoclast fusion (Zhu et al., 2013), which potentially explains the numerous pre-osteoclasts seen with the addition of RvE1, however, mono- and binuclear cells were not counted

due to time restraints, therefore, this was not verified. Similar results were reported in the study by Kholy et al. (2018), which showed an inhibition of murine osteoclastogenesis with RvE1 (100 nM; ~35 ng/ml) in the presence of TNF. Another study reported inhibition of osteoclast differentiation in RAW264.7 cells at 50 nM and 100 nM showing similar results (Funaki et al., 2018). Lastly, Herrera et al. (2008) also observed osteoclast inhibition with 1, 3 and 10 ng/ml in cells isolated from mouse bone marrow with 3 ng/ml being the most effective.

Additionally, RvE1 also showed an inhibitory effect on bone resorption. However, the inhibition was non-significant and varied between 2.5-8.8 % with one donor exhibiting no effect. Notably, calcium phosphate coated plates were used to assess the degree of bone resorption, which may have led to different results compared to testing on an actual bone substrate. Herrera et al. (2008) reported reduced bone resorption in the presence of RvE1, using dentin slices in murine bone marrow osteoclasts. This ability of RvE1 to supress resorption was also observed in RAW264.7 cells in using a fluorescent bone resorption assay kit with calcium phosphate-coated plates (Funaki et al., 2018). Notably, the experiments in this thesis could not be repeated with more donors due to the plates being discontinued, and due to lack of time the assay could not be optimised with bone slices or with the fluorescent bone resorption kit. Experiments were attempted on ivory discs, however, osteoclasts differentiated very slowly and even after 3 weeks, they were still in their precursor state and failed to become mature osteoclasts (data not shown). Furthermore, it was challenging to evaluate the resorbed area due to various ridges on the discs caused by cutting of the ivory.

Interestingly, despite RvE1's inhibitory effect in healthy osteoclasts under TNF-driven conditions, RvE1 showed no effect on the osteoclast inhibition in RA osteoclasts. In contrast, RvD1, which showed no effect on healthy donors, significantly inhibited osteoclastogenesis in RA samples under TNF-driven conditions, which led to 15.6±2.4 % inhibition. Additionally, RvD1 did not have an effect on bone resorption. This was in juxtaposition to the findings of Benabdoun et al. (2019), who showed an inhibition of bone resorption with 500 nM of RvD1 on hydroxyapatite matrix with osteoclasts differentiated from primary human monocytes, as well as in murine bone explants. This suggests that higher concentration of RvD1 may be needed in order to inhibit bone resorption. The

study also showed an inhibition of osteoclasts, however, this was not done in human osteoclasts but with RAW 264.7 cells.

Due to differences between osteoclasts differentiated from monocytes and pre-DCs, the effect of SPMs was also tested in pre-DC-derived osteoclasts. Overall, no effect of SPMs was observed on osteoclastogenesis from pre-DCs differentiated from leukocyte cones. Notably, due to very low pre-DC counts in whole blood, the experiments were done with leukocyte cones, however, it was not possible to investigate the effect of SPMs in RA osteoclasts as cones are only available for healthy blood. SPMs were added on day 4 or 5, however, this time-point may be too late to observe an effect as osteoclasts from pre-DCs differentiate faster than from monocytes and by day 5, mature osteoclasts are visible. Therefore, an earlier time-point may be more effective. Another, and more likely reason for no effect of SPMs on pre-DCs can be due to their different phenotypes or varying expression of SPM receptors. FPR2 receptor (RvD1, 17-HDHA, and MaR1 receptor) was not expressed on osteoclasts derived from pre-DCs at all, while CMKLR1 (RvE1, 17-HDHA receptor) and LTB4R (RvE1, MaR1 receptor) were only slightly expressed, with LTB4R showing higher expression (figure 3.8; table 3.4). Low expression of these SPM receptors could be the reason why none of these SPMs showed an effect on osteoclastogenesis. Notably, SPM receptor expression at protein level was not evaluated on osteoclasts from pre-DCs, therefore, only their RNAseq transcript expression can be compared.

Additionally, when comparing monocyte-derived osteoclasts, LTB4R expression at the protein level was significantly higher in healthy compared to RA osteoclasts while CMKLR1 was similarly expressed in healthy and RA osteoclasts. The higher expression of LTB4R receptor in healthy than in RA also suggests that even though RvE1 interacts with both receptors (LTB4R and CMKLR1), LTB4R may be the main receptor for monocyte-derived osteoclast inhibition. This could explain why RvE1 did not have an effect on monocyte-derived osteoclastogenesis in RA. This also corresponds with Herrera et al. (2008) who suggested that LTB4R receptor is the main receptor responsible for modulation of osteoclastogenesis by RvE1. On the other hand, RvD1 most likely inhibited osteoclastogenesis in RA via FPR2 receptor, as its other receptor GPR32 was not expressed on monocytes or osteoclasts. This was also reported by Benabdoun et al. (2019) who confirmed that RvD1 apart from GPR32 also signals via FPR2 receptor, as its silencing resulted in higher

osteoclastogenesis and bone resorption. Additionally, it is not entirely clear why RvD1 inhibits osteoclastogenesis in RA but not in healthy donors as the protein expression of FPR2 on osteoclasts was expressed in both conditions. Notably, only one isoform of FPR2 was tested at the protein level, therefore, it is possible that if another isoform is responsible for binding the FPR2 receptor and for functional outcomes of RvD1, it cannot be detected with the antibody/western blot.

Gene transcript expression of healthy and RA osteoclasts in the presence of SPMs under inflammatory conditions was also investigated in order to get an insight into the osteoclastogenic and inflammatory pathways. Despite the RvE1's inhibitory effect on osteoclasts under TNF-driven conditions in healthy osteoclasts, it slightly enhanced the gene expression of NFATc1, which plays a key role in osteoclast fusion, activation, differentiation and bone resorption via TRAP, DC stamp and Cathepsin K (Zhao et al., 2010; Kim & Kim, 2014; Wehrhan et al., 2019). However, the fold-change was not bigger than 2, which suggests very subtle and non-significant differences in the presence of SPMs. The reason for slight increase in NFATc1 and inhibition of osteoclasts with RvE1 could also be due to histone modifications. If a repressive modification was present on NFATc1 promoter, it would lead to transcriptional silencing, blocking the activation of the promoter, thus could explain inhibition of osteoclastogenesis (Rohatgi et al., 2018; Woolcock, 2022). Additionally, as reported by Zhu et al. (2013), RvE1 did not have a significant effect on NFATc1 protein expression, however, RvE1 decreased its binding to the DC-stamp promoter. This shows that RvE1 can act in the nucleus by regulating DC-stamp thus decrease osteoclastogenesis and osteoclast fusion. However, the effect of RvE1 on DC-stamp was not observed in these experiments. Notably, the mentioned study used murine bone marrow cells, where 10 nM (~3.5 ng/ml) of RvE1 was used, with the highest inhibition observed after 4 days of continuous incubation with RvE1. Surprisingly, RvD1 did not have a significant effect on gene transcripts despite its inhibition of osteoclastogenesis in RA samples. However, despite its non-significance, OSCAR, NFATc1, and PU.1 expression was slightly decreased in all 3 donors, which corresponds with the functional outcomes. Therefore, as mentioned above, different time-points should be tested.

For future work, fusion of osteoclasts can be tested with live imaging to investigate whether the inhibition of osteoclasts by SPMs prevents the fusion of pre-osteoclasts or whether a different mechanism is involved. Additionally, mono- and binuclear cells in osteoclast cultures can be counted to observe whether lower number of osteoclasts correlates with higher number of osteoclast precursors, evaluating the levels of osteoclastogenic fusion. Next, fluorescent bone resorption assay kit (Cosmo Bio USA) can be used to determine bone resorption in the presence of SPMs. Additionally, higher SPM concentrations can be tested to assess the effect of RvE1 and RvD1 on bone resorption in healthy and RA osteoclasts, respectively. Furthermore, the effect of SPMs on DC-derived osteoclasts can be evaluated at earlier time-point (day 3) as the addition on day 4 and 5 may be too late to observe an inhibitory effect. To get a deeper understanding of the mechanisms and signalling pathways responsible for functional outcomes of SPMs, experiments involving for example various SPM receptor inhibitors, gene silencing via small interfering RNA (siRNA), overexpression of a specific receptor, or CRISPR-cas9 would have to be conducted. Downstream pathways can also be investigated after the SPM receptor activation, however many of these SPM receptors modulate the same pathways, which can make the analysis challenging. Finally, the effect of SPMs on osteoclastogenic genes was only tested at one time-point, therefore, for a better understanding of the effect of SPMs on the transcript of these genes, various time-points can be tested as some genes can be upregulated/downregulated in less or more than 24h after the SPM addition (day 6), which was the time-point used in this thesis.

In summation, this work provides novel insights into the inhibitory effects of RvE1 and RvD1 on osteoclastogenesis under TNF-driven conditions in healthy and RA osteoclasts. This was the first time the effect of SPMs was tested on osteoclasts differentiated from primary human cells. The results suggest that RvE1 can inhibit osteoclastogenesis in the presence of TNF in healthy donors likely via LTB4R, with the additional signalling through CMKLR1. Additionally, RvD1 inhibited osteoclastogenesis under inflammatory conditions in RA, which was done presumably via FPR2 receptor. Notably, no effect of SPMs was observed on osteoclasts differentiated from healthy pre-DCs, most likely due to low SPM receptor expression. Additionally, a potential inhibitory effect of RvE1 on bone resorption has also been observed, however, these results were very donor

dependent. Based on power calculation, a minimum of 743 patients are required for 80% power, assuming a 5% significance level using 2-tailed test. Notably, this sample size is not feasible and indicated that these results are insignificant. RvD1 did not inhibit bone resorption in RA osteoclasts.

This work also investigates various osteoclastogenic gene expression in order to uncover the mechanisms of action of SPMs, however, no significant effect of any of the SPMs was observed. Overall, none of the SPMs showed an inhibitory effect on osteoclastogenic genes, thus, different mechanism is involved in osteoclast inhibition with RvE1 and RvD1. As osteoclasts are highly metabolic cells and metabolic alterations were observed in RA myeloid compartment when compared to healthy monocytes (McGarry et al., 2021), the link between osteoclast inhibition and metabolism is further observed in chapter 5.

4.4 Conclusion

This chapter focused on the activity of SPMs on osteoclasts in health and RA. Even though these SPMs are still in their early stage of investigation, they are emerging as novel potential therapeutics which could cease inflammation and restore the balance between osteoclasts and osteoblasts thus prevent further osteoclastogenesis and bone erosion in RA. The results showed that RvE1 inhibits osteoclastogenesis under TNF-driven conditions in healthy donors, while RvD1 inhibits osteoclast differentiation in patients with RA. However, no effect on bone resorption was observed. Additionally, no effect of SPMs was observed on osteoclasts differentiated from DC precursors. More research is now needed to elucidate the mechanism of actions of SPMs in osteoclasts and their resolution pathways. Notably, osteoclasts are highly metabolically active cells, therefore it is necessary to understand metabolic differences in health and RA as there is limited research when it comes to metabolism of osteoclasts in the presence of SPMs. Moreover, SPMs have shown an effect on mitochondrial respiration in murine macrophages (Calderin et al., 2022), therefore the effect of SPMs on metabolism needs to be studied in order to understand downstream pathways, which could potentially be targeted in order to decrease inflammation, osteoclastogenesis, and bone resorption in RA.

Chapter 5 Metabolism of osteoclasts and their precursors in health and rheumatoid arthritis

5.1 Introduction

Glucose is the main source of energy for cellular metabolism and can be further catabolised by the following processes: glycolysis, Krebs cycle (also known as tricarboxylic acid (TCA cycle)), and oxidative phosphorylation (OXPHOS). As a result, adenosine triphosphate (ATP), an energy-carrying molecule, is formed (Bonora et al., 2012). Glycolysis produces far less ATP then OXPHOS, with the final product of 2 ATP molecules compared to 30-32 ATP molecules generated by OXPHOS. ATP in glycolysis is produced by the conversion of glucose into 2 molecules of acetyl coenzyme A (acetyl coA) via a series of reactions. Acetyl coA then enters the Krebs cycle, generating 2 ATP molecules, 6 nicotinamide adenine dinucleotide (NADH) molecules and 2 flavin adenine dinucleotide ($FADH_2$) molecules and 2 carbon dioxide (CO_2) molecules (Sanchez-Lopez et al., 2019). NADH and $FADH_2$ further enter the electron transport chain (ETC, also known as respiratory chain), where a proton gradient across the inner membrane is created by proton pumping (reviewed in Arnold & Finley, 2023). These protons are carried to the mitochondrial matrix via ATP synthase with a concentration gradient generating larger amount of ATP molecules as a part of OXPHOS (figure 5.1). The number of ATP molecules is dependent on the flow of protons through the ATPase and electron transport, therefore the number of ATP molecules differs (Deshpande & Mohiuddin, 2022).

As a result of activity of proton pumps, mitochondrial membrane potential is generated. Its role is to store energy, which is used by ATP synthase for the ATP production in the process of OXPHOS. As a result, mitochondrial membrane potential is reduced. On the other hand, if the ATP synthase rotates in the other direction, ATP can be hydrolysed and mitochondrial membrane potential can be generated (Zorova et al., 2018). The mitochondrial membrane potential is a key player in ETC and is essential for maintaining homeostasis of the mitochondria by maintaining an electrochemical gradient needed for the production of ATP (Baranov et al., 2021; Vasan et al., 2022; Zorova et al., 2018). If the mitochondrial membrane potential is disrupted, it leads to mitochondrial dysfunction and can

further cause the loss of viability, apoptosis, higher reactive oxygen species (ROS) production, or different pathologies, like RA (Gutiérrez et al., 2017; Liu et al., 2021; Ma et al., 2022; Promila et al., 2023). Additionally, hypoxia or inflammatory factors like TNF or IFN gamma in the synovial environment can lead to mutations in mitochondrial DNA, which can further lead to higher ROS production (Harty et al., 2011; Ma et al., 2022). These alterations can contribute to cellular damage including inflammation and the development of RA (Fearon et al., 2016; Ma et al., 2022). However, the mechanism behind mitochondrial dysfunction in RA is not well understood (Ma et al., 2022; Zorova et al., 2018).

Even though glycolysis is much less effective in the production of ATP compared to OXPHOS, it is the preferred metabolic pathway for many fast-proliferating cells like cancer cells or in various inflammatory conditions like RA under hypoxia, which is common in inflamed joints due to large number of cells (Sanchez-Lopez et al., 2019; Soto-Heredero et al., 2020). Additionally, higher ATP production by glycolysis under hypoxia can contribute to a higher cell proliferation, osteoclastogenesis, and bone resorption in RA (Ganapathy-Kanniappan & Geschwind, 2013). As RA patients exhibit enhanced utilisation of glycolytic pathways compared to healthy individuals, it has been speculated whether glucose metabolism could be considered a target for RA. Additionally, compared to healthy cells, RA $CD14^+$ monocytes are metabolically reprogrammed to become inflammatory macrophages, which exhibit an altered metabolism resulting in upregulated glycolysis, higher oxygen consumption, higher mitochondrial mass, increased mitochondrial respiration, and enhanced ATP synthesis, indicative of increased mitochondrial activity (McGarry et al., 2021).

Despite prior research suggesting metabolic alterations in RA compared to healthy myeloid compartment (McGarry et al., 2021), there is only limited research on the metabolism of osteoclasts and their precursors in RA compared to healthy individuals. Additionally, the mechanisms of action responsible for the altered metabolic state in RA compared to healthy cells remain unknown. Therefore, the aim of this chapter was to elucidate the drivers of this altered metabolic state in RA compared to healthy monocytes and understand the metabolic changes in osteoclasts and their precursors and to observe the effect of SPMs on metabolism. Thus, the expression of 7 metabolic enzymes, namely glucose transporter 1

(GLUT1), Acetyl-CoA carboxylase 1 (ACC1), Succinate Dehydrogenase Complex Flavoprotein Subunit A (SDHA), Glucose-6-phosphate dehydrogenase (G6PD), pyruvate kinase muscle isozyme (PKM), carnitine palmitoyltransferase 1A (CPT1A), and cytochrome C (CytC) was investigated (figure 5.1). These enzymes are involved in glycolysis, OXPHOS, fatty acid synthesis, which are SPM precursors, and oxidation process, and their expression was compared in healthy and RA monocytes (figure 5.1). Apart from metabolic enzymes, this chapter also explored the effect of 4 metabolic dyes in monocytes, macrophages and osteoclasts, namely 2-NBDG (glucose uptake), BodiPy FL C16 (fatty acid uptake), MitoTracker Deep Red FM (MitoTracker DR, mitochondrial mass), and TMRM (mitochondrial membrane potential) (figure 5.1). Additionally, ATP and superoxide production together with the mitochondrial oxygen consumption, basal and maximal respiration revealed the metabolic differences in healthy and RA osteoclasts and their precursors. In summary, evaluation of the metabolism and metabolic pathways in osteoclasts and their precursors was essential for the understanding of their actions on osteoclastogenesis and bone resorption.

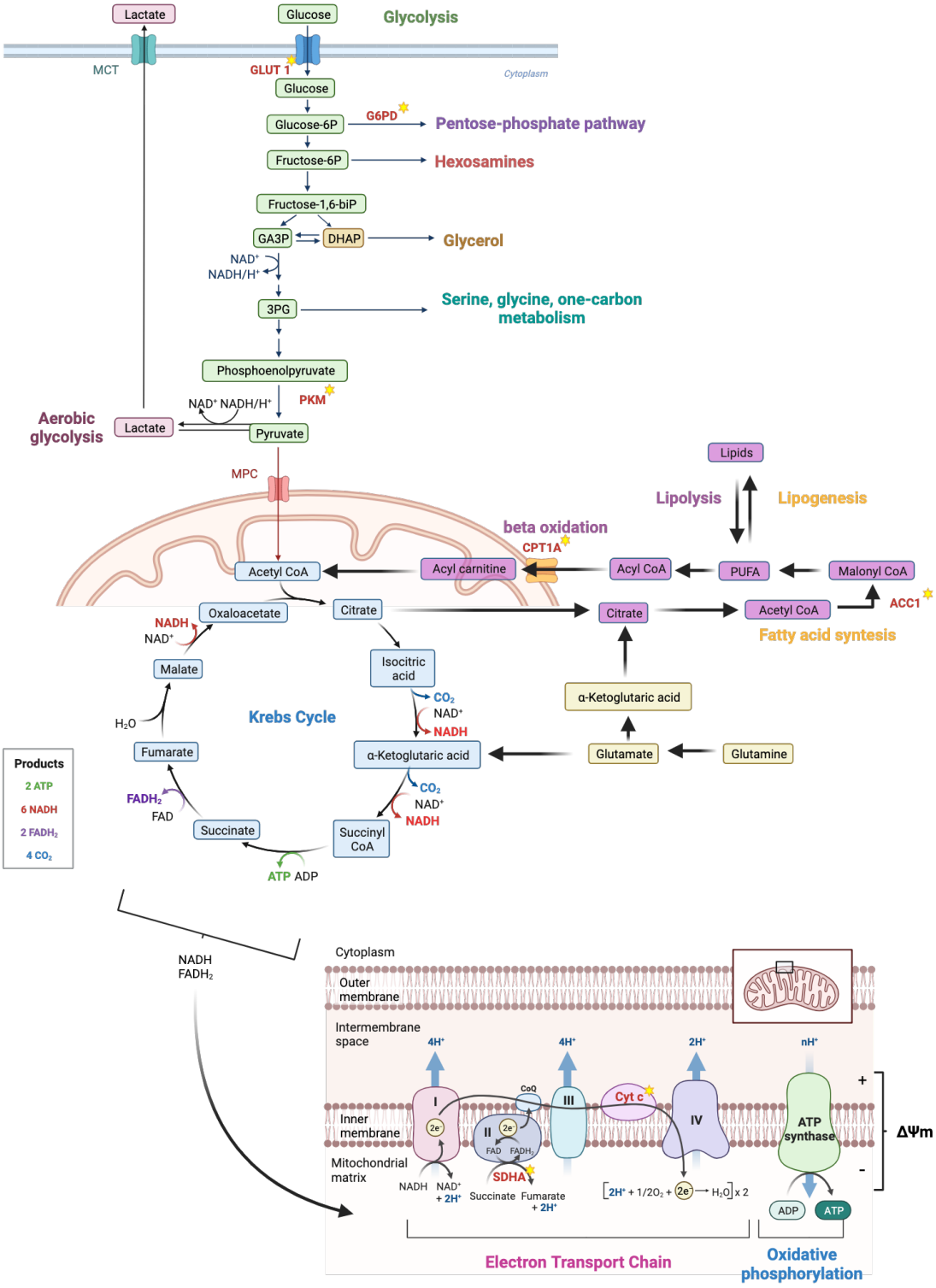

Figure 5.1 The metabolism of glucose including glycolysis, Krebs cycle, electron transport chain, and OXPHOS.

Glycolysis results in 2 ATP molecules, 2 NADH molecules and 2 pyruvates, which then enter the Krebs cycle. Krebs cycle generates 1 ATP, 3 NADH, 1 FADH2 and 2 CO_2 molecules, which is doubled as 2 pyruvate molecules are generated and each of them enters the Krebs cycle. The produced NADH and $FADH_2$ molecules are further used in electron transport chain (ETC) as electron donors. Electrons then move in the inner membrane via protein complexes (I-IV) to pump protons across the inner membrane creating proton gradient and mitochondrial membrane potential (ΔΨm), which are necessary for the ATP production via ATP synthase in the OXPHOS process. Metabolic enzymes targeted in further experiments are marked with a yellow star. Made in BioRender.

5.2 Results

5.2.1 Metabolic changes in health and RA

Prior research has shown discrepancies in metabolic states between healthy and RA myeloid compartment (Fearon et al., 2022; Hanlon et al., 2022; McGarry et al., 2021; see section 5.1), however, the metabolic alterations in healthy and RA osteoclasts and their precursors are not well understood. To investigate whether particular aspects are altered and are thus contributing to the prior observations, $CD14^+$ monocytes were stained with different metabolic enzymes with distinct role in glucose metabolism, including glycolysis (GLUT1, PKM), pentose-phosphate pathway (G6PD), ETC/OXPHOS (SDHA, CytC), and lipid metabolism (ACC1, CPT1A). The staining of metabolic enzymes was conducted in order to understand whether they are perturbed and contribute to the altered metabolic set-points. Additionally, cells were also stained with metabolic dyes measuring glucose uptake (2-NBDG), fatty acid uptake (Bodipy C16), mitochondrial mass/number of mitochondria (Mitotracker DR), and mitochondrial membrane potential (TMRM). All the enzymes and dyes were compared to single-stained and unstained controls and the cells were gated as live singlets (figure 5.2).

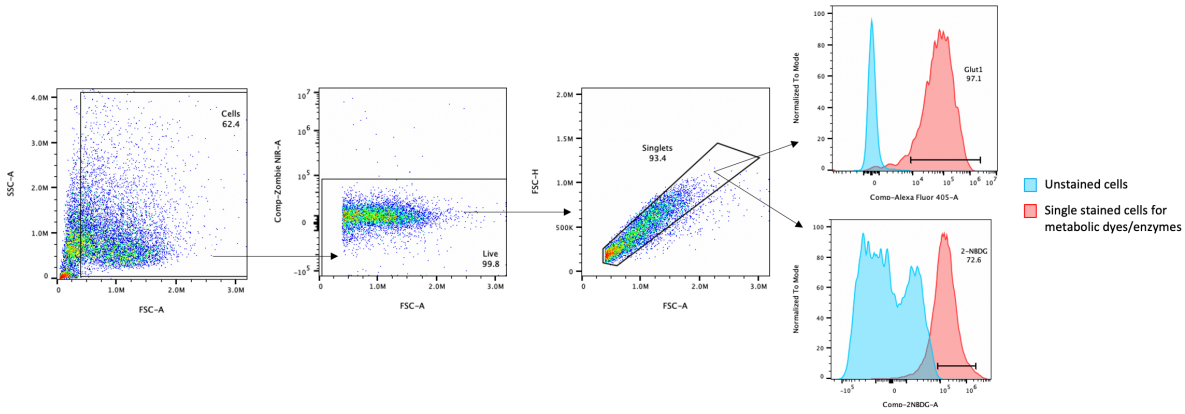

Figure 5.2 Representative image for staining of the metabolic dyes and enzymes.
$CD14^+$ monocytes were gated as single, live cells (Zombie NIR negative). An example of 1 metabolic dye (2-NBDG) and 1 metabolic enzyme (Glut1) is shown based on single-stained cells (red) compared to unstained cells (blue). SSC-A – side scatter area, FSC-A – forward scatter area, FSC-H – forward scatter height.

In initial experiments, the expression of the above-mentioned metabolic enzymes was tested in healthy and RA monocytes (figure 5.3). Despite some donor variability, the overall enzyme expression in healthy and RA samples was comparable suggesting similar expression. Therefore, based on these findings it is

unlikely that published metabolic differences between healthy and RA monocytes (McGarry et al., 2021) are due to the altered expression of these enzymes.

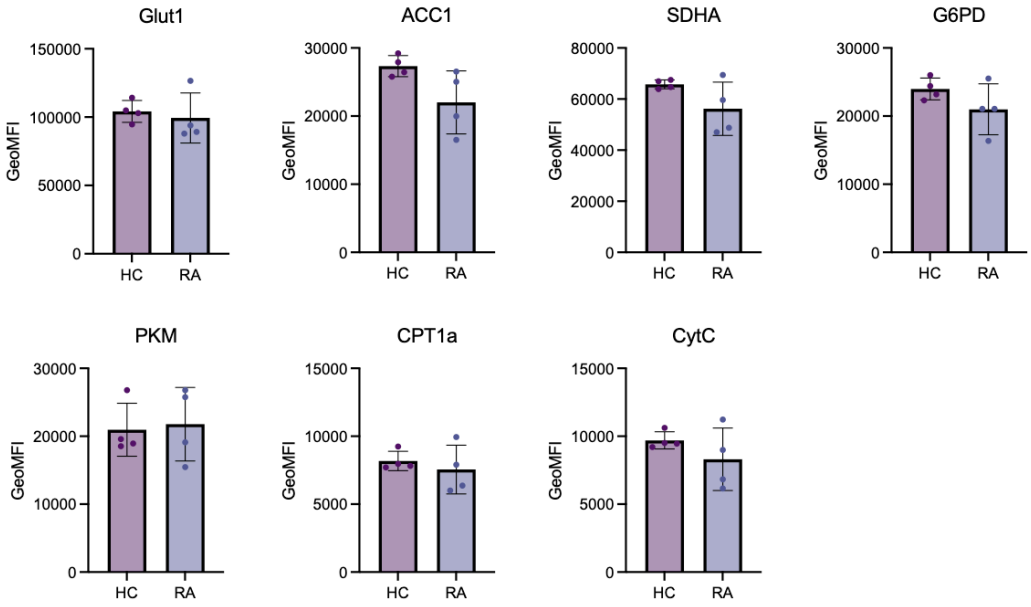

Figure 5.3 Metabolic enzyme expression in healthy and RA monocytes.
Geometric mean fluorescence intensity (GeoMFI) was measured for Glut1, ACC1, SDHA, G6PD, PKM, CPT1a and CytC in healthy (HC, purple bars) and RA (blue bars) monocytes (n=4). Parametric unpaired t-test was used to establish significance, after the samples passed the Shapiro-Wilk's normality test. None of the results were significant. Individual dots represent individual donors. Error bars show mean±SD.

After no significant differences in the expression of metabolic enzymes in healthy and RA monocytes, further work was no longer focused on exploring the mechanism of actions responsible for the altered metabolic state in RA monocytes mentioned by McGarry et al. (2021) but was rather focused on overall metabolic changes. Therefore, to investigate and confirm prior observations that there are differences in metabolic states between healthy monocytes and those from RA patients, studies were undertaken using metabolic dyes. Specifically, RA monocytes showed significantly higher glucose and fatty acid uptake and enhanced mitochondrial membrane potential compared to healthy monocytes. Additionally, they also exhibited significant increase in the signal intensity for Mitotracker DR, suggesting either higher number of mitochondria or larger mitochondria. However, further experiments would be required for clarification; therefore, for simplicity, an increased Mitotracker DR intensity will be referred to as "increase in mitochondria". Overall, this suggests that RA monocytes are more metabolically active than healthy monocytes despite similar expression of

metabolic enzymes (figure 5.4). Consistent with McGarry et al. (2021), higher uptake of MitoTracker dye was observed, showing an increase in mitochondria. The other parameters were not measured in the mentioned study.

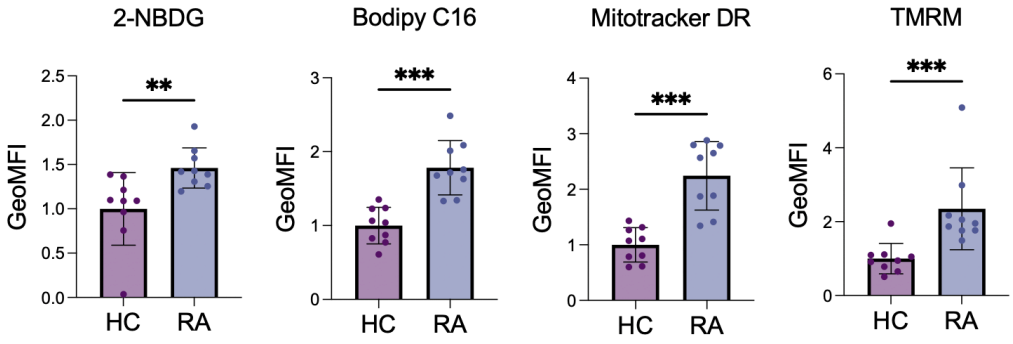

Figure 5.4 Metabolic dyes in healthy and RA monocytes.
Geometric mean fluorescence intensity (GeoMFI) was measured for 2-NBDG, Bodipy C16, MitoTracker DR, and TMRM metabolic dyes on healthy (HC, purple; N=9) and RA (blue; N = 9) live monocytes. Statistical significance was assessed via Mann-Whitney unpaired non-parametric test, after a failed Shapiro-Wilk's normality test: **p ≤ 0.002, ***p ≤ 0.0005.

After observing and confirming the metabolism of monocytes, the metabolism of macrophages and osteoclasts was also studied to find out whether the metabolic changes are retained throughout cellular differentiation to alternative maturation states. It should be noted, that within the experimental setup, the number of donors per condition varied due to several factors. For instance, as PBMCs were frozen prior to the experiments, several donors took longer to differentiate into osteoclasts with some of them not being able to differentiate into osteoclasts at all. Therefore, these donors were excluded from the analysis. Similarly, conditions with very few/no cells after gating were excluded. Notably, RA donors were more robust than healthy donors, were better at differentiating into osteoclasts, and were less likely to die, despite the same isolation and storing procedure. To assess the uptake of various metabolic dyes in osteoclasts and pre-osteoclasts, cells were gated as live, single cells (figure 5.2). As it is not possible to fully separate mature osteoclasts from their precursors in cell cultures, both populations were included in the analysis.

The results showed that in both mature macrophage and osteoclast, glucose and fatty acid uptake was significantly increased in RA compared to healthy donors (figure 5.5 A, B). In contrast, no significant differences were observed in

mitochondrial membrane potential and mitochondrial mass/number of mitochondria between healthy and RA macrophage (figure 5.5 A) and osteoclast (figure 5.5 B).

Overall, despite no difference in metabolic enzyme expression, RA monocytes showed a significant increase in glucose uptake, fatty acid uptake, mitochondrial membrane potential and increase in mitochondria, suggesting that RA monocytes might be more metabolically active. Additionally, higher glucose and fatty acid uptake was maintained throughout the differentiation into macrophages and osteoclasts.

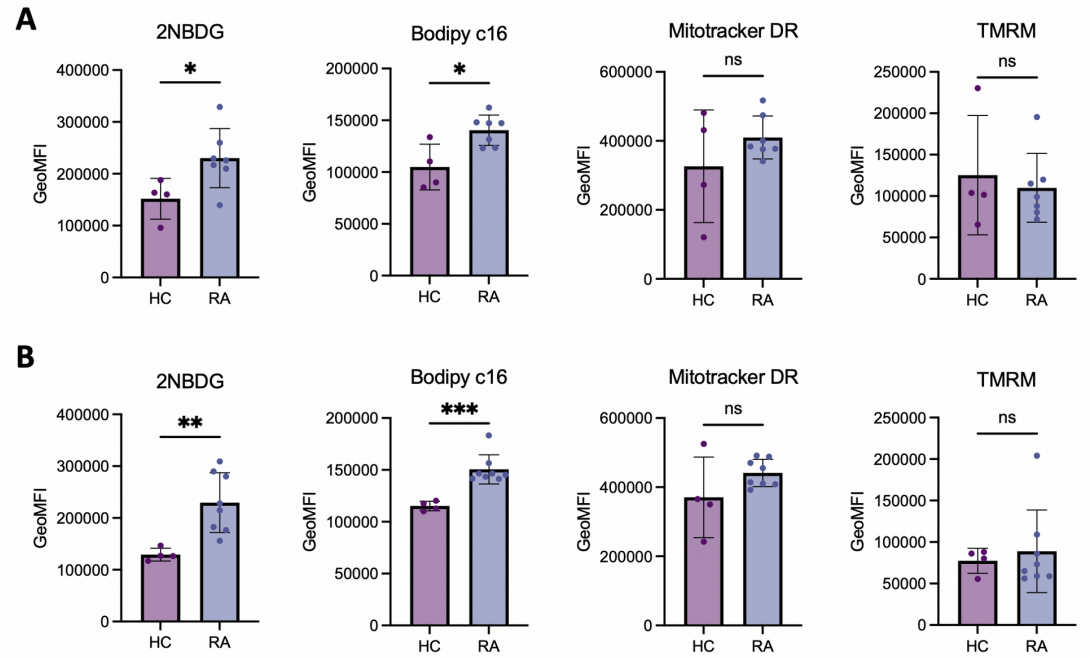

Figure 5.5 Comparison of metabolic dyes in healthy and RA macrophages and osteoclasts. Geometric mean fluorescence intensity (GeoMFI) of 2-NBDG, Bodipy C16, MitoTracker DR, and TMRM was measured for healthy (HC, purple; N=4) and RA (blue; N=7-8) macrophages **(A)** and osteoclasts **(B)** in the live, singlet population. Statistical significance was measured with the unpaired parametric t-test after the samples passed the normality test. Significance is shown with an asterisk; *p ≤ 0.05, **p ≤ 0.005, ***p ≤ 0.0005, ns – not significant. Individual dots represent individual donors. Error bars show mean±SD.

5.2.2 ATP production in healthy and RA monocytes and the impact of SPMs stimulation

After observing a difference in the metabolism of osteoclasts and their precursors, overall ATP production was measured to investigate whether its expression differs in health and RA, and in different cell types. The results showed comparable ATP

levels in healthy and RA monocytes (figure 5.6 A). To understand the balance between glycolysis or OXPHOS with regards to ATP production in the myeloid compartment, oligomycin and 2DG inhibitors were added. Oligomycin (OXPHOS inhibitor) and 2DG glucose analogue (glycolysis inhibitor) were added individually or in a combination as controls. The data showed higher ATP production in the presence of oligomycin than compared to 2DG at 10 or 100 ng/ml, which suggests that both, healthy and RA monocytes, use primarily glycolysis. Additionally, RA monocytes showed slightly higher ATP production via glycolysis compared to healthy monocytes, however, this difference was not significant (figure 5.6 A). SPMs were also added to observe whether they can regulate ATP production, however, no difference in either healthy or RA monocytes in the presence of SPMs was observed (figure 5.6 B, C, respectively).

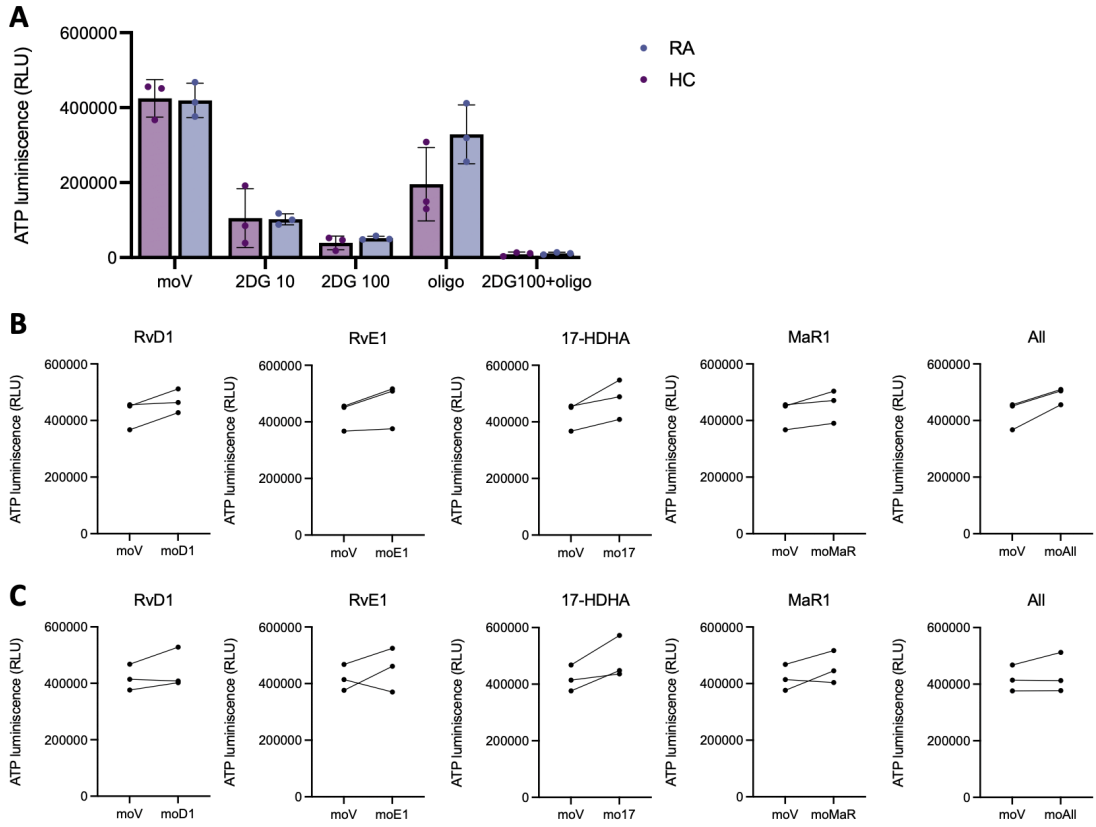

Figure 5.6 ATP production in healthy and RA monocytes.
A - ATP production with glycolysis and OXPHOS inhibitors (2DG and oligomycin, respectively) compared to the monocyte control with added ethanol as a vehicle (moV). 2DG was added at 10 mM, 100 mM, while oligomycin was added at 1 µM. The controls were also added in combination with 100 mM of 2DG and 1 µM of oligomycin. **B** - ATP production in healthy monocytes with the addition of 10 ng/ml of SPMs, namely RvD1 (moD1), RvE1 (moE1), 17-HDHA (mo17), MaR1 (moMaR), and their combination (moAll) compared to their monocyte control with added vehicle (moV). **C** - ATP production in RA monocytes with the addition of 10 ng/ml of individual SPMs and their combination compared to their monocyte control with vehicle (moV). Paired t-test was conducted for statistical significance after passing the Shapiro-Wilk's normality test, however, all results were non-significant (n=3 for healthy and RA).

To further elaborate on the metabolism of osteoclasts, the overall ATP production was measured under TNF-driven conditions, however, similarly to monocytes, no difference between healthy and RA osteoclasts was observed, and similarly to monocytes, the ATP production was mostly driven by glycolysis (figure 5.7 A). Additionally, no effect was observed with any of the SPMs in healthy or RA osteoclasts, either (figure 5.7 B, C, respectively). The effect of SPMs on macrophages was not tested due to limited number of cells and donors and also because osteoclasts are the main focus of interest for this work.

In summary, there is no substantial difference in ATP production between healthy and RA osteoclasts and monocytes. Similarly, none of the SPMs exhibited a notable effect on ATP production.

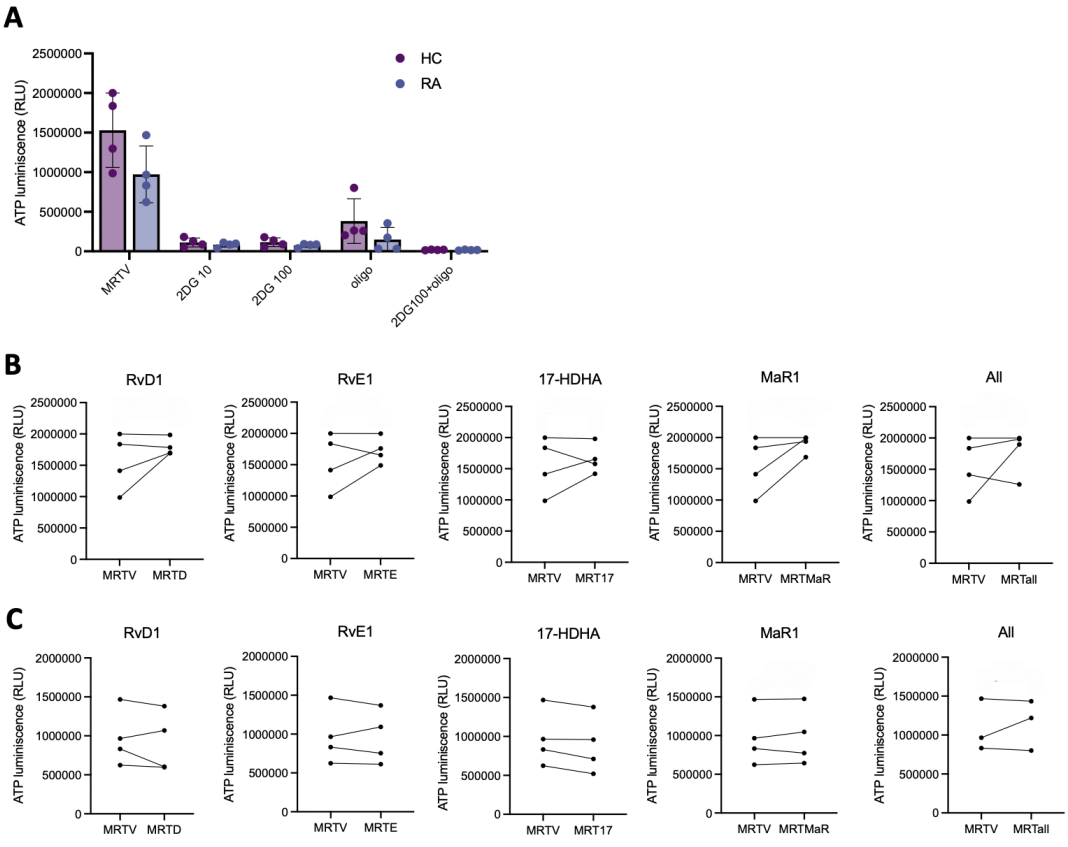

Figure 5.7 ATP production in healthy and RA osteoclasts.
A - ATP production with glycolysis and OXPHOS inhibitors (2DG and oligomycin, respectively) compared to the osteoclast control differentiated with M-CSF, RANKL, TNF and vehicle (MRTV). 2DG was added at 10 mM, 100 mM, while oligomycin was added at 1 µM. The controls were also added in combination with 100 mM of 2-DG and 1 µM of oligomycin. **B** - ATP production in healthy osteoclasts with the addition of 10 ng/ml of SPMs, namely RvD1 (MRTD), RvE1 (MRTE), 17-HDHA (MRT17), MaR1 (MRTMaR), and their combination (MRTall). Parametric paired t-test was conducted for statistical significance after passing the normality test. No significant results were observed (n=4). **C** - ATP production in RA osteoclasts with the addition of individual SPMs (n=4) and their combination (N=3). Parametric paired t-test was conducted for statistical significance after passing the normality test. No significant results were observed.

5.2.3 The effect of SPMs on mitochondrial superoxide production in healthy and RA osteoclasts

Despite no effect of SPMs on the ATP production, the MitoSOX assay was conducted on osteoclasts under TNF-driven conditions in the presence of SPMs to establish their role on superoxide regulation. In explanation of the assay, after the penetration of the dye into live mitochondria, the MitoSOX dye gets oxidised by mitochondrial superoxide, which emits bright red colour. The brighter the signal, the more superoxide is present. Notably, this technique only shows superoxide, not other ROS or reactive nitrogen species (RNS). To measure the levels of other ROS/RNS, different detection kits or fluorescent probes could be used (Gardiner et al., 2020).

In healthy osteoclasts in the presence of TNF, RvE1 showed a significant effect on the inhibition of superoxide with an average inhibition of 33.4±18.2%, varying from 12-64%. The other SPMs lead to a mixed effect on the superoxide production (figure 5.8 A). The inhibition can also be observed in the representative microscope images, where the addition of RvE1 noticeably decreased superoxide levels resulting in less bright red colour compared to the control and the other conditions. The image with the addition of RvE1 was also more comparable to the negative control with very low signal, confirming its inhibitory effect (figure 5.8 B). Additionally, 17-HDHA also showed an inhibitory effect, resulting in less bright microscope images, similar to the ones with RvE1, however, the results were not significant.

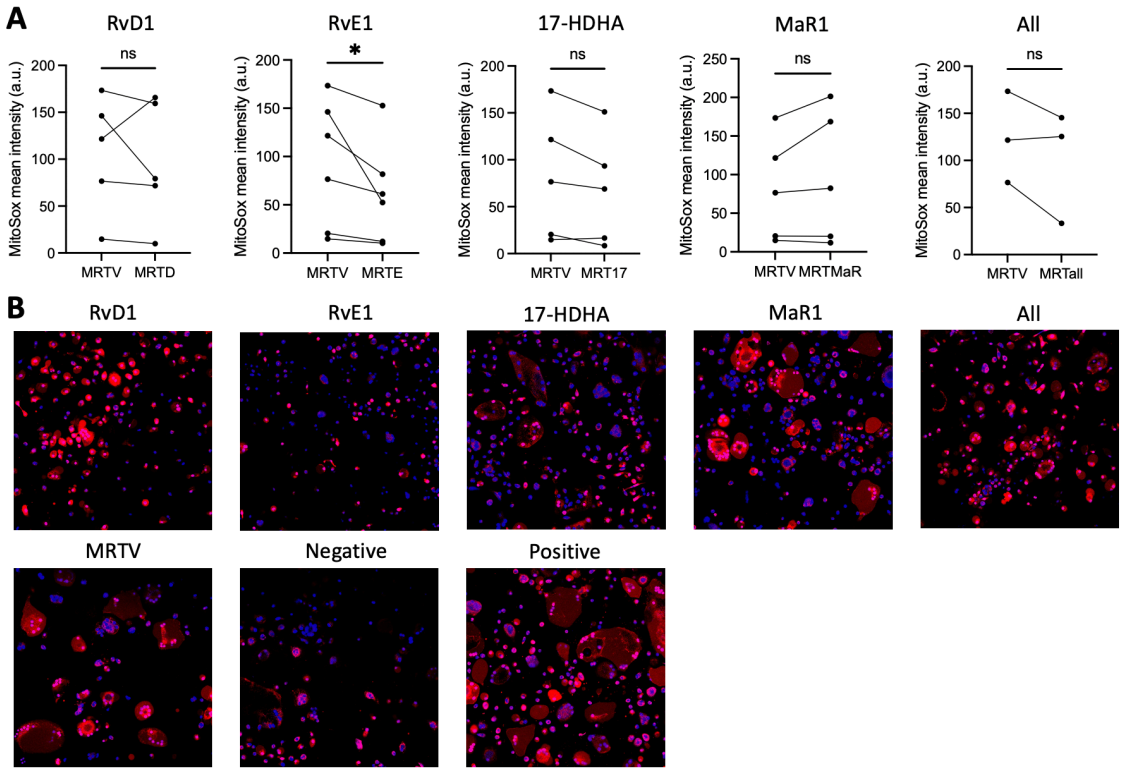

Figure 5.8 MitoSOX assay in healthy osteoclasts with the addition of SPMs.
A - MitoSOX mean intensity was measured for individual cells of every microscope image in the presence of 10 ng/ml of SPMs, namely RvD1 (MRTD), RvE1 (MRTE), 17-HDHA (MRT17), MaR1 (MRTMaR), and a combination of all SPMs (MRTall) compared to the osteoclast control differentiated in the presence of 25 ng/ml of M-CSF, 25 ng/ml of RANKL, 10 ng/ml of TNF and vehicle (MRTV). Parametric paired t-test was used for significance after passing the normality test; *$p \leq 0.05$. **B** - Confocal microscope images of osteoclasts with MitoSOX dye. The brighter the colour, the more superoxide is present in mitochondria. Menadione was used as a positive control, while Mito-TEMPO was used as a negative control. All the SPMs were compared to the MRTV control.

Unlike in healthy osteoclasts, RvE1 did not inhibit superoxide production in RA osteoclasts. However, RvD1 together with 17-HDHA lead to a significant decrease of superoxide in osteoclasts in every RA donor. The inhibition with RvD1 resulted in 36.4±12.4% decrease in the superoxide production ranging between 28.6-54.8% while the addition of 17-HDHA showed 22.4±7.3% reduction with the span between 14-30% (figure 5.9 A). Therefore, the inhibition by RvD1 was slightly more pronounced compared to 17-HDHA. Additionally, representative images are shown, where the addition of RvD1 and 17-HDHA led to less bright signal than in the control and other conditions (figure 5.9 B). The other SPMs including their combination did not have an inhibitory effect in RA osteoclasts.

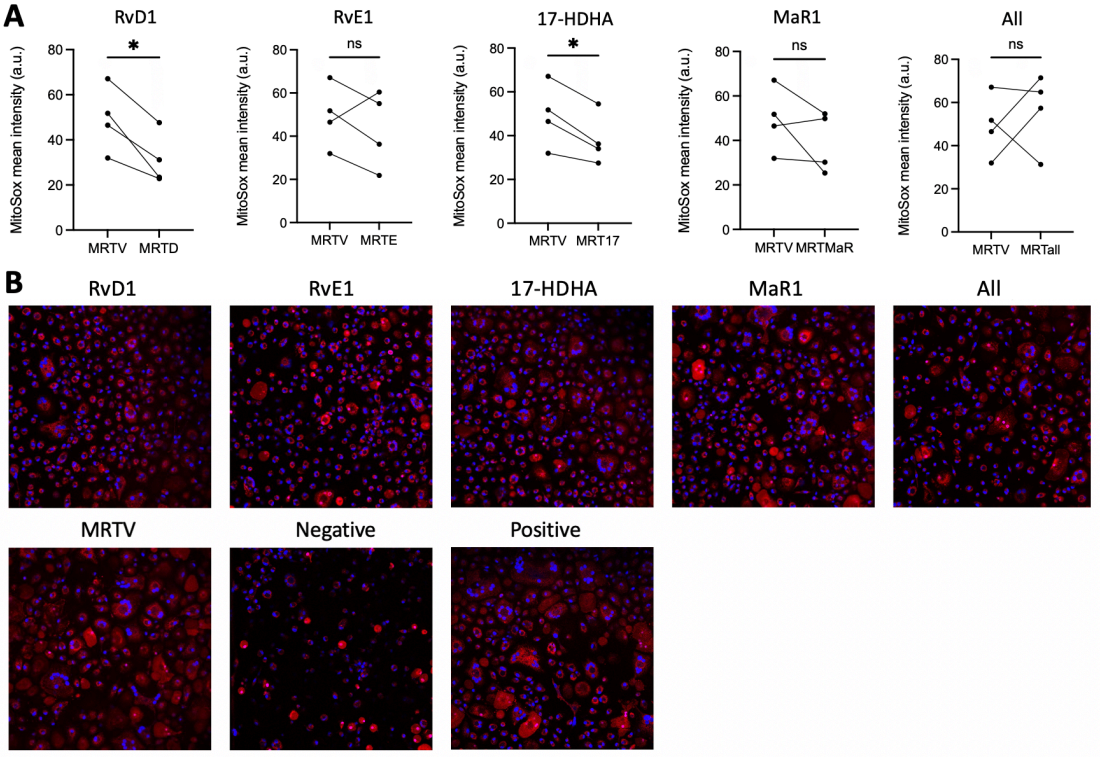

Figure 5.9 MitoSOX assay in RA osteoclasts with the addition of SPMs.
A - MitoSOX mean intensity was measured for individual cells of every microscope image with various 10 ng/ml of SPMs, namely RvD1 (MRTD), RvE1 (MRTE), 17-HDHA (MRT17), MaR1 (MRTMaR), and a combination of all SPMs (MRTall). Osteoclasts differentiated in the presence of M-CSF, RANKL, TNF, and vehicle (MRTV) were used as a control. Paired t-test was used for significance after passing the normality test; *p ≤ 0.05. **B** - Representative confocal microscope images of RA osteoclasts with MitoSOX dye. The brighter the colour, the more superoxide is present in mitochondria. Menadione was used as a positive control, while Mito-TEMPO was used as a negative control. All the SPMs were compared to the MRTV control.

5.2.4 The effect of SPMs on mitochondrial respiration in health and RA

After certain SPMs showed an inhibitory effect on the production of superoxide, the effect of SPMs was tested with a Seahorse Mito Stress assay conducted on healthy and RA monocytes. The oxygen consumption rate (OCR) was measured for mitochondrial respiration in live cells at baseline, and with the addition of oligomycin (blocks ATP synthase), Carbonyl cyanide 3-chlorophenylhydrazone (CCCP; uncoupling agent that disrupts mitochondrial membrane potential), and the combination of rotenone and antimycin A (inhibitors of complex I and III, respectively) (Agilent.com). Based on these measurements, several parameters providing more complex information about the mitochondrial function could be calculated (figure 5.10):

- Basal respiration – energetic demand of the cell at baseline
- ATP production – ATP produced by the mitochondria to meet the energetic needs of the cell
- Proton leak – respiration not coupled to ATP production, can be a sign of damaged mitochondria
- Maximal respiration – maximal respiratory rate the cell can achieve after respiratory chain operates at its maximum
- Spare respiratory capacity – ability of the cell to respond to energetic demand, which can show the cell's fitness
- Non-mitochondrial oxygen consumption – it is important for assessing mitochondrial respiration

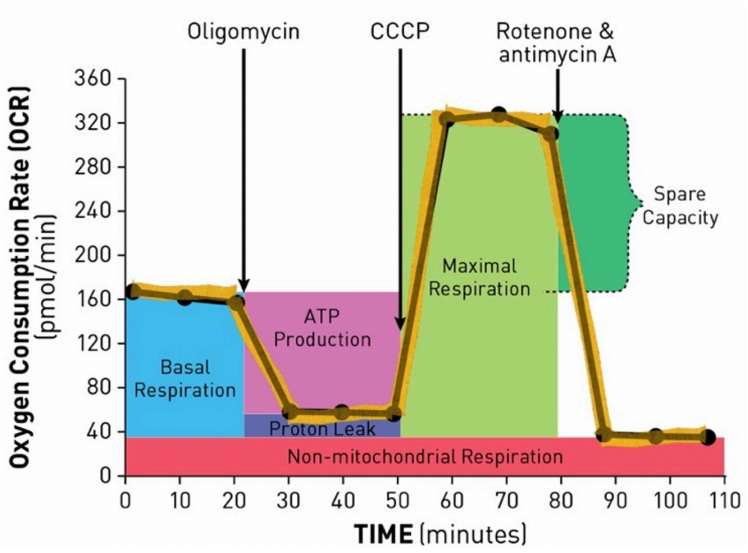

Figure 5.10 Seahorse cell mito-stress test for mitochondrial respiration.
The graph shows the calculations for different metabolic parameters like non-mitochondrial oxygen consumption, basal respiration, maximal respiration, proton leak, ATP production and spare respiratory capacity with the addition of oligomycin, Carbonyl cyanide 3-chlorophenylhydrazone (CCCP), and rotenone & antimycin A (Agilent.com).

The Seahorse data showed higher OCR production in healthy monocytes compared to RA (5.11 A), however, it is important to mention that although the assay had 5-6 technical replicates it is only based on 1 healthy and 1 RA donor. Initial data showed that healthy monocytes had increased maximal respiration compared to basal respiration, therefore their spare respiratory capacity was higher, which is essential for the cell's viability and the higher the value of this theoretical maximum respiratory capacity, the better, as it gives the cell the ability to meet higher energetic requirements. In contrast, RA monocytes appeared to be close to

using their maximal capacity to respire as their basal and maximal respiration was comparable (figure 5.11A). This suggests that RA monocytes have a very low spare respiratory capacity, which could hinder their ability to cope with various forms of stress. This could further affect ATP production and lead to cell death (Marchetti et al., 2020).

Notably, the effect of SPMs differed in healthy and RA monocytes. In healthy monocytes, all SPMs reduced OCR levels. Additionally, basal respiration, maximal respiration, and the ATP production was decreased in the presence of the SPMs (figure 5.11 B). In RA monocytes, however, only 17-HDHA and MaR1 decreased the OCR levels, while RvE1 and RvD1 showed comparable OCR levels to the control. Moreover, while 17-HDHA and MaR1 showed subtle inhibition in basal and maximal respiration and ATP production, RvD1 and RvE1 did not have an effect on the respiration and only subtly increased the ATP production (figure 5.11 C). The effect of SPMs, however, was more pronounced in healthy compared to RA monocytes. This shows that SPMs could have an impact on mitochondrial respiration, however, their effect varies in health and RA and more donors are needed for a better understanding.

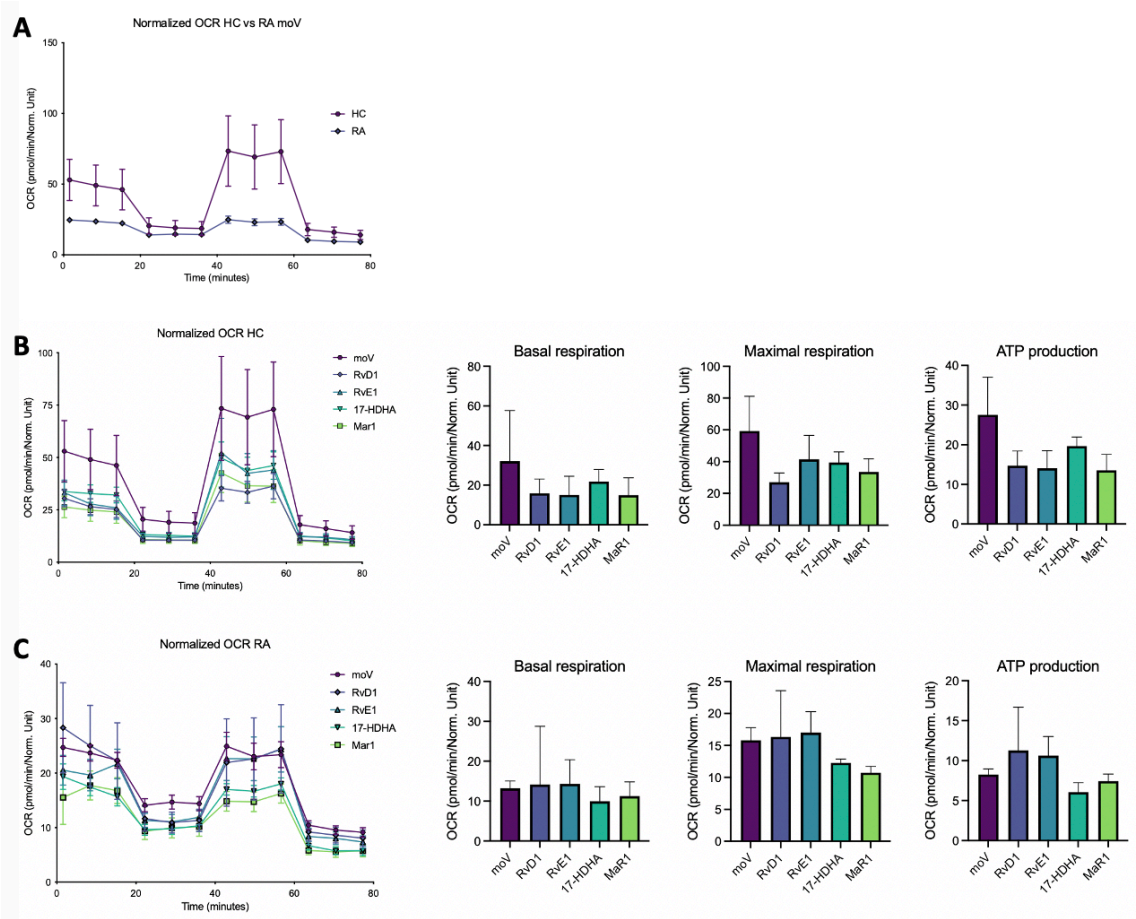

Figure 5.11 Cellular respiration in healthy and RA monocytes in the presence of SPMs. **A -** Normalised oxygen consumption rate (OCR) values are shown for the healthy (HC) and RA monocytes with vehicle control (moV). **B -** Calculated OCR parameters, namely basal respiration, maximal respiration, and ATP production of healthy (HC) monocytes in the presence of SPMs compared to the control (moV). **C** - OCR levels in RA monocytes in the presence of SPMs compared to the monocyte control (MoV). The graphs were plotted using Prism 9 software as mean ± SEM for 1 healthy and 1 RA donor with 5-6 technical replicates.

5.3 Discussion

This chapter focused on investigating the metabolism of healthy and RA osteoclasts and their precursors, as it has been shown that the metabolism of healthy and RA monocytes is very distinct (McGarry et al., 2021). Additionally, based on the previous chapter, some effects of selected SPMs were observed on osteoclastogenesis, where RvE1 and RvD1 inhibited osteoclast differentiation under TNF-driven conditions in healthy and RA donors, respectively (see chapter 4). Therefore, understanding the metabolic changes is not only essential for unravelling the mechanisms of action of SPMs but also for shedding light on the interplay between metabolism and osteoclastogenesis in the context of health and RA.

The findings in this chapter revealed significant increase in glucose uptake, fatty acid uptake, increase in mitochondria, and mitochondrial membrane potential in RA compared to healthy monocytes, despite similar expression of metabolic enzymes. The reason for a high glucose uptake but similar GLUT1 expression, for example, could be due to various post-translational modifications, like phosphorylation, which could make the receptor more active in RA compared to healthy monocytes. This could explain why the expression levels in health and RA are comparable, but glucose uptake is increased in RA and not in healthy monocytes (Lemos Duarte & Devi, 2020) Additionally, there are several GLUT isoforms, for example GLUT2, GLUT3, GLUT4, and GLUT5, which were not tested in this thesis. Therefore, it is also plausible that the enhanced glucose uptake was driven via these isoforms and not through the primary GLUT1 receptor (Sibiak et al., 2022). In a study using human THP-1 cells, GLUT3 levels were higher in monocytes than GLUT1 levels, while the other isoforms – GLUT2, GLUT4, and GLUT5 were not expressed (Fu et al., 2004). However, it was also shown that the levels of GLUT1 and glucose uptake are increased in RA and other inflammatory conditions such as SLE (Zezina et al., 2020), which would not be fully consistent with the results observed in this thesis as GLUT1 was not increased in RA. Notably, healthy and RA monocytes used for the metabolic assays were frozen prior to the experiments, which might have also affected the metabolic response. Therefore, for future work, fresh samples should be evaluated.

Additionally, the increase in glucose and fatty acid uptake in RA monocytes was maintained throughout the differentiation into macrophages and osteoclasts. In contrast, the mitochondrial mass/number of mitochondria and the mitochondrial membrane potential remained comparable between healthy and RA osteoclasts and macrophages. Notably, the osteoclast population used for the assessment of metabolic dyes did not only consist of pure mature osteoclasts. As cells in osteoclast co-cultures, namely osteoclasts, pre-osteoclasts and macrophages are all $OSCAR^{+}$, it is a technical limitation of this assay to distinguish different subsets and look at the uptake of metabolic dyes only on osteoclasts (Bianco et al., 1987). Overall, this comparison indicates that the differences in the mitochondrial mass/number of mitochondria and the mitochondrial membrane potential between healthy and RA cells diminish throughout the differentiation process.

Interestingly, although RA monocytes exhibit enhanced metabolic activity, the overall ATP production between healthy and RA monocytes was comparable with no substantial differences observed. One hypothesis for similar ATP production in healthy and RA monocytes despite higher glucose and fatty acid uptake, higher membrane potential, and increased mitochondria in RA monocytes could be due to higher utilisation of glycolysis compared to OXPHOS in RA monocytes. This would suggest that even though RA monocytes have higher glucose uptake, they rely more on glycolysis, which yields less ATP than OXPHOS. Even though the fatty acid uptake and mitochondrial membrane potential was increased, which could suggest higher activity in the process of OXPHOS, an increase in mitochondria, possibly showing higher mitochondrial mass, was also more pronounced in RA monocytes, which could mean mitochondrial impairment. This would be consistent with McGarry et al. (2021), who observed bigger mitochondrial mass in RA monocytes and linked it to mitochondrial dysfunction. Dysfunctional mitochondria could then lead to limited ATP production, as ATP could be hydrolysed, which would also explain higher mitochondrial membrane potential (Zorova et al., 2018). Moreover, mitochondrial damage, caused by hypoxia or the presence of inflammatory factors (e.g., TNF), could lead to higher ROS production and lower ATP, which would also support these results of higher mitochondrial activity in RA monocytes but similar ATP levels to healthy monocytes (Ma et al., 2022). Another study tested monocytes and macrophages from coronary artery disease, which showed predisposition of these cells to promote inflammation by elevated glucose consumption, ATP production and cytokine release compared to healthy cells (Shirai et al., 2016). However, in this thesis, no difference in overall ATP levels was observed between healthy and RA monocytes, therefore, another hypothesis, besides mitochondrial dysfunction, could be that RA cells show higher energetic demands than healthy cells. Thus, as they are primed to become inflammatory macrophages, it is possible that they produce more ATP but also use more ATP, which could then result in similar overall ATP levels between RA and healthy cells. This hypothesis could also be supported by the data from Seahorse showing that RA monocytes operate at their maximum capacity, suggesting they are more active (Agilent.com). However, only 1 healthy and 1 RA donor was tested, therefore additional experiments are required to fully test this hypothesis.

The observations in monocytes were also reflected in the osteoclast compartment, where no difference in the ATP production was observed in osteoclasts derived from healthy or RA individuals. This could be due to reprogramming of the metabolism of RA osteoclasts where they switch to higher glycolysis despite having enough oxygen, which would lead to the production of lactate (Ghanbari Movahed et al., 2019). This is known as the Warburg effect and is common in cancer cells or fast-proliferating cells. It only results in 2 ATPs and reduced ROS production as OXPHOS is not the main pathway of glucose utilisation. Increased glucose uptake could instead of ATP also be used for the synthesis of amino acids for proliferation and cell growth (Ghanbari Movahed et al., 2019). In summation, further experiments are needed to fully comprehend why ATP production remains comparable in health and RA, despite higher metabolic activity of RA cells. Finally, no effect of SPMs was observed on ATP production in osteoclasts and monocytes, suggesting that SPMs do not alter the overall production of ATP.

Despite no effect of SPMs on ATP production, RvE1 exhibited an inhibitory effect on superoxide production in healthy osteoclasts under TNF-driven conditions (33.4±18.2%). Superoxide is the main ROS and is highly produced in inflammatory conditions like RA or during joint inflammation (Lee et al., 2021). It is mostly generated from the ETC in mitochondria and too much production can lead to joint destruction, cell damage, articular degeneration, pain, or various chronic diseases (Indo et al., 2015; Lee et al., 2021). Therefore, the inhibition of superoxide in mitochondria can reduce inflammation and further joint destruction (Di Cesare Mannelli et al., 2013). Interestingly, in RA osteoclasts, RvE1 did not have an effect on superoxide inhibition, however, RvD1 and 17-HDHA managed to reduce the production of superoxide. RvD1 inhibited its release by 36.4±12.4%, while 17-HDHA by 22.4±7.3%, suggesting that it could have an impact on the metabolic activity of the cells. A similar pattern of the actions of RvE1 and RvD1 was observed in the previous chapter (chapter 4) where RvE1 showed an inhibitory effect in healthy osteoclasts, while RvD1 inhibited osteoclastogenesis in RA osteoclasts under TNF-driven conditions. These results may suggest a link between reduced superoxide production and the ability of these SPMs to inhibit osteoclastogenesis.

The effect of SPMs on metabolism was also further studied with Seahorse experiments, where some differences were observed between their effect in healthy and RA monocytes, although only 1 healthy and 1 RA donor was tested. The results showed more pronounced effect on healthy compared to RA monocytes, where in RA monocytes RvE1 and RvD1 did not influence basal and maximal respiration, and only had a subtle effect on mitochondrial ATP production, while in healthy monocytes all SPMs showed an inhibitory effect on mitochondrial respiration and ATP production. The reason why RvE1 and RvD1 showed no effect on respiration in RA could be due to inflammatory environment, because of which RA monocytes were primed to become inflammatory cells, which could overrule the effect of SPMs, thus showing less pronounced effect compared to healthy. Additionally, mitochondrial dysfunction that is often associated with RA patients and was also suggested based on the results from metabolic dyes described above could be another reason why RA monocytes were less prone to the actions of SPMs (Panga et al., 2019). However, more donors would be needed for a better understanding of the actions of SPMs on mitochondrial respiration. Due to time and cell limitations, it was not possible to fully investigate all aspects within this thesis, and thus it would be interesting to investigate mitochondrial respiration of healthy and RA osteoclasts and the effect of SPMs in osteoclasts and their precursors. It would also be worth using the metabolic dyes and metabolic enzyme assays in osteoclasts and their precursors in the presence of SPMs, to explore the effect of SPMs on mitochondrial metabolism and their mechanisms of action in health and RA.

5.4 Conclusion

In conclusion, RA monocytes demonstrated enhanced metabolic activity, and this difference in glucose and fatty acid uptake persisted throughout their differentiation into macrophages and osteoclasts. While RA monocytes also showed higher mitochondrial membrane potential and increase in mitochondria compared to healthy monocytes, these differences were no longer observed in differentiated cells. Despite the increased metabolic activity in the RA myeloid compartment, no changes were observed in the expression of metabolic enzymes or ATP production when compared to healthy cells. Nevertheless, higher metabolic state may suggest increased inflammation, osteoclastogenesis and bone

resorption in RA patients. Additionally, when testing the effect of SPMs, RvE1 significantly decreased the production of superoxide in healthy osteoclasts under TNF-driven conditions, while RvD1 and 17-HDHA inhibited superoxide levels in RA osteoclasts when exposed to TNF, which might be beneficial in reducing osteoclastogenesis and inflammation. Further investigations are required to determine the drivers of this altered state and reveal potential novel pathways that could be therapeutically targeted to simultaneously mitigate inflammation and bone erosion.

Chapter 6 General discussion

Rheumatoid arthritis is a chronic autoimmune disease with an estimated overall prevalence of 0.81% in adults in the United Kingdom, where women are affected approximately three times more than men (ratio of 2.7:1) (Gardiner et al., 2018). To date, there is no effective cure for RA and current therapeutics are not efficacious in all individuals, therefore, several studies have focussed on the effect of pro-resolving mediators, which could lead to the remission of symptoms. Specialised pro-resolving mediators have shown the potential to resolve inflammation, reduce bone resorption and osteoclast differentiation, protect from oxidative stress, inhibit pro-inflammatory cytokines, and enhance healing, however, their mechanism of action, is not well understood (Funaki et al., 2018; Norling et al., 2016; Leuti et al., 2019; Chiang & Serhan, 2020; Ali et al., 2021). Moreover, they are naturally produced, therefore, they are not immunosuppressive, which is a major concern for side effects of current biologics like anti-TNF therapies (Fattori et al., 2020; Serhan, 2017; Norling et al., 2016).

This thesis initially investigated the expression of known SPM receptors (mainly CMKLR1, FPR2, and LTB4R) on monocytes and osteoclasts, as to this date, there is only limited research on SPM receptors, especially in osteoclasts differentiated from primary human cells. RNAseq analysis revealed differences between healthy and RA monocytes with CMKLR1 exhibiting significantly higher expression in healthy monocytes, FPR2 showed significantly increased expression in RA, and LTB4R was similarly expressed (chapter 3). When these SPM receptors were tested at the protein level by western blot, significantly higher expression of LTB4R was noted in healthy monocytes and osteoclasts, while CMKLR1 and FPR2 were similarly expressed. This led to the hypothesis that SPMs binding to LTB4R, specifically RvE1 and MaR1, might have more pronounced effect in healthy than in RA monocytes and osteoclasts; assuming LTB4R is their primary receptor.

Once the SPM receptors were investigated, further experiments were focused on the effect of four SPMs, namely RvE1, RvD1, MaR1 and 17-HDHA. Notably, previous studies have shown that RvE1 and RvD1 have an effect on the inhibition of osteoclastogenesis, however, their impact has not been tested on osteoclasts differentiated from healthy and RA primary human cells (RvE1 - Kholy et al., 2018;

Funaki et al., 2018; Herrera et al., 2008; RvD1 - Benabdoun et al., 2019; Yuan et al., 2010; Klein et al., 2022). Additionally, to the best of my knowledge, the effect of 17-HDHA and MaR1, has not been previously tested in regards of osteoclastogenesis, however, DHA, which is their precursor was shown to be able to inhibit osteoclastogenesis in cell lines (Boeyens et al., 2014; Xie et al., 2019), murine models (Kishikawa et al., 2019; Ma et al., 2023), and osteoclasts differentiated from primary human cells (Kasonga et al., 2015). Therefore, work in this thesis aimed to explore the potential of these SPMs on inhibiting osteoclast differentiation from primary human cells. The findings showed that none of the selected SPMs exhibited a significant effect on osteoclastogenesis under steady-state conditions (no TNF) in healthy or RA osteoclasts. However, in the presence of TNF, RvE1 inhibited osteoclastogenesis in healthy osteoclasts (15.01±6.65% inhibition), possibly due to the prevention of pre-osteoclast fusion as reported by Zhu et al. (2013), who tested an effect of RvE1 in *in vitro* murine models, but further experiments would be needed for confirmation. Interestingly, RvE1's inhibitory effect was not observed in RA osteoclasts, while RvD1 showed inhibitory actions on osteoclast differentiation in the presence of TNF in RA osteoclasts (15.58±2.43% inhibition) but had no effect in healthy cells (chapter 4). The SPM's inhibitory effect in the presence of TNF might be attributed to TNF-induced upregulation of several inflammatory pathways like NF-kB, MAPK, ERK, pI3K, JNK, p38, and AKT (Luo et al., 2018; Zha et al., 2018, Lee et al., 2001; Kitaura et al., 2022). RvE1 and RvD1 as pro-resolving lipids have the ability to inhibit these pathways in order to reduce inflammation and osteoclast differentiation. For example, RvE1 and RvD1 can signal via MAPK/ERK and PI3K/AKT to block NF-kB, therefore these SPMs might be more effective once these pathways are upregulated (Kholy et al., 2018; Funaki et al., 2018; Li et al., 2020; Keinan et al., 2013). To fully investigate this, new studies should be undertaken to evaluate the associated signalling cascades.

Additionally, RvE1 and RvD1 were assessed for their impact on bone resorption, however, the results were non-significant. It is possible that RvE1 could have a potential to inhibit bone resorption, as it reduced bone resorption in 3 donors and 1 donor remained unchanged, however due to heterogeneity of healthy and RA individuals, more donors would be needed for confirmation. Notably, this was tested with calcium phosphate coated plates, which were discontinued, therefore

the experiments could not be repeated with more donors. This was in contrast to previous studies, where RvE1 showed inhibitory effect on bone resorption. This was observed in murine osteoclasts differentiated on dentin slices and RAW264.7 cells differentiated on calcium-phosphate plates, however, higher concentration of SPMs was used (Herrera et al., 2008; Funaki et al., 2018). RvD1 has also previously shown an inhibitory effect on bone resorption using osteoclasts differentiated from primary human monocytes on hydroxyapatite matrix, as well as in murine bone explants (Benabdoun et al., 2019). Notably, these studies used much higher concentrations than the one used in this thesis (500 nM compared to 26.6 nM (10 ng/ml)), therefore, higher concentration of SPMs could be tested in future experiments. Furthermore, SPMs are dissolved in ethanol, which was one of the reasons why a lower concentration of SPMs was tested. Thus, the possible effect of ethanol also has to be further investigated at higher concentrations. Additionally, bone resorption plates used for these experiments were used after their expiry date and could not be reorder as they were discontinued, therefore, fluorescent bone resorption assay kit (COSMO BIO USA) could be used as an alternative.

Based on the SPM receptor expression and the actions of SPMs, it can be postulated that RvE1 acts primarily via LTB4R receptor, which was previously suggested by Herrera et al. (2008). Higher expression of this receptor at the protein level in healthy compared to RA osteoclasts could explain why RvE1 is only effective in reducing osteoclast differentiation in healthy and not in RA cells. On the other hand, as GPR32 receptor was not expressed in healthy or RA monocytes or in healthy osteoclasts, RvD1's signalling was most likely induced via FPR2 receptor. The importance of this receptor was also confirmed in a study by Benabdoun et al. (2019), who showed that silencing of FPR2 leads to higher osteoclastogenesis. Even though the expression of FPR2 at the protein level was comparable between healthy and RA monocytes and osteoclasts, its expression at the transcript level was significantly higher in RA than in healthy monocytes. However, there are several isoforms of FPR2, while the antibody used for western blot only targeted one of them, which could mean that even though the expression of the targeted isoform was comparable, the expression of the other isoforms might differ, which would have to be further tested for example by qPCR, electrophoresis (Harvey & Cheng, 2016), mass spectrometry (Hale, 2013), or long-read RNA sequencing (for

example Oxford Nanopore) (Miller et al., 2022). Additionally, the interaction between FPR2 and RvD1 has not been solved at a molecular level and it is currently unclear how they bind to each other and how/if it differs between the various isoforms. Therefore, the more pronounced effect of RvD1 in RA compared to healthy cells may be attributed to the interaction with isoforms that were not detected by the antibody. Additionally, post-translational modifications like glycosylation, phosphorylation, palmitoylation and ubiquitination (Lemos Duarte & Devi, 2020), could also have an impact on the activity of the receptor and downstream pathways, which could be another possibility for the observed inhibitory effect in RA but not in healthy cells despite similar receptor expression.

This thesis also looked into various osteoclastogenic pathways, however, only very subtle effect of SPMs on transcript expression was observed in healthy and RA osteoclasts and none of the observed differences was bigger than a 2-fold change (chapter 4). After the comparison of healthy and RA osteoclasts, the only difference was observed in the expression of NFATc1, which is an important transcription factor for osteoclastogenesis (Zhao et al., 2010). In the presence of RvE1, 17-HDHA and the combination of all SPMs, NFATc1 expression was increased in healthy osteoclasts compared to their control with no SPM and compared to RA osteoclasts. Even though RvE1 was shown to inhibit osteoclastogenesis, it increased the levels of NFATc1 in healthy osteoclasts but not in RA. This could be attributed to the presence of repressive histone 3 lysine 27 tri-methylation (H3K27me3) modification, which if present on NFATc1 promoter would lead to transcriptional silencing, which would block the activation of the promoter, thus lead to inhibition of osteoclastogenesis (Rohatgi et al., 2018; Woolcock, 2022). Previous research in the lab identified various changes in activating histone 3 lysine 4 tri-methylation (H3K4me3) or repressing H3K27me3 modifications, alongside different histone-modifying enzymes and regulators in RA when compared to healthy controls. The results suggested perturbed epigenetic and transcriptomic profiles in RA monocytes and responses *in vivo* (Woolcock, 2022; Ansalone et al., 2021). To further understand whether this is the case, Chip-seq would have to be conducted in order to assess either the activating H3K4me3 or repressing H3K27me3 modifications.

Lastly, the metabolism of osteoclasts and their precursors was examined as healthy and RA cells are very distinct and perturbation in RA myeloid compartment has been previously observed (McGarry et al., 2021). The results in this thesis revealed significant increase in glucose uptake, fatty acid uptake, mitochondrial membrane potential. Additionally, an increase in Mitotracker DR signal was observed, which could correspond to either higher mitochondrial mass or increased number of mitochondria in RA compared to healthy monocytes, however imaging studies would be required to determine whether this signal corresponds to mitochondrial size or mitochondrial content. This increased metabolic activity of RA monocytes was observed despite no significant difference in the overall ATP production and similar expression of metabolic enzymes (GLUT1, ACC1, SDHA, G6PD, PKM, CPT1a, CytC). The reason for similar ATP production and metabolic enzyme expression in healthy and RA monocytes could be due to different mechanisms, which were summarised in chapter 5. One possibility is that despite higher glucose and fatty acid uptake, RA monocytes have higher utilisation of glycolysis compared to OXPHOS, yielding less ATP. This was also suggested by the preliminary Seahorse data, where healthy monocytes showed higher oxygen consumption rate when compared to RA, which suggests lower OXPHOS engagement in RA monocytes (Hanlon et al., 2022; Monsour et al., 2022). Although fatty acid uptake and higher mitochondrial membrane potential were increased under TNF settings, the mitochondrial mass/number of mitochondria was also increased, suggesting impairment, which could lead to lower ATP production and higher ROS production (Ma et al., 2022). Furthermore, RA monocytes might produce more ATP but also use more ATP, which could explain comparable ATP production and similar enzyme expression to healthy donors. Furthermore, RA monocytes showed to operate at their maximal respiratory capacity, while healthy monocytes have higher spare respiratory capacity, which is crucial for the cell's viability (chapter 5). Therefore, variations in metabolic profiles of healthy and RA monocytes can affect the impact of SPMs, as indicated in the preliminary Seahorse data. This data demonstrated that the effect of SPMs on basal respiration, maximal respiratory capacity, and mitochondrial ATP production was increased in healthy monocytes, while no difference was observed in the presence of RvE1 and RvD1 in RA monocytes. Notably, none of the results (based on technical replicates) were significant and only 1 healthy and 1 RA donor was tested. Another explanation for the more pronounced effects of SPMs in healthy rather than in RA

monocytes could be that RA monocytes are primed to become pro-inflammatory, and the inflammatory environment may override the actions of SPMs on the mitochondrial respiration. Additionally, as mentioned above, mitochondrial dysfunction in RA monocytes might be another reason why the effect of SPMs is not as pronounced as in healthy cells. Interestingly, the difference in glucose and fatty acid uptake persisted throughout the differentiation into osteoclasts, however, the mitochondrial mass/number of mitochondria, and the membrane potential were no longer significantly distinct. More experiments, such as Seahorse, testing of metabolic dyes and enzymes, are needed to better understand the differences in metabolism in mature osteoclasts and their precursors in the presence and absence of SPMs.

Even though SPMs did not exhibit an effect on the ATP production and only showed a subtle effect on mitochondrial respiration, their impact was further tested on mitochondrial superoxide production in health and RA. The data showed that RvE1 reduced mitochondrial superoxide production in healthy osteoclasts, which is the main ROS responsible for mitochondrial damage. In contrast, in RA osteoclasts, RvD1 and 17-HDHA inhibited superoxide production, while RvE1 no longer had an inhibitory effect. One explanation for the inhibition in superoxide production but no effect on basal and maximal respiration, and the ATP production could be due to upregulation of superoxide dismutase, which can neutralise superoxide production. Previous research showed that RvE1 and RvD1 can increase levels of superoxide dismutase and glutathione peroxidase (Bozkurt et al., 2023). Higher expression of superoxide dismutase can convert superoxide into hydrogen peroxide, which can be further converted into water by glutathione peroxidase (Koju et al., 2019). Therefore, the current data suggest that RvE1 and RvD1 inhibit osteoclastogenesis in healthy and RA osteoclasts, respectively, via the inhibition of superoxide (Laha et al., 2022).

In conclusion, this thesis showed differential expression of SPM receptors in health and RA providing a deeper insight into the metabolism of healthy and RA monocytes and osteoclasts. The data suggested that despite similar metabolic enzyme expression and ATP production, RA monocytes exhibited potentially higher metabolic activity, as they showed higher glucose and fatty acid uptake, increased mitochondrial membrane potential, and higher mitochondrial

mass/number of mitochondria when compared with healthy monocytes. Moreover, higher glucose and fatty acid uptake in RA compared to healthy monocytes was maintained in osteoclasts. Additionally, RvE1 and RvD1 showed an inhibitory effect on osteoclast differentiation in health and RA under TNF-driven conditions, respectively, which was associated with reduced superoxide production. Finally, as not all RA therapeutics are effective in every individual, SPMs or their pathways could be beneficial as a potential treatment in RA, which might reduce the side effects that are associated with current treatment. However, further research is needed to investigate the drivers of the altered metabolic profile in RA and to understand the resolution pathways that could be potentially targeted in order to reduce inflammation, osteoclastogenesis, and bone resorption.

Impact of COVID-19

Due to the COVID-19 pandemic, clinics and the lab were closed for the first half a year of my PhD. Therefore, no healthy or RA samples could be obtained, and no experiments could be conducted. Even after the re-opening of the lab and clinics, it was still very challenging to obtain RA samples. Therefore, the work of this PhD thesis shifted from the original plan of generating and analysing my own RNAseq datasets towards bioinformatic analysis of pre-existing datasets generated in our lab group. Additionally, due to time constraints some experiments could not be repeated, which resulted in limited number of donors.

Conferences

Riedlova, P., Woolcock, K., Ansalone, C., Goodyear, C. S., (2023, November 10-15). The Effect of Resolvin E1 and Resolvin D1 Specialised Pro-resolving Mediators on the inhibition of Osteoclastogenesis [Conference poster presentation]. ***American College of Rheumatology (ACR)***, San Diego, California, USA.

Riedlova, P., Almeida L., Ansalone, C., Sood, S., Everts, B., Goodyear, C. S., (2023, March 9-11). Investigating metabolic variations in osteoclasts and their myeloid precursors within rheumatoid arthritis [Conference poster presentation]. ***European Workshop for Rheumatology Research (EWRR)***, Dublin, Ireland.

Riedlova, P., Almeida L., Ansalone, C., Sood, S., Everts, B., Goodyear, C. S., (2022, November 10-14). Altered Metabolic State in Myeloid Precursors and Mature Cells Within Rheumatoid Arthritis [Conference poster presentation]. ***American College of Rheumatology (ACR)***, Philadelphia, Pennsylvania, USA.

Riedlova, P., Ansalone, C., Woolcock, K., Sood, S., Goodyear, C. S., (2022, June 29-July 1). Evaluation of specialized pro-resolving mediators and their receptors in osteoclast lineage cells from health and diseases [Conference poster presentation]. ***8th European Workshop for Lipid Mediators (8EWLM)***, Stockholm, Sweeden.

Almeida, L., Riedlova, P., Goodyear, C. S., Everts, B., (2022, December 14-15). Metabolic dysregulation in human myeloid cells in rheumatoid arthritis [Conference poster presentation]. ***Dutch society for immunology***, Amsterdam, The Netherlands.

Published papers

Riedlova, P., Sood, S., Goodyear, C. S., & Ansalone, C. (2023). Differentiation of functional osteoclasts from human peripheral blood CD14+ monocytes. *Journal of Visualized Experiments*, (191). https://doi.org/10.3791/64698

Kok, F. O., Wang, H., Riedlova, P., Goodyear, C. S., & Carmody, R. J. (2021). Defining the structure of the NF-κb pathway in human immune cells using quantitative proteomic data. *Cellular Signalling*, *88*, 110154. https://doi.org/10.1016/j.cellsig.2021.110154

Appendices

Media

Complete α-MEM media

- 500 ml Alpha Minimum Essential Medium (α-MEM; Gibco)
- 10% Heat Inactivated Fetal Bovine Serum (FBS; Gibco)
- 5 ml Penicilin/streptomycin (Sigma)
- 5 ml L-glutamine (Gibco)

Complete RPMI media

- 500 ml Roswell Park Memorial Institute (RPMI; Gibco)
- 10% Heat Inactivated FBS (Gibco)
- 5 ml Penicilin/streptomycin (Sigma)
- 5 ml L-glutamine (Gibco)

Buffers and solutions

Cell separation buffer

- 500 ml dPBS (Gibco)
- 1% Heat Inactivated Fetal Bovine Serum (FBS; Gibco)
- 2 mM EDTA (Invitrogen)

FACS buffer

- 500 ml PBS
- 2% FBS
- 2 mM EDTA

TRAP fixative solution

- 12.5 ml citrate solution
- 32.5 ml acetone
- 5 ml 37% formaldehyde

TRAP staining solution

For 1 ml:

- 900 µL distilled water
- 10 µL Fast Garnet Solution (5 µL Fast Garnet + 5 µL Sodium Nitrite)
- 10 µL Napthol
- 40 µL Acetate
- 50 µL Tartrate (1M - 2.8 g of K-Na Tartrate Tetrahydrate (MW 282.23; C4H4KNaO6*4H2O) in 10 mL H2O)

2x RT master mix for cDNA synthesis

- 2 µL of 10X RT buffer
- 0.8 µL 25X dNTP Mix (100 mM)
- 2 µL of 10X RT Random Primers
- 1 µL of MultiScribe™ Reverse Transcriptase
- 4.2 µL Nuclease-free water

qPCR master mix

For 1 sample:

- 5 µl Power Sybr green dye (Invitrogen, 4367659)
- 3.8 µl RNase free water
- 0.1 µl forward primer
- 0.1 µl reverse primer

TBST

- 1x Tris-buffered saline
- 0.1% Tween

Milk blocking buffer

- 5% non-fat dried milk
- 50 ml 1x Tris-buffered saline
- 0.1% Tween

PFA

- 500 ml PBS
- 2% para formaldehyde

2% formaldehyde

- 50 ml dH_2O
- 2% methanol-free formaldehyde

0.1% Triton

- PBS
- 0.1% Triton X-100

2% BSA

- 50 ml PBS
- 2% bovine serum albumin

MitoSOX master mix

- 500 ml PBS
- 5 µM MitoSOX dye (Invitrogen)
- 4 µM Hoechst 33342 nuclei staining (stock = 16.2 mM; Invotrogen)

Seahorse media

- 50 ml basal Seahorse media with no serum (Agilent Technologies)
- 4 mM glutamine
- 5.5 mM glucose
- 1 mM penicillin/streptomycin
- 1 mM sodium pyruvate (Gibco)

- pH of 7.4

Cell-Tak solution

- 41.3 µL Cell-Tak (Corning)
- 2.5 ml 0.1 M sodium bicarbonate ($NaHCO_3$) solution

Sulforhodamine B (SRB) sodium salt solution

- 0.2 g SRB (Sigma-Aldrich)
- 50 ml 1% acetic acid

List of references

Abdolmaleki, F., Kovanen, P., Mardani, R., Gheibi-hayat, S., Bo, S. and Sahebkar, A. (2019). Resolvins: Emerging Players in Autoimmune and Inflammatory Diseases. *Clinical Reviews in Allergy & Immunology*, 58(1), pp.82-91

Agidigbi, T. S., & Kim, C. (2019). Reactive oxygen species in osteoclast differentiation and possible pharmaceutical targets of ROS-mediated osteoclast diseases. *International Journal of Molecular Sciences*, *20*(14), 3576. doi:10.3390/ijms20143576

Agilent.com (2023). *Seahorse XF Cell mito stress test kit user guide - agilent*. Available at: https://www.agilent.com/cs/library/usermanuals/public/XF_Cell_Mito_Stress_Test_Kit_User_Guide.pdf

Akchurin, T., Aissiou, T., Kemeny, N., Prosk, E., Nigam, N., & Komarova, S. V. (2008). Complex Dynamics of osteoclast formation and death in long-term cultures. *PLoS ONE*, *3*(5). doi:10.1371/journal.pone.0002104

Aletaha, D. and Blüml, S., (2016). Therapeutic implications of autoantibodies in rheumatoid arthritis. *RMD Open*, 2(1), p.e000009

Aliko, A., Ciancaglini, R., Alushi, A., Tafaj, A., & Ruci, D. (2011). Temporomandibular joint involvement in rheumatoid arthritis, systemic lupus erythematosus and systemic sclerosis. *International Journal of Oral and Maxillofacial Surgery*, *40*(7), 704–709. https://doi.org/10.1016/j.ijom.2011.02.026

Alnaeeli, M., & Teng, Y.-T. A. (2009). Dendritic cells differentiate into osteoclasts in bone marrow microenvironment in vivo. *Blood*, *113*(1), 264–265. doi:10.1182/blood-2008-09-180836

Amaral, F., Oliveira, T., Calderaro, D., Ferreira, G. and Teixeira, M., 2016. Advance in Therapies for Rheumatoid Arthritis. Immune Rebalancing, pp.15-36.

Amarasekara, D. S., Yun, H., Kim, S., Lee, N., Kim, H., & Rho, J. (2018). Regulation of osteoclast differentiation by cytokine networks. *Immune Network*, *18*(1). https://doi.org/10.4110/in.2018.18.e8

Anderson, H. C. (2003). Matrix vesicles and calcification. *Current Rheumatology Reports*, *5*(3), 222–226. doi:10.1007/s11926-003-0071-z

Angelotti F, Parma A, Cafaro G, Capecchi R, Alunno A, Puxeddu I. One year in review (2017): pathogenesis of rheumatoid arthritis. *Clin Exp Rheumatol*. 2017;35(3):368-378

Ansalone, C., Cole, J., Chilaka, S., Sunzini, F., Sood, S., Robertson, J., Siebert, S., McInnes, I. B., & Goodyear, C. S. (2021). TNF is a homoeostatic regulator of distinct epigenetically primed human osteoclast precursors. *Annals of the Rheumatic Diseases*, *80*(6), 748–757. https://doi.org/10.1136/annrheumdis-2020-219262

Arai, F., Miyamoto, T., Ohneda, O., Inada, T., Sudo, T., Brasel, K., Miyata, T., Anderson, D. M., & Suda, T. (1999). Commitment and differentiation of osteoclast precursor cells by the sequential expression of C-FMS and receptor activator of nuclear factor KB (rank) receptors. *The Journal of Experimental Medicine*, *190*(12), 1741–1754. https://doi.org/10.1084/jem.190.12.1741

Arnardottir, H., Dalli, J., Norling, L., Colas, R., Perretti, M. and Serhan, C. (2016). Resolvin D3 Is Dysregµlated in Arthritis and Reduces Arthritic Inflammation. *The Journal of Immunology*, 197(6), pp.2362-2368

Arnold, P.K. and Finley, L.W.S. (2023) 'Regulation and function of the mammalian tricarboxylic acid cycle', *Journal of Biological Chemistry*, 299(2), p. 102838. doi:10.1016/j.jbc.2022.102838.

Auréal, M., Machuca-Gayet, I. and Coury, F. (2020) 'Rheumatoid arthritis in the view of osteoimmunology', *Biomolecules*, 11(1), p. 48. doi:10.3390/biom11010048.

Balan, S., Saxena, M., Bhardwaj, N. (2019). Dendritic cell subsets and locations. *International Review of Cell and Molecular Biology*, 1–68. doi:10.1016/bs.ircmb.2019.07.004

Balas, L., Guichardant, M., Durand, T., & Lagarde, M. (2014). Confusion between protectin D1 (PD1) and its isomer protectin DX (PDX). an overview on the dihydroxy-docosatrienes described to date. *Biochimie*, *99*, 1–7. doi:10.1016/j.biochi.2013.11.006

Baranov, S. *et al.* (2021) 'Two hit mitochondrial-driven model of synapse loss in neurodegeneration', *Neurobiology of Disease*, 158, p. 105451. doi:10.1016/j.nbd.2021.105451.

Barden, A. E., Moghaddami, M., Mas, E., Phillips, M., Cleland, L. G., & Mori, T. A. (2016). Specialised pro-resolving mediators of inflammation in inflammatory arthritis. *Prostaglandins, Leukotrienes and Essential Fatty Acids*, *107*, 24–29. https://doi.org/10.1016/j.plefa.2016.03.004

Barnes, P., 2009. How corticosteroids control inflammation: Quintiles Prize Lecture 2005. British Journal of Pharmacology, 148(3), pp.245-254.

Baum, R. and Gravallese, E., 2013. Impact of Inflammation on the Osteoblast in Rheumatic Diseases. *Current Osteoporosis Reports*, 12(1), pp.9-16.

Bazan, N. G. (2006). Neuroprotectin D1 (NPD1): A dha-derived mediator that protects brain and retina against cell injury-induced oxidative stress. *Brain Pathology*, *15*(2), 159–166. https://doi.org/10.1111/j.1750-3639.2005.tb00513.x

Bazan, N. G. (2009). Cellular and molecular events mediated by docosahexaenoic acid-derived neuroprotectin D1 signaling in photoreceptor cell survival and brain protection. *Prostaglandins, Leukotrienes and Essential Fatty Acids*, *81*(2–3), 205–211. https://doi.org/10.1016/j.plefa.2009.05.024

Benabdoun, H. A., Kulbay, M., Rondon, E.-P., Vallières, F., Shi, Q., Fernandes, J., Fahmi, H., & Benderdour, M. (2019). In vitro and in vivo assessment of the proresolutive and antiresorptive actions of Resolvin D1: Relevance to arthritis. *Arthritis Research & Therapy*, *21*(1). https://doi.org/10.1186/s13075-019-1852-8

Bhagavatham, S. K., Kannan, V., Darshan, V. M., & Sivaramakrishnan, V. (2021). Nucleotides modulate synoviocyte proliferation and osteoclast differentiation in macrophages with potential implications for rheumatoid arthritis. *3 Biotech*, *11*(12). doi:10.1007/s13205-021-03052-8

Bianco, P., Costantini, M., Dearden, L. C., & Bonucci, E. (1987). 'Expression of tartrate-resistant acid phosphatase in bone marrow macrophages'. *Basic and applied histochemistry*, 31(4), 433–440.

Bird, P., Hall, S., Nash, P., Connell, C., Kwok, K., Witcombe, D. and Thirunavukkarasu, K., (2019). Treatment outcomes in patients with seropositive versus seronegative rheumatoid arthritis in Phase III randomised clinical trials of tofacitinib. *RMD Open*, 5(1), p.e000742.

Bolamperti, S., Villa, I., & Rubinacci, A. (2022). Bone Remodeling: An operational process ensuring survival and bone mechanical competence. *Bone Research*, *10*(1). doi:10.1038/s41413-022-00219-8

Bonora, M. *et al*. (2012) "ATP synthesis and storage," *Purinergic Signalling*, 8(3), pp. 343–357. Available at: https://doi.org/10.1007/s11302-012-9305-8.

Bouchareychas, L., Grössinger, E. M., Kang, M., Qiu, H., & Adamopoulos, I. E. (2017). Critical role of LTB4/Blt1 in IL-23–induced synovial inflammation and osteoclastogenesis via NF-KB. *The Journal of Immunology*, *198*(1), 452-460. doi:10.4049/jimmunol.1601346

Boyce, B. and Xing, L. (2007). The RANKL/RANK/OPG pathway. *Current Osteoporosis Reports*, 5(3), pp.98-104.

Bullock, J., Rizvi, S., Saleh, A., Ahmed, S., Do, D., Ansari, R. and Ahmed, J., (2018). Rheumatoid Arthritis: A Brief Overview of the Treatment. *Medical Principles and Practice*, 27(6), pp.501-507.

Calderin, E. P., Zheng, J.-J., Boyd, N. L., McNally, L., Audam, T. N., Lorkiewicz, P., Hill, B. G., & Hellmann, J. (2022). Exercise-induced specialized proresolving mediators stimulate AMPK phosphorylation to promote mitochondrial respiration in macrophages. *Molecular Metabolism*, *66*, 101637. https://doi.org/10.1016/j.molmet.2022.101637

Cappariello, A., Maurizi, A., Veeriah, V., & Teti, A. (2014). The great beauty of the osteoclast. *Archives of Biochemistry and Biophysics*, *558*, 70–78. https://doi.org/10.1016/j.abb.2014.06.017

Capulli, M., Paone, R., & Rucci, N. (2014). Osteoblast and osteocyte: Games without frontiers. *Archives of Biochemistry and Biophysics*, *561*, 3–12. doi:10.1016/j.abb.2014.05.003

Carbone, L., Vasan, S., Elam, R., Gupta, S., Tolaymat, O., Crandall, C., Wactawski-Wende, J., & Johnson, K. C. (2020). The Association of Methotrexate, sulfasalazine, and hydroxychloroquine use with fracture in postmenopausal women with rheumatoid arthritis: Findings from the Women's Health initiative. *JBMR Plus*, *4*(10). https://doi.org/10.1002/jbm4.10393

Cash, J., Norling, L. and Perretti, M. (2014). Resolution of inflammation: targeting GPCRs that interact with lipids and peptides. *Drug Discovery Today*, 19(8), pp.1186-1192.

Cezar, T. L., Martinez, R. M., Rocha, C. D., Melo, C. P., Vale, D. L., Borghi, S. M., . . . Casagrande, R. (2019). Treatment with Maresin 1, a docosahexaenoic acid-derived pro-resolution lipid, protects skin from inflammation and oxidative stress caused by UVB irradiation. *Scientific Reports, 9*(1). doi:10.1038/s41598-019-39584-6

Chacko, B.K. *et al*. (2014) 'The Bioenergetic Health Index: A new concept in mitochondrial translational research', *Clinical Science*, 127(6), pp. 367–373. doi:10.1042/cs20140101.

Chatterjee, A., Komshian, S., Sansbury, B., Wu, B., Mottola, G., Chen, M., Spite, M. and Conte, M., 2017. Biosynthesis of proresolving lipid mediators by vascular cells and tissues. *The FASEB Journal*, 31(8), pp.3393-3402.

Chatzidionysiou, K., Emamikia, S., Nam, J., Ramiro, S., Smolen, J., van der Heijde, D., Dougados, M., Bijlsma, J., Burmester, G., Scholte, M., van Vollenhoven, R., & Landewé, R. (2017). Efficacy of glucocorticoids, conventional and targeted synthetic disease-modifying antirheumatic drugs: A systematic literature review informing the 2016 update of the EULAR recommendations for the management of rheumatoid arthritis. *Annals of the Rheumatic Diseases*, *76*(6), 1102–1107. https://doi.org/10.1136/annrheumdis-2016-210711

Chiang, N. and Serhan, C.N. (2017) "Structural elucidation and physiologic functions of specialized pro-resolving mediators and their receptors,"

Molecular Aspects of Medicine, 58, pp. 114–129. Available at: https://doi.org/10.1016/j.mam.2017.03.005.

Chiang, N., de la Rosa, X., Libreros, S., Pan, H., Dreyfuss, J. M., & Serhan, C. N. (2021). Cysteinyl-specialized proresolving mediators link resolution of infectious inflammation and tissue regeneration via TRAF3 activation. Proceedings of the National Academy of Sciences, 118(10). doi:10.1073/pnas.2013374118

Chiang, N., Sakuma, M., Rodriguez, A. R., Spur, B. W., Irimia, D., & Serhan, C. N. (2022). Resolvin T-series reduce neutrophil extracellular traps. Blood, 139(8), 1222–1233. doi:10.1182/blood.2021013422

Chiurchiù, V., Leute, A. and Maccarrone, M., 2018. Bioactive Lipids and Chronic Inflammation: Managing the Fire Within. *Frontiers in Immunology*, 9.

Choi, S. and Lee, K., 2018. Clinical management of seronegative and seropositive rheumatoid arthritis: A comparative study. *PLOS ONE*, 13(4), p.e0195550.

Combe, B., Landewe, R., Daien, C., Hua, C., Aletaha, D., Álvaro-Gracia, J., Bakkers, M., Brodin, N., Burmester, G., Codreanu, C., Conway, R., Dougados, M., Emery, P., Ferraccioli, G., Fonseca, J., Raza, K., Silva-Fernández, L., Smolen, J., Skingle, D., Szekanecz, Z., Kvien, T., van der Helm-van Mil, A. and van Vollenhoven, R., 2016. 2016 update of the EULAR recommendations for the management of early arthritis. Annals of the Rheumatic Diseases, 76(6), pp.948-959.

Conte, F., Menezes-de-Lima, O., Verri, W., Cunha, F., Penido, C., & Henriques, M. (2010). Lipoxin a4 attenuates zymosan-induced arthritis by modulating endothelin-1 and its effects. *British Journal of Pharmacology*, *161*(4), 911–924. https://doi.org/10.1111/j.1476-5381.2010.00950.x

Dai, X. and Stanley, E.R., (2003). Colony-Stimulating Factor-1 (CSF-1). *Encyclopedia of Hormones*, pp.274-284.

Dalli, J., Chiang, N., & Serhan, C. N. (2015). Elucidation of novel 13-series Resolvins that increase with atorvastatin and clear infections. Nature Medicine, 21(9), 1071–1075. doi:10.1038/nm.3911

Dalli, J., Colas, R. A., & Serhan, C. N. (2013). Novel N-3 immunoresolvents: Structures and actions. *Scientific Reports*, *3*(1). doi:10.1038/srep01940

De Kleer, I., Willems, F., Lambrecht, B., & Goriely, S. (2014). Ontogeny of myeloid cells. *Frontiers in Immunology*, *5*. doi:10.3389/fimmu.2014.00423

De la Rosa, X., Norris, P. C., Chiang, N., Rodriguez, A. R., Spur, B. W., & Serhan, C. N. (2018). Identification and complete stereochemical assignments of the new Resolvin conjugates in tissue regeneration in human tissues that stimulate proresolving phagocyte functions and tissue

regeneration. The American Journal of Pathology, 188(4), 950–966. doi:10.1016/j.ajpath.2018.01.004

Deshpande, O.A. and Mohiuddin, S.S. (2022) *Biochemistry, oxidative phosphorylation*, *National Library of Medicine*. Statpearls. Available at: https://pubmed.ncbi.nlm.nih.gov/31985985/.

Devaraj, N., (2018). The difficult rheumatology diagnosis. *Ethiopian Journal of Health Sciences*, 28(1), p.101.

Di Cesare Mannelli, L. *et al*. (2013) 'Therapeutic effects of the superoxide dismutase mimetic compound me2do2a on experimental articular pain in rats', *Mediators of Inflammation*, 2013, pp. 1–11. doi:10.1155/2013/905360.

Dubé, L., Spahis, S., Lachaîne, K., Lemieux, A., Monhem, H., Poulin, S.-M., … Levy, E. (2022). Specialized pro-resolving mediators derived from n-3 polyunsaturated fatty acids: Role in metabolic syndrome and related complications. Antioxidants & Redox Signaling, 37(1–3), 54–83. doi:10.1089/ars.2021.0156

Dyall, S.C. *et al*. (2022) 'Polyunsaturated fatty acids and fatty acid-derived lipid mediators: Recent advances in the understanding of their biosynthesis, structures, and functions', *Progress in Lipid Research*, 86, p. 101165. doi:10.1016/j.plipres.2022.101165.

El Kholy, K., Freire, M., Chen, T., & Van Dyke, T. E. (2018). Resolvin E1 promotes bone preservation under inflammatory conditions. *Frontiers in Immunology, 9*. doi:10.3389/fimmu.2018.01300

Epelman, S., Lavine, K. J., & Randolph, G. J. (2014). Origin and functions of tissue macrophages. Immunity, 41(1), 21–35. doi:10.1016/j.immuni.2014.06.013

Everts, V., Delaissé, J. M., Korper, W., Jansen, D. C., Tigchelaar-Gutter, W., Saftig, P., & Beertsen, W. (2002). The bone lining cell: Its role in cleaning howship's lacunae and initiating Bone Formation. *Journal of Bone and Mineral Research, 17*(1), 77–90. doi:10.1359/jbmr.2002.17.1.77

Faccio, R., Choi, Y., Teitelbaum, S. and Takayanagi, H. (2011). The Osteoclast. *Osteoimmunology*, pp.141-185.

Fata, J., Kong, Y., Li, J., Sasaki, T., Irie-Sasaki, J., Moorehead, R., Elliott, R., Scully, S., Voura, E., Lacey, D., Boyle, W., Khokha, R. and Penninger, J., (2000). The Osteoclast Differentiation Factor Osteoprotegerin-Ligand Is Essential for Mammary Gland Development. *Cell*, 103(1), pp.41-50.

Fearon, U., Canavan, M., Biniecka, M., & Veale, D. J. (2016). Hypoxia, mitochondrial dysfunction and synovial invasiveness in rheumatoid

arthritis. *Nature Reviews Rheumatology*, *12*(7), 385–397. doi:10.1038/nrrheum.2016.69

Fearon, U., Hanlon, M. M., Floudas, A., & Veale, D. J. (2022). Cellular metabolic adaptations in rheumatoid arthritis and their therapeutic implications. *Nature Reviews Rheumatology*, *18*(7), 398–414. doi:10.1038/s41584-022-00771-x

Feher, J., (2017). Calcium and Phosphorus Homeostasis II. *Quantitative Human Physiology*, pp.933-945.

Feng, X. and Teitelbaum, S. (2013). Osteoclasts: New Insights. *Bone Research*, 1(1), pp.11-26.

Fennen, M., Pap, T. and Dankbar, B. (2016) 'Smad-dependent mechanisms of inflammatory bone destruction', *Arthritis Research & Therapy*, 18(1). doi:10.1186/s13075-016-1187-7.

Ferreira, I., Falcato, F., Bandarra, N., & Rauter, A. P. (2022). Resolvins, Protectins, and Maresins: Dha-derived specialized pro-resolving mediators, biosynthetic pathways, synthetic approaches, and their role in inflammation. *Molecules*, *27*(5), 1677. https://doi.org/10.3390/molecules27051677

Flak, M. B., Koenis, D. S., Sobrino, A., Smith, J., Pistorius, K., Palmas, F., & Dalli, J. (2019). GPR101 mediates the pro-resolving actions of rvd5n-3 DPA in arthritis and infections. *Journal of Clinical Investigation*, *130*(1), 359–373. https://doi.org/10.1172/jci131609

Fleetwood, A., Achuthan, A. and Hamilton, J., 2016. Colony Stimulating Factors (CSFs). *Encyclopedia of Immunobiology*, pp.586-596.

Florencio-Silva, R., Sasso, G. R., Sasso-Cerri, E., Simões, M. J., & Cerri, P. S. (2015). Biology of bone tissue: Structure, function, and factors that influence bone cells. *BioMed Research International*, *2015*, 1–17. doi:10.1155/2015/421746

Franz-Odendaal, T. A., Hall, B. K., & Witten, P. E. (2005). Buried alive: How osteoblasts become osteocytes. *Developmental Dynamics*, *235*(1), 176–190. doi:10.1002/dvdy.20603

Fu, Y., Maianu, L., Melbert, B. R., & Garvey, W. T. (2004). Facilitative glucose transporter gene expression in human lymphocytes, monocytes, and macrophages: A role for glut isoforms 1, 3, and 5 in the immune response and foam cell formation. *Blood Cells, Molecules, and Diseases*, *32*(1), 182–190. https://doi.org/10.1016/j.bcmd.2003.09.002

Funaki, Y., Hasegawa, Y., Okazaki, R., Yamasaki, A., Sueda, Y., Yamamoto, A., Yanai, M., Fukushima, T., Harada, T., Makino, H., & Shimizu, E. (2018).

Resolvin E1 inhibits osteoclastogenesis and bone resorption by suppressing il-17-induced rankl expression in osteoblasts and RANKL-induced osteoclast differentiation. *Yonago Acta Medica*, *61*(1), 008–018. https://doi.org/10.33160/yam.2018.03.002

Galli, F., Varani, M., Trapasso, F., Tetti, S., & Signore, A. (2022). Radiolabeling of monocytes, NK cells and dendritic cells and quality controls. Nuclear Medicine and Molecular Imaging, 299-304. doi:10.1016/b978-0-12-822960-6.00187-3

Ganapathy-Kanniappan, S. and Geschwind, J.-F.H. (2013) "Tumor glycolysis as a target for cancer therapy: Progress and prospects," *Molecular Cancer*, 12(1), p. 152. Available at: https://doi.org/10.1186/1476-4598-12-152.

Gao, L. *et al.* (2013) "Resolvin E1 and chemokine-like receptor 1 mediate bone preservation," *The Journal of Immunology*, 190(2), pp. 689–694. Available at: https://doi.org/10.4049/jimmunol.1103688.

Gardiner, B., Dougherty, J. A., Ponnalagu, D., Singh, H., Angelos, M., Chen, C.-A., & Khan, M. (2020). Measurement of oxidative stress markers in vitro using commercially available kits. *Measuring Oxidants and Oxidative Stress in Biological Systems*, 39–60. doi:10.1007/978-3-030-47318-1_4

Gasser, J. A., & Kneissel, M. (2017). Bone Physiology and biology. *Molecular and Integrative Toxicology*, 27–94. doi:10.1007/978-3-319-56192-9_2

Ghanbari Movahed, Z. *et al.* (2019) 'Cancer cells change their glucose metabolism to overcome increased ROS: One step from cancer cell to cancer stem cell?', *Biomedicine & Pharmacotherapy*, 112, p. 108690. doi:10.1016/j.biopha.2019.108690.

Goldring, S. R. (2015). The osteocyte: Key player in regulating bone turnover. *RMD Open*, *1*(Suppl 1). doi:10.1136/rmdopen-2015-000049

Gomez, E.A. et al. (2020) 'Blood pro-resolving mediators are linked with synovial pathology and are predictive of DMARD responsiveness in rheumatoid arthritis', Nature Communications, 11(1). doi:10.1038/s41467-020-19176-z.

Gossec, L. (2018). Monitoring of disease and treatment of patients with rheumatic disease. *Handbook of Systemic Autoimmune Diseases*, 97–125. doi:10.1016/b978-0-444-63887-8.00005-0

Granot, T., Senda, T., Carpenter, D. J., Matsuoka, N., Weiner, J., Gordon, C. L., … Farber, D. L. (2017). Dendritic cells display subset and tissue-specific maturation dynamics over human life. *Immunity*, *46*(3), 504–515. doi:10.1016/j.immuni.2017.02.019

Gutiérrez, L., Stepien, G., Gutiérrez, L., Pérez-Hernández, M., Pardo, J., Pardo, J., Grazú, V., & de la Fuente, J. M. (2017). Nanotechnology in drug discovery and development. *Comprehensive Medicinal Chemistry III*, 264–295. https://doi.org/10.1016/b978-0-12-409547-2.12292-9

Habouri, L., El Mansouri, F. E., Ouhaddi, Y., Lussier, B., Pelletier, J.-P., Martel-Pelletier, J., Benderdour, M., & Fahmi, H. (2017). Deletion of 12/15-lipoxygenase accelerates the development of aging-associated and instability-induced osteoarthritis. *Osteoarthritis and Cartilage*, *25*(10), 1719–1728. https://doi.org/10.1016/j.joca.2017.07.001

Hadjicharalambous, C., Alpantaki, K., & Chatzinikolaidou, M. (2021). Effects of nsaids on pre-osteoblast viability and osteogenic differentiation. *Experimental and Therapeutic Medicine*, *22*(1). https://doi.org/10.3892/etm.2021.10172

Hanlon, M. M., McGarry, T., Marzaioli, V., Amaechi, S., Song, Q., Nagpal, S., Veale, D. J., & Fearon, U. (2022). Rheumatoid arthritis macrophages are primed for inflammation and display bioenergetic and functional alterations. *Rheumatology*, *62*(7), 2611–2620. https://doi.org/10.1093/rheumatology/keac640.

Harty, L. C., Biniecka, M., O'Sullivan, J., Fox, E., Mulhall, K., Veale, D. J., & Fearon, U. (2011). Mitochondrial mutagenesis correlates with the local inflammatory environment in arthritis. *Annals of the Rheumatic Diseases*, *71*(4), 582–588. https://doi.org/10.1136/annrheumdis-2011-200245

Headland, S. and Norling, L. (2015). The resolution of inflammation: Principles and challenges. *Seminars in Immunology*, 27(3), pp.149-160.

Heidari B. (2011). Rheumatoid Arthritis: Early diagnosis and treatment outcomes. *Caspian journal of internal medicine*, *2*(1), 161–170.

Herrera, B.S. *et al*. (2008) "An endogenous regulator of inflammation, resolvin E1, modulates osteoclast differentiation and bone resorption," *British Journal of Pharmacology*, 155(8), pp. 1214–1223. Available at: https://doi.org/10.1038/bjp.2008.367.

Hoeffel, G., Wang, Y., Greter, M., See, P., Teo, P., Malleret, B., … Ginhoux, F. (2012). Adult langerhans cells derive predominantly from embryonic fetal liver monocytes with a minor contribution of yolk sac–derived macrophages. Journal of Experimental Medicine, 209(6), 1167–1181. doi:10.1084/jem.20120340

Huang, R., Vi, L., Zong, X., & Baht, G. S. (2020). Maresin 1 resolves aged-associated macrophage inflammation to improve bone regeneration. *The FASEB Journal*, *34*(10), 13521–13532. https://doi.org/10.1096/fj.202001145r

Huang, W. (2007). Signaling and transcriptional regulation in osteoblast commitment and differentiation. *Frontiers in Bioscience*, *12*(8–12), 3068. doi:10.2741/2296

Hughes, F.M. *et al*. (2021) 'Specialized proresolution mediators in the bladder: Annexin-A1 normalizes inflammation and bladder dysfunction during bladder outlet obstruction', *American Journal of Physiology-Renal Physiology*, 321(4). doi:10.1152/ajprenal.00205.2021.

Hwang, S.-M., Chung, G., Kim, Y., & Park, C.-K. (2019). The role of Maresins in inflammatory pain: Function of macrophages in wound regeneration. *International Journal of Molecular Sciences*, *20*(23), 5849. https://doi.org/10.3390/ijms20235849

Hwang, S.-Y. and Putney, J.W. (2011) "Calcium signaling in osteoclasts," *Biochimica et Biophysica Acta (BBA) - Molecular Cell Research*, 1813(5), pp. 979–983. Available at: https://doi.org/10.1016/j.bbamcr.2010.11.002.

Indo, H.P. *et al*. (2015) 'A mitochondrial superoxide theory for oxidative stress diseases and aging', *Journal of Clinical Biochemistry and Nutrition*, 56(1), pp. 1–7. doi:10.3164/jcbn.14-42.

Inui, K., & Koike, T. (2016). Combination therapy with biologic agents in rheumatic diseases: Current and future prospects. *Therapeutic Advances in Musculoskeletal Disease*, *8*(5), 192–202. https://doi.org/10.1177/1759720x16665330

Ito, S. and Hata, T. (2004). Crystal Structure of RANK Ligand Involved in Bone Metabolism. *TRAIL (TNF-Related Apoptosis-Inducing Ligand)*, pp.19-33.

Jaén, R. I., Sánchez-García, S., Fernández-Velasco, M., Boscá, L., & Prieto, P. (2021). Resolution-based therapies: The potential of lipoxins to treat human diseases. Frontiers in Immunology, 12. doi:10.3389/fimmu.2021.658840

Jang, D., Lee, A.-H., Shin, H.-Y., Song, H.-R., Park, J.-H., Kang, T.-B., … Yang, S.-H. (2021). The role of tumor necrosis factor alpha (TNF-α) in autoimmune disease and current TNF-α inhibitors in therapeutics. *International Journal of Molecular Sciences*, *22*(5), 2719. doi:10.3390/ijms22052719

Jung, T. W., Chung, Y. H., Kim, H.-C., Abd El-Aty, A. M., & Jeong, J. H. (2018). Protectin DX attenuates LPS-induced inflammation and insulin resistance in adipocytes via AMPK-mediated suppression of the NF-KB pathway. *American Journal of Physiology-Endocrinology and Metabolism*, *315*(4). https://doi.org/10.1152/ajpendo.00408.2017

Kajiya, H. (2012). Calcium signaling in osteoclast differentiation and bone resorption. *Advances in Experimental Medicine and Biology*, 917–932. https://doi.org/10.1007/978-94-007-2888-2_41

Kapellos, T. S., Bonaguro, L., Gemünd, I., Reusch, N., Saglam, A., Hinkley, E. R., & Schultze, J. L. (2019). Human monocyte subsets and phenotypes in major chronic inflammatory diseases. Frontiers in Immunology, 10. doi:10.3389/fimmu.2019.02035

Karsdal, M. A., Larsen, L., Engsig, M. T., Lou, H., Ferreras, M., Lochter, A., … Foged, N. T. (2002). Matrix metalloproteinase-dependent activation of latent transforming growth factor-β controls the conversion of osteoblasts into osteocytes by blocking osteoblast apoptosis. *Journal of Biological Chemistry*, *277*(46), 44061–44067. doi:10.1074/jbc.m207205200

Kasonga, A., Deepak, V., Kruger, M. and Coetzee, M., 2015. Arachidonic Acid and Docosahexaenoic Acid Suppress Osteoclast Formation and Activity in Human CD14+ Monocytes, *In vitro*. *PLOS ONE*, 10(4), p.e0125145.

Katsimbri, P. (2017). The biology of normal bone remodelling. European Journal of Cancer Care, 26(6). https://doi.org/10.1111/ecc.12740

Keffer, J., Probert, L., Cazlaris, H., Georgopoulos, S., Kaslaris, E., Kioussis, D., & Kollias, G. (1991). Transgenic mice expressing human tumour necrosis factor: A predictive genetic model of arthritis. *The EMBO Journal*, *10*(13), 4025–4031. https://doi.org/10.1002/j.1460-2075.1991.tb04978.x

Keinan, D., Leigh, N., Nelson, J., De Oleo, L., & Baker, O. (2013). Understanding resolvin signaling pathways to improve oral health. *International Journal of Molecular Sciences, 14*(3), 5501-5518. doi:10.3390/ijms14035501

Kester, M., Karpa, K. and Vrana, K., 2012. Inflammatory Disorders. Elsevier's Integrated Review Pharmacology, pp.161-172.

Khan, F. U., Khongorzul, P., Raki, A. A., Rajasekaran, A., Gris, D., & Amrani, A. (2022). Dendritic cells and their immunotherapeutic potential for treating type 1 diabetes. *International Journal of Molecular Sciences*, *23*(9), 4885. https://doi.org/10.3390/ijms23094885

Kidger, S. V. (2017). The impact of the synovial environment and GM-CSF on the myeloid compartment in rheumatoid arthritis. PhD thesis, University of Glasgow.

Kim, J.H. and Kim, N. (2014) “Regulation of NFATC1 in osteoclast differentiation,” *Journal of Bone Metabolism*, 21(4), p. 233. Available at: https://doi.org/10.11005/jbm.2014.21.4.233.

Kimura, K., Kitaura, H., Ishida, M., Hakami, Z., Saeed, J., Sugisawa, H. and Takano-Yamamoto, T., (2015). Effect of Macrophage Colony-Stimulating Factor Receptor c-Fms Antibody on Lipopolysaccharide-Induced Pathological Osteoclastogenesis and Bone Resorption. *Interface Oral Health Science 2014,* pp.259-267.

Köhler, B., Günther, J., Kaudewitz, D. and Lorenz, H., 2019. Current Therapeutic Options in the Treatment of Rheumatoid Arthritis. Journal of Clinical Medicine, 8(7), p.938.

Komano, Y., Nanki, T., Hayashida, K., Taniguchi, K., & Miyasaka, N. (2006). *Arthritis Research & Therapy*, *8*(5). https://doi.org/10.1186/ar2046

Kornu, R., Dao, K., Orozco, C. and Patel, R., 2012. Rheumatology. *Medical Secrets*, pp.247-290.

Kostoglou-Athanassiou, I., Athanassiou, P., Lyraki, A., Raftakis, I. and Antoniadis, C., 2012. Vitamin D and rheumatoid arthritis. *Therapeutic Advances in Endocrinology and Metabolism*, 3(6), pp.181-187.

Koźmiński, P., Halik, P., Chesori, R. and Gniazdowska, E., 2020. Overview of Dual-Acting Drug Methotrexate in Different Neurological Diseases, Autoimmune Pathologies and Cancers. *International Journal of Molecular Sciences*, 21(10), p.3483.

Kremer, J., Lawrence, D., Petrillo, G., Litts, L., Mullaly, P., Rynes, R., Stocker, R., Parhami, N., Greenstein, N., Fuchs, B., Mathur, A., Robinson, D., Sperling, R. and Bigaouette, J., 1995. Effects of high-dose fish oil on rheumatoid arthritis after stopping nonsteroidal antiinflammatory drugs clinical and immune correlates. *Arthritis & Rheumatism*, 38(8), pp.1107-1114.

Krishnamoorthy, N., Abdulnour, R. E., Walker, K. H., Engstrom, B. D., & Levy, B. D. (2018). Specialized proresolving mediators in innate and adaptive immune responses in airway diseases. *Physiological Reviews, 98*(3), 1335-1370. doi:10.1152/physrev.00026.2017

Krishnamoorthy, S., Recchiuti, A., Chiang, N., Yacoubian, S., Lee, C., Yang, R., . . . Serhan, C. N. (2010). Resolvin D1 binds human phagocytes with evidence for proresolving receptors. *Proceedings of the National Academy of Sciences, 107*(4), 1660-1665. doi:10.1073/pnas.0907342107

Kubatzky, K.F., Uhle, F. and Eigenbrod, T. (2018) “From macrophage to osteoclast – how metabolism determines function and activity,” *Cytokine*, 112, pp. 102–115. Available at: https://doi.org/10.1016/j.cyto.2018.06.013.

Lacombe, J., Karsenty, G., & Ferron, M. (2013). Regulation of lysosome biogenesis and functions in osteoclasts. *Cell Cycle*, *12*(17), 2744–2752. https://doi.org/10.4161/cc.25825

Lange, U., Teichmann, J., Müller-Ladner, U., & Strunk, J. (2005a). Increase in bone mineral density of patients with rheumatoid arthritis treated with anti-TNF-α antibody: A prospective open-label pilot study. *Rheumatology*, *44*(12), 1546–1548. https://doi.org/10.1093/rheumatology/kei082

Laria, A., Lurati, A., Marrazza, M., Mazzocchi, D., Re, K. A., & Scarpellini, M. (2016). The macrophages in rheumatic diseases. Journal of inflammation research, 9, 1–11. https://doi.org/10.2147/JIR.S82320

Lee, H.-R. *et al.* (2021) 'Reduction of oxidative stress in peripheral blood mononuclear cells attenuates the inflammatory response of fibroblast-like synoviocytes in rheumatoid arthritis', *International Journal of Molecular Sciences*, 22(22), p. 12411. doi:10.3390/ijms222212411.

Levy, B., Clish, C., Schmidt, B., Gronert, K., & Serhan, C. (2001). Lipid mediator class switching during acute inflammation: signals in resolution. *Nature Immunology*, *2*(7), 612-619. doi: 10.1038/89759

Li, Q. F., Hao, H., Tu, W. S., Guo, N., & Zhou, X. Y. (2020). Maresins: anti-inflammatory pro-resolving mediators with therapeutic potential. *European review for medical and pharmacological sciences*, *24*(13), 7442–7453. https://doi.org/10.26355/eurrev_202007_21913

Li, Z. H., Si, Y., Xu, G., Chen, X. M., Xiong, H., Lai, L., Zheng, Y. Q., & Zhang, Z. G. (2017). High-dose PMA with RANKL and MCSF induces THP-1 cell differentiation into human functional osteoclasts in vitro. *Molecular Medicine Reports*, *16*(6), 8380–8384. https://doi.org/10.3892/mmr.2017.7625

Libreros, S., Shay, A. E., Nshimiyimana, R., Fichtner, D., Martin, M. J., Wourms, N., & Serhan, C. N. (2021). A new E-series resolvin: Rve4 stereochemistry and function in efferocytosis of inflammation-resolution. Frontiers in Immunology, 11. doi:10.3389/fimmu.2020.631319

Liu, C., Fan, D., Lei, Q., Lu, A., & He, X. (2022). Roles of Resolvins in chronic inflammatory response. *International Journal of Molecular Sciences*, *23*(23), 14883. https://doi.org/10.3390/ijms232314883

Liu, S., Liu, S., He, B., Li, L., Li, L., Wang, J., Cai, T., Chen, S., & Jiang, H. (2021). OXPHOS deficiency activates global adaptation pathways to maintain mitochondrial membrane potential. *EMBO Reports*, *22*(4). https://doi.org/10.15252/embr.202051606

López-Vicario, C., Rius, B., Alcaraz-Quiles, J., García-Alonso, V., Lopategi, A., Titos, E., & Clària, J. (2016). Pro-resolving mediators produced from EPA and DHA: Overview of the pathways involved and their mechanisms in metabolic syndrome and related liver diseases. *European Journal Of Pharmacology*, *785*, 133-143. doi: 10.1016/j.ejphar.2015.03.092

Ma, C. *et al.* (2022) 'Mitochondrial dysfunction in rheumatoid arthritis', *Biomolecules*, 12(9), p. 1216. doi:10.3390/biom12091216.

Malmström, V., Catrina, A. and Klareskog, L., (2016). The immunopathogenesis of seropositive rheumatoid arthritis: from triggering to targeting. Nature Reviews Immunology, 17(1), pp.60-75.

Marchetti, P. *et al.* (2020) 'Mitochondrial spare respiratory capacity: Mechanisms, regulation, and significance in non-transformed and cancer cells', *The FASEB Journal*, 34(10), pp. 13106–13124. doi:10.1096/fj.202000767r.

Markey, K. and Hill, G. (2017). Cytokines in Hematopoietic Stem Cell Transplantation. *Cytokine Effector Functions in Tissues*, pp.219-236.

Marsh, S. A., Arthur, H. M., & Spyridopoulos, I. (2017). The secret life of nonclassical monocytes. *Cytometry Part A*, *91*(11), 1055–1058. doi:10.1002/cyto.a.23280

Matic, I., Matthews, B. G., Wang, X., Dyment, N. A., Worthley, D. L., Rowe, D. W., … Kalajzic, I. (2016). Quiescent bone lining cells are a major source of osteoblasts during adulthood. *Stem Cells*, *34*(12), 2930–2942. doi:10.1002/stem.2474

Matsuo, K., & Irie, N. (2008). Osteoclast–Osteoblast Communication. *Archives of Biochemistry and Biophysics*, *473*(2), 201–209. doi:10.1016/j.abb.2008.03.027

Matsuura, Y., Kikuta, J., Kishi, Y., Hasegawa, T., Okuzaki, D., Hirano, T., Minoshima, M., Kikuchi, K., Kumanogoh, A., & Ishii, M. (2018). *in vivo*visualisation of different modes of action of biological dmards inhibiting osteoclastic bone resorption. *Annals of the Rheumatic Diseases*. https://doi.org/10.1136/annrheumdis-2017-212880

Matzelle, M., Gallant, M., Condon, K., Walsh, N., Manning, C., Stein, G., Lian, J., Burr, D. and Gravallese, E., 2012. Resolution of inflammation induces osteoblast function and regulates the Wnt signaling pathway. *Arthritis & Rheumatism*, 64(5), pp.1540-1550.

McDonald, M. M., Khoo, W. H., Ng, P. Y., Xiao, Y., Zamerli, J., Thatcher, P., … Phan, T. G. (2021). Osteoclasts recycle via osteomorphs during Rankl-stimulated bone resorption. *Cell*, *184*(5). doi:10.1016/j.cell.2021.02.002

McGarry, T., Hanlon, M. M., Marzaioli, V., Cunningham, C. C., Krishna, V., Murray, K., Hurson, C., Gallagher, P., Nagpal, S., Veale, D. J., & Fearon, U. (2021). Rheumatoid arthritis CD14 + monocytes display metabolic and inflammatory dysfunction, a phenotype that precedes clinical manifestation of disease. *Clinical & Translational Immunology*, *10*(1). https://doi.org/10.1002/cti2.1237

McInnes, I. and Schett, G., (2011). The Pathogenesis of Rheumatoid Arthritis. *New England Journal of Medicine*, 365(23), pp.2205-2219.

Mirjam, K., & Broos, C. E. (2019). Immunological manifestations in sarcoidosis. Sarcoidosis, 37-54. doi:10.1016/b978-0-323-54429-0.00003-3

Miron, R. J., & Zhang, Y. F. (2012). Osteoinduction. *Journal of Dental Research*, *91*(8), 736–744. doi:10.1177/0022034511435260

Monie, T. P. (2017). A snapshot of the innate immune system. The Innate Immune System, 1-40. doi:10.1016/b978-0-12-804464-3.00001-6

Mu, Q., Zhou, H., Xu, Y., He, Q., Luo, X., Zhang, W., & Li, H. (2020). NPD1 inhibits excessive autophagy by targeting RNF146 and Wnt/ß-catenin pathway in cerebral ischemia-reperfusion injury. *Journal of Receptors and Signal Transduction*, *40*(5), 456–463. https://doi.org/10.1080/10799893.2020.1756325

Murakami, A., Matsuda, M., Harada, Y., & Hirata, M. (2017). Phospholipase C-related, but catalytically inactive protein (PRIP) up-regulates osteoclast differentiation via calcium-calcineurin-NFATC1 signaling. *Journal of Biological Chemistry*, *292*(19), 7994–8006. https://doi.org/10.1074/jbc.m117.784777

Muto, A., Mizoguchi, T., Udagawa, N., Ito, S., Kawahara, I., Abiko, Y., Arai, A., Harada, S., Kobayashi, Y., Nakamichi, Y., Penninger, J., Noguchi, T. and Takahashi, N. (2011). Lineage-committed osteoclast precursors circulate in blood and settle down into bone. *Journal of Bone and Mineral Research*, 26(12), pp.2978-2990.

Nguyen, J., & Nohe, A. (2017). Factors that affect the osteoclastogenesis of raw264.7 cells. *Journal of Biochemistry and Analytical Studies*, *2*(1). https://doi.org/10.16966/2576-5833.109

Nielsen, M. C., Andersen, M. N., & Møller, H. J. (2019). Monocyte isolation techniques significantly impact the phenotype of both isolated monocytes and derived macrophages   in vitro. Immunology, 159(1), 63-74. doi:10.1111/imm.13125

Nordberg, L., Lillegraven, S., Aga, A., Sexton, J., Olsen, I., Lie, E., Berner Hammer, H., Uhlig, T., van der Heijde, D., Kvien, T. and Haavardsholm, E., (2018). Comparing the disease course of patients with seronegative and seropositive rheumatoid arthritis fulfilling the 2010 ACR/EULAR classification criteria in a treat-to-target setting: 2-year data from the ARCTIC trial. *RMD Open*, 4(2), p.e000752.

Norling, L.V. and Perretti, M. (2020) 'Proresolving lipid mediators enhance PMN-mediated bacterial clearance', Proceedings of the National Academy of Sciences, 117(17), pp. 9148–9150. doi:10.1073/pnas.2004241117.

O'Neill, L. A. J. (2015). A broken Krebs cycle in macrophages. Immunity, 42(3), 393–394. doi:10.1016/j.immuni.2015.02.017

O'Neill, L. A. J., & Pearce, E. J. (2015). Immunometabolism governs dendritic cell and macrophage function. Journal of Experimental Medicine, 213(1), 15–23. doi:10.1084/jem.20151570

Özgül Özdemir, R. B., Soysal Gündüz, Ö., Özdemir, A. T., & Akgül, Ö. (2020). Low levels of pro-resolving lipid mediators lipoxin-A4, Resolvin-D1 and resolvin-E1 in patients with rheumatoid arthritis. *Immunology Letters*, *227*, 34–40. https://doi.org/10.1016/j.imlet.2020.08.006

Pabón-Porras, M., Molina-Ríos, S., Flórez-Suárez, J., Coral-Alvarado, P., Méndez-Patarroyo, P., & Quintana-López, G. (2019). Rheumatoid arthritis and systemic lupus erythematosus: Pathophysiological mechanisms related to innate immune system. SAGE Open Medicine, 7, 205031211987614. doi: 10.1177/2050312119876146

Panga, V., Kallor, A. A., Nair, A., Harshan, S., & Raghunathan, S. (2019). Mitochondrial dysfunction in rheumatoid arthritis: A comprehensive analysis by integrating gene expression, protein-protein interactions and gene ontology data. *PLOS ONE*, *14*(11). https://doi.org/10.1371/journal.pone.0224632

Park, J. H., Lee, N. K., & Lee, S. Y. (2017). Current Understanding of RANK Signaling in Osteoclast Differentiation and Maturation. *Molecµles and cells*, 40(10), 706–713.

Parvizi, J. and Kim, G., (2010). Osteoclasts. *High Yield Orthopaedics*, pp.337-339.

Patel, A. A., Ginhoux, F., & Yona, S. (2021). Monocytes, macrophages, dendritic cells and neutrophils: An update on lifespan kinetics in health and disease. *Immunology*, *163*(3), 250–261. https://doi.org/10.1111/imm.13320

Pettit, A. R., Ji, H., von Stechow, D., Müller, R., Goldring, S. R., Choi, Y., … Gravallese, E. M. (2001). Trance/Rankl knockout mice are protected from bone erosion in a serum transfer model of arthritis. *The American Journal of Pathology*, *159*(5), 1689–1699. doi:10.1016/s0002-9440(10)63016-7

Pinto, N., Klein, Y., David, E., Polak, D., Steinberg, D., Mizrahi, G., Khoury, Y., Barenholz, Y., & Chaushu, S. (2023). Resolvin D1 improves allograft osteointegration and directly enhances osteoblasts differentiation. *Frontiers in Immunology*, *14*. https://doi.org/10.3389/fimmu.2023.1086930

Porcheray, F., Viaud, S., Rimaniol, A.-C., Léone, C., Samah, B., Dereuddre-Bosquet, N., … Gras, G. (2005). Macrophage activation switching: An asset for the resolution of inflammation. Clinical and Experimental Immunology, 142(3), 481–489. doi:10.1111/j.1365-2249.2005.02934.x

Promila, L., Joshi, A., Khan, S., Aggarwal, A., & Lahiri, A. (2023). Role of mitochondrial dysfunction in the pathogenesis of rheumatoid arthritis:

Looking closely at fibroblast- like synoviocytes. *Mitochondrion*, *73*, 62–71. https://doi.org/10.1016/j.mito.2023.10.004

Radford, K., Shortman, K., & O'Keeffe, M. (2014). Dendritic cells in autoimmune disease. The Autoimmune Diseases, 175–186. doi:10.1016/b978-0-12-384929-8.00012-5

Rajakariar R, Yaqoob MM, Gilroy DW (2006). COX-2 in Inflammation and Resolution. Molecular Interventions, 6(4), 199-207. doi: 10.1124/mi.6.4.6

Ramos-Junior, E., Leite, G., Carmo-Silva, C., Taira, T., Neves, K., & Colón, D. et al. (2016). Adipokine Chemerin Bridges Metabolic Dyslipidemia and Alveolar Bone Loss in Mice. *Journal Of Bone And Mineral Research*, *32*(5), 974-984. doi: 10.1002/jbmr.3072

Rana, A.K. *et al*. (2018) "Monocytes in rheumatoid arthritis: Circulating precursors of macrophages and osteoclasts and, their heterogeneity and plasticity role in Ra Pathogenesis," *International Immunopharmacology*, 65, pp. 348–359. Available at: https://doi.org/10.1016/j.intimp.2018.10.016.

Recchiuti, A., Mattoscio, D., & Isopi, E. (2019). Roles, actions, and therapeutic potential of specialized pro-resolving lipid mediators for the treatment of inflammation in cystic fibrosis. *Frontiers in Pharmacology*, *10*. doi:10.3389/fphar.2019.00252

Rider, P., Carmi, Y. and Cohen, I., 2016. Biologics for Targeting Inflammatory Cytokines, Clinical Uses, and Limitations. International Journal of Cell Biology, 2016, pp.1-11.

Rocamonde, B., Carcone, A., Mahieux, R., & Dutartre, H. (2019). HTLV-1 infection of myeloid cells: From transmission to immune alterations. *Retrovirology*, *16*(1). https://doi.org/10.1186/s12977-019-0506-x

Rochefort, G. Y., Pallu, S., & Benhamou, C. L. (2010). Osteocyte: The unrecognized side of Bone Tissue. Osteoporosis International, 21(9), 1457–1469. https://doi.org/10.1007/s00198-010-1194-5

Rodriguez, A. R., Spur, B. W. (2020). First total syntheses of the pro-resolving lipid mediators 7(s),13(r),20(s)-resolvin T1 and 7(s),13(r)-resolvin T4. Tetrahedron Letters, 61(6), 151473. doi:10.1016/j.tetlet.2019.151473

Sadiku, P., & Walmsley, S. R. (2019). Hypoxia and the regulation of myeloid cell metabolic imprinting: Consequences for the inflammatory response. *EMBO Reports*, *20*(5). doi:10.15252/embr.201847388

Sahni, V., & Van Dyke, T. E. (2023). Immunomodulation of periodontitis with spms. *Frontiers in Oral Health*, 4. https://doi.org/10.3389/froh.2023.1288722

Sakthiswary, R., Uma Veshaaliini, R., Chin, K.-Y., Das, S., & Sirasanagandla, S. R. (2022). Pathomechanisms of bone loss in rheumatoid arthritis. *Frontiers in Medicine*, *9*. https://doi.org/10.3389/fmed.2022.962969

Salhotra, A., Shah, H. N., Levi, B., & Longaker, M. T. (2020). Mechanisms of bone development and repair. *Nature Reviews Molecular Cell Biology*, *21*(11), 696–711. doi:10.1038/s41580-020-00279-w

Sanchez-Lopez, E., Cheng, A. and Guma, M. (2019) "Can metabolic pathways be therapeutic targets in rheumatoid arthritis?," *Journal of Clinical Medicine*, 8(5), p. 753. Available at: https://doi.org/10.3390/jcm8050753.

Sansbury, B.E. and Spite, M. (2016) "Resolution of acute inflammation and the role of Resolvins in immunity, thrombosis, and Vascular Biology," *Circulation Research*, 119(1), pp. 113–130. Available at: https://doi.org/10.1161/circresaha.116.307308.

Santos, A., Bakker, A. D., & Klein-Nulend, J. (2009). The role of osteocytes in Bone Mechanotransduction. *Osteoporosis International*, *20*(6), 1027–1031. doi:10.1007/s00198-009-0858-5

Sawa, N., Fujimoto, H., Sawa, Y., & Yamashita, J. (2019). Alternating differentiation and dedifferentiation between mature osteoblasts and osteocytes. *Scientific Reports*, *9*(1). doi:10.1038/s41598-019-50236-7

Sayegh, S., El Atat, O., Diallo, K., Rauwel, B., Degboé, Y., Cavaignac, E., Constantin, A., Cantagrel, A., Trak-Smayra, V., Alaaeddine, N., & Davignon, J.-L. (2019). Rheumatoid synovial fluids regulate the immunomodulatory potential of adipose-derived mesenchymal stem cells through a TNF/NF-KB-dependent mechanism. *Frontiers in Immunology*, *10*. https://doi.org/10.3389/fimmu.2019.01482

Schaffler, M.B. and Kennedy, O.D. (2012) 'Osteocyte signaling in Bone', *Current Osteoporosis Reports*, 10(2), pp. 118–125. doi:10.1007/s11914-012-0105-4.

Scherer, H., Häupl, T., & Burmester, G. (2020). The etiology of rheumatoid arthritis. *Journal Of Autoimmunity*, *110*, 102400. doi: 10.1016/j.jaut.2019.102400

Schett, G., (2007). Cells of the synovium in rheumatoid arthritis. Osteoclasts. *Arthritis Res Ther* **9,** 203

Scott, D., 2010. Arthritis in the Elderly. *Brocklehurst's Textbook of Geriatric Medicine and Gerontology*, pp.566-576.

Serhan, C. N. (2014). Pro-resolving lipid mediators are leads for Resolution Physiology. *Nature*, *510*(7503), 92–101. doi:10.1038/nature13479

Serhan, C. N., & Levy, B. D. (2018). Resolvins in inflammation: Emergence of the pro-resolving superfamily of mediators. *Journal of Clinical Investigation, 128*(7), 2657–2669. doi:10.1172/jci97943

Serhan, C. N., Chiang, N., & Dalli, J. (2018). New pro-resolving N-3 mediators bridge resolution of infectious inflammation to tissue regeneration. *Molecular Aspects of Medicine*, 64, 1–17. doi:10.1016/j.mam.2017.08.002

Serhan, C. N., Libreros, S., & Nshimiyimana, R. (2022). E-series resolvin metabolome, biosynthesis and critical role of stereochemistry of specialized pro-resolving mediators (spms) in inflammation-resolution: Preparing spms for Long Covid-19, human clinical trials, and targeted Precision Nutrition. *Seminars in Immunology*, *59*, 101597. doi:10.1016/j.smim.2022.101597

Serhan, C.N. (2020) "Nutrients and gene expression in inflammation," *Principles of Nutrigenetics and Nutrigenomics*, pp. 457–467. Available at: https://doi.org/10.1016/b978-0-12-804572-5.00061-6.

Sharma-walia, N., & Chandrasekharan, J. (2015). Lipoxins: Nature'S way to resolve inflammation. *Journal of Inflammation Research*, 181. doi:10.2147/jir.s90380

Shea, B., Swinden, M., Tanjong Ghogomu, E., Ortiz, Z., Katchamart, W., Rader, T., Bombardier, C., Wells, G. and Tugwell, P., 2013. Folic acid and folinic acid for reducing side effects in patients receiving methotrexate for rheumatoid arthritis. *Cochrane Database of Systematic Reviews*.

Shirai, T. *et al*. (2016) 'The glycolytic enzyme PKM2 bridges metabolic and inflammatory dysfunction in coronary artery disease', *Journal of Experimental Medicine*, 213(3), pp. 337–354. doi:10.1084/jem.20150900.

Sibiak, R., Ozegowska, K., Wender-Ozegowska, E., Gutaj, P., Mozdziak, P., & Kempisty, B. (2022). FETOMATERNAL expression of glucose transporters (gluts)—biochemical, cellular and clinical aspects. *Nutrients*, *14*(10), 2025. https://doi.org/10.3390/nu14102025

Silva, B. and Bilezi fan, J. (2015). Parathyroid hormone: anabolic and catabolic actions on the skeleton. *Current Opinion in Pharmacology*, 22, pp.41-50.

Smolen, J., Aletaha, D. and McInnes, I. (2016). Rheumatoid arthritis. *The Lancet*, 388(10055), pp.2023-2038.

Smolen, J., Aletaha, D., Barton, A., Burmester, G., Emery, P., Firestein, G., Kavanaugh, A., McInnes, I., Solomon, D., Strand, V. and Yamamoto, K., (2018). Rheumatoid arthritis. Nature Reviews Disease Primers, 4(1).

Smolen, J., Landewé, R., Breedveld, F., Dougados, M., Emery, P., Gaujoux-Viala, C., Gorter, S., Knevel, R., Nam, J., Schoels, M., Aletaha, D., Buch, M.,

Gossec, L., Huizinga, T., Bijlsma, J., Burmester, G., Combe, B., Cutolo, M., Gabay, C., Gomez-Reino, J., Kouloumas, M., Kvien, T., Martin-Mola, E., McInnes, I., Pavelka, K., van Riel, P., Scholte, M., Scott, D., Sokka, T., Valesini, G., van Vollenhoven, R., Winthrop, K., Wong, J., Zink, A. and van der Heijde, D., 2010. EULAR recommendations for the management of rheumatoid arthritis with synthetic and biological disease-modifying antirheumatic drugs. *Annals of the Rheumatic Diseases*, 69(6), pp.964-975.

Sodin-Semrl, S., Spagnolo, A., Barbaro, B., Varga, J., & Fiore, S. (2004). Lipoxin A4 counteracts synergistic activation of human fibroblast-like synoviocytes. *International Journal of Immunopathology and Pharmacology*, *17*(1), 15–25. https://doi.org/10.1177/039463200401700103

Soto-Heredero, G. *et al*. (2020) "Glycolysis – a key player in the inflammatory response," *The FEBS Journal*, 287(16), pp. 3350–3369. Available at: https://doi.org/10.1111/febs.15327.

Stein, K. C., & Frydman, J. (2019). The stop-and-go traffic regulating protein biogenesis: How translation kinetics controls proteostasis. *Journal of Biological Chemistry*, *294*(6), 2076–2084. https://doi.org/10.1074/jbc.rev118.002814

Sulicka-Grodzicka, J. et al. (2022) 'Chemerin as a potential marker of resolution of inflammation in COVID-19 infection', Biomedicines, 10(10), p. 2462. doi:10.3390/biomedicines10102462

Tahir, S., & Steffens, S. (2021). Nonclassical monocytes in Cardiovascular Physiology and disease. *American Journal of Physiology-Cell Physiology*, *320*(5). doi:10.1152/ajpcell.00326.2020

Takegahara, N., Kim, H., Mizuno, H., Sakaue-Sawano, A., Miyawaki, A., Tomura, M., Kanagawa, O., Ishii, M., & Choi, Y. (2016). Involvement of receptor activator of nuclear factor-KB ligand (RANKL)-induced incomplete cytokinesis in the polyploidization of osteoclasts. *Journal of Biological Chemistry*, 291(7), 3439–3454. https://doi.org/10.1074/jbc.m115.677427

Tanaka, Y. (2020). Rheumatoid arthritis. *Inflammation and Regeneration*, *40*(1). doi:10.1186/s41232-020-00133-8

Taylor, P. C. (2020). Update on the diagnosis and management of early rheumatoid arthritis. *Clinical Medicine*, *20*(6), 561–564. doi:10.7861/clinmed.2020-0727

Teitelbaum, S. (2007). Osteoclasts: What Do They Do and How Do They Do It? *The American Journal of Pathology*, 170(2), pp.427-435.

Thomas, R., Guise, T., Yin, J., Elliott, J., Horwood, N., Martin, T. and Gillespie, M., 1999. Breast Cancer Cells Interact with Osteoblasts to Support Osteoclast Formation1. *Endocrinology*, 140(10), pp.4451-4458.

Thümmler, K., Williams, M. T., Kitson, S., Sood, S., Akbar, M., Cole, J. J., Hunter, E., Soutar, R., & Goodyear, C. S. (2022). Targeting 3D chromosomal architecture at the rank loci to suppress myeloma-driven osteoclastogenesis. *OncoImmunology*, *11*(1). https://doi.org/10.1080/2162402x.2022.2104070

Tsou, C.-L., Peters, W., Si, Y., Slaymaker, S., Aslanian, A. M., Weisberg, S. P., Mack, M., & Charo, I. F. (2007). Critical roles for CCR2 and MCP-3 in monocyte mobilization from bone marrow and recruitment to inflammatory sites. *Journal of Clinical Investigation*, *117*(4), 902–909. https://doi.org/10.1172/jci29919

Tsukasaki, M. and Takayanagi, H. (2019). Osteoimmunology: evolving concepts in bone–immune interactions in health and disease. *Nature Reviews Immunology*, 19(10), pp.626-642.

Vasan, K. *et al*. (2022) "Genes involved in maintaining mitochondrial membrane potential upon electron transport chain disruption," *Frontiers in Cell and Developmental Biology*, 10. Available at: https://doi.org/10.3389/fcell.2022.781558.

Vik, A., Dalli, J., & Hansen, T. V. (2017). Recent advances in the chemistry and biology of anti-inflammatory and specialized pro-resolving mediators biosynthesized from N-3 docosapentaenoic acid. Bioorganic & Medicinal Chemistry Letters, 27(11), 2259–2266. doi:10.1016/j.bmcl.2017.03.079

Vuoti, E., Lehenkari, P., Tuukkanen, J., Glumoff, V., & Kylmäoja, E. (2023). Osteoclastogenesis of human peripheral blood, bone marrow, and cord blood monocytes. *Scientific Reports*, *13*(1). doi:10.1038/s41598-023-30701-0

Wacleche, V., Tremblay, C., Routy, J.-P., & Ancuta, P. (2018). The biology of monocytes and dendritic cells: Contribution to HIV pathogenesis. *Viruses*, *10*(2), 65. https://doi.org/10.3390/v10020065

Wakefield, R. J., Gibbon, W. W., Conaghan, P. G., O'Connor, P., McGonagle, D., Pease, C., Green, M. J., Veale, D. J., Isaacs, J. D., & Emery, P. (2000). The value of sonography in the detection of bone erosions in patients with rheumatoid arthritis: a comparison with conventional radiography. *Arthritis and rheumatism*, *43*(12), 2762–2770. https://doi.org/10.1002/1529-0131(200012)43:12<2762::AID-ANR16>3.0.CO;2-#

Walker, M. E., Souza, P. R., Colas, R. A., & Dalli, J. (2017). 13-Series Resolvins mediate the leukocyte-platelet actions of Atorvastatin and pravastatin in inflammatory arthritis. The FASEB Journal, 31(8), 3636–3648. doi:10.1096/fj.201700268

Wang, B., Dong, Y., Tian, Z., Chen, Y., & Dong, S. (2021). The role of dendritic cells derived osteoclasts in bone destruction diseases. *Genes & Diseases*, *8*(4), 401–411. doi:10.1016/j.gendis.2020.03.009

Wang, R.X. and Colgan, S.P. (2017) "Special pro-resolving mediator (SPM) actions in regulating gastro-intestinal inflammation and gut mucosal immune responses," *Molecular Aspects of Medicine*, 58, pp. 93–101. Available at: https://doi.org/10.1016/j.mam.2017.02.002.

Woolcock, K. (2022) "Dysregulation of bivalent promoters in circulating monocytes in inflammatory diseases", *PhD thesis, University of Glasgow*.

Wu, J., Li, Y., Fang, X., Teng, Y., & Xu, Y. (2021). Decreased Serum Maresin 1 Concentration Is Associated With Postmenopausal Osteoporosis: A Cross-Sectional Study. *Frontiers in Medicine*, *8*. https://doi.org/10.3389/fmed.2021.759825

Xu, L., Chang, C., Jiang, P., Wei, K., Zhang, R., Jin, Y., Zhao, J., Xu, L., Shi, Y., Guo, S., & He, D. (2022). Metabolomics in rheumatoid arthritis: Advances and review. *Frontiers in Immunology*, *13*. https://doi.org/10.3389/fimmu.2022.961708

Xue, J., Xu, L., Zhu, H., Bai, M., Li, X., Zhao, Z., … Su, Y. (2020). CD14+CD16− monocytes are the main precursors of osteoclasts in rheumatoid arthritis via expressing tyro3tk. *Arthritis Research & Therapy*, *22*(1). doi:10.1186/s13075-020-02308-7

Yao, Y., Cai, X., Ren, F., Ye, Y., Wang, F., Zheng, C., … Zhang, M. (2021). The macrophage-osteoclast axis in osteoimmunity and osteo-related diseases. *Frontiers in Immunology*, *12*. doi:10.3389/fimmu.2021.664871

Zaninelli, T.H., Fattori, V. and Verri, W.A. (2021) 'Harnessing inflammation resolution in arthritis: Current understanding of specialized pro-resolving lipid mediators' contribution to arthritis physiopathology and future perspectives', *Frontiers in Physiology*, 12. doi:10.3389/fphys.2021.729134.

Zanna, M. Y., Yasmin, A. R., Omar, A. R., Arshad, S. S., Mariatulqabtiah, A. R., Nur-Fazila, S. H., & Mahiza, M. I. (2021). Review of dendritic cells, their role in clinical immunology, and distribution in various animal species. International Journal of Molecular Sciences, 22(15), 8044. doi:10.3390/ijms22158044

Zezina, E., Sercan-Alp, O., Herrmann, M., & Biesemann, N. (2020). Glucose transporter 1 in rheumatoid arthritis and autoimmunity. *WIREs Systems Biology and Medicine*, *12*(4). https://doi.org/10.1002/wsbm.1483

Zhao, B., Grimes, S. N., Li, S., Hu, X., & Ivashkiv, L. B. (2012). TNF-induced osteoclastogenesis and inflammatory bone resorption are inhibited by transcription factor RBP-J. *Journal of Experimental Medicine*, *209*(2), 319–334. https://doi.org/10.1084/jem.20111566

Zhao, Q. *et al*. (2010) “NFATC1: Functions in osteoclasts,” *The International Journal of Biochemistry & Cell Biology*, 42(5), pp. 576–579. Available at: https://doi.org/10.1016/j.biocel.2009.12.018.

Zhao, Z., Hou, X., Yin, X., Li, Y., Duan, R., Boyce, B. F., & Yao, Z. (2015). TNF induction of NF-KB RELB enhances RANKL-induced osteoclastogenesis by promoting inflammatory macrophage differentiation but also limits it through suppression of NFATC1 expression. *PLOS ONE*, *10*(8). https://doi.org/10.1371/journal.pone.0135728

Zhou, H., & Wu, L. (2017). The development and function of dendritic cell populations and their regulation by mirnas. *Protein & Cell*, *8*(7), 501–513. https://doi.org/10.1007/s13238-017-0398-2

Zhu, M., Van Dyke, T.E. and Gyurko, R. (2013) “Resolvin E1 regulates osteoclast fusion *via* dc-stamp and NFATC1,” *The FASEB Journal*, 27(8), pp. 3344–3353. Available at: https://doi.org/10.1096/fj.12-220228.

Zorova, L.D. *et al*. (2018) “Mitochondrial membrane potential,” *Analytical Biochemistry*, 552, pp. 50–59. Available at: https://doi.org/10.1016/j.ab.2017.07.009.